

**DNA DAMAGE RESPONSES IN THE  
CONTEXT OF THE CELL DIVISION CYCLE**

**Simona Giunta**

*St John's College*



*A dissertation submitted for the degree of  
Doctor of Philosophy  
at the  
University of Cambridge*

**Wellcome Trust and Cancer Research UK Gurdon Institute,  
Department of Zoology**

**2010**

# STATEMENT

---

The work presented in this thesis was undertaken in the laboratory of Professor Stephen P. Jackson at the Wellcome Trust and Cancer Research UK Gurdon Institute, in fulfilments of the requirements for the degree of Doctor of Philosophy. I am a member of the Department of Zoology and of St John's College, Cambridge.

This thesis and the experiments presented therein represent the outcome of my own independent work and were carried out entirely by myself, unless otherwise stated in the text.

No part of this thesis has already been, or is presently being, submitted for any other degree, diploma or qualification. In addition, this dissertation does not exceed the word limit for the Biology Degree Committee.

Simona Giunta

University of Cambridge

2010

# ABSTRACT

---

## DNA damage responses in the context of the cell division cycle

Simona Giunta

During my PhD, I have investigated aspects of the DNA damage response (DDR) in the context of three different cellular scenarios: DNA damage signalling in response to double-strand breaks during mitosis, coordination of DNA replication with DNA damage responses by regulation of the GINS complex, and checkpoint activation by the prototypical checkpoint protein Rad9. Here, I show that mitotic cells treated with DNA break-inducing agents activate a ‘primary’ DDR, including ATM and DNA-PK-dependent H2AX phosphorylation and recruitment of MDC1 and the MRN complex to damage sites. However, downstream DDR events and induction of a DNA damage checkpoint are inhibited in mitosis, with full DDR activation only ensuing when damaged mitotic cells enter G1. In addition, I provide evidence that induction of a primary DDR in mitosis is biologically important for cell viability. The GINS complex is an evolutionarily conserved component of the DNA replication machinery and may represent an ideal candidate for transferring the DNA damage signal to the replication apparatus. Here, I show the identification of a consensus ‘SQ’ PIKK phosphorylation motif at the carboxyl end of the GINS complex subunit, Psf1. In *Saccharomyces cerevisiae*, switching the conserved serine to a glutamic acid is lethal, indicating that the site is crucial for the protein’s function. Moreover, in human cells, I identified UV-DDB, a heterodimeric complex involved in NER repair, as a binding partner that specifically interacts with the Psf1 C-terminus *in vitro*. Finally, I discuss my findings in characterizing functional interactions between Rad9 and Chk1 in *S. cerevisiae*. I show that specific consensus CDK sites within Rad9 N-terminus are essential to enable Chk1 phosphorylation and activation, and that MCPH1, a human homologue of Rad9, may share a conserved function in binding and activating Chk1, underscoring the evolutionary conservation of checkpoint activation mechanisms.

To my little sister *Giulia*  
that I missed in these four years  
when, from being a child,  
she became a woman

## ACKNOWLEDGMENTS

---

I am deeply indebted to my PhD supervisor and mentor Professor *Steve Jackson*, for allowing me to conduct my PhD studies in his laboratory, for his enlightening suggestions, helpful assistance and guidance throughout my PhD.

I am extremely grateful to all past and present members of the Jackson lab. In particular, I thank *Rinma Belotserkovskaya* for collaborating on the mitotic DDR project, *Robert Driscoll* for his support, practical advice and stimulating discussions, and my colleagues *Yaron Galanty* and *Pablo Huertas* for help, supervision and assistance during my work. I also want to thank *Jeanine Harrigan*, *Sophie Polo*, *Josep Forment*, *Kyle Miller*, *Julia Coates*, *Sonja Flott*, *Naria Guerini* and *Ross Chapman* for providing answers to my endless queries. I am grateful to *Kate Dry* for her careful reading of this thesis.

During this work, I have collaborated with many great colleagues and I wish to extend my thanks to *Muriel Grenon*, *Noel Lowndes*, *Alessandro Sartori*, *Jon Pines* and the whole *Pines Lab*. I also thank *Nigel*, *Al*, *Alex*, the *Computing*, *Graphic* and *Media teams*, and everyone at the *Gurdon Institute* for making it such a special environment to work in.

Very special thanks go to my family, my parents *Maurizio & Fiorella*, my sisters *Federica & Giulia*, my grandparents and all my friends in Italy, in the UK and all over the world, for their constant moral support, encouragement and endless love. I owe special thanks to *Alistair Field* for having been there every step of the way, from the first to the last of these pages, and for having proof read them too.

# CONTENTS

---

## TABLE OF CONTENTS

STATEMENT	1
ABSTRACT	2
ACKNOWLEDGMENTS	4
CONTENTS	5
<b>TABLE OF CONTENTS</b>	<b>5</b>
<b>LIST OF FIGURES</b>	<b>9</b>
<b>LIST OF DIAGRAMS</b>	<b>11</b>
<b>LIST OF TABLES</b>	<b>12</b>
ABBREVIATIONS	13
INTRODUCTION	16
<b>1 GENERAL INTRODUCTION</b>	<b>17</b>
<b>1.1 FOREWORD</b>	<b>17</b>
<b>1.2 THE CELL DIVISION CYCLE</b>	<b>18</b>
1.2.I The cell cycle phase of mitosis: brief but important	19
1.2.II Licensing replication: assembly and function of the pre-replicative complex	22
1.2.III Entry into the synthesis phase	26
1.2.IV The fork: elongation of DNA synthesis by the core DNA replication machinery	28
<b>1.3 DNA DAMAGE RESPONSES</b>	<b>31</b>
1.3.I Signalling cascades in response to DNA double strand breaks during interphase	32
1.3.II Maintaining genome integrity during DNA replication: DNA damage in S-phase	42
<b>1.4 DNA, CHROMATIN, CHROMOSOMES: ORGANIZATION OF THE GENETIC INFORMATION</b>	<b>46</b>
1.4.I The impact of chromatin environment over DDR and repair	48
1.4.II Work presented in this thesis	52

<b>2</b>	<b>MATERIALS AND METHODS</b>	<b>55</b>
2.1	SOURCES FOR CHEMICALS, BUFFERS AND SOLUTIONS	55
2.2	ANTIBODIES	55
2.3	PLASMIDS	57
2.4	SYNTHETIC PEPTIDES	58
2.5	NUCLEIC ACID METHODS	59
2.6	ANALYTICAL BIOCHEMISTRY AND PROTEIN METHODS	61
2.7	IMMUNOFLUORESCENCE AND IMAGING	65
2.8	FLOW CYTOMETRY	66
2.9	BACTERIA RELATED TECHNIQUES	67
2.10	HUMAN TISSUE CULTURE METHODS	68
2.11	YEAST MATERIALS AND METHODS	71

---

**RESULTS**

<b>3</b>	<b>DNA DAMAGE SIGNALLING IN RESPONSE TO DSBs DURING MITOSIS</b>	<b>79</b>
3.1	SUMMARY	79
3.2	INTRODUCTION	81
3.2.I	DNA damage responses in mitosis: a one hour long gap in our knowledge	81
3.2.II	Mitosis and cancer: clinical relevance	85
3.3	RESULTS	88
3.3.I	Analyzing DNA damage responses in the context of mitosis: a matter of synchronization	88
3.3.II	Phosphorylation of histone variant H2AX in mitosis: differences and similarities to interphase	93
3.3.III	Activation of apical PIKK kinases ATM and DNA-PK leads to H2AX phosphorylation in mitosis	101
3.3.IV	Mitotic MDC1 is recruited to IRIF and is competent to bind $\gamma$ H2AX	104
3.3.V	The Mre11-Rad50-Nbs1 complex localizes to DSB sites in mitosis and may serve to hold DNA ends together	107
3.3.VI	53BP1 fails to be recruited to sites of DNA damage during mitosis	108
3.3.VII	Investigating the mechanisms of 53BP1 exclusion in mitosis	113
3.3.VIII	Impact of mitotic chromatin structure on the DDR	115
3.3.IX	Association of ubiquitin conjugates with DNA damage sites is absent during mitosis	118
3.3.X	Localization analysis of the E3 ubiquitin ligases RNF8, RNF168 and BRCA1 in unperturbed and challenged mitosis	121
3.3.XI	The E3 ubiquitin ligases RNF8 is not recruited to mitotic IRIF	121
3.3.XII	RNF168 is not recruited to DNA damage foci in mitosis, but localizes to kinetochores	129
3.3.XIII	The DDR mediator BRCA1 is also excluded from mitotic IRIF	130

3.3.XIV	Absence of a DNA damage checkpoint in mitosis correlates with failed activation of checkpoint kinases	132
3.3.XV	Mitotic cells mark sites of DSBs prior to full DDR activation in G1	134
3.3.XVI	Biological significance of the ‘primary’ DDR in mitosis	137
<b>3.4</b>	<b>DISCUSSION</b>	<b>141</b>
3.4.I	Analysis of DNA damage responses in mitosis: exclusion of secondary DDR factors from IRIF	141
3.4.II	Modulation of DNA damage checkpoint during mitosis	144
3.4.III	Biological significance of the primary DDR in mitosis: marking and tethering	146
3.4.IV	Absence of DNA damage repair in mitosis	147
3.4.V	Different kinetics of DDR activation: breathing chromatin versus mitotic chromosomes	149
<b>3.5</b>	<b>CONCLUSIONS AND FUTURE PROSPECTIVE</b>	<b>150</b>
<b>4</b>	<b>ANALYSIS OF THE GINS COMPLEX SUBUNIT PSF1</b>	<b>153</b>
<b>4.1</b>	<b>SUMMARY</b>	<b>153</b>
<b>4.2</b>	<b>INTRODUCTION</b>	<b>154</b>
4.2.I	The GINS complex is an evolutionarily conserved component of the replisome	154
4.2.II	Structural organization of the GINS complex in the context of the DNA replication fork	159
4.2.III	Functional relevance of Psf1 carboxyl terminal domain in mediating initiation of replication	161
4.2.IV	Alternative roles for the GINS complex: do all roads come from Rome?	162
<b>4.3</b>	<b>RESULTS</b>	<b>166</b>
<b>4.4</b>	<b>ANALYSIS OF THE GINS SUBUNIT PSF1 IN HUMAN CELLS</b>	<b>166</b>
4.4.I	Psf1 and Psf2 subunits of the GINS complex contain an evolutionarily conserved DNA damage related motif at the C-terminus	166
4.4.II	A candidate approach to test the BRCT phospho-peptide binding hypothesis	168
4.4.III	Mass spectrometry screen for substrates binding to the Psf1 C-terminus	171
4.4.IV	UV-DDB protein complex binds to Psf1 C-terminus in vitro	172
4.4.V	Phosphorylation of human Psf1 after DNA damage	175
4.4.VI	Analysis of Psf1 subunit of the GINS complex in the cell cycle	179
<b>4.5</b>	<b>A C-TERMINAL MOTIF OF PSF1 IS ESSENTIAL FOR THE GINS COMPLEX ACTIVITY IN SACCHAROMYCES CEREVISIAE</b>	<b>185</b>
4.5.I	Analysis of the conserved SQ motif at the C-terminus of Psf1	185
4.5.II	Analysis of <i>S. cerevisiae</i> psf1 null and ‘SQ’ motif mutant strains	185
4.5.III	Analysis of the psf1-S187A mutant	188
4.5.IV	Analysis of psf1-S187A and psf1-S187E mutants in a psf1-1 strain	188
4.5.V	Psf1-S187E is a dominant negative mutant in budding yeast	195
4.5.VI	A multicopy suppressor screening of psf1-S187E lethality	197
4.5.VII	Phosphorylation of Psf1 SQXF motif in <i>S. cerevisiae</i>	199
4.5.VIII	Identification of Psf1 interacting partners in budding yeast	200

<b>4.6 DISCUSSION AND CONCLUSION</b>	<b>202</b>
4.6.I Conserved SQXF motif on human Psf1 binds to the UV-DDB complex	202
4.6.II Physiological roles for Psf1 in cell cycle progression in human cells	205
4.6.III Psf1 serine 187 is important for cell viability in <i>S. cerevisiae</i>	208
4.6.IV Identification of novel Psf1 binding partners in <i>S. cerevisiae</i>	210
4.6.V Open questions and future directions	211
<b>5 RAD9 CONSENSUS CDK PHOSPHORYLATION SITES REGULATE CHK1</b>	
<b>ACTIVATION IN BUDDING YEAST</b>	<b>215</b>
<b>5.1 SUMMARY</b>	<b>215</b>
<b>5.2 INTRODUCTION</b>	<b>216</b>
5.2.I Rad9 as the prototypical DNA damage checkpoint adaptor protein	216
5.2.II Rad9 mediates activation of the checkpoint kinases	217
5.2.III Rad9's role in activating Chk1	220
<b>5.3 RESULTS</b>	<b>222</b>
5.3.I Rad9 contains consensus CDK phosphorylation sites within its N-terminal CAD	222
5.3.II Site-directed mutagenesis of 5 consensus CDK sites in Rad9	223
5.3.III Failed Chk1 phosphorylation and activation in the rad9-4A mutant	225
5.3.IV Physical interactions between Rad9 and Chk1	231
5.3.V Microcephalin is a novel candidate homologue of budding yeast Rad9	232
<b>5.4 DISCUSSION AND CONCLUSION</b>	<b>238</b>
5.4.I Functional activity for Rad9 consensus CDK sites in Chk1 activation	238
5.4.II Phosphorylation of Rad9 by CDK enables interaction with Chk1	240
5.4.III MCPH1, a new homologue of <i>S. cerevisiae</i> Rad9 in higher eukaryotes	241
5.4.IV Open questions and future directions	242
<b>DISCUSSION AND CONCLUSIONS</b>	<b>244</b>
<b>6 GENERAL DISCUSSION</b>	<b>245</b>
<b>REFERENCES</b>	<b>254</b>
<b>APPENDIX</b>	<b>278</b>
<b>PUBLICATIONS</b>	<b>279</b>

## LIST OF FIGURES

1. Impact of DNA damage on cell cycle distribution in U2OS cells .....	Pg. 90
2. Consequences of prolonged nocodazole treatment in U2OS cells .....	92
3. A slight increase in $\gamma$ H2AX levels during mitosis in HeLa cells .....	95
4. $\gamma$ H2AX forms foci in response to DNA damaging agents during mitosis .....	96
5. $\gamma$ H2AX foci have brighter fluorescent intensities in mitotic cells than in interphase cells .....	98
6. H3 pS10 localization and modifications in interphase and mitosis and its relationship to $\gamma$ H2AX foci .....	99
7. DSBs on mitotic DNA bridges are marked by $\gamma$ H2AX foci .....	100
8. ATM and DNA-PK mediate $\gamma$ H2AX IRIF formation in mitosis .....	102
9. ATM is activated by DNA damage and phosphorylates selected substrates in mitosis .....	103
10. MDC1 localizes to sites of DSB after induction of DNA damage during mitosis .....	105
11. The hyper-phosphorylated mitotic MDC1 binds to $\gamma$ H2AX .....	106
12. The MRN subunit Nbs1 is recruited to IRIF in mitosis .....	108
13. 53BP1 is excluded from DNA damage-induced foci during mitosis .....	110
14. 53BP1 is actively excluded from IRIF upon entry into mitosis .....	112
15. Methylated marks on histones H3K79 and H4K20 are retained in mitosis .....	114
16. Conserved consensus CDK sites for PDB binding are not responsible for mitotic exclusion of 53BP1 from IRIF .....	115
17. 53BP1 forms IRIF following Calyculin A-induced PCC .....	117
18. Ubiquitin conjugates do not accumulate to IRIF in mitotic cells .....	120
19. Free and conjugated ubiquitin levels are constant during the cell cycle .....	121
20. RNF8 accumulates to mitotic structures, centrosomes and kinetochores, but does not co-localize with $\gamma$ H2AX IRIF in mitosis .....	124
21. Mitotic RNF8 is competent to bind to MDC1 phospho-peptides .....	126
22. RNF8 forms IRIF at late mitotic stages, however 53BP1 focal accumulation does not occur until re-entry into the following G1 .....	128
23. RNF168 is excluded from mitotic chromatin and IRIF until late mitosis .....	129
24. BRCA1 is excluded from mitotic chromatin and fails to localize to sites of DSB during mitosis .....	132
25. Presence of DSBs does not trigger a DNA damage checkpoint delay in the progression through mitosis and re-entry into G1 .....	134

26. The absence of DNA damage checkpoint in mitosis correlates with impaired activation of Chk1, Chk2 and other canonical ATM targets .....	135
27. Exclusion of 53BP1 from mitotic IRIF precedes its association with IRIF and checkpoint activation in G1 .....	136
28. Proficient phosphorylation of Chk2 T68 upon re-entry into G1 .....	137
29. Primary DDR in mitosis is biologically important for cell survival .....	139
30. Primary DDR in mitosis promotes DSB repair in the following cell cycle .....	141
31. Multispecies alignment of Psf1 and Psf2 proteins sequences .....	169
32. Peptide pull-down experiments and WB for selected candidates .....	171
33. Silver stained gel and selection of bands for identification by MS .....	172
34. Psf1 C-terminus peptides bind to DDB1 and the interaction is stabilized by phosphorylation .....	174
35. Full-length GST-Psf1 expression, purification and pull-downs .....	175
36. Addressing Psf1 phosphorylation <i>in vitro</i> and <i>in vivo</i> .....	178
37. Psf1 Phospho-S173 rabbit polyclonal antibody tests .....	179
38. Level of endogenous and transiently-transfected Psf1 proteins is unchanged after DNA damage .....	180
39. Psf1 down-regulation affects progression through S-phase .....	182
40. Down-regulation of <i>PSF1</i> by siRNA causes reduction in protein level of other GINS subunits .....	183
41. Localization of human Psf1 is altered by DNA damage following irradiation ...	184
42. Conservation of fungal Psf1 carboxyl terminus and SQFF motif .....	186
43. Yeast <i>psf1</i> deletion mutant is unviable and lethality is rescued by a plasmid copy of <i>PSF1</i> .....	187
44. Conservation of fungal Psf1 carboxyl terminus and SQFF motif .....	188
45. Spot test for <i>psf1-S187A</i> colony formation upon treatment with DNA damaging agents .....	189
46. Lethality of Psf1 <sup>S187E</sup> in the <i>psf1-1</i> mutant strain .....	191
47. <i>Psf1-S187E</i> displays hyper-sensitivity to specific DNA damaging agents, whereas <i>psf1-S187A</i> behaves like a wild-type strain .....	193
48. Proficient Rad53 phosphorylation and activation of the G1/S checkpoint in <i>psf1</i> mutant strains .....	195
49. HA-Psf1 does not co-IP MCM2 subunit of the MCM complex .....	196
50. <i>Psf1-S187E</i> is a dominant negative mutant of yeast <i>PSF1</i> .....	197
51. Screen for suppressors of <i>psf1-S187E</i> mutant lethality at 37°C .....	199
52. Yeast Psf1 phosphorylation sites upon incubation with HU .....	200

53. Factors interacting with full-length Psf1 upon incubation with HU in <i>S. cerevisiae</i> .....	202
54. Rad9 consensus CDK sites within the N-terminal CAD region .....	224
55. Expression of <i>rad9</i> CDK mutants .....	225
56. Rad9 S83, T110, T125 and T143 are required for Chk1 phosphorylation .....	227
57. <i>Rad9-4A</i> mutant is not proficient in mediating phosphorylation of Chk1 during late S-phase and in mitosis .....	228
58. Sensitivity assay of Rad9 CDK mutants .....	230
59. A small amount of Chk1 binds to Rad9 N-terminus <i>in vitro</i> .....	233
60. Identification of a novel CAD region in human MCPH1, which shares conserved CDK sites with scRad9 and binds to human Chk1 .....	235
61. Strategy for the design of Rad9-h/ggMCPH1 hybrid constructs .....	237

## LIST OF DIAGRAMS

1. Possible mechanisms of action of the CMG helicase complex during DNA unwinding .....	Pg. 25
2. The eukaryotic replication fork .....	30
3. Schematic structure of a prototypical DNA damage PIKK, ATM .....	34
4. Signalling cascade amplification .....	36
5. 53BP1 structural features and domains .....	39
6. The two-step DDR signalling cascade .....	40
7. From DNA to chromatin to chromosomes, through multiple compaction steps ..	47
8. Mitotic data support the existence of a positive feedback loop between recruitment of DDR mediators and checkpoint activation .....	146
9. Ordered assembly of the replisome for initiation of replication in <i>S. cerevisiae</i> ..	157
10. The GINS complex activities at the replication fork during DNA synthesis .....	159
11. The molecular structure of the human GINS complex .....	161
12. Highly conserved, exposed phenylalanine 176 on Psf1 may regulate interaction with DDB1 .....	204
13. Rad9 protein structural features and domains .....	217
14. Modes of Rad53 activation through the Rad9 adaptor protein .....	220

## LIST OF TABLES

1. Antibodies .....	Pg. 55
2. Plasmid constructs .....	57
3. Synthetic peptides .....	58
4. Yeast culture media .....	71
5. Yeast strains used in this study .....	72
6. <i>In silico</i> search for C-terminal consensus (S/T)QXF peptide motifs across the human genome .....	168
7. Synthetic peptides of Psf1 and Psf2 used for pull-downs experiments .....	171
8. Psf1 peptides-binding proteins identified by mass spectrometry .....	173
9. Proteins interacting with full length Psf1 .....	201

## ABBREVIATIONS

---

4NQO	4-nitroquinoline 1-oxide
53BP1	p53 binding protein 1
5-FOA	5-fluoro-orotic acid
aa	amino acids
APC/C	anaphase promoting complex/cyclosome
ARS	autonomously replicating sequences
ATM	ataxia telangiectasia, mutated
ATMi	ATM inhibitor (KU-55933)
ATP	adenosine triphosphate
ATR	ataxia telangiectasia, mutated and RAD3-related
BRCA1/2	breast cancer 1/2
BRCT	BRCA1 carboxyl-terminal
CAD	Chk1-activation domain
Cdc	cell division cycle proteins
CDK	cyclin-dependent kinase
Cdt1	cdc10-dependent transcript 1
CMG	Cdc45-MCM2-7-GINS
CPT	camptothecin
Csm3	chromosome segregation in meiosis 3
DAPI	4,6 diamidino-2-phenylindole
DDB1/2	DNA damage binding protein 1/2
DDK	Dbf4-Cdc7 kinase
DDR	DNA damage response
DNA	deoxyribonucleic acid
DNA-PKcs	DNA-dependent protein kinase, catalytic subunit
DNA-PKi	DNA-dependent protein kinase inhibitor (NU-7441)
dNTPs	deoxyribonucleoside triphosphates
DSB	double strand break
FACS	fluorescence activated cell sorting

FAT	FRAP-ATM-TRRAP
FATC	FAT C-terminus
FRAP	FKBP12-rapamycin-associated protein
GFP	green fluorescent protein
GINS	go ichi nii san; (sld)5, (Psf)1, (Psf)2, (Psf)3 in Japanese
$\gamma$ H2AX	phosphorylated form of H2AX (histone H2A variant)
H3K79me2	di-methylated histone H3 lysine 79
H4K20me2	di-methylated histone H4 lysine 20
HDACi	histone de-acetylase inhibitor
HEAT	huntingtin, elongation factor 3, protein phosphatase 2A, and TOR
HNE	HeLa nuclear extract
HP1	heterochromatin protein 1
HR	homologous recombination
HU	hydroxyurea
IB	immunoblot
IF	immunofluorescence
IP	immunoprecipitation
IR	ionizing radiation
IRIF	IR-induced foci
K.D.	knock-down
K.O.	knock-out
MC	mitotic catastrophe
MCM	mini-chromosome maintenance
MCPH1	microcephalin 1
MDC1	mediator of DNA damage checkpoint 1
MMS	methylmethane sulphonate
MPF	maturation/mitosis-promoting factor
Mrc1	mediator of replication checkpoint protein 1
Mre11	meiotic recombination repair protein 11
MRN	Mre11-Rad50-Nbs1
MS/MS	tandem mass spectrometry
Nbs1	Nijmegen breakage syndrome 1
NER	nucleotide excision repair
ORC	origin recognition complex

ORF	open reading frame
PCNA	proliferating cell nuclear antigen
PIKK	phosphatidylinositol 3-kinase-like kinase
Pol	(DNA) polymerase
Pre-IC	pre-initiation complex
Pre-RC	pre-replicative complex
Psf1/2/3	partner of Sld5 1/2/3
PTM	post-translational modifications
Rad9	radiation sensitive 9
RFC	replication factor C
RNF8/168	RING finger protein 8/168
RPA	replication protein A
SAC	spindle assembly checkpoint
SCD	S/TQ (serine/threonine-glutamine) cluster domain
SDS-PAGE	sodium dodecyl sulphate-polyacrylamide gel electrophoresis
siRNA	small interfering ribonucleic acid
Sld5	synthetic lethal with <i>Dpb11-1 5</i>
SSB	single strand break
TCA	trichloroacetic acid
TLS	translesion synthesis
Tof1	Top1-associated factor 1
Top1/2	(DNA) topoisomerase I/II
TopBP1	(DNA) topoisomerase II binding protein 1
TOR	target of rapamycin
TRRAP	transformation/transcription domain-associated protein
TSA	tricostatin A
U	units
UIM	ubiquitin-interacting motif
UTR	untranscribed region
UV	ultra-violet radiation
WB	western blot
WCE	whole cell extract
WM	wortmannin
WT	wild-type

## INTRODUCTION

---

# 1 GENERAL INTRODUCTION

## 1.1 Foreword

*“Homo mundus minor”*

*Boethius (524 A.D.)*

A historical perspective on cancer aetiology needs to embrace the origins of multi-cellularity, the secular evolutionary process that brought individual cells together. In the XVII century, Robert Hooke first uncovered the fundamental structural and functional unit of all living organisms, the cell; centuries of ongoing studies followed to unravel not only the mystery of how cells function and act, but also how they interact to form a living being. Cancer is a cellular phenomenon that stems from the breakdown of the universal laws of nature that govern multi-cellularity. Biological laws have evolved to enforce self-killing when a dysfunctional cell no longer contributes to the wellbeing of the organism as a whole. Selfishly, the cancer cell goes against these rules of co-existence and, if driven by an expansionistic pursuit, leads to the formation of a tumour that may result in the death of the organism. Such a short-sighted, egocentric plan initiated from a single cell occurs through circumventing rigid molecular restrains and is facilitated by modern lifestyle and the drastic, often evolution-independent, increase in longevity. As we keep postponing the antagonistic pleiotropy called ageing, we draw ourselves closer to the edge (of evolution), where cancer awaits.

## 1.2 The cell division cycle

*“Therefore, I reasoned that study of the cell cycle responsible for the reproduction of cells was important and might even be illuminating about the nature of life”*

*Sir Paul Nurse (Autobiography, 2001)*

The mammalian cell cycle describes the process whereby a cell replicates its DNA and divides to produce two genetically identical daughter cells. Essentially, two types of cell cycle control mechanisms exist: a cascade of protein phosphorylations that act as an “engine” to relay a cell from one stage to the next and a set of checkpoints that monitor completion of critical events and delay progression to the next stage if necessary.

The first type of control involves a highly regulated protein family, the kinases. Activation requires the association between a cyclin, the core of each complex and the essential regulatory subunit, and a cyclin-dependent kinase (CDK), the catalytic subunit. The activity of the cyclin-CDK complexes is regulated by an intricate network of events including induction and degradation of the cyclin subunit, phosphorylation and dephosphorylation of the CDK subunit and binding of CDK inhibitors to the cyclin-CDK complex. The phosphorylation events regulate the length of each cell cycle phase and transition to the next phase (Collins et al., 1997; Funk, 1999).

The second type of cell cycle regulation, the checkpoint control, involves complex signal transduction pathways at the G1/S, G2/M transitions and in S phase to mitosis to detect errors in DNA replication and chromosome segregation. When these checkpoints are activated, for example by DNA damage, signals are relayed to the cell cycle machinery to cause a delay in cycle progression and avoid acquisition of mutation. Therefore these checkpoints integrate cell cycle regulations with DNA repair, the integrity of which is essential to maintain genetic stability. Mutations in the checkpoint components may lead to aberrant cell cycle progression in the presence of stimuli such as DNA damage and eventually to genetic instability.

### **1.2.1      *The cell cycle phase of mitosis: brief but important***

*“Nothing we have learned about mitosis since it was discovered a century ago is as dazzling as the discovery itself”*

*(Mazia, 1987)*

The eukaryotic cell division cycle consists of four distinct phases: gap phase 1 (G1), synthesis phase (S-phase), gap phase 2 (G2) and mitosis (M-phase). G1, S and G2 phases are collectively termed interphase, characterized by cell growth and replication of the genetic material, of which the nucleus is the repository. The cell cycle culminates in the terminal phase of mitosis, whereby cell division results in two identical daughter cells. Although the fundamental aspects of cell duplication and division are similar in all eukaryotes, the duration of the cell cycle varies greatly between organisms. Budding yeasts, for examples, can complete an entire cell cycle in approximately 90 minutes (Forsburg and Nurse, 1991), whereas the mammalian cell cycle takes about 24 hours. Mitosis is the shortest cell cycle stage, lasting approximately one hour. Although brief, mitosis is a complex biological phenomenon, essential for the continuation of life. M-phase can be divided into two major events, karyokinesis and cytokinesis. Karyokinesis, the process of nuclear division, is commonly subdivided into different stages, based on changes in chromosome structure and behaviour. The onset of mitosis is defined by the condensation of nuclear chromatin into mitotic chromosomes and nuclear envelope breakdown, a stage called prophase. In pro-metaphase, kinetochores are formed on the centromeres of mitotic chromosomes, allowing microtubules attachment. In metaphase, chromosomes are aligned along the spindle equatorial plane by the spindle fibres. During anaphase, microtubules pull chromosomes apart at the kinetochores. As well as equal division of the genetic information, a successful mitosis must ensure that all other cellular

components are distributed to the two daughter cells, through the process of cytokinesis. In telophase, cytokinesis and karyokinesis are completed, the cell physically splits in two, and the nuclear envelope reassembles around the two sets of chromatids located at opposite poles to re-establish a nuclear environment for each of the two daughter cells (Norbury and Nurse, 1992). Microscope observations of visually dramatic events during mitosis lead to an approximate subdivision into phases merely based on gross morphological changes. A new way of classifying mitotic transitions is based on the molecular dynamics of each step (Pines and Rieder, 2001). Indeed, mitosis is highly regulated by complex molecular mechanisms. The onset of mitosis is marked by the transition between G2 and M-phase, a crucial checkpoint for the cell. The G2/M boundary is susceptible to stress signals and initiates a reversible arrest, preventing cells from entering mitosis under challenged conditions and until DNA replication is completed (Bernhard et al., 1995). Once the G2/M boundary is overcome, chromatin is compacted, the nuclear envelope disassembles and the cell becomes committed to mitosis.

Activation of the MPF (maturation/mitosis-promoting factor), a complex made of cyclin B/CDK1, is a critical step in driving cells into mitosis (Nurse, 1990). In interphase, newly synthesized cyclin B/CDK1 complexes are kept inactivated by Myt1 and Wee1 inhibitory phosphorylations on threonine 14 and tyrosine 15 of CDK1 (Parker and Piwnicka-Worms, 1992; Tuel-Ahlgren et al., 1996; Liu et al., 1997). In early mitosis, Cdc25, a dual-specificity phosphatase, removes the inhibitory phosphorylations, enabling cyclin B/CDK1 activation (Coleman and Dunphy, 1994; Lew and Kornbluth, 1996). Activated cyclin B/CDK1 complexes, in turn, phosphorylate specific substrates to promote events such as chromosome condensation and mitotic spindle assembly, enabling mitotic entry. Regulation of mitotic cyclin/CDK complexes is tightly controlled through positive and

negative feedback loops, involving a complex network of kinases and phosphatases (reviewed in Perry and Kornbluth, 2007).

Once the chromosomes are aligned in metaphase, a further checkpoint step, the so-called spindle assembly checkpoint (SAC), is in place to ensure that condensed sister chromatids are successfully attached to the spindle *via* their kinetochores before anaphase can proceed (Rieder and Salmon, 1998). The SAC directly inhibits the APC/C (anaphase promoting complex/cyclosome), a large ubiquitin ligase complex that targets selected substrates for ubiquitylation, mediating entry into anaphase and subsequent cytokinesis. Major effectors of the SAC are Mad2 and BubR1 that are enriched at loosely attached kinetochores, and prevent mitotic exit by inhibiting the APC from targeting Cyclin B and Securin for degradation. The cell remains arrested until the Mad2 and BubR1 signals are attenuated, when stable bipolar attachment of all chromosomes to the spindle is achieved. Once the SAC is satisfied, APC-mediated proteolysis of selected substrates drives cells into anaphase (Peters, 2006). The end of mitosis is marked by a rapid degradation of Cyclin B by the APC-Cdc20 complex, which causes the loss of CDK1 activity, allowing for the formation of a midbody and a new nuclear envelope (Kramer et al., 2000). The midbody is a transient structure made of compacted bundles of microtubules, containing proteins required for chromosome segregation and mitotic exit. Ultimately, cytokinesis completes the mitotic division into two identical daughter cells. Several molecular details remain to be elucidated in the complex series of events leading to cell division. In particular, the control of the APC complex during mitosis, including its ability to selectively recognise different substrates, is still largely unknown.

### ***1.2.II Licensing replication: assembly and function of the pre-replicative complex***

In eukaryotic cells, regulatory mechanisms are in place to ensure that DNA synthesis occurs once every cell cycle to faithfully replicate each section of the nuclear genome (Blow and Laskey, 1988). The origins of replication are specific points in the genome licensed for replication initiation, which are fired once in a single S-phase. Eukaryotic origins of replication represent DNA platforms for the assembly of protein complexes, leading to the formation of two bi-directional DNA replication forks. Whereas bacterial chromosomes typically have a single origin of replication, eukaryotic cells initiate replication at multiple locations across the genome. Initiation of replication is a highly ordered and regulated process that involves a plethora of factors (reviewed in Diffley and Labib, 2002). The pre-replicative complex (pre-RC) is a multi-protein complex first assembled on the replication origin during G1. The formation of the pre-RC in eukaryotes involves early replication factors such as ORC, Cdc6, Cdt1 and MCM2-7. The origin recognition complex (ORC) is made of six highly conserved protein subunits and is the earliest factor to bind to replication origins. ORC was first shown in *Xenopus* egg extracts to be essential for initiation of replication (Carpenter et al., 1996; Romanowski et al., 1996; Rowles et al., 1996), a function conserved across the eukaryotic domain. Loading of ORC to replication origins is a highly regulated process, influenced by DNA recognition and ATP binding and hydrolysis. Despite being structurally and functionally conserved, ORC mechanism and timing of interaction with origins varies between different eukaryotes. In *Saccharomyces cerevisiae*, ORC specifically recognizes a region of ~30 base pairs of DNA within an autonomously replicating sequence (ARS; Bell and Stillman, 1992). Specific DNA elements, such as the ARS sequences have yet to be identified in higher eukaryotes, suggesting that DNA sequence alone does not define the origin of replication. In addition,

although ORC is constitutively associated with DNA throughout the cell cycle in yeast, *Xenopus* and mammalian ORC is removed from chromatin in mitosis (Carpenter et al., 1996; Romanowski et al., 1996; Natale et al., 2000; Tatsumi et al., 2000). ORC binding to DNA serves as a highly conserved assembly platform to recruit additional members of the pre-RC, including the loading factors Cdc6 (cell division cycle protein 6; Nishitani and Nurse, 1995; Coleman et al., 1996; Tanaka et al., 1997) and Cdt1 (cdc10-dependent transcript 1; Maiorano et al., 2000; Nishitani et al., 2000) that play a role in limiting DNA replication to once each cell cycle. Additional players are involved in positively and negatively regulating assembly of factors into the pre-RC. For instance, in *Xenopus* eggs and human cells, geminin was shown to be a negative regulator of Cdt1 and its rapid degradation at the metaphase-anaphase transition enables Cdt1 recruitment to early-replicating origins (Wohlschlegel et al., 2000; Tada et al., 2001) and renders chromatin competent for replication initiation. Cdc6 and Cdt1, recruited independently by ORC, in turn, function synergistically to load the heterohexameric MCM (mini-chromosome maintenance) protein complex to chromatin. The MCM2-7 hexamer plays an evolutionarily conserved role in DNA replication initiation (for a comprehensive review, see Kearsey and Labib, 1998). In addition to MCM's role at the pre-RC as a component required to license DNA for replication, MCM functions at the replication fork as the replicative DNA helicase. Indeed, the MCM complex remains associated with the fork during S-phase and plays a role ahead of the fork as an helicase to unwind the DNA duplex, with a 3' to 5' polarity shown for the archaeal MCM (Kelman et al., 1999; Chong et al., 2000; Shechter et al., 2000). A plethora of biochemical data in archaea, yeast and more recently human cells have shown that a MCM sub-complex of MCM4, 6 and 7 proteins possesses intrinsic, ATP-dependent, 3' to 5' helicase activity (Ishimi, 1997; You et al., 1999; Lee and Hurwitz, 2000). Elegant studies performed by Matthew Bochman and

Anthony Shwacha have found that, while both MCM2-7 and MCM4,6,7 are capable of binding to single stranded DNA (ssDNA), MCM4,6,7 binding to both ssDNA and double stranded DNA (dsDNA) is faster and more efficient. However, the MCM2-7 heterohexamer does display helicase activity *in vitro*, but only when a putative MCM 2/5 ATP-dependent gate is closed, suggesting that conformational changes, mimicked by removal of the MCM2 and 5 subunits, may have regulatory significance in controlling MCM enzymatic activity (Bochman and Schwacha, 2007; Bochman et al., 2008; Bochman and Schwacha, 2008).

New data show that the MCM2-7 ring binds to Cdc45 and GINS, suggesting that the CMG (Cdc45-MCM2-7-GINS) super-complex may be responsible for DNA unwinding in eukaryotes (Diagram 1), with Cdc45 and GINS acting as cofactors of the helicase (Moyer et al., 2006). However, the mechanism of action of MCM as a replicative helicase is unclear. Nevertheless, several models have been suggested for the helicase action: (1) in the ‘wedge model’ or ‘steric-exclusion model’, one of the newly synthesized strand moves through the central helicase channel, preventing annealing at the DNA duplex junction (Diagram 1B; Patel and Picha, 2000). This would be in agreement with data inferring that MCM preferably binds ssDNA. A variation of the wedge model is the ‘ploughshare model’ where MCM moves on dsDNA and another protein serves to separate the two strands as they exit from the helicase (Takahashi et al., 2005). A strong candidate for this role is the GINS complex (Diagram 1A). (2) In the ‘torsional model’, the MCM creates negative superhelical stress by rotating the DNA strands and inducing displacement of base pairing (Patel and Picha, 2000). (3) In the ‘rotatory pump model’, similarly to the torsional model, MCM acts as rotary motor but the rotatory movement along the DNA helical axis occurs at a distance from the replication fork. Fixed MCM complexes pump the DNA through the

ring in opposite directions, generating superhelical stress that unwinds the DNA placed between the two MCMs (Laskey and Madine, 2003). This is an appealing model that would reconcile data that MCM preferentially binds to unreplicated DNA (Madine et al., 1995; Krude et al., 1996; Dimitrova et al., 1999) and that the MCM helicase does not co-localize with the replication fork during S-phase (Madine et al., 1995; Krude et al., 1996; Ritzi et al., 1998; Dimitrova et al., 1999).

**DIAGRAM 1. Possible mechanisms of action of the CMG helicase complex during DNA unwinding**



**Content not visible due to copyright limitations**

The CMG complex collaborates in the separation of the two DNA strands at the replication fork. Given GINS has been shown to have higher affinity to ssDNA, it is located in the replication bubble. In A, MCM2–7 pumps dsDNA through its inner channel by helical rotation in an ATP-dependent manner, destabilizing the double helix. In this model, GINS complex function more passively as a structural element resembling a strand displacement blade, or 'ploughshare' to sterically separate the two strands, preventing re-annealing of unwound DNA and providing room for the activity of the polymerases (A). On the other hand, in B, GINS is located in front of the MCM2–7 complex and play a more active role in DNA unwinding (B). To date, it is still unclear if the eukaryotic MCM acts as dsDNA translocase (A) or binds ssDNA during DNA unwinding.

Image from Boskovic et al., 2007

In spite of a compelling amount of evidence pointing to a role for the MCM as the eukaryotic replicative helicase, additional details are required to clarify certain discrepancies and to fully elucidate MCM function as a helicase (reviewed in Aparicio et al., 2006).

### ***1.2.III Entry into the synthesis phase***

Formation of pre-RCs and their activation are regulated in *trans*, by cell cycle-dependent control of replication licensing factors, and in *cis*, by structural features that aid selection of replication origins. Once the potential sites for replication are marked by the pre-RCs, CDK activity is required to enable single firing of each replication origin and timely initiation of DNA synthesis. It is noteworthy, however, that a differential regulation exists in the timing of origin firing. The so-called ‘early’ origins are activated as cells enter S-phase, whereas the ‘late’ origins, often associated with heterochromatic regions, are fired later in S-phase (Bousset and Diffley, 1998; Donaldson et al., 1998) and often progress into G2 with ongoing replication. Licensed origins are activated for replication by CDK and DDK cell cycle kinases. In this context, CDK comprises Cdk2 associated with the S-phase specific cyclins A and E (Krude et al., 1997). DDK (Dbf4-dependent kinase) follows an analogous mechanism of activation, where the catalytic subunit Cdc7 is activated upon cell cycle regulated accumulation of the Dbf4 regulatory partner at the G1/S boundary. When cells transit from G1 into S-phase, the pre-RCs are converted into pre-ICs (pre-initiation complexes). In budding yeast, several proteins are localized at the pre-IC: Mcm10, Sld2, Sld3, Dpb11, Cdc45, DNA polymerase  $\epsilon$ , GINS complex (consisting of Sld5, Psf1, Psf2 and Psf3) and replication protein-A (RPA; consisting of Rfa1, Rfa2 and Rfa3). The laboratory of Dr Hiro Araki has shown that in *S. cerevisiae* CDK activity is

required for the initiation of replication by phosphorylating two members of the pre-IC, Sld2 and Sld3 (Masumoto et al., 2002). Phosphorylated Sld2 binds to the twin BRCT (BRCA1 carboxyl-terminal) domains at the carboxyl terminus of Dpb11 (Tak et al., 2006), the homologue of fission yeast Cut5, that, in turn, regulates Sld2-Sld3 interactions. Phosphorylated Sld3, facilitated by the Dpb11-mediated interaction with Sld2 (Tanaka et al., 2007), recruits another important pre-IC factor, Cdc45 (Kamimura et al., 2001). Sld2 and Sld3 are the major targets of CDK-dependent phosphorylation required for initiation of replication, because mimicking CDK-phosphorylation on Sld2 and Sld3 is sufficient to bypass the requirement for CDK in DNA replication (Zegerman and Diffley, 2007). In addition, Dpb11 plays an essential role in recruiting the GINS complex to the pre-IC (Takayama et al., 2003). In human cells, however, loading of MCM, GINS and Cdc45 requires the Ctf4, RecQL4 and Mcm10 proteins, but not TopBP1, the human homologue of Dpb11 (Im et al., 2009), indicating that distinct but partially overlapping mechanisms exist in replication complex assembly across different species. The exact functions of many pre-IC proteins are still largely unknown, although many remain associated with the replication machinery during replication fork elongation, suggesting that they may be required for helicase activity, such as mediated by MCM2-7, GINS and Cdc45, or contribute to DNA synthesis in other ways (Aparicio et al., 1997; Pacek et al., 2006).

The final step in replication initiation is the loading of the replicative polymerases, DNA polymerase (pol)  $\alpha$ ,  $\delta$  and  $\epsilon$  (Hubscher et al., 2002). The pre-IC factor, Mcm10, recruits and stabilizes DNA pol  $\alpha$ -primase at the replication fork (Ricke and Bielinsky, 2004; Chattopadhyay and Bielinsky, 2007; Zhu et al., 2007), which coincides with initiation of replication.

CDK activity not only promotes replication initiation at the G1/S transition but has also been shown to negatively regulate replication, in order to prevent re-replication and preserve genomic stability during S-phase. CDK-dependent phosphorylation events inhibit pre-RC formation as cells progress through the cell cycle by directly targeting members of the pre-RC complex. For example, in budding yeast, Cdc6 is phosphorylated and targeted for degradation in late G1 (Drury et al., 1997; Drury et al., 2000). ORC is also a target for CDK modification (Nguyen et al., 2001; Vas et al., 2001) although the mechanisms of ORC functional inhibition by CDK phosphorylation are unclear. Furthermore, the MCM complex's cytoplasmic re-localization in G2 depends on CDK activity, as inactivation of CDK results in stable maintenance of the MCM complex in the nucleus (Labib et al., 1999; Nguyen et al., 2000). In addition, the MCM subunit Mcm2 is phosphorylated by DDK (Jiang and Hunter, 1997; Lei et al., 1997; Brown and Kelly, 1998; Weinreich and Stillman, 1999). Possibly, this could act as a way to regulate activation of the MCM helicase, of which Mcm2 is allegedly an inhibitory subunit.

#### ***1.2.IV The fork: elongation of DNA synthesis by the core DNA replication machinery***

The eukaryotic DNA polymerases  $\alpha$ ,  $\delta$  and  $\epsilon$  share similar conserved catalytic sites, yet play different roles in the elongation of the replication fork (Nasheuer et al., 2002; Takeda and Dutta, 2005). DNA pol  $\alpha$  works in a four-subunit complex with DNA primase to synthesize short tracts of ribonucleotides that act as primers for leading and lagging strand synthesis. The RNA primer made by the primase enzyme is then extended by pol  $\alpha$ . The function of DNA pol  $\alpha$  in this process is a primary requirement for replication, being the only replicative polymerase that can perform *de novo* DNA synthesis on ssDNA. DNA pol

$\delta$  and DNA pol  $\epsilon$  instead need a pre-existing 3'-OH priming DNA end onto which they can attach nucleotides (Hubscher et al., 2002). Due to the low processivity of DNA pol  $\alpha$  (~30 nucleotides) and lack of proofreading activity, most DNA synthesis is carried out by either pol  $\delta$  and/or pol  $\epsilon$ , which are more processive and contain proofreading exonuclease activities. Thus, after primer synthesis, a polymerase switch occurs with DNA pol  $\alpha$  being replaced at the start of leading strand synthesis and during initiation of every fragment on the lagging strand (Takeda and Dutta, 2005). Inherently, DNA polymerases have a 5' to 3' DNA processivity, signifying that only one of the parental DNA strands will be replicated continuously; the so-called leading strand. On the other hand, the other strand, named 'lagging', is replicated in relatively short 'Okasaki' fragments (Diagram 2b). Replication of leading and lagging strands requires a particularly robust coordination between DNA synthesis and unwinding, possibly achieved through factors, such as the GINS complex, which have been shown to bind both the MCM helicase and DNA polymerases. Although DNA pol  $\delta$  has been implicated in lagging-strand replication (Garg and Burgers, 2005a) and DNA pol  $\epsilon$  in leading-strand replication (Pursell et al., 2007), it is formally possible that the two polymerases participate in replicating both strands. The series of RNA-DNA hybrid fragments on the lagging strand require additional processing to promote their maturation into a continuous strand. The DNA-flap endonuclease Fen1 removes the RNA primers coordinately to the helicase/endonuclease activity of Dna2, and with RNase H; following DNA pol  $\delta$  action, the Okasaki fragments are ligated by DNA ligase I (reviewed in Garg and Burgers, 2005b).

Association of the DNA polymerase auxiliary factor PCNA (proliferating cell nuclear antigen) is required to increase processivity of DNA synthesis (Jonsson and Hubscher, 1997). The ring-shaped homotrimeric processivity factor PCNA encircles dsDNA and acts

as a ‘sliding clamp’ to prevent dissociation of polymerases from the DNA. The loading of the PCNA ring onto dsDNA is mediated by the conserved heteropentameric clamp loader protein complex called replication factor C (RFC), a member of the AAA+ family of proteins (Bowman et al., 2005), which recognizes RNA-DNA hybrids at the fork. RFC and PCNA, together with RPA, are required for the polymerase switch to DNA pol  $\delta$  and DNA pol  $\epsilon$ , thereby triggering ensuing replication.

## **DIAGRAM 2. The eukaryotic replication fork**

**Content not visible due to copyright limitations**

Origins of replication are marked by pre-RC on multiple distinct locations across the genome (a). Licensed replication origins are fired and replication is initiated (b). The MCM helicase complex remains associated with the fork during S-phase and plays a role ahead of the fork as a helicase to unwind the DNA duplex (see text for details). The eukaryotic replication fork comprises a plethora of proteins that contribute to DNA replication and its fidelity. MCM-dependent unwinding allows access to the DNA polymerases, pol  $\alpha$ , in complex with the DNA primase, and the replicative polymerases  $\delta$  and pol  $\epsilon$ . Additional factors include the replication processivity clamp PCNA, loaded by the RFC complex, RPA, which binds ssDNA regions during fork progression, and factors that are involved in monitoring fork integrity. In *S. cerevisiae*, these are the checkpoint mediators Mrc1, Tof1, Csm3 and Rrm3. DNA topoisomerases I and II act to relieve the torsional stress caused by the DNA topology at the replication fork (c).

Image from Branzei and Foiani, 2010

Progression of the replication fork causes topological problems such as positive supercoiling and concatenation ahead of the replication fork, counteracted by the action of

topoisomerases I and II, respectively, which nick the DNA backbone to release the torsional stress (Diagram 2c; Nadal, 2007). Termination of replication occurs when two opposing forks meet and the newly synthesized DNA is ligated.

### **1.3 DNA damage responses**

The maintenance of an intact genome is a pivotal aspect of cellular homeostasis. Upon the formation of DNA lesions, the cell promptly onsets a complex DNA damage response (DDR). The DDR network orchestrates a wide range of cellular events; these comprise sensing the lesion, arresting the cell cycle, coordinately with the repair of the damage, ultimately leading to resumption of the physiological cellular metabolism (Zhou and Elledge, 2000; Rouse and Jackson, 2002).

On a daily basis, the DNA in the cell sustains a wide diversity of lesions, caused *via* exogenous as well as endogenous sources. DNA double strand breaks (DSBs) are breaks that encompass both strands of the DNA helix and are undoubtedly the gravest cytotoxic form of damage for eukaryotic cells (Khanna and Jackson, 2001). DSBs occur following exposure to ionizing radiations (IR) or radiomimetic drugs, including cancer chemotherapeutics. Physiological cellular processes, such as V(D)J recombination during immunoglobulin gene rearrangement and stalled replication forks during DNA synthesis, are also causes of DSBs (Bassing and Alt, 2004). Failure to repair DSBs causes genomic instability and can lead to tumourigenesis and other age-related diseases (reviewed in Jackson and Bartek, 2009).

### ***1.3.1 Signalling cascades in response to DNA double strand breaks during interphase***

The molecular signal-transduction cascade that unfolds following DSB induction in mammalian cells has been intensively investigated in the context of interphase. Simplistically, the cascade comprises of two major stages and follows a hierarchical mode of activation: from an initial sensing of the lesion, activation of apical DDR kinases and amplification of the signal *via* mediator proteins, the signal is subsequently relayed to downstream effectors responsible for events leading to cell cycle arrest and DSB repair by homologous recombination (HR) or non-homologous end joining (NHEJ) pathways, before resumption of the cell cycle.

At the apex of the DDR following a DSB, ‘sensor’ proteins are able to detect damaged DNA, possibly due to altered chromatin structure or perturbation in DNA-processing activities, such as replication and transcription. Although the exact molecular mechanisms are still unclear, the Mre11-Rad50-Nbs1 (MRN) complex is believed to directly sense damaged DNA and has been pinpointed as the upstream mediator in the activation of the DDR, being one of the first factors to be recruited to the DNA ends upon formation of a DSB (Mirzoeva and Petrini, 2001). Furthermore, the Ku70/Ku80 heterodimer, which displays high affinity for DNA ends in a sequence-independent manner (reviewed in Downs and Jackson, 2004), also plays an early role in the DDR by sensing free DNA ends following DSB formation.

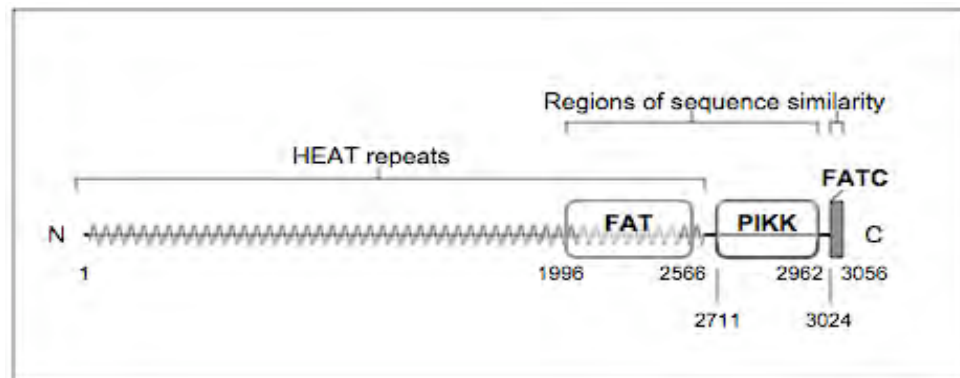
The major apical protein kinase that orchestrates the intricate network of responses to DSBs is ATM (ataxia telangiectasia mutated; Khanna et al., 2001; Shiloh, 2003). ATM is recruited to the site of break by interactions with the MRN sensor complex (Uziel et al.,

2003; Falck et al., 2005) and becomes activated through auto-phosphorylation on serine 1981 (S1981; Bakkenist and Kastan, 2003; Abraham and Tibbetts, 2005; Lee and Paull, 2005) and acetylation on lysine 3016 by the histone acetyltransferase (HAT) Tip60 (Sun et al., 2007). MRN-dependent DNA unwinding and tethering activities are required to recruit ATM firstly to the direct proximity of the DNA ends, and in turn, to promote ATM binding to the chromatin around the break (Williams et al., 2007). Furthermore, the MRN complex possesses nucleolytic activity, acting both as an exo- and an endonuclease (Paull and Gellert, 1998). Our laboratory has shown that MRN endonucleolytic activity is important for resection of the DSBs and it synergizes with another nuclease, CtIP (Sartori et al., 2007), in response to DSBs. It is currently unclear whether MRN activity as a nuclease is directly involved in ATM activation. Evidence from the laboratory of Vincenzo Costanzo shows that in *Xenopus*, ssDNA oligonucleotides, generated as a by-product of MRN-dependent resection, stimulate ATM activation (Jazayeri et al., 2008).

Mutations in the *ATM* gene are responsible for ataxia telangiectasia (Savitsky et al., 1995), a recessive human genetic disorder characterized by immunodeficiency, hyper-sensitivity to radiation, genomic instability and cancer predisposition, impaired motor skills caused by cerebellar degeneration (ataxia) and red veins in the eyes (telangiectasias). The proximal kinase ATM belongs to the PIKK (phosphatidylinositol 3-kinase-like kinase) family of protein kinases. PIKK family members include ATM, ATR (ATM and RAD3-related), DNA-PKcs (DNA-dependent protein kinase catalytic subunit), TRRAP, mTOR/FRAP (mammalian target of rapamycin) and SMG1/ATX. The PIKK family is structurally unique. These large PIKK polypeptides, up to 450 kDa in size, display a highly divergent amino-terminus made of  $\alpha$ -helical HEAT repeat units (Perry and Kleckner, 2003; Brewerton et al., 2004) and strong sequence homology in the carboxyl-terminal catalytic

domain. This kinase domain is flanked by two loosely conserved regions, the FAT (FRAP/ATM/TRRAP) and the FATC (FAT C-terminus) domain, residing at the very carboxyl end of the protein (Durocher and Jackson, 2001).

**DIAGRAM 3. Schematic structure of a prototypical DNA damage PIKK, ATM**

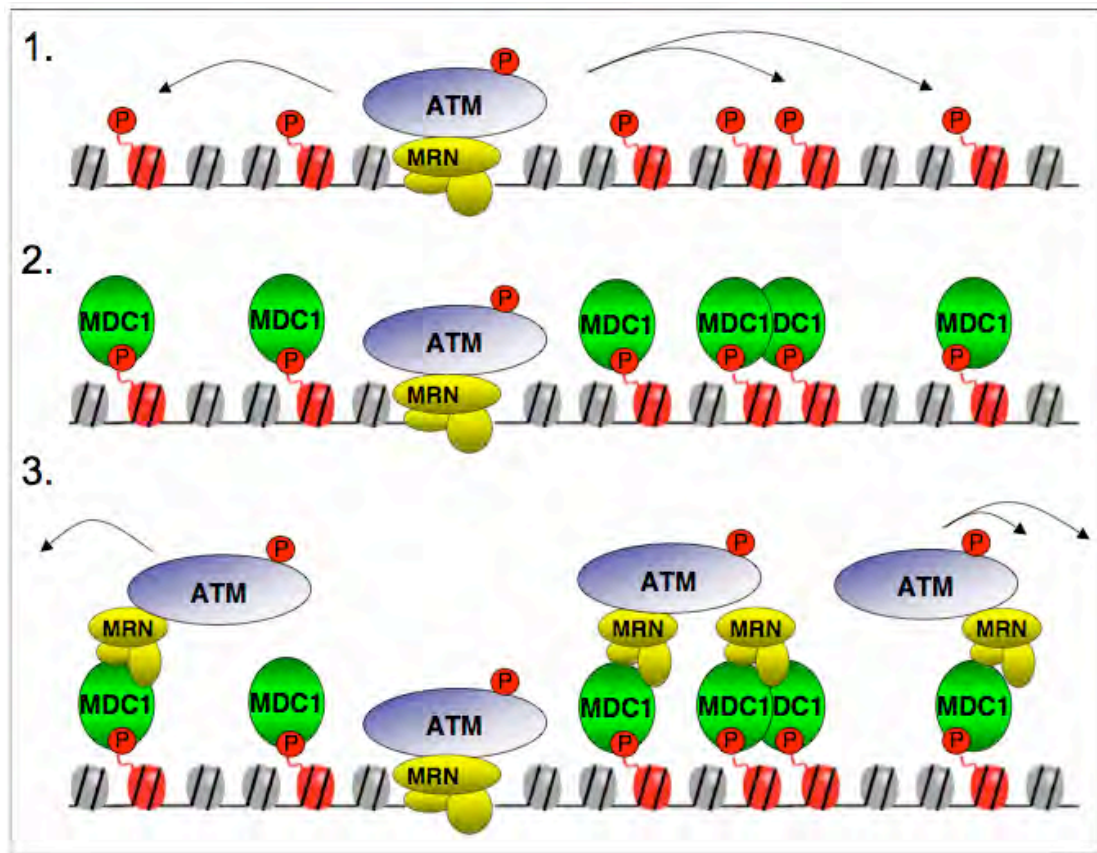


The schematic outline of ATM domain structure is shown. ATM is a 370 kDa phospho-protein, comprising 49 HEAT (Huntingtin, Elongation factor 3, A subunit of protein phosphatase 2A, and TOR1) repeats from the N-terminus to the C-terminus, up to amino acid 2661. The FAT, PIKK catalytic and FACT domains are located at the C-terminus and display strong sequence similarity.

The nuclear PIKKs, ATM, ATR and DNA-PK serve as serine/threonine kinases in response to DNA damage. ATM and DNA-PK are directly activated by induction of DNA DSBs. By contrast, ATR activation requires generation of ssDNA, which may occur during replication stress, at sites of replication fork stalling or as a consequence of processing of DNA DSB ends, where ssDNA-binding protein RPA coats resected DNA breaks. However, the mode of recruitment of these DNA damage-induced PIKKs to the sites of DNA insults is analogous. A C-terminal PIKK interaction motif on Nbs1, ATRIP and Ku80 is required for the recruitment to DSBs of ATM, ATR and DNA-PKcs, respectively, and, importantly, for PIKK-dependent activation of the DNA damage signalling cascade (Falck et al., 2005). This outlines the close relationship between these protein kinases and provides a regulatory mechanism to control their recruitment to damaged chromatin.

A prime PIKK target at sites of DNA damage is the histone H2A variant H2AX, whose derivative phosphorylated on serine 139 (S139) is referred to as  $\gamma$ H2AX. This post-translational modification on H2AX C-terminus tail spreads over many kilo-bases of DNA flanking the DSB site and leads to amplification of the DNA damage signal (Celeste et al., 2002; Celeste et al., 2003).  $\gamma$ H2AX is regarded as a hallmark of DSBs and can be cytologically visualized by fluorescent microscopy as discrete nuclear punctate ‘dots’, called IR-induced foci (IRIF; Rogakou et al., 1998). Phospho-S139 of  $\gamma$ H2AX acts as a docking site for the recruitment of the DDR-mediator protein MDC1. MDC1 binds H2AX phospho-epitope *via* its C-terminal tandem BRCT domain (Stucki et al., 2005), creating megabase-sized  $\gamma$ H2AX-MDC1 foci. MDC1 bound to  $\gamma$ H2AX on the chromatin flanking the DSB promotes phospho-dependent recruitment of MRN-ATM, inducing a positive feedback loop to amplify the DNA damage signalling cascade (Stucki and Jackson, 2004). Indeed, MDC1 has been shown to bind to the MRN complex and to be required for its focal enrichment to DSBs and propagation of the DDR signalling (Diagram 4; Goldberg et al., 2003; Stewart et al., 2003). It is noteworthy that, although MRN localizes to DSB sites earlier than MDC1 as a sensor complex, MRN enrichment to DSB-flanking DNA is mediated by interactions with MDC1. The dual role of MRN places the complex in two essential steps of the DDR: first, as a sensor of the damaged DNA, MRN promotes early recruitment of ATM to the immediate proximity of the break; and second, following an increase in the local concentration of activated ATM, H2AX phosphorylation and recruitment of MDC1, MRN acts as a mediator generating a landing platform for ATM, promoting ATM assembly at the DSB-flanking chromatin and amplifying the DNA damage signal.

**DIAGRAM 4. Signalling cascade amplification**



DNA damage signalling cascade is amplified to relay the signal to downstream effectors. MRN senses the DNA DSB and binds to the broken DNA ends. MRN-dependent recruitment of ATM leads to its activation by auto-phosphorylation and formation of  $\gamma$ H2AX (1). The ATM-dependent phosphorylation of H2AX recruits the (BRCT)<sub>2</sub> domains of MDC1 on the chromatin flanking the DSB site (2). MDC1 contributes to amplification of the signalling cascade by promoting recruitment of MRN-ATM and inducing a positive feedback loop to amplify the DNA damage signalling (3). 'P' indicates phosphorylation.

ATM targets a plethora of diverse substrates for phosphorylation in response to DSBs. ATM-mediated phosphorylation of MDC1 on 'TQXF' motifs is required for the subsequent recruitment of the RING-finger E3 ubiquitin ligase RNF8, *via* phospho-dependent binding through RNF8 FHA domain (Huen et al., 2007; Kolas et al., 2007; Mailand et al., 2007). Similarly to tandem BRCT domains, the FHA domain is a phospho-binding motif that regulates protein-protein interactions in an inducible manner in response to selected stimuli (Durocher et al., 1999). Several FHA- and BRCT-containing proteins

have been implicated in the DDR network, providing molecular interfaces for specific, and reversible, ligand binding. RNF8 produces DSB-associated ubiquitylations on histones H2A and H2AX, where a lysine side chain covalently binds to ubiquitin through an isopeptide linkage, creating a template for the recruitment of a second E3 ubiquitin ligase, RNF168, to DSB sites. RNF168 is retained to the DSB-flanking chromatin *via* its two UIMs (ubiquitin-interacting motifs). The ubiquitin-binding domains of RNF168 enable its focal accumulation on chromatin primed by RNF8-dependent ubiquitylation. In turn, similarly to RNF8, RNF168 interacts with the E2 conjugating enzyme Ubc13, and promotes additional ubiquitylation of damaged chromatin by catalyzing the formation of lysine 63-linked ubiquitin conjugates on H2A-type histones (Doil et al., 2009; Stewart et al., 2009). RNF8/RNF168-mediated ubiquitylation is postulated to impact on the chromatin arrangement surrounding the DSB, opening up the chromatin to allow recruitment of downstream factors, including the mediator protein 53BP1 (p53-binding protein 1) and another E3 ubiquitin ligase, BRCA1 (breast cancer protein 1). It is currently unclear whether the epistatic recruitment of the two RING-finger ubiquitin ligases RNF8 and RNF168 and subsequent chromatin remodelling events are mediated by broadening the spectrum of substrates targeted for ubiquitylation or increasing the local concentration to reach a critical threshold in the ubiquitylation gradient. Nevertheless, the amplification of ubiquitin conjugates at the DSB-flanking chromatin is pivotal for local changes in chromatin structure near DNA-break sites and represents a turning point in the DDR cascade that enables localization of downstream proteins and propagation of the DSB signal.

The aforementioned opening up of the chromatin is believed to allow the exposure of histone marks normally embedded into the globular domain of the nucleosome, such as

methyations on histone H4 lysine 20 (H4K20) and histone H3 lysine 79 (H3K79), which serve as docking sites for the 53BP1 tandem-Tudor domain to promote 53BP1 retention in IRIF (Huyen et al., 2004; Botuyan et al., 2006). Once at the site of damage, 53BP1 is phosphorylated by ATM in its N-terminal region and cooperates in the amplification of the DNA damage signalling pathway (Schultz et al., 2000; Anderson et al., 2001; Rappold et al., 2001). 53BP1 plays a role in the activation of the G2/M cell cycle arrest (DiTullio et al., 2002; Fernandez-Capetillo et al., 2002; Wang et al., 2002) and knock-down of 53BP1 results in genomic instability (Ward et al., 2003). In addition, novel evidence points to a role for 53BP1 in increasing chromatin mobility and bringing DNA ends into close proximity, facilitating repair of DSBs by NHEJ (reviewed in FitzGerald et al., 2009). 53BP1 is postulated to play a similar role in physiological processes such as class switch recombination and long-range V(D)J recombination (Manis et al., 2004; Ward et al., 2004; Difilippantonio et al., 2008). 53BP1 also contains two tandem BRCT motifs at its C-terminus. The BRCT domains of 53BP1 do not seem to be required for its recruitment to IRIF or for its repair function (Ward et al., 2006) and their significance in the context of the DDR is currently unclear.

## DIAGRAM 5. 53BP1 structural features and domains

**Content not visible due to copyright limitations**

53BP1 contains several PIKK consensus phosphorylation sites (S/TQ) in its N-terminus. *In vivo*, ATM has been shown to target both serines 25 and 29. Similarly to other DDR mediators, 53BP1 contains two tandem BRCT domains at its very C-terminus. In addition, 53BP1 contains a tandem Tudor domain that allows its recruitment to sites of damage as well as binding to the kinetochore during unperturbed mitosis. LC8 binding sites and two potential KEN (KENXXXN) motifs may represent sequences interacting with the APC.

Image by Adams and Carpenter, 2006

In addition to promoting 53BP1 recruitment, ubiquitylated templates enable Rap80-dependent targeting of BRCA1/BARD1, Abraxas and Brcc36 to sites of DNA damage (Wang and Elledge, 2007). BRCA1 thereby initiates further ubiquitylation events that facilitate DNA damage signalling and DSB repair. The striking feature of the sequential recruitment of three E3 ubiquitin ligases to the sites of DNA damage emphasizes the importance of post-translational modifications, such as ubiquitylation, in regulating chromatin structure and fine-tuning the assembly of numerous DDR factors to the DSB-flanking chromatin, to convey the DNA damage signal to the cell. In addition, recent data point to the coordination of ubiquitylation with SUMOylation events, where the attachment of small ubiquitin-related modifier (SUMO) to target proteins promotes the productive association of 53BP1, BRCA1 and RNF168 to DSB sites (Galanty et al., 2009; Morris et al., 2009).

The temporal differences in the recruitment dynamics of various DDR factors are reflected in their accumulation at damaged sites within the IRIF focal structures. In cells treated with DSB-inducing agents, IRIF can be visualized indirectly by performing immunostaining with specific antibodies, or directly by expressing fluorescently-tagged proteins (van

Veelen et al., 2005). Within seconds, DSBs can thus be detected as large nuclear aggregates containing MRN,  $\gamma$ H2AX, MDC1 and RNF8. The appearance of ubiquitin conjugates (stained by the FK2 antibody) and RNF168, as well as the assembly of 53BP1 and BRCA1 into nuclear foci can be detected seconds after binding of the aforementioned early DDR factors to the DSB compartments and, kinetically, represent a second wave of recruitment.

**DIAGRAM 6. The two-step DDR signalling cascade**



**Content not visible due to copyright limitations**

This diagram shows the *early wave* of chromatin assembly to follow a linear epistatic phosphorylation-driven cascade, initiated by ATM activation and H2AX phosphorylation, followed by the local accumulation of MDC1, MRN and RNF8 to the DSB-flanking chromatin. RNF8-regulated transition depends on ubiquitylation of H2A-type histones for the recruitment of RNF168 to the DSB. The RNF8/RNF168-mediated ubiquitin-dependent chromatin alterations render the local chromatin permissive for the assembly of DDR factors belonging to the *late wave* of recruitment, such as 53BP1 and BRCA1. Thus, the recruitment to sites of DNA damage of 53BP1 and BRCA1 can be envisaged as part of a second step in the DDR, subsequent to an RNF8-regulated transition.

Image by Mailand et al., 2007

DNA insults induce temporary halts of cellular proliferation at specific points during the cell cycle, providing time for the DNA damage repair machinery to mend the lesion before the cell resumes proliferation (Hartwell and Weinert, 1989). These so-called cell cycle checkpoints can occur at the G1/S boundary in order to prevent replication of damaged DNA, at the G2/M transition to avoid propagation of DNA lesions and unreplicated DNA to the progeny cells, and can act within S-phase to monitor and maximize high fidelity DNA replication. The proximal PIKK kinases ATM and ATR, together with other mediating factors, enable the recruitment and activation of the downstream checkpoint kinases. In mammalian cells, two checkpoint effector kinases have been identified: Chk1 and Chk2 (reviewed in Bartek and Lukas, 2003). Chk2 is mainly activated by ATM, a step involving Chk2 dimerization and *in trans* auto-phosphorylation, and functions to activate G1/S and intra-S-phase checkpoints. On the other hand, Chk1 is mainly subjected to ATR phosphorylation and plays a more prominent role in the G2/M checkpoint and in response to perturbed replication. Nevertheless, it is noteworthy that a certain degree of cross-talk, along with partial functional redundancy, exists between Chk1 and Chk2 (Bartek and Lukas, 2003). The activation of these checkpoint kinases is pivotal to channel the DDR signal to downstream targets, mediating arrest in the cell cycle, as well as a variety of nuclear and cellular responses, including transcriptional modulation. On the other hand, a permanent DNA damage signal, as emanated from an unreparable lesion, may activate cellular phenomena like apoptosis or senescence (Jackson and Bartek, 2009).

### ***1.3.II Maintaining genome integrity during DNA replication: DNA damage in S-phase***

DNA replication is undoubtedly one of the most fascinating processes in biology. In human cells, the 3.4 billion base pairs of the haploid genome are faithfully duplicated to ensure error-free transmission of the genetic information to the next generation. During eukaryotic replication, several mechanisms of surveillance exist that monitor replication fork initiation, progression, fidelity, termination and continuation into G2 and mitosis upon completion of DNA replication. The inherently fragile nature of the DNA and its handling by the replication fork may represent sources of mutational damage that impact both on cellular and organismal survival. The concerted effort of S-phase checkpoint pathways normally ensures preservation of genome stability during DNA synthesis. Three types of S-phase checkpoints exist depending on their triggering stimuli. First, the replication checkpoint is initiated in response to stalling of replication forks due to alteration in the DNA structure, deoxyribonucleoside triphosphates (dNTPs) depletion or torsional stress caused by fork-to-fork or fork-to-transcription complex collision. Second, the intra-S-phase checkpoint is activated any time during S-phase when DNA damage is generated, even at a distance from the replicons. ATR plays a major role in activating the replication checkpoint, which depends on the replication fork. On the other hand, the intra-S-phase checkpoint is primarily signalled by ATM kinase (reviewed in Bartek et al., 2004). Finally, the existence and molecular nature of the checkpoint that prevents mitotic entry until DNA synthesis is completed is still under debate. In human cells, Cdc6 has been suggested to monitor completion of DNA replication before entry into mitosis (Clay-Farrace et al., 2003).

Replication forks can stall upon encountering protein-DNA complexes or due to depletion of the nucleotide pools. These pause sites, where a barrier in replication fork progression is met, can become fragile sites in the genome (Casper et al., 2002), highly susceptible to breakage and recombination. Additionally, unusual or highly repetitive DNA sequences may create DNA secondary structure that induce replication slow zones, which are also highly prone to chromosome fragility (for review, see Labib and Hodgson, 2007). Progression of the replication fork through these regions is slowed down and paused by the replisome components Mrc1 and Tof1 (orthologues of vertebrate Claspin and Timeless, respectively). Mrc1 and Tof1 are involved in modulating the pace of DNA synthesis in unperturbed circumstances and are especially important during replication of expanded triplet nucleotide repeats (Shishkin et al., 2009; Voineagu et al., 2009). To prevent fork collapsing, leading to formation of a highly cytotoxic DNA DSBs, stalled forks are maintained stable by activation of the replication checkpoint. Central to this response are ATM and ATR. In yeast, these are Mec1 and Tel1 (*S. cerevisiae*) or Rad3 and Tel1 (*Schizosaccharomyces pombe*). While ATM responds mostly to DSBs to prevent recombination events at the replication forks, ATR acts at stalled replication forks, where the presence of ssDNA-binding protein RPA mediates ATR stabilization (Zou and Elledge, 2003). Also, RPA serves as a recruiting platform for the checkpoint clamp loader Rad17, which, in turn, recruits the PCNA-like checkpoint complex 9-1-1 (Rad9-Rad1-Hus1). Phosphorylation of the 9-1-1 complex by ATR serves to amplify the checkpoint signal and relay it to the transducer kinases Chk1 and Chk2. These factors trigger a global checkpoint response throughout the nucleus by targeting substrates for phosphorylation, preventing the firing of late replication origins and entry into mitosis (see review by Branzei and Foiani, 2010). Furthermore, the checkpoint kinases act to further promote fork stability and preventing replication fork demise (Donaldson and Blow, 2001). In budding yeast,

Mec1/ATR and Rad53/Chk2 are also required to prevent fork collapse and replisome disassembly from the stalled forks. Finally, the replication checkpoint signals for replication fork restart and is directly involved in controlling the process of replication resumption (Kai and Wang, 2003; Liberi et al., 2005; Sabbioneda et al., 2005; Lopes et al., 2006).

The action of unwinding DNA ahead of the replication fork induces torsional stress that manifests itself as positive supercoils in front of the fork or precatenates between the replicated duplexes, resolved by Top1 and Top2 topoisomerases, respectively (reviewed in Wang, 2002). Additional topological strains are exerted when the replication fork meets the transcription machinery. The proximity between two replication bubbles increases topological stress and slows down fork progression. In this case, Top1 releases the positive supercoils (Tuduri et al., 2009), while Top2 seems to be involved in the formation of chromatin loops to protect the transcription apparatus during DNA replication (Bermejo et al., 2009). The collisions between the transactions of replication and transcription can be head-on or in-line (Cook, 1999). The latter, co-directional collision occurs when the fork at the leading strand makes contact with the rear of the RNA polymerase; although replication is slowed down, the fork does not collapse, as the mRNA transcript can be used as a primer to resume DNA synthesis (Pomerantz and O'Donnell, 2008). On the other hand, a head-on collision represents the opposite scenario, when the front of the RNA polymerase collides with the fork at the lagging strand. Head-on collisions can cause fork collapse, leading to DSBs and transcription-associated recombination that may cause genomic instability (Olavarrieta et al., 2002).

In addition to intrinsic barriers to replication fork progression, the replisome can encounter sites of DNA damage arising from endogenously-occurring or exogenously-induced DNA-damage. Such lesions include bulky lesions, such as UV photoproducts, covalent DNA crosslinks and DSBs. These DNA insults can be produced at DNA loci outside the active replicon and can be met by the fork during elongation. When encountering DNA damage, the semi-discontinuous DNA replication becomes discontinuous on both strands. The formation of new primers allows the replication fork to leave a gap on both strands where the DNA is damaged and progress, leaving the lesion behind the fork. The damage is then dealt with by two DNA damage tolerance pathways, translesion synthesis (TLS) polymerases or the template switch pathway characterized by HR repair (for a comprehensive review, see Kogoma, 1997). More complex lesions, like inter-strand cross-links, are repaired by a concerted effort of three pathways: the Fanconi anemia, HR and TLS polymerase pathways (Niedzwiedz et al., 2004). In S-phase, DSBs may also arise as a consequence of replication fork collapse, when the entire replisome becomes dissociated from the fork or, perhaps, physiologically as a consequence of topological strain. Formation of DSBs during S-phase activates the ATM/ATR-dependent intra-S-phase checkpoint, which leads to the unfolding of the DDR signalling cascade, activation of Chk1 and Chk2 kinases, and cell cycle delay (Chapter 1.3.I). In addition, ATM- and ATR-dependent inhibition of Cdk2/Cyclin E and Cdc7/Dbf4 S-phase kinases induces silencing of late replication origins (Santocanale and Diffley, 1998). This appears to be at least in part mediated by ATM-dependent inhibitory phosphorylation on Cdk2 preventing loading of Cdc45 and firing of new origins (Costanzo et al., 2000). Additionally, the ATM-dependent checkpoint pathway acts together with the nuclease Sae2 and Mre11 to prevent formation of cruciform DNA structures when the elongating forks encounters an unrepaired DSB (Doksani et al., 2009). Although the fork encountering the break is

irreversibly dismantled, the other forks within the replicon can continue replication (Branzei and Foiani, 2010).

Interestingly, the responses activated by DSBs during replication are also involved in monitoring timing of DNA synthesis and origin firing in the absence of DNA damage. Novel data in *Xenopus* extracts suggests that ATM and ATR regulate inhibition of Cdk2 and Cdc7 S-phase kinases through a negative feedback loop to physiologically inhibit origin firing following initiation of replication in unchallenged conditions (Shechter et al., 2004).

#### **1.4 DNA, chromatin, chromosomes: organization of the genetic information**

The processes of DNA replication, DNA repair, transcription and other long-range DNA transactions in the nucleus are coupled with genome-wide disruption and reorganization of chromatin. In all eukaryotic cells, DNA is tightly compacted into a hierarchically organized structure called chromatin. The basic unit of chromatin is the nucleosome. The nucleosome core particle consists of 146 base pairs of DNA wrapped around an octamer of two each of the histones H2A, H2B, H3, H4. The resulting structure is a 10 nm chromatin fibre often referred to as ‘beads-on-a-string’ (Kornberg, 1974). A more compact and repressive higher order chromatin structure is known as the 30 nm fibre, which is achieved through recruitment of the linker histone H1 or “architectural” chromatin-associated factors such as heterochromatin protein 1 (HP1). The exact organization of the 30 nm fibre is under considerable debate. In general, either “solenoid” models, wherein the nucleosomes are gradually coiled around a central axis, or more open “zig-zag” models

that adopt higher-order self-assemblies, have been described (Allis et al., 2007). Recent evidence, including X-ray structures using model systems involving four nucleosomes point towards a fibre arrangement more consistent with a zig-zag arrangement (Khorasanizadeh, 2004). Organization into higher order chromatin domains (300-700 nm) also occurs, although the extent to which these associations give rise to meaningful functional “chromosome territories” remains unclear (Allis et al., 2007).

**DIAGRAM 7. From DNA to chromatin to chromosomes through multiple compaction steps**



**Content not visible due to copyright limitations**

DNA undergoes several levels of compaction to be packaged inside the 0.1  $\mu\text{m}$  of the human nucleus; the DNA double helix-core histones complex is tightly packed into chromatin fibres. Chromatin is coiled into higher-order structures, up to being compacted into a typical metaphase chromosome.

Image modified from [micro.magnet.fsu.edu/cells/nucleus/chromatin.html](http://micro.magnet.fsu.edu/cells/nucleus/chromatin.html)

Higher order structures of chromatin have historically been defined as either euchromatic or heterochromatic, based on the nuclear staining pattern of dyes used to visualize DNA in cells. Euchromatin is decondensed chromatin and may be transcriptionally active or inactive, whereas heterochromatin is generally defined as highly compacted and silenced

chromatin. It may exist as permanently silent chromatin (constitutive heterochromatin) or repressed (facultative heterochromatin) in some cells, during a specific cell cycle or developmental stage (Allis et al., 2007).

#### ***1.4.1 The impact of chromatin environment over DDR and repair***

Higher-order chromatin structure may hinder accessibility of proteins to the DNA. In numerous nuclear processes, including replication, transcription and DNA repair, it is essential for their respective molecular machineries to be able to rapidly access individual regions of the genome. Although transactions on the DNA helix require more than simply increased accessibility to the DNA, modulation of the chromatin template is a critical step in all these processes. The inherent flexibility of chromatin and the dynamic nature of the nucleosome allow modulation of the steric hindrance between core histones and DNA, improving accessibility.

Covalent post-translational modifications (PTMs) impact on chromatin organization in an antithetic manner, to promote or hinder accessibility to DNA. PTMs include reversible chemical modification of histones and may be removed, subsequently re-establishing the original chromatin environment. Numerous enzymatic regulatory complexes are responsible for a wide range of PTMs, including acetylation, methylation, phosphorylation, SUMOylation and ubiquitylation (Kouzarides, 2007). Any single core histone can accommodate distinct PTMs in a large number of combinations. The combinatorial pattern of PTMs and its functional outcome is at the centre of the histone code hypothesis (Strahl and Allis, 2000), where an epigenetic marking system functions to regulate '*chromatin-templated processes, with far reaching consequences for cell fate decisions*' (Jenuwein and

Allis, 2001). In addition, cross-talk between the distinct modifications adds yet another layer of complexity in deciphering the histone codes in physiological and pathological contexts. Often, priming PTMs are required to allow further modifications to take place, regulating functional outcome in an epistatic manner. For instance, cell cycle dependent phosphorylations of Chk2 by Plk3 on sites adjacent to the ATM-target residue threonine 68 (T68) primes DNA damage-dependent phosphorylation, facilitating Chk2 activation (Bahassi et al., 2006). Epigenomes can be encoded by combinations of PTMs that act not only on histones but also on non-histone proteins.

DNA damage repair is a DNA-dependent activity that has to overcome the chromatin accessibility barrier. A paradigmatic example of PTMs occurring following the induction of a DSB is the phosphorylation of the histone variant, H2AX.  $\gamma$ H2AX accumulates at sites of DSBs and extends up to a megabase of DNA flanking the DSB, generating domains visible *via* fluorescent microscopy within minutes post-IR and may persist for several hours (Rogakou et al., 1998), playing a role in the amplification of the DDR signalling cascade. Although the exact significance of this chromatin modification upon DSB formation is still unknown, functional studies revealed that cells lacking  $\gamma$ H2AX repair damage more slowly and display gross chromosomal rearrangements than control cells, indicating a role for  $\gamma$ H2AX in maintenance of genomic stability (Celeste et al., 2002). Furthermore, core histones in the proximity of the break are subjected to extensive modifications by E3 ubiquitin ligases that increase the local concentration of ubiquitin, impacting on chromatin conformation. The joined effort of RNF8 and RNF168 at the chromatin flanking the DSB site surpasses the threshold of ubiquitylation required to enable opening of the chromatin and recruitment of downstream mediators, like 53BP1 and BRCA1. The timely recruitment of these E3 ubiquitin ligases to the break site serves to alter

chromatin-binding requirements in a way to tailor the protein recruitment dynamics, offering a multilayered spatio-temporal regulation through promoting chromatin remodelling events.

As aforementioned, DSB-induced PTMs play a key role in local restructuring of chromatin to enable access of the DDR machinery and repair of the lesion. PTMs can promote physical changes in histone distribution, including displacement, exchange, sliding and re-assembly of the nucleosome. Penny Jeggo's laboratory has recently provided several lines of evidence indicating that DSBs associated with heterochromatic regions are particularly reliant on ATM signalling to induce remodelling of dense chromatin regions and provide accessibility to the DNA break, ultimately enabling its repair (Goodarzi et al., 2008). Therefore, the status of chromatin directly impacts on propagation of DNA damage signals and on the physical mending of the DNA insult. Conversely, it is tempting to speculate that chromatin plasticity facilitates genomic surveillance. This notion is strengthened by data from Oscar Fernandez-Capetillo and colleagues, which engineered a murine stem cell system expressing reduced levels of the linker histone H1. The linker histone H1 enables compaction of the nucleosomal array into tightly packaged chromatin fibres; thus, cells expressing 50% the physiological level of H1, displayed a more open chromatin configuration. The increased plasticity of chromatin directly correlated to a hyper-responsiveness to DSBs, displaying enhanced DDR signalling and hyper-activated checkpoint. The cells were hyper-resistant to DNA damaging agents and showed faster repair kinetics than control cells. These phenotypical changes were recapitulated by using TSA (trichostatin A), a HDACi (histone de-acetylase inhibitor) that induces chromatin relaxation. This work complements previous work showing that deletion of *S. cerevisiae* linker histone Hho1 leads to a hyper-HR phenotype (Downs et al., 2003). These and other

experimental data substantiate the existence of a profound cross-talk between regulation of chromatin conformations by PTMs and unfolding of the DDR, and are especially relevant in view of DSBs being reported to trigger DDR-dependent global relaxation processes (Ziv et al., 2006; Goodarzi et al., 2009). Such global relaxation of chromatin could facilitate responses to DNA breaks by enabling faster access of DDR factors to the DSB sites to facilitate genomic surveillance and repair. An intriguing scenario recently presented is the ‘breathing’ chromatin status typical of pluripotent stem cells. Transcriptional up-regulation of chromatin remodellers, such as Chd1 (Gaspar-Maia et al., 2009), increases openness of chromatin. In parallel, stem cells are characterized by faster dynamics in their DDR than other cells, together with accelerated and high fidelity repair of DSBs by preferentially using HR. Such findings also suggest that chromatin conformation acts as a switch to select between repair pathways. A more rigid and compacted DNA conformation may hinder resection of DSBs and recruitment of HR promoting factors, such as BRCA1, leading to NHEJ repair. On the other hand, a more open chromatin status may favour resection of DNA and enables HR.

Recently, Evi Soutoglou and Tom Misteli (2008) engineered a novel way to trigger a complete DDR cascade in the absence of DNA damage. In their system, immobilization of DDR factors on chromatin was sufficient to onset a typical DDR response, leading to checkpoint activation. They monitored the outcome of the stable tethering of factors including Nbs1, Mre11, MDC1 and ATM to DNA, which caused phosphorylation of  $\gamma$ H2AX and activation of the full physiological downstream cascade. This phenomenon was ATM and DNA-PK dependent (Soutoglou and Misteli, 2008). This work emphasizes the importance of the association between molecules and chromatin in the activation, amplification and maintenance of the DNA damage response.

#### **1.4.II      *Work presented in this thesis***

The maintenance of genomic integrity is of critical importance to living organisms, because DNA contains the genetic instructions essential for life. Cells are endowed with remarkably complex pathways that help repair the damage to protect genomic stability.

In this thesis, I explore how DNA damage responses change depending on the cell cycle stage and examine the cross-talk between the cell cycle machinery and the DNA damage response network. In chapter 3, I uncover the signalling cascade in response to DNA damage during mitosis in human cells, outline the complex inter-relationship between DDR and chromatin structural and epigenetic statuses, and show that the mitosis-specific DDR is biologically important for cell viability. In chapter 4, I analyze the role of Psf1, a subunit of the GINS complex, in human and yeast cells; I also characterize a consensus DNA damage phospho-motif at the C-terminus of the protein, which is important for cell viability in budding yeast. Finally, chapter 5 includes the analysis of *S. cerevisiae* Rad9 regulation by CDK and how this impacts on the activation of the checkpoint kinase Chk1.

The results presented here underlie the complex relationship between cellular pathways required for genomic stability and those needed for cell cycle progression, and furthermore suggests that additional, as yet, undiscovered mechanisms work to influence, regulate and coordinate these molecular networks to promote cellular homeostasis.



## MATERIALS AND METHODS

---

## 2 MATERIALS AND METHODS

### 2.1 Sources for chemicals, buffers and solutions

All chemicals were purchased from Sigma Aldrich, Acros Organics or Fisher Scientific. Radiochemicals were from Amersham Biosciences. Restriction enzymes and modifying enzymes were purchased from Roche or New England Biolabs. Stock solutions, buffers for molecular biology, buffers and solution for SDS-PAGE or other biochemical techniques were prepared as described in Sambrook et al., (1989), unless otherwise stated.

### 2.2 Antibodies

The antibodies listed in Table 1 were used in this thesis for immunoblotting (IB; chapter 2.6.V), immunofluorescence (IF; chapter 2.7.I) and/or immunoprecipitation (IP; 2.6.VI).

**TABLE 1. Antibodies**

<b>Antigen</b>	<b>Species</b>	<b>Reference/Supplier</b>	<b>Dilution</b>
53BP1	Rabbit	Novus Biologicals	IF 1:500 /IB 1:1000
53BP1 pS25	Rabbit	Bethyl	IB 1:1000
$\alpha$ -tubulin	Mouse	Sigma	IF 1:500/IB 1:1000
$\beta$ -actin	Mouse	Abcam	IB 1:5000
$\gamma$ H2AX	Mouse	Upstate	IF 1:1000/IB 1:1000
$\gamma$ H2AX	Rabbit	Cell Signalling	IF 1:250
ATM	Rabbit	Calbiochem/Merck	IP 2 $\mu$ g/IB 1:100
ATM pS1981	Mouse	Cell Signalling	IB 1:1000
BRCA1 (D20)	Rabbit	Santa Cruz	IF 1:250/IB 1:1000

Table 1, cont'd...

Antigen	Species	Reference/Supplier	Dilution
CENP-F	Rabbit	Abcam	IF 1:500
Chk1	Mouse	Santa Cruz	IB 1:1000
Chk1 pS345	Rabbit	Cell Signalling	IB 1:1000
Chk2	Rabbit	Abcam	IB 1:1000
Chk2 pT68	Rabbit	Cell Signalling	IB 1:1000
DDB1	Goat	Abcam	IB 1:1000
DDB2	Rabbit	(El-Mahdy et al., 2006)	IB 1:1000
DNA-PKcs pT2609	Rabbit	Abcam	IB 1:1000
FLAG (M2)	Mouse	Sigma	IP 2 µg/IB 1:1000
GST	Mouse	Santa Cruz	IB 1:1000
H2A acidic patch	Rabbit	Upstate	IB 1:1000
H2AX	Rabbit	Abcam	IB 1:5000
H3 pS10	Mouse	Abcam	IF 1:500/IB 1:2000
H3K79me2	Rabbit	Abcam	IB 1:1000
H4	Mouse	Abcam	IB 1:2000
H4K20me2	Rat	Abcam	IB 1:1000
HA	Mouse	Covance	IP 2 µg/IB 1:2000
KAP1	Rabbit	Santa Cruz	IB 1:1000
KAP1 pS824	Rabbit	Bethyl	IB 1:125
scMCM2 (y-N19)	Goat	Insight Biotechnology	IP 2 µg/IB 1:500
MCM7 (141.2)	Mouse	Santa Cruz	IB 1:500
MCPH1	Rabbit	Bethyl	IB 1:1000
MDC1	Rabbit	(Goldberg et al., 2003)	IB 1:5000
MDC1 pS329pT331	Rabbit	(Chapman and Jackson, 2008)	IF 1:250
MRE11 (12D7)	Mouse	Genetex/Abcam	IB 1:1000
NBS1 (1D3)	Mouse	Genetex/Abcam	IB 1:1000
scPGK1	Mouse	Invitrogen	IB 1:1000
PSF1	Rabbit	Steve Bell	IF 1:200/IB 1:1000
PSF1 pS173	Rabbit	This study; Eurogenetec	IB 1:500
PSF2	Rabbit	Steve Bell	IB 1:500
scRad9	Rabbit	Noel Lowndes	IB 1:10000
RAD50 (13B3)	Mouse	Genetex/Abcam	IB 1:2000
scRad53	Rabbit	Noel Lowndes	IB 1:5000
RPA (RPA2/34)	Mouse	Lab vision	IB 1:2500
RNF168	Rabbit	(Stewart et al., 2009)	IB 1:1000
RNF8	Rabbit	(Tuttle et al., 2007)	IB 1:1000
SLD5	Rabbit	Steve Bell	IB 1:500
SMC1	Rabbit	Bethyl	IB 1:10000
SMC1 pS966	Rabbit	Bethyl	IB 1:5000
TopBP1	Rabbit	Abcam	IB 1:1000
Ub-H2A	Mouse	Upstate	IB 1:1000
Ub-conjugated (FK2)	Mouse	BIOMOL	IF 1:250

All antibodies are raised against human proteins, unless denoted by the prefix 'sc' (*S. cerevisiae*).

## 2.3 Plasmids

Plasmids used in this study are shown in Table 2.

**TABLE 2. Plasmid constructs**

#	Plasmid	Source	Description
1	pcDNA 3.1	Addgene	Mammalian expression vector
2	Psf1-2HA	This study	hPsf1 N-terminally double-HA-tagged cloned <i>XhoI/BamHI</i> into pcDNA 3.1
3	Psf1-2HA-A	This study	hPsf1 S173A in pcDNA 3.1 (#2 derived)
4	Psf1-2HA-E	This study	hPsf1 S173E in pcDNA 3.1 (#2 derived)
5	pGEX-4T.3	GE Healthcare	Bacterial expression vector
6	Psf1-GST	This study	hPsf1 cloned <i>XhoI/BamHI</i> into pGEX-4T.3
7	Psf1-GST-A	This study	hPsf1 S173A in pGEX-4T.3 (#6 derived)
8	Psf1-GST-E	This study	hPsf1 S173E in pGEX-4T.3 (#6 derived)
9	pRS413	Stratagene	Yeast shuttle vector containing a CEN/ARS replication system and <i>HIS3</i> marker gene
10	pRS416	Stratagene	Yeast shuttle vector containing a CEN/ARS replication system and <i>URA3</i> marker gene
11	Psf1-3HA ( <i>URA3</i> )	This study	scPsf1 N-terminally triple-HA-tagged cloned <i>XhoI/EcoRI</i> into pRS413
12	Psf1-3HA ( <i>HIS3</i> )	This study	scPsf1 N-terminally triple-HA-tagged cloned <i>XhoI/EcoRI</i> into pRS416
13	Psf1-3HA-A	This study	scPsf1 S187A in pRS413 (#12 derived)
14	Psf1-3HA-E	This study	scPsf1 S187E in pRS413 (#12 derived)
15	pRS414	Stratagene	Yeast shuttle vector containing a CEN/ARS replication system and <i>TRP1</i> marker gene
16	Rad9-3HA	A. Hammet	scRad N-terminally triple-HA-tagged cloned into pRS414
17	Rad9-3HA-1	This study	scRad9 S83A in pRS414 (#16 derived)
18	Rad9-3HA-2	This study	scRad9 T110A in pRS414 (#16 derived)
19	Rad9-3HA-3	This study	scRad9 T125A in pRS414 (#16 derived)
20	Rad9-3HA-4	This study	scRad9 T143A in pRS414 (#16 derived)
21	Rad9-3HA-4M	This study	scRad9 S83A, T110A, T125A, T143A in pRS414 (#16 derived)
22	Rad9-3HA-5M	This study	scRad9 S56A, S83A, T110A, T125A, T143A in pRS414 (#16 derived)
23	Rad9	This study	scRad9 cloned <i>XhoI/EcoRI</i> into pRS414 with 1.2 kb promoter and 1 kb terminator
24	Rad9-1	This study	scRad9 S83A in pRS414 (#23 derived)
25	Rad9-2	This study	scRad9 T110A in pRS414 (#23 derived)
26	Rad9-3	This study	scRad9 T125A in pRS414 (#23 derived)
27	Rad9-4	This study	scRad9 T143A in pRS414 (#23 derived)

Table 2, cont'd...

#	Plasmid	Source	Description
28	Rad9-4M	This study	scRad9 S83A, T110A, T125A, T143A in pRS414 (#23 derived)
29	Rad9-5M	This study	scRad9 S56, S83A, T110A, T125A, T143A in pRS414 (#23 derived)
30	Rad9 N-term-GST	This study	scRad9 1-498 bp N-terminus fragment cloned <i>XhoI/EcoRI</i> in pGEX-4T.3
31	MCPH1 N-term-GST	This study	hMCPH1 1-756 bp N-terminus fragment cloned in pGEX-4T.1
32	Rad9hMCPH1 hybrid	This study	hMCPH1 N-terminus (1-609) and scRad9 (435-end) in pCR® Blunt II TOPO® vector
33	Rad9ggMCPH1 hybrid	This study	ggMCPH1 N-terminus (1-557) and scRad9 (435-end) in pCR® Blunt II TOPO® vector

## 2.4 Synthetic peptides

Biotinylated synthetic peptides used for pull-downs experiments in this study (Table 3). All peptides were synthesized by Pepceuticals (Bristol, UK), except for the H2AX and  $\gamma$ H2AX peptides made by Graham Bloomberg (Department of Biochemistry, University of Bristol, UK).

TABLE 3. Synthetic peptides

Name	Synthetic peptide
H2AX	Biotin-SGS-ATVGP KAPSGGKKATQASQEY-COOH
$\gamma$ H2AX (pSer139)	Biotin-SGS-ATVGP KAPSGGKKATQA(pS)QEY-COOH
MDC1	Biotin-SGS-AVQSM EDEPTQAFML-NH <sub>2</sub>
MDC1 (pT719)	Biotin-SGS-AVQSM EDEP(pT)QAFML-NH <sub>2</sub>
Psf1	Biotin-SGS-GTSCVLLKKN SQHFLPR-NH <sub>2</sub>
Psf1 (pS173)	Biotin-SGS-GTSCVLLKKN(pS)QHFLPR-NH <sub>2</sub>
Psf1 (pS173, F176A)	Biotin-SGS-GTSCVLLKKN(pS)QHALPR-NH <sub>2</sub>
Psf2	Biotin-SGS-YKLRTNLQPLESTQSQDF-COOH
Psf2 (pS182)	Biotin-SGS-YKLRTNLQPLESTQ(pS)QDF-COOH

SGS indicates a serine-glycine-serine flexible linker; (pS) denotes the phosphorylated residue.

## **2.5 Nucleic acid methods**

### **2.5.I Quantitation**

Nucleic acids were quantified by spectrophotometry using a NanoDrop ND-1000 Spectrophotometer (Labtech International) and measured at OD<sub>260nm</sub>. Concentrations were calculated using the following formula: 1 OD<sub>260nm</sub> = 37 ng/μl.

### **2.5.II Polymerase Chain Reaction (PCR)**

PCRs contained 100 ng template DNA, 5 μl 10x reaction buffer without MgCl<sub>2</sub>, 1.5 mM MgCl<sub>2</sub>, 1 mM dATP, 1 mM dCTP, 1 mM dGTP, 1 mM dTTP, 500 nM of each primer and 3 units (U) polymerase and H<sub>2</sub>O to 50 μl final volume. Expand High Fidelity PCR System (Roche) was used. Reactions were performed in a Dyad Peltier thermal cycler according to the standard conditions: 94°C, 2 min (1 cycle); 94°C, 1 min; primer dependent annealing temperature, 1 min; 72°C, 1.2 min per kb amplification of predicted product (30 cycles); 72°C, 10 min final elongation.

### **2.5.III Site directed mutagenesis**

Site directed mutagenesis was performed according to the QuickChange site directed mutagenesis procedure (Stratagene) but with a maximum of 10 complementary bases between the oligonucleotide primers. Oligonucleotides harbouring the respective altered bases were ordered from Sigma Aldrich. The PCR reaction mixture was amplified using the following standard conditions: 94°C, 30 sec (one cycle); 94°C, 1 min; 52°C 1 min; 68°C, 1 min per 1 kb plasmid (16 cycles). 10 U *DpnI* was added to the mixture and the

reaction incubated for 1 hour at 37°C. XL-1 Blue or TOP10 chemically competent *E. coli* bacterial cells were then transformed with 5 µl of the digestion (Chapter 2.9.I).

#### **2.5.IV    *Agarose gel electrophoresis and DNA purification***

DNA was electrophoresed in a 0.8%-1.0% agarose gel, made in 1x TBE (89 mM Tris-borate, 2 mM EDTA) containing 1 µg/ml ethidium bromide, using an agarose gel apparatus. Samples were diluted in 6x loading buffer (25% glycerol, 0.125% w/v bromophenol blue, 0.125% w/v xylene cyanol). DNA was visualised by UV illumination. DNA was extracted from agarose gels using the Qiaquick gel extraction kit (Qiagen) according to the manufacturer's instructions.

#### **2.5.V     *Restriction digestion analysis***

PCR products and plasmid DNA were digested in a total volume of 25 µl containing 5 U of each restriction enzyme (Roche or New England Biolabs) and 2.5 µl of 10x incubation buffer supplied by the manufacturer and incubated at 37°C for 1 hour. Vector DNA was purified by agarose gel electrophoresis followed by extraction with the Qiaquick gel extraction kit (Qiagen).

#### **2.5.VI    *DNA ligation***

Gel purified and digested PCR products were mixed with target digested and dephosphorylated vector DNA at a molecular ratio of 5:1. 2x ligation buffer and 1 U of T4 rapid DNA ligase (Roche) were added and reactions incubated for 60 min at room temperature (RT).

### ***2.5.VII DNA sequencing and sequence analysis***

DNA sequencing reactions were performed by John Lester in the DNA sequencing facility of the Department of Biochemistry, University of Cambridge, UK. Computational analysis of the chromatographic data was performed by using Sequencer (Gene Codes Corporation) and DNA Strider (CEA, France). All plasmid constructs used or constructed for the work in this thesis were confirmed by sequencing analysis.

## **2.6 Analytical biochemistry and protein methods**

### ***2.6.I Measurement of protein concentration***

The concentration of proteins present in extracts was determined by the BioRad protein assay. Typically, 1  $\mu$ l of extract was added to 1 ml of a 5x dilution of BioRad protein assay dye reagent. To determine the protein concentration, the absorption at a wavelength of 595 nm was determined with a Pharmacia Ultraspec 2100 spectrophotometer.

### ***2.6.II SDS-PAGE***

Protein electrophoresis was by using sodium dodecyl sulphate polyacrylamide gel electrophoresis (SDS-PAGE) and the BioRad Mini-Protean II or Criterion midi-gel apparatus. Standard recipes for stacking and separating gels were used (Sambrook et al., 1989) and were polymerized by addition of 0.1% ammonium persulphate (APS) and 0.1% TEMED. All samples/extracts were diluted in 2x SDS sample buffer (100 mM Tris-HCl pH 6.8, 20% glycerol, 4% SDS, 715 mM  $\beta$ -Mercaptoethanol, 0.2% w/v bromophenol blue) and denatured by incubation at 95°C for 5 min immediately before loading.

Electrophoresis was at 90-180V in 1x protein running buffer (25 mM Tris-base, 190 mM glycine, 0.1% SDS) until SeeBlue (Invitrogen) and Precision Plus Dual Color (BioRad) protein standard markers migrated at the appropriate position on the separating gel.

### ***2.6.III Coomassie staining***

The SDS-PAGE gel was incubated with Coomassie blue staining solution (0.25% w/v Coomassie brilliant blue R250, 10% isopropanol, 10% acetic acid) for at least 1 hour at RT. The staining solution was removed and destaining solution (5% acetic acid) was added in repeated 30 min washes until the non-protein background staining was removed.

### ***2.6.IV Silver staining***

The SDS-PAGE gel was fixed in a solution of 50% methanol, 12% acetic acid, 0.5 ml/l formaldehyde (37%) overnight. After two 30 min washes in 50% methanol, the gel was incubated 1 min with 0.2 g/l sodium thiosulphate ( $\text{Na}_2\text{S}_2\text{O}_3$ ) solution, followed by three 30 sec washing steps in double distilled water ( $\text{ddH}_2\text{O}$ ). The gel was incubated in silver solution (2 g/l  $\text{AgNO}_3$ , 0.75 ml/l 37% formaldehyde) for 40 min at 4°C. After two 30 sec washes, the gel was developed in staining solution (60 g/l sodium carbonate, 4 mg/ml sodium thiosulphate and 0.5 ml/l 37% formaldehyde) for 1-15 min. The reaction was stopped by incubation in 1% glacial acetic acid. Careful handling using sterile plastic-ware was used to avoid contamination with keratins throughout this procedure.

### ***2.6.V Protein transfer and western blotting***

Proteins from SDS-PAGE were transferred onto nitrocellulose membrane (Protran BA85, Schleicher & Schuell) in transfer buffer (25 mM Tris-base, 190 mM glycine, 20%

methanol) for 70-90 min at 300 mA by the Mini-Protean 2 apparatus (BioRad). Transfer efficiency and sample loading were confirmed using Ponceau protein stain (0.2% w/v Ponceau S, 3% w/v TCA, 3% w/v 5-sulphosalicylic acid). Ponceau staining was removed by washing with Tris buffered saline (pH 7.5) containing 0.1% Tween 20 (TBS-T) before western blotting. The membrane was blocked in TBS-T supplemented with 5% w/v non-fat dried milk or 3% w/v bovine serum albumin (BSA) for 30-60 min. The membrane was then incubated for 1 hour at RT or overnight at 4°C in primary antibody (Table 1; IB) diluted in the desired blocking solution. The membrane was washed three times for 15 min with TBS-T and incubated with secondary antibody (Dako/Sigma) diluted 1/10000 in TBS-T plus 5% milk for 1 hour. The membrane was washed three times for 15 min before antibody detection by chemiluminescence using the ECL or ECL-Advance system (Amersham Biosciences) according to supplied protocol and X-ray medical films (AX, Konica), processed using a Compact X4 developer (Xograph). Immunoblotted membranes were stripped in buffer (2 % SDS, 62.5 mM Tris-HCl pH 6.7, 100 mM  $\beta$ -Mercaptoethanol) for 45 min at 50°C and washed extensively in TBS-T, before blocking. Western blotting was performed again as described above.

#### ***2.6.VI Immunoprecipitation***

Cells were harvested and lysed on ice in lysis buffer (20 mM HEPES pH 7.9, 450 mM NaCl, 1.5 mM MgCl<sub>2</sub>, 1 mM EGTA, 0.1% Tween20, 10% glycerol) or Benzonase lysis buffer (25mM Tris pH 7.5, 2 mM MgCl<sub>2</sub>, 0.5% NP-40 and 40 mM NaCl for 10 min, then increased to 450 mM NaCl for 30 min), supplemented with phosphatase (Sigma-Aldrich) and protease (Roche) inhibitor cocktails. Lysates were cleared by centrifugation at 14,000 revolutions per minute (rpm) for 15 min at 4°C and diluted to 150 mM NaCl. Extracts were subsequently incubated with Protein A- or G-coated Dynabeads (Invitrogen) pre-bound to

2 µg of antibody for 2 hour at 4°C. Beads were extensively washed and then boiled for 5 min in SDS-sample buffer (0.0625 M Tris-HCl pH 8.7, 2% SDS, 5% β-Mercaptoethanol, 10% glycerol, 0.01% Bromophenol Blue).

### ***2.6.VII Peptide pull-downs***

1 mg of U2OS whole cell extract (WCE) – obtained by lysing cells in lysis buffer as described in 2.6.VI – or HeLa nuclear extract (CilBiotech) was diluted in an equal volume of binding buffer (TBS, 10% glycerol, 1 mM DTT) and incubated with 10-40 µl of streptavidin Dynabeads (Dyna) saturated with biotinylated peptides (Table 3) for 1 hour at 4°C. Beads were washed extensively with TBS-T and bound proteins were eluted in SDS-sample buffer. Phosphatase (Sigma-Aldrich) and protease (Roche) inhibitor cocktails were added to all buffers used.

### ***2.6.VIII GST pull-downs***

Purified GST-protein fusions on glutathione-sepharose 4B beads (GE Healthcare; see 2.11.II) were washed with and resuspended in equal volume of TEN100 buffer (20 mM Tris pH 7.4, 0.1 mM EDTA and 100 mM NaCl). GST-protein fusion on beads was incubated with the extract of choice for 1 hour at 4°C. Beads were washed four times with NTEN buffer (20 mM Tris pH 7.4, 0.1 mM EDTA, 300 mM NaCl and 0.5% NP40) and bound proteins were eluted by boiling for 5 min in SDS-sample buffer and visualized by Coomassie staining (2.6.III) or western blotting (2.6.V).

## **2.6.IX *In vitro phosphorylation and kinase assays***

1 µg of purified GST-fusion proteins was incubated with 95 µM of ATP (adenosine triphosphate), 0.37 MBq of [ $\gamma$ <sup>32</sup>P]-ATP (10 µCi/µl; Amersham) or 1 µg of purified Cyclin A/CDK2 (Upstate) or Chk1 (provided by Melanie Blasius) in GST pull-down buffer (Chapter 2.6.VIII) for 30 min at 30°C. After GST pull-down, samples were resolved by SDS-PAGE followed by western blotting, except for experiments using [ $\gamma$ <sup>32</sup>P]-ATP that were followed by autoradiography with autoradiography films (Hyperfilm MP, Amersham).

## **2.7 Immunofluorescence and imaging**

### **2.7.1 *Immunostaining***

Cells were grown on coverslips or harvested by mitotic shake-off and attached to poly-L-lysine-coated coverslips with a cytospin centrifuge at 500 rpm for 5 min. All following procedures were performed at RT. Cells were fixed with 2% paraformaldehyde for 20 min, washed three times with phosphate buffered saline (PBS), permeabilised with 0.2% Triton X-100 in PBS for 5 min and blocked with 5% BSA in PBS/0.1%Tween-20 for 10 min. Primary antibodies used are listed in Table 1 (IF). Incubation with primary antibodies was for 45 min followed by three washes with PBS and a 30 min incubation with the corresponding secondary antibodies: Alexa-Fluor 488 (green), 594 (red) and 647 (far red) at 1:1000 (Invitrogen). Coverslips were washed three times with PBS and mounted with Vectashield mounting medium containing 4,6 diamidino-2-phenylindole (DAPI; Vector Laboratories).

## **2.7.II     *Imaging and processing***

Images were acquired with a Radiance 2100 confocal microscope (BioRad) with a 40x or 60x objective and processed by Photoshop (Adobe). Foci counting and fluorescent intensity were automatically performed using Volocity software (Improvision).

## **2.8     Flow cytometry**

### **2.8.I     *Analysis of DNA content and cell cycle distribution***

Approximately  $1 \times 10^5$  human cells or  $1 \times 10^7$  yeast cells were harvested and fixed with 70% ethanol at 4°C overnight, followed by washes with PBS and incubation for 30 min with RNase A (250 µg/ml) and propidium iodide (PI; 12.5 µg/ml) at 37°C. Human and yeast cells were analyzed by FACS (fluorescence activated cell sorting) on a CyAn flow cytometer (Beckman Coulter) or with a Beckman Coulter FACSCalibur machine with BD CellQuest software. Data were analyzed with FlowJo software (Tree Star, Inc.).

### **2.8.II     *Cell cycle regulation of protein expression***

$1 \times 10^6$  human cells were harvested and the Flow Kit staining protocol was followed (BD Biosciences). In brief, cells were washed by adding 1 ml staining buffer, containing Dulbecco's phosphate-buffered saline (DPBS) with 2% w/v heat-inactivated foetal bovine serum (FBS) and 0.09% w/v sodium azide, pH 7.4. (0.2 µm-pore filtered). Centrifugation at 1000 rpm for 3 min was followed by resuspension into 80 µl BD Cytotfix/Cytoperm buffer for 30 min at RT. Cells were washed with 1 ml of BD Perm/Wash buffer and then incubated with primary antibodies in 50 µl of BD Perm/Wash buffer for 1 hour, followed by a wash and incubation with 1:100 dilution of Alexa-fluorescent secondary antibodies

for 1 hour. A final wash was followed by treatment with RNase and staining with PI and processing by FACS, as described above (2.8.I).

## **2.9 Bacteria related techniques**

### **2.9.I Bacterial transformation**

Autoclaved Luria-Bertani media (LB; 10 g/l tryptone, 5 g/l yeast extract, 5 g/l NaCl, pH 7.5) were used to grow liquid bacterial cultures by shaking at 225 rpm at 37°C for 12 hours. To select for bacteria transformed with a plasmid conferring resistance to antibiotics, a final concentration of 50 µg/ml of ampicillin or 35 µg/ml of kanamycin were included in liquid cultures or plates prior to inoculation or streaking. Heat shock was used to transform chemically competent XL-1 Blue cells (Stratagene) or TOP10 cells (Invitrogen) and amplify *E. coli*-yeast shuttle vectors, cloning products and site directed mutagenesis products. 50 µl of cells were thawed on ice and gently mixed with plasmid DNA and incubated on ice for 30 min. The tube was then placed in a water bath for 30 sec and chilled on ice for 1 min. 250 µl of SOC (Invitrogen) were added and the bacterial culture incubated at 37°C at 225 rpm for 1-2 hours before plating all on LB/agar plates containing the appropriate antibiotic for selection. Single colonies were grown into ~5 ml LB liquid medium, containing the appropriate antibiotic, overnight and harvested by centrifugation. Plasmid DNA was isolated by mini-prep procedure using a Qiaprep miniprep kit (Qiagen) according to the manufacturer's instructions.

## **2.9.II     *Recombinant protein expression and purification***

Expression of recombinant protein was done with BL21 (DE3) pLysS cells (Invitrogen). A single colony of bacteria was used to inoculate a 20 ml LB culture (supplemented with the appropriate selective antibiotic) and grown overnight shaking at 37°C. In the morning, culture was inoculated to a starting OD<sub>600nm</sub> of 0.06. Cells were then grown to an OD<sub>600nm</sub> of 0.6 before being cooled in a shaking water incubator for 30 min at 15°C before isopropyl-β-D-thiogalactopyranoside (IPTG) was added at final concentration of 0.1 mM. Cells were then incubated at 37°C for 3-4 hours or at 15°C overnight and harvested by centrifugation. Cells were resuspended in ice-cold PBS, sonicated with Bioruptor sonication device at 40% amplitude, lysed with 20% Triton X-100 and centrifuged. Soluble and pellet fractions were analyzed by SDS-PAGE followed by coomassie staining. 20-40 μl of a 50% slurry of glutathione sepharose beads was added to the supernatant for 1 hour at 4°C and beads were recovered by centrifugation and used for GST pull-down experiments.

## **2.10 Human tissue culture methods**

### **2.10.I     *Cell culture***

U2OS, HeLa, BJ and MRC5 cells were cultured in standard Dulbecco modified Eagle's minimal essential medium (DMEM; Sigma-Aldrich) supplemented with 10% FBS (BioSera), 2 mM L-glutamine, 100 U/ml penicillin, and 100 μg/ml streptomycin (Sigma-Aldrich). The medium for U2OS cells stably expressing GFP-MDC1 (Kolas et al., 2007), GFP-RNF8 (Mailand et al., 2007), GFP-53BP1 and GFP-RNF168 (Yaron Galanty) was supplemented with 0.5 mg/ml G418 (Gibco, Invitrogen).

### ***2.10.II Treatment with DDR inhibitors and DNA-damaging agents***

ATM (KU-55933) and DNA-PK (NU-7441) inhibitors were from KuDOS Pharmaceuticals and Chk1/2 inhibitor AZD7762 was from AstraZeneca (Zabludoff et al., 2008). IR treatment was with a Faxitron X-ray machine (Faxitron X-ray Corporation, Illinois, USA). Phleomycin (Duchefa Biochemie) was added at 30 µg/ml. Where appropriate, ATM and DNA-PK inhibitors (20 µM and 2 µM, respectively) were applied to culture medium 1 hour prior to DSB induction. Chk1 inhibitor was added (50 nM final concentration) 3 hours prior to phleomycin treatment. Cells were processed for analyses 30 min after IR or phleomycin treatment.

### ***2.10.III Transfection of plasmid DNA***

Human cells plated for a 25-50% confluency and washed into 2 ml of DMEM low-serum Q-only (DMEM supplemented with 5% w/v FCS and glutamine) before transfection. Chemical transfection was performed using Fugene 6 (Roche), or Lipofectamine 2000 (Invitrogen) reagents according to manufacturer's instructions. Briefly, DNA-transfection complexes were prepared in 0.5 ml Optimem (Invitrogen) by the addition of 12 µl of Fugene 6 reagent, and 2-5 µg of plasmid DNA, incubating at room temperature for 15 min. DNA-transfection complex mixture was gently and evenly added to the plate. Cells were monitored for optimal protein expression at ~24 and ~48 hours following transfection.

### ***2.10.IV Transfection of siRNA***

All siRNA duplexes were purchase from MWG-Biotech or Dharmacon (Thermo) and were transfected into cells at ~25% confluency by using Oligofectamine reagent (Invitrogen) according to manufacturer's instructions, to a final concentration of 80 nM. Typically, cells

were left in DMEM low-serum Q-only transfection medium for 24 hours, before washing into standard medium. Cells harvested for experiments ~48 or ~72 hour post-transfection.

### ***2.10.V Cell synchronization techniques***

The thymidine-nocodazole method includes 16-22 hours pre-synchronization with a single-thymidine-block using 2.5 mM of thymidine, followed by cells being extensively washed and released into fresh medium. After 8-10 hours, nocodazole was added to a final concentration 40 ng/ml for 3-4 hours to accumulate cells in early mitosis. For nocodazole-only synchronization, cells were incubated with 100 ng/ml nocodazole for 18-20 hours.

### ***2.10.VI Cell survival assay***

Mitotic cells obtained by shake-off of the cultures pre-synchronised by thymidine-nocodazole were treated with ATM and DNA-PKcs inhibitors for 1 hour and irradiated with 0.5, 1, 2 or 4 Gy. 30 min later, cells were extensively washed to remove inhibitors and/or nocodazole, counted and plated. Asynchronous cells were plated 24 hours prior to the treatments. Cells were left for 10-14 days at 37°C to allow colony formation. Colonies were stained with 0.5% crystal violet/20% ethanol and counted. Results were normalized to plating efficiencies. Statistical analysis was performed using the R Language for Statistical Computing. Coefficients and corresponding p-values were calculated separately for mitotic and asynchronous cells, using the linear modelling function in R by the following model:  $\log(y) = \beta_0 + \beta_1 IR + \beta_2 IR^2 + \beta_3 t + \beta_4 IR * t$ , where  $y$  is the percentage of cells surviving,  $IR$  is the radiation level in Gy, and  $t$  is the treatment (encoded as 0 for DMSO and 1 for ATMi/DNA-PKi). The quadratic term was included since the response curve is nonlinear.

## 2.11 Yeast materials and methods

### 2.11.1 Yeast media

Yeast was grown in autoclaved YPA medium or autoclaved THULL synthetic medium (Table 4) supplemented with 2% glucose unless otherwise indicated. THULL medium was used to select for the marker genes *URA3*, *TRP1*, *HIS3* or *LEU2* where indicated. Unless otherwise stated, cells were grown at 30°C. For long-term storage at -80°C, 15% glycerol was added to a saturated culture. For short-term storage, yeast strains were stored on yeast extract–peptone–dextrose medium with adenine (YPAD) agar plates at 4°C.

**TABLE 4. Yeast culture media**

<b>Medium</b>	<b>Recipe</b>
YPAD	Per litre: 20 g bactopectone, 10 g yeast extract, 40 mg adenine hemisulphate. Glucose was added to 2% after autoclaving. 20 g of bactoagar was added for media plates.
THULL	Per litre: 1.2 g yeast nitrogen base (without amino acids), 5 g ammonium sulphate, 10 g succinic acid, 6 g NaOH, 0.8 g amino acid (aa) dropout mix. Glucose was added to 2% after autoclaving. 20 g of bactoagar was added for plates.
Aa dropout mix	1 g of each adenine, arginine, cysteine, threonine, and 0.5 g of each asparagines, isoleucine, methionine, phenylalanine, proline, serine, tyrosine, valine.
100X aa stock	Per litre: 10 g aa (tryptophan, histidine, leucine or lysine) were dissolved in 1 litre of ddH <sub>2</sub> O. For uracil, 10 g were dissolved in 0.1 M NaOH. Solutions were filter sterilised.
SC-URA	Per litre: As THULL, plus 100 mg each of leucine, tryptophan, histidine and lysine added from 100X stocks after autoclaving.
SC-LEU	Per litre: As THULL, plus 100 mg each of uracil, tryptophan, histidine and lysine added from 100X stocks after autoclaving.
SC-TRP	Per litre: As THULL, plus 100 mg each of leucine, uracil, histidine and lysine added from 100X stocks after autoclaving.
SC-HIS	Per litre: As THULL, plus 100 mg each of leucine, tryptophan, uracil and lysine added from 100X stocks after autoclaving.
5-FOA	Per 250 ml: 0.25 g 5-FOA, 0.5 g aa dropout mix, 1.7 g yeast nitrogen base without aa, 25 mg leucine, 25 mg lysine, 25 mg tryptophan, 25 mg histidine, 12.5 mg uracil, 25 ml 20% glucose, 100 ml sterile ddH <sub>2</sub> O, 5 g bactoagar, cooled to 55°C.

## 2.11.II Yeast strains and genotypes

**TABLE 5. Yeast strains used in this study**

<b>Strain</b>	<b>Background</b>	<b>Genotype</b>	<b>Reference/Source</b>
W303-1A	<i>MATa ade2-1 can1-100 his3-11,15 leu2-3,112 trp1-lura3-1 RAD5</i>	W303	Robert Driscoll
W303-1B	<i>MATα ade2-1 can1-100 his3-11,15 leu2-3,112 trp1-lura3-1 RAD5</i>	W303	Robert Driscoll
W303	Diploid of W303-1A and W303-1B	W303	This study
SGY01	<i>MATa 3HA-PSF1::HIS3</i>	W303	This study
SGY02	<i>MATa 3HA-psf1-S187A::HIS3</i>	W303	This study
SGY03	<i>MATa 3HA-psf1-S187E::HIS3</i>	W303	This study
SGY04	<i>MATa HIS3::</i>	W303	This study
SGY05	Diploid <i>psf1Δ::kanMX6 / PSF1</i>	W303	This study
SGY06	<i>psf1Δ::kanMX6 3HA-PSF1::URA3</i>	W303	This study
SGY07	<i>psf1Δ::kanMX6 3HA-PSF1::HIS3</i>	W303	This study
SGY08	<i>psf1Δ::kanMX6 3HA-PSF1::URA3 3HA-PSF1::HIS3</i>	W303	This study
SGY09	<i>psf1Δ::kanMX6 3HA-PSF1::URA3 3HA-psf1-S187A::HIS</i>	W303	This study
SGY10	<i>psf1Δ::kanMX6 3HA-psf1-S187A::HIS</i>	W303	This study
SGY11	<i>psf1Δ::kanMX6 3HA-PSF1::URA3 3HA-psf1-S187E::HIS</i>	W303	This study
YYT4	<i>MATa ade2-1 can1-100 his3-11, 15 leu2-3,112 trp1-1 ura3-1 bar1 psf1-1</i>	W303	(Takayama et al., 2003)
SGY12	<i>psf1-1 3HA-PSF1::HIS3</i>	W303	This study
SGY13	<i>psf1-1 3HA-psf1-S187A::HIS3</i>	W303	This study
SGY14	<i>psf1-1 3HA-psf1-S187E::HIS3</i>	W303	This study
SGY15	<i>psf1-1 HIS3::</i>	W303	This study
YSC1178	<i>MATa his3Δ1 leu2Δ0 met15Δ0 ura3Δ0 HIS3MX6 PSF1-TAP</i>	W303	(Ghaemmaghmi et al., 2003)
RDY072	<i>mec1Δ::TRP1 sml1-1</i>	W303	Robert Driscoll
SGY16	<i>rad9Δ::URA3 3FLAG-CHK1</i>	W303	This study
SGY17	As SGY16 + <i>RAD9::TRP1</i>	W303	This study
SGY18	As SGY16 + <i>rad9-S83A::TRP1</i>	W303	This study
SGY19	As SGY16 + <i>rad9-T110A::TRP1</i>	W303	This study
SGY18	As SGY16 + <i>rad9-T125A::TRP1</i>	W303	This study
SGY19	As SGY16 + <i>rad9-T143A::TRP1</i>	W303	This study
SGY20	SGY16 + <i>rad9-S83A, T110A, T143A::TRP1</i>	W303	This study
SGY21	As SGY16 + <i>rad9-S83A, T110A, T125A, T143A::TRP1</i>	W303	This study
SGY22	As SGY16 + <i>rad9-S56A, S83A, T110A, T125A, T143A::TRP1</i>	W303	This study
Cdc28as1	<i>ura3-1, leu2-3,112, trp1-1, his3-11,15, ade2-1, can1-100, GAL+cdc28as1</i>	W303	(Bishop et al., 2000)

### **2.11.III Construction of yeast strains**

Deletion of genes was carried out using PCR-mediated targeted gene disruption method (Baudin et al., 1993). Double mutants were created where possible by crossing *MATa* and *MATα* strains to create a heterozygous diploid, and subsequent sporulation of this diploid to form tetrads was followed by dissection and replica plating to determine correct genotype of the resulting spores. 3x FLAG-epitope tagged genes were created by PCR-mediated targeted gene tagging. p3FLAG-KanMX was used as template for generation of a PCR product that introduces three copies of the FLAG epitope just upstream of the termination codon of the *CHK1* gene by HR (Gelbart et al., 2001), using especially designed primers. PCR products were gel-purified and transformed into yeast cells (Chapter 2.11.IV). Gene disruption was confirmed by diagnostic PCR from genomic DNA prepared from resistant colonies (Chapter 2.11.VI) using primers upstream of the disrupted gene and inside the disruption cassette. Gene tagging was confirmed by western blotting.

### **2.11.IV Yeast transformation**

A modified version of the lithium acetate procedure (Ito et al., 1983) was used. Approximately  $1 \times 10^8$  logarithmically growing yeast cells were harvested by centrifugation at 3000 rpm for 3 min, washed in 1 ml H<sub>2</sub>O, followed by one wash in 1 ml 1x TE/LiAc (0.1 M lithium acetate, 10 mM Tris-HCl pH 7.5, 1 mM EDTA). Cells were resuspended in 50 μl 1x TE/LiAc and 1-2 μg of plasmid DNA or disruption construct were added. 25 μl of sonicated salmon sperm DNA (10 mg/ml, previously denatured at 95°C for 5 min before being placed on ice) and 300 μl of PLATE solution (40% polyethylene glycol 3350, 0.1 M lithium acetate, 10 mM Tris-HCl pH 7.5, 1 mM EDTA) were added, before incubation at

30°C for 1 hour. The yeast suspension was then heat-shocked at 42°C for 15 min before washing and resuspension in 0.5 ml ddH<sub>2</sub>O. Aliquots of 200 µl were plated on appropriate media plates containing or lacking the required selection and grown for 2-3 days at 30°C.

#### **2.11.V Plasmid shuffle**

The plasmid shuffle method (Bender and Pringle, 1991) consists of using a null mutation in chromosomal gene *PSF1*, rescued by the wild-type version on a *URA3* selectable plasmid. Because *psf1Δ* is lethal, diploid cells heterozygous for *psf1* null allele were transformed with wild-type *PSF1*-containing *URA3* plasmid and sporulated. The strain containing the wild-type plasmid and null mutation for *PSF1* was selected by replica-plating on 5-fluoro-orotic acid (5-FOA); 5-FOA is a chemical toxin that kills Ura<sup>+</sup> yeast cells. This strain was transformed with plasmids that contain mutant variants of *psf1* or wild-type *PSF1* on a *HIS3* plasmid. The *PSF1*-Ura<sup>+</sup> plasmid can be shuffled out of the transformed cells by selecting against the presence of *URA3* in 5-FOA-containing medium. Mutant alleles may rescue the lethality of the chromosomal *psf1* mutation and can thus be studied further.

#### **2.11.VI Genomic DNA preparation**

Yeast genomic DNA was prepared as described by Kaiser et al. (1994). In brief, 5 ml of saturated cultures were resuspended in 0.5 ml of 1 M sorbitol, 0.1 M EDTA pH 8.0 and incubated with 12.5 µl of 4 mg/ml Zymolyase 100-T (ICA) for 1 hour at 37°C. Following centrifugation, the pellet was resuspended in 0.5 ml of 50 mM Tris-HCl pH 7.4, 20 mM EDTA, 1% SDS and incubated at 65°C for 30 min. 0.2 ml of 5 M potassium acetate was

added and incubated on ice for 1 hour. Supernatant resulting from centrifugation was added to one volume of 100% isopropanol, and then incubated for 5 min at room temperature before brief centrifugation. Precipitated DNA was air-dried and resuspended in 0.3 ml of TE (10 mM Tris-HCl pH 7.4, 1 mM EDTA). 15  $\mu$ l of a 1 mg/ml solution of RNase A was added and incubated at 37°C for 30 min. Precipitate resulted from adding 0.03 ml of 3 M sodium acetate and 0.2 ml of 100% isopropanol followed by centrifugation. The pellet was air-dried before resuspension in 0.2 ml of TE pH 7.4.

### ***2.11.VII Denatured whole cell extracts with TCA preparation***

Denatured protein extracts were prepared by trichloroacetic acid (TCA) extraction (as described by Foiani et al., 1994).  $1 \times 10^8$  cells of log phase cultures were centrifuged at 3000 rpm for 3 min at 4°C and resuspended in 100  $\mu$ l of 20% TCA with an equal volume of acid-washed glass beads. The cells were lysed in a FastPrep (setting 4.5; Bio101) for 50 sec and the supernatant recovered in a fresh microcentrifuge tube. The glass beads were washed with 200  $\mu$ l of 5% TCA and the supernatants combined and then centrifuged for 10 min at 13200 rpm. The pellet was then resuspended in 100  $\mu$ l of SDS-sample buffer, boiled at 95°C for 5 min before loading, typically 10-15  $\mu$ l, on SDS-PAGE gels.

### ***2.11.VIII Preparation of native whole cell extract***

Native protein extracts were prepared from mid-log yeast cultures (500 ml) harvested by centrifugation, washed twice with H<sub>2</sub>O and resuspended in an equal volume of 2x extraction buffer (200 mM Hepes-KOH pH 7.9, 300 mM potassium acetate, 20 mM magnesium acetate, 0.2% NP-40, 4 mM EDTA, 20% glycerol, 2x protease inhibitors, 2

mM DTT) before disruption in a Constant Cell Disruption System (Constant Systems) at 20000 pounds per square inch (psi) and 4°C. The recovered extract was centrifuged at 13500 rpm for 15 min at 4°C, the supernatant removed to a fresh tube and stored at -80°C.

### ***2.11.IX Yeast cell cycle synchronization in G1***

To arrest cells in G1, *MATa* cells were grown from OD<sub>600nm</sub> of 0.06 to 0.2-0.3 and treated 10 µg/ml of α-factor for 1-2 hour (Paulovich and Hartwell, 1995). The efficiency (>95%) of the arrest was confirmed by light microscopy, determining the ratio of un-budded to budded cells. Cells were then either harvested directly or synchronously released into the cell cycle by washing with YPAD to eliminate the α-factor.

### ***2.11.X Purification of TAP-tagged proteins***

6-10 litres of yeast culture expressing tandem affinity purification (TAP) tagged protein were processed as described in 2.13.VIII. Supernatant was added to pelleted and resuspended in same volume of Tampon A (50 mM Tris pH 7.5, 100 mM NaCl, 1.5 mM MgCl<sub>2</sub>, 0.15% NP40, 1x protease and phosphatase inhibitors) with 50% IgG sepharose overnight at 4°C. Washed with Tampon de Corte (Tampon A + 1 mM DTT) and added 1 ml Tampon de Corte and 100 U of TEV protease overnight at 4°C. Supernatant was filtered through a chromatography column (BioRad) and 3 ml Tampon B (10 mM Tris pH 8, 150 mM NaCl, 1 mM Mg-Acetate, 2 mM CaCl<sub>2</sub>, 10 mM β-Mercaptoethanol, 1 mM Imidazole, 0.1% NP40) with 3 µl 1M CaCl<sub>2</sub> and 300 µl 50% calmodulin beads were added overnight at 4°C. Beads were washed on column with Tampon B and TAP-tagged proteins were eluted in Tampon B plus 5 mM EGTA.

### ***2.11.XI Growth curves***

For growth curves, cells were grown overnight to saturation in 5 ml YPAD. Cultures were then diluted to an OD<sub>600nm</sub> of 0.06 and grown to an OD<sub>600nm</sub> of 0.3 in 10 ml YPAD. Cultures were then re-diluted to an OD<sub>600nm</sub> of 0.06 in 10 ml YPAD and the absorbance measured for 3-8 hours.

### ***2.11.XII Sensitivity assays***

Sensitivity assays of different yeast strains to increased temperature, DNA damaging agents, IR and ultra-violet radiation (UV) were carried out by inoculating a single colony and incubating the culture overnight at 30°C to saturation. Cells were then diluted to a density of  $1.75 \times 10^7$  in sterile ddH<sub>2</sub>O and ~5 µl of 5- or 10-fold serial dilutions were spotted onto YPAD or the appropriate synthetic selective medium containing hydroxyurea (HU), methane methylsulphonate (MMS), camptothecin (CPT) or phleomycin as required. Cells were similarly diluted on YPAD plates and allowed to dry before IR and UV irradiation. Plates were incubated for 2-3 days at 30°C, or 23°C and 37°C for temperature-sensitivity analysis.

## RESULTS

---

### **3 DNA DAMAGE SIGNALLING IN RESPONSE TO DSBs DURING MITOSIS**

#### **3.1 Summary**

The DDR comprises an intricate network of pathways that coordinates cellular reactions to DNA insults. Cellular responses to DNA damage range from arrest of the cell cycle, repair of DNA lesions, to the re-establishment of cellular homeostasis. In mammalian cells, the signalling cascade initiated in response to DSBs has been extensively investigated in interphase cells. Yet, the molecular events following induction of DSBs during mitosis are still somewhat elusive.

Here, I show that mitotic cells treated with DSB-inducing agents activate a ‘primary’ DDR comprised of early signalling events including activation of the protein kinases ATM and DNA-PK, histone H2AX phosphorylation together with recruitment of MDC1 and the Mre11-Rad50-Nbs1 (MRN) complex to damage sites. However, mitotic cells display no detectable recruitment of the E3 ubiquitin ligases RNF8, RNF168 and BRCA1, or accumulation of the mediator protein 53BP1, at DSB sites, indicating that ‘secondary’ DNA damage responses are inhibited in mitosis. Furthermore, DNA damage signalling is attenuated in mitotic cells, with full DDR activation only ensuing when a DSB-containing mitotic cell enters G1. In addition, induction of DSBs does not trigger a DNA damage checkpoint arrest once the cell is committed to mitosis. Accordingly, I show that phosphorylation of certain downstream ATM substrates in response to DSB induction, including the DNA damage checkpoint kinases Chk1 and Chk2, is impaired during mitosis.

Finally, I provide evidence that induction of a primary DDR in mitosis, including  $\gamma$ H2AX marking of DSBs and MRN-mediated end-tethering, is biologically important for cell viability, as it may facilitate the induction of a full DDR and repair of the DNA lesion in the more favourable chromatin environment of the G1 cell.

## **3.2 Introduction**

### ***3.2.1 DNA damage responses in mitosis: a one hour long gap in our knowledge***

Albeit extensively investigated in the context of interphase cells, the precise mechanisms and functions of the DDR in mitotic cells are still poorly understood. During the 1960s, analyses of living cells following irradiation revealed the existence of defined points of arrest in the progression through the cell cycle. Remarkably, irradiation of cells that displayed a mitotic status, visually identified by marked chromatin condensation and absence of nuclear envelope, failed to halt cell cycle progression and continued through the process of cell division, giving rise to two daughter cells (Swann, 1957; Mazia, 1961). The observations that mitotic cells seemed unresponsive to IR prompted speculations that no checkpoint, and therefore no DNA damage responses, existed in mitosis. Interestingly, the time frame after the G2/M transition when cells became unresponsive to irradiation was named a ‘point of no return’ (Mazia, 1961). This dramatic appellation emphasized the early understanding of the potentially detrimental repercussions for the cell to ignore DNA lesions and continue to orchestrate the series of events that lead to cell division. More recent studies have shown that vertebrate cells can delay mitosis, or even reverse mitotic progression if exposed to IR during a newly defined ‘antephase’ point – between late G2 to mid prophase – when chromatin condensation is actively taking place in preparation for entry into mitosis and cell division (Pines and Rieder, 2001; Matsusaka and Pines, 2004; Chin and Yeong, 2009). The antephase checkpoint has acquired increasing importance over recent years. It acts to complement two established checkpoints: the prior G2/M checkpoint that acts to monitor completion of DNA replication and absence of DNA damage before preceding into mitosis; and the spindle assembly checkpoint (SAC), which

ensures accurate spindle assembly on all mitotic chromosomes, before allowing the transition into anaphase and mitotic exit. Knowledge of the existence of an antephasis checkpoint stems from experimental observations showing that exposure to stress signals in early prophase cells that have initiated chromatin compaction yet retain an intact nuclear envelope, triggers a temporal delay and a reversion into a G2 status (Carlson, 1969a; Carlson, 1969b; Rieder and Cole, 1998; Matsusaka and Pines, 2004) and my own observations). Following antephasis, and once the cell has passed the 'point of no return', marked by nuclear envelope breakdown in late prophase, the cell becomes committed to completing mitosis even in the presence of DNA damage (Rieder and Cole, 1998). Nonetheless, the rate of mitotic progression can be affected by the amount of DNA damage: whilst relatively low levels of damage do not delay M-phase exit, more substantial damage can interfere with the structure and functions of kinetochores, resulting in a significantly prolonged mitosis due to the need to satisfy the SAC (Mikhailov et al., 2002). Thus, DNA breaks *per se* do not hinder mitotic progression and do not appear to induce activation of a DNA damage checkpoint (Rieder and Salmon, 1998), unless they affect spindle assembly and kinetochore attachment, leading to activation of the SAC.

Laboratory induction of DNA damage on cultured cells is an artificial scenario that may mimic particularly challenging *in vivo* conditions, including exposure to chemotherapy, radiotherapy and highly mutagenic compounds. On the other hand, the understanding of how cells deal with DSBs that arise endogenously during physiological progression into mitosis is also of high relevance. The mitotic spindle itself can cause DSBs by a breakage-fusion-bridge mechanism, as marked by the appearance of  $\gamma$ H2AX local accumulation. Recent evidence suggests that the DSBs are specifically localized at centromeres, particularly vulnerable sites subjected to the spindle-induced tensional forces during

mitosis. Furthermore, spindle-generated DSBs are mainly found in centromere-containing micronuclei (Guerrero et al., 2009). As both spindle defects and increased  $\gamma$ H2AX signals correlate with aneuploidy, these phenomena may underlie malignant transformation, promoting tumorigenesis.

It is noteworthy that a defined threshold exists in the number of DSBs required to elicit the activation of the G2/M checkpoint. About 10-20 DSBs are the minimum required to induce cell cycle arrest and prevent entry into mitosis (Deckbar et al., 2007). It is therefore possible to envisage a scenario where less than 20 DSBs, endogenously arising after completion of S-phase or during G2 and following exposure to less than 0.4 Gy of IR, may be carried through into mitosis. Experimental evidence shows that cells containing less than 20 DSBs can complete mitosis in a timely manner, suggesting that low numbers of DSBs, enough to slip under the radar of the G2/M checkpoint, would not reverse entry into mitosis through activation of the 'antephase' checkpoint nor the SAC. It would be interesting to continue monitoring these cells during subsequent cell cycles to establish whether the presence of a few DSBs is compatible with error-free segregation or if it will lead to chromosomal imbalances.

Interestingly, several DDR components have been found to play roles in regulating chromosome segregation in the absence of DNA damage. The recruitment of DDR factors to mitotic structures during unperturbed mitosis has been reported; for example, ATM, ATR, DNA-PKcs, p53, TopBP1, BRCA1, Chk1 and Chk2 associate with centrosomes in mitosis (Hsu and White, 1998; Tsvetkov et al., 2003; Reini et al., 2004; Tritarelli et al., 2004; Zhang et al., 2007), while 53BP1 is found at kinetochores (Jullien et al., 2002). These mitotic compartmentalizations correlate to functional activity of these proteins in the

process of cell division. 53BP1, for instance, is loaded to the kinetochore during prophase, where it co-localizes with CENP-E. In metaphase, it is released only if all chromosomes are aligned correctly on the equatorial plate, suggesting that 53BP1 may play a physiological role in controlling mitotic progression into anaphase (Jullien et al., 2002). Another report also pinpointed *Xenopus* 53BP1 as a suppressor of mitotic catastrophe (Xia et al., 2001). In addition, Chk1 is directly regulated by CDK1-dependent phosphorylation (Shiromizu et al., 2006) and is required for several aspects of cell division, ranging from regulation of the SAC, transcriptional inhibition of mitotic cyclin/CDK genes, to controlling chromosome segregation and cytokinesis (Kramer et al., 2004; Zachos et al., 2007; Peddibhotla et al., 2009). MDC1 was also recently shown to directly bind the APC/C (anaphase-promoting complex/cyclosome; Coster et al., 2007) and to regulate mitotic progression by enabling cdc20-mediated activation of the APC in the metaphase-to-anaphase transition (Townsend et al., 2009). These data further underscore the link between cell cycle regulation and the DNA damage cascade.

In budding yeast, canonical DNA damage components such as the apical DDR kinases Mec1 (the yeast homologue of ATR) and Tel1 (homologous to ATM) directly influence mitotic progression in the presence of DNA damage, and are interlinked with intrinsic mitotic checkpoints, promoting activation of the SAC upon cytotoxic stress (Kim and Burke, 2008). Nevertheless, to date, there is no clear evidence to suggest a DNA damage-dependent role for these DDR factors in the mitosis of mammalian cells.

Collectively, these data point toward a scenario whereby DSBs fail to activate a DNA damage checkpoint and to elicit DNA damage responses in the context of mitosis in mammalian cells. Nevertheless, the presence of  $\gamma$ H2AX foci in mitotic cells treated with IR

(Nakamura et al., 2006; Kato et al., 2008) suggests that DSBs generated during mitosis are not left unnoticed by the DDR machinery. Indeed, it would be difficult to envisage a scenario where the presence of extremely cytotoxic lesions such as DSBs is uncared for while meticulous multistep regulations act to maintain mitotic fidelity.

### **3.2.II      *Mitosis and cancer: clinical relevance***

Just like normal cells, all cancer cells multiply through the process of cellular division. Therefore, mitosis is fundamental to propagation of life and, at the same end, to the process of tumourigenesis. A main cellular feature of cancer cells is the abnormal hyperproliferation. Human cells have implemented a plethora of molecular machineries to ensure faithful duplication of an undamaged genome and accurate partitioning during cell division. Thus, the fast paced rate of division typical of many cancers does not warrant controlled proliferation and fidelity of duplication. Cancer often results from the accumulation of mutational damage in genes that control cell cycle progression, arrest, as well as cell death. Therefore, deregulation of the cell division cycle is a causative trait of cancer cells. Moreover, mitotic index values are used to measure the proliferative capacities of a specific cell type within a tissue. High mitotic index is regarded as a biological marker for aggressive and often invasive tumours. For these reasons, mitosis has been an important target for anti-cancer therapy (reviewed in Sudakin and Yen, 2007). Currently, aside from surgery, systemic chemotherapy represents the main line of action for the treatment of cancer. Anti-mitotic drugs are chemotherapeutics that disrupt assembly of the mitotic spindle, affecting cell division. Active classes of drugs in cancer treatment, such as taxanes and vinca alkaloids, are anti-mitotic toxins that stabilize and depolymerize microtubules, respectively. However, these conventionally developed anti-mitotic agents

affect all dividing cells, causing severe toxicity to healthy tissues. Furthermore, intrinsic or acquired resistance to anti-mitotic drugs is observed when cancer cells tolerate gross chromosomal instability and continue to divide. Chromosomal instability is associated with poor patient prognosis and causes further exacerbation of cancer cell abnormalities. Notably, however, a new generation of anti-neoplastic drugs is being investigated, using novel classes of anti-mitotics that target functional aspects of the mitotic regulatory system. Inhibitors against mitotic kinases, including Polo-like kinases, Aurora and others, are currently entering clinical trials. Being over-expressed in cancer, new compounds against these proteins have high potential as targets for anticancer treatment and may reduce side effects compared to conventional treatments.

Another important aspect of mitosis in the context of cancer treatment is the inherent ability of mitotic cells to trigger cell death through induction of mitotic catastrophe (MC). MC is a mechanism of delayed reproductive death caused by abnormal mitosis that leads to micronucleation. The pathway of MC may be activated as an anti-proliferative response of tumour cells or may be induced by anti-mitotic and cytotoxic agents and is particularly relevant in absence of p53 and when apoptotic pathways are impaired. However, cells may escape death through MC *via* a so-called mitotic restitution pathway, activating endocycles and resulting in giant polyploid cells. This mechanism of survival may also cause resistance to anti-mitotics (Erenpreisa and Cragg, 2001).

In light of the extreme radio-sensitivity of mitotic cells (our observations and Stobbe et al., 2002), mitosis is an ideal target for anti-cancer treatment. Fast-dividing cells subjected to mitotic DNA damage readily undergo cell death. On the other hand, mitosis may also have a causative effect other than merely an incidental role, in disrupting genomic integrity and

promoting tumourigenesis. In fact, damaged mitotic cells may over-ride the cell death pathway, leading to malignant transformations. Therefore, several mechanisms exist by which aberrant mitotic control affects both the onset and continuance of tumourigenesis as well as responses to anti-mitotic chemotherapy and cancer prognosis. Strikingly, while anti-mitotic agents are at the forefront in developing novel strategies in cancer control, little is known about the molecular mechanisms following induction of DNA damage in mitosis. Therefore, more data are urgently required to gain a better understanding of the mitotic process and the molecular details subsequent to its perturbation.

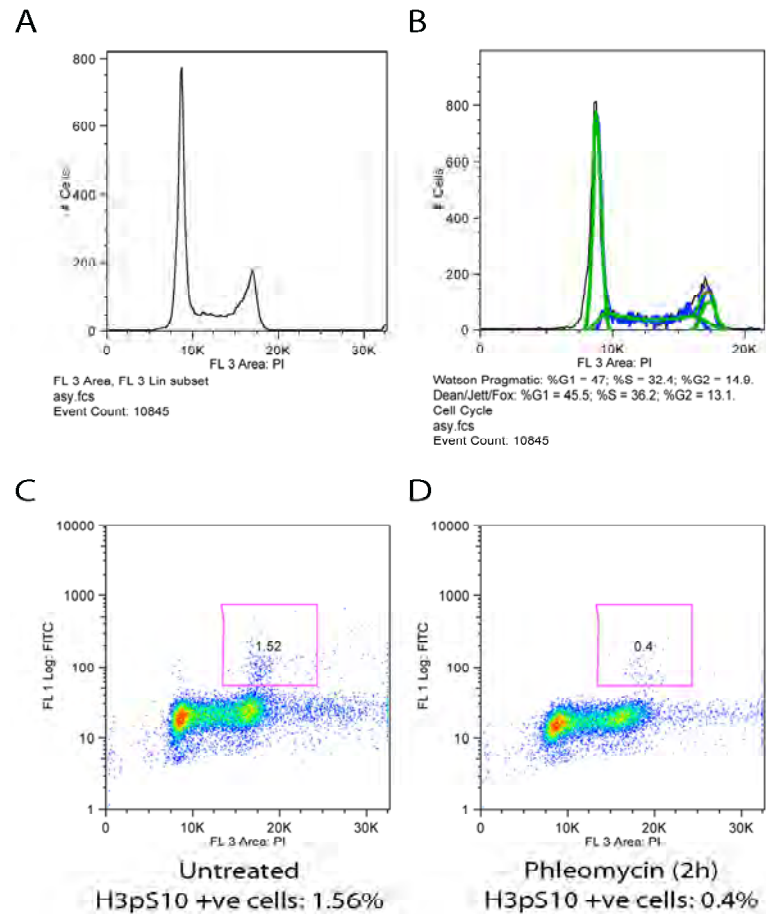
### 3.3 Results

#### 3.3.1 *Analyzing DNA damage responses in the context of mitosis: a matter of synchronization*

The study of molecular events occurring during mitosis is hindered by the brevity of this cell cycle phase. Generally, the distribution over the cell cycle of an asynchronous population of cultured human osteosarcoma cancer cell line U2OS, as monitored by FACS, shows that a majority of cells is found in G1 (up to 50%); the remaining fifty percent is divided between S-phase and G2/M, with approximately 35-40% of cells in S-phase versus ~15% for G2/M (Figure 1A and 1B). However, a major limitation of cell cycle analysis using flow cytometry techniques is that it does not allow discrimination between G2 and M-phases of the cell cycle, as the DNA content is the same. Histone H3 phosphorylated on serine 10 (H3 pS10) is a post-translational modification highly enriched during chromatin compaction at the onset of prophase and marks chromosomes throughout mitosis, representing a canonical marker of mitotic cells. Immunofluorescence staining of this modification with antibodies against H3pS10 allows readily detection and discrimination of mitotic cells within an asynchronous population. Mitotic indices, measured manually by quantification of H3 pS10-positive cells using immunostaining, or by automated analysis *via* flow cytometry (Juan and Darzynkiewicz, 2004), revealed that approximately 1.5-3% of asynchronously growing U2OS cells were undergoing mitosis at any one time (Figure 1C and data not shown). This small proportion makes it hard to study cells during mitosis. Thus, before presenting data on the mitotic DNA damage signalling in response to DSBs, I will briefly present novel methodologies that I have developed to overcome specific limitations in the study of the mitotic DDR.

A major issue in analyzing DNA damage related events in mitosis is the negative effect that DNA damaging agents exert over the mitotic index. The mitotic population is drastically reduced upon treatment with DSB-inducing agents, including IR and phleomycin (Figure 1D and Figure 2B), a DNA-intercalating agent known to cause DSBs throughout the cell cycle (Moore, 1988). If the damage were inflicted before antepase, robust activation of the G2/M checkpoint would prevent entry of damaged cells into mitosis. On the other hand, cells damaged during mitosis can progress through mitosis and back into G1 within 1 hour post-treatment, due to the absence of a mitotic DNA damage checkpoint. Therefore, the analyses performed in my studies do not exceed a 30-minute incubation following treatment with DNA damaging agents, allowing retention and monitoring of cells damaged during mitosis. Limiting incubation to 30-minutes post-damage and use of H3 pS10 to mark mitotic cells allowed visualization of an adequate number of mitotic cells in immunofluorescence analyses, without need for synchronization. Thus, for all immunofluorescences shown in this study, asynchronous cell populations were used.

**FIGURE 1. Impact of DNA damage on cell cycle distribution in U2OS cells**



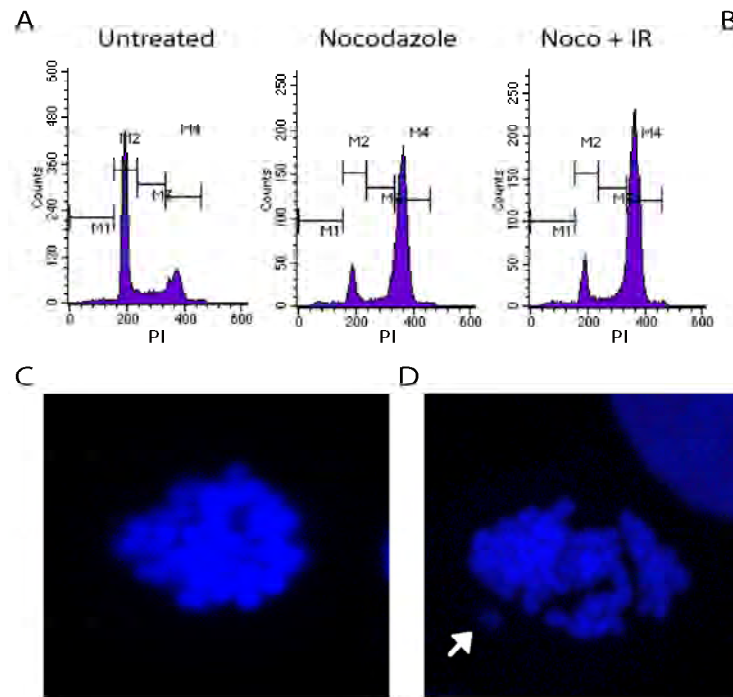
FACS profile of untreated, asynchronously growing U2OS cells (A) and corresponding quantification using two cell cycle modelling algorithms: the Watson Pragmatic, blue line (G1 = 47%; S = 32.4%; G2/M = 14.9%) and the Dean/Jett/Fox method, green line (G1 = 45.5%; S = 36.2%; G2/M = 13.1%) (B). Mitotic cells, as measured by H3 pS10 (purple boxes), are about 1.52% in untreated asynchronous U2OS cells (C) and decrease to 0.4% after 2 hours treatment with phleomycin (D).

Harvesting of a large numbers of mitotic cells was required for cell extracts, western blotting and for flow cytometry analyses. Given that mitotic cells represent such a minor proportion of an asynchronous culture, I used synchronization methods to enrich for the mitotic population. Initially, I used the microtubule depolymerizing agent, nocodazole, to arrest cells at prophase. Nocodazole-arrested cells displayed a chromosomal arrangement typical of prophase cells (Figure 2C), due to their inability to align chromosomes on the metaphase equatorial plate and progress into metaphase. U2OS cells were incubated in the

presence of 100 ng/ml of nocodazole for 20 hours and synchronization was monitored by flow cytometric analysis of the DNA content: 74% of cells were found in G2/M post-synchronization, with 11% and 15% of cells remaining in G1 and in S-phase, respectively (Figure 2A).

Nocodazole is extensively used to synchronize cells in mitosis; yet, microtubule-disrupting agents have been previously shown to induce p53-dependent stress responses in human cells (Tishler et al., 1995). Indeed, nocodazole caused severe stress to the cells, as monitored by an increased  $\gamma$ H2AX signal (Figure 2B). DAPI staining of several U2OS cells exposed to prolonged nocodazole treatment revealed disrupted cellular morphology, abnormal chromatin arrangement and obvious multinucleation, indicative of apoptosis (Figure 2C, 2D and 2E). Chromosomal aberrations caused by prolonged SAC activation and, eventually, escape from the nocodazole block and endoreduplication are highly relevant in the context of chemotherapeutic treatments with anti-mitotic drugs (Dalton and Yang, 2009). Thus, the nocodazole-induced stress signal, as monitored by extensive  $\gamma$ H2AX phosphorylation in western blotting (Figure 2B) and in immunofluorescence (data not shown), rendered the use of synchronization by prolonged exposure to nocodazole unsuitable for investigation of DNA damage signalling in mitosis.

**FIGURE 2. Consequences of prolonged nocodazole treatment in U2OS cells with or without DNA damage induction**



**Content not visible due to copyright limitations**

U2OS cells were incubated with or without 100 ng/ml nocodazole for 20 hours, followed by treatment with 5 Gy of IR or mock irradiation. Cells were then collected for FACS, IF and WB analyses. Nocodazole-induced synchronization arrested a high proportion of cells in G2/M (74%), and this was unchanged after irradiation (A). Arrest of U2OS cells with nocodazole gives rise to  $\gamma$ H2AX detection *via* WB. However, the  $\gamma$ H2AX signal is further increased upon treatment with 5 Gy of IR. It is noteworthy that the reduction seen in H3 pS10 levels upon IR treatment of asynchronous cells reflects a reduction in the proportion of mitotic cells following DNA damage (B; panel B from Collaborator). DAPI staining of DNA after nocodazole arrest in prophase (C). Certain cells show broken chromosomes (arrow) and abnormal DNA conformations (D). Bulky, multinucleated cells, possibly in the process of apoptosis, were also observed in nocodazole-arrested samples (E).

To minimize exposure of cells to nocodazole, other methods of synchronization were tested. I optimized a synchronization protocol using a thymidine-nocodazole method. Thymidine is commonly used to arrest cells at the G1/S boundary. As thymidine also induces cytotoxic stress, cells were subjected to a single thymidine block of 16 hours. Following release from thymidine, cells took from 8 to 10 hours to progress into S-phase and reach G2/M (Figure 5). Therefore, after thymidine pre-synchronization, cells were released into fresh medium for approximately 8 hours. After the release, a short incubation

with nocodazole – from 3 to a maximum of 4 hours – formed a mitotic trap, where cells progressing into mitosis were blocked in prophase. This novel single-thymidine-nocodazole block gave a much more efficient mitotic arrest, as shown by FACS (in HeLa cells, Figure 25; and in U2OS, Figure 27), a drastic reduction in abnormal and multinucleated cells, and a partial reduction in the levels of  $\gamma$ H2AX signal compared to nocodazole synchronization (data not shown). Therefore, the single thymidine-nocodazole arrest was the preferred choice of synchronization in subsequent experiments, except for immunofluorescences where asynchronous cells were used. In addition, to obtain an essentially pure mitotic population, mitotic shake off of synchronized cells was performed at all times.

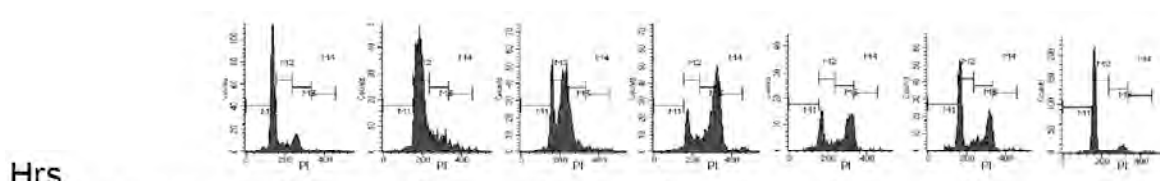
Multiple cell lines were used during the course of this study, to confirm that the results obtained were not cell line specific. The human cervical cancer cell line HeLa was subjected to similar synchronization methods as U2OS and responded in a comparable manner. In addition, asynchronous populations of BJ and MRC5 primary fibroblasts were used for immunofluorescence experiments to verify certain key molecular mechanisms in untransformed cells offering a cellular scenario closer to the physiological environment.

### ***3.3.II Phosphorylation of histone variant H2AX in mitosis: differences and similarities to interphase***

$\gamma$ H2AX is a robust read-out of the presence of DNA DSBs in cells. In interphase cells exposed to DSB-inducing agents, histone H2AX becomes rapidly and extensively phosphorylated in the chromatin flanking the damaged regions. This phosphorylation is PIKK-dependent and is a hallmark of unrepaired DSBs (Rogakou et al., 1998; Paull et al.,

2000). In mitosis, it is unclear whether  $\gamma$ H2AX signal is associated with substantial changes in chromatin compaction under unchallenged conditions. It has hitherto been shown that ATM-dependent phosphorylation of H2AX can occur during unperturbed mitosis and this is thought to be unrelated to the DDR (Huang et al., 2005b; Ichijima et al., 2005; McManus and Hendzel, 2005; Kato et al., 2008). Immunofluorescence analysis of untreated mitotic cells arising from an asynchronous population did not show an overt H2AX staining in any of the cell lines used (Figure 4). Therefore, the reported pan-nuclear  $\gamma$ H2AX staining, and especially its intensity in mitosis, may be a cell-line specific phenomenon or may be due to the method of synchronization, including prolonged nocodazole incubation, used in many studies. However, I cannot exclude that detection of a subtle increase in  $\gamma$ H2AX staining during mitosis may require sensitive analytical methods, often incompatible with the use of non-synchronized samples. To address physiological H2AX phosphorylation by western blotting, HeLa cells were released from thymidine block in G1/S and their progression was monitored for 12 hours. A mild increase in  $\gamma$ H2AX levels occurred after 9 hours, concomitantly with an increase in H3pS10 signal and chromatin compaction induced upon entry into mitosis (Figure 3). Therefore, a small amount of H2AX phosphorylation may be constitutively induced upon entry into mitosis in certain cell lines. Accordingly, a recent report showed that ATM is constitutively activated upon entry into mitosis in the absence of DNA damage (Oricchio et al., 2006).

**FIGURE 3. A slight increase in  $\gamma$ H2AX levels during mitosis in HeLa cells**

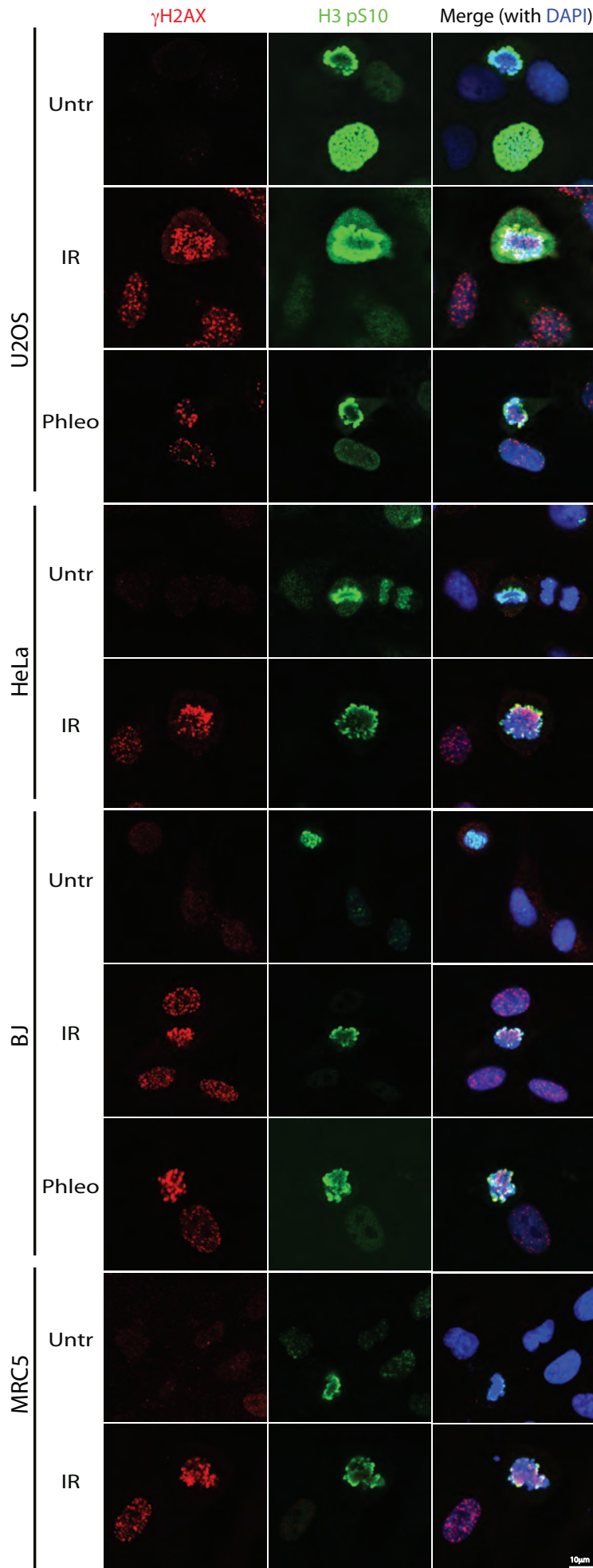


**Content not visible due to copyright limitations**

HeLa cells were released from incubation with 2.5 mM of thymidine and progression through the cell cycle was monitored by FACS (Simona Giunta; numbers on FACS images were left unmodified, although small, not to interfere with the images) and using cell cycle markers in WB (Collaborator). Cyclin D3 levels increase as cells entered S-phase. Cyclin B stabilization and H3 S10 phosphorylation indicate entrance into mitosis.

To monitor how mitotic cells respond to DNA damaging agents, I assessed  $\gamma$ H2AX focus formation in mitotic cells arising from asynchronously growing human U2OS, HeLa, BJ and MRC5 cell cultures (Figure 4). Importantly, multiple discrete  $\gamma$ H2AX foci were detected only in mitotic cells that had been exposed to IR or the radiomimetic drug phleomycin, but were not readily observed in untreated mitotic cells (Figure 4). Thus, genotoxic agents specifically induce  $\gamma$ H2AX focal accumulation in mitotic cells, indicative of DSBs. Similar to interphase cells, a few  $\gamma$ H2AX foci were observed in mitotic cells under untreated conditions, possibly representing DSBs arising from endogenous sources (Deckbar et al., 2007; Kato et al., 2009).

**FIGURE 4.  $\gamma$ H2AX forms foci in response to DNA damaging agents during mitosis**

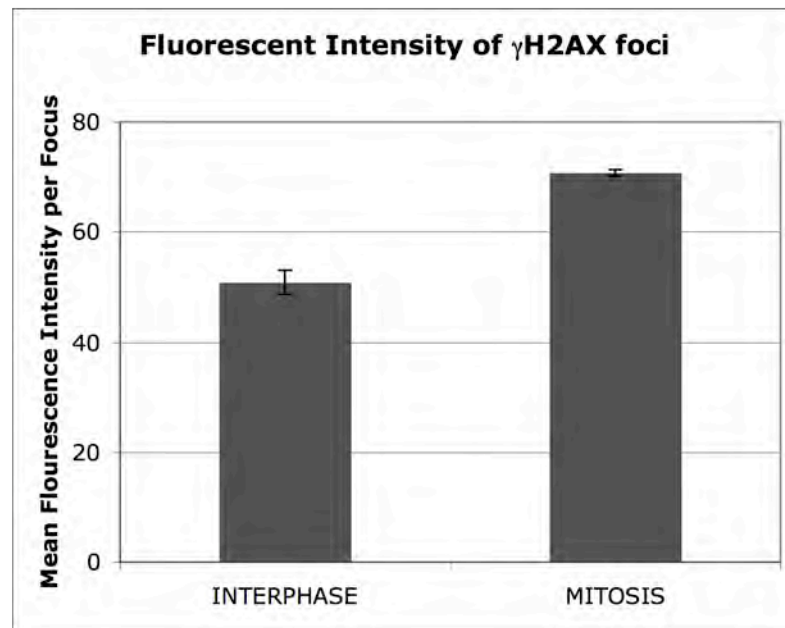


Asynchronous U2OS, HeLa, BJ and MRC5 cells were co-stained for  $\gamma$ H2AX together with histone H3pS10 to mark mitotic chromosomes. In untreated samples, mitotic cells do not show  $\gamma$ H2AX staining, similarly to cells in interphase. Upon treatment with 5 Gy of IR or 30  $\mu$ g/ml phleomycin (Phleo) and harvesting after 30 minutes, formation of  $\gamma$ H2AX foci occurs in both mitotic and interphase cells in all cell lines analyzed.

Collectively, the above findings indicate that the early  $\gamma$ H2AX focus formation at sites of damage is a common feature of both the mitotic and the interphase DDR. Nonetheless, differences exist in the basal level of H2AX phosphorylation; low levels of constitutively phosphorylated  $\gamma$ H2AX and active ATM might occur in mitotic cells to produce an underlying DDR signal. While the function, if any, of this is unknown, one possibility is that it increases the sensitivity of genome surveillance, leading to the ready activation of the DDR upon the presence of genotoxic stress in mitosis.

Although my studies indicated that DNA damage-induced  $\gamma$ H2AX foci form in mitotic cells with similar kinetics to interphase cells, quantification of  $\gamma$ H2AX mean fluorescent intensity per focus performed using Volocity software (Improvision, Coventry, UK) indicated that  $\gamma$ H2AX foci in mitosis display stronger fluorescent intensity than in interphase cells (Figure 5). Similar observations have been described in mitotic chromosomes of mouse germ cells (Forand et al., 2004), suggesting that this is not a human cancer cell-specific phenomenon. Although this observation may simply correlate with a brighter DAPI signal due to highly compacted DNA, it may also suggest that the peculiar chromatin conformation of mitotic cells may aid, rather than impede, the spreading of the  $\gamma$ H2AX modification forming larger DSB foci in mitosis. The histone variant H2AX is estimated to be present once every  $\sim$ 10 nucleosomes (Rogakou et al., 1998). It is therefore tempting to speculate that the close proximity of nucleosomes in compacted mitotic chromatin could facilitate the spreading and extent of H2AX phosphorylation.

**FIGURE 5.  $\gamma$ H2AX foci have brighter fluorescent intensities in mitotic cells than in interphase cells**

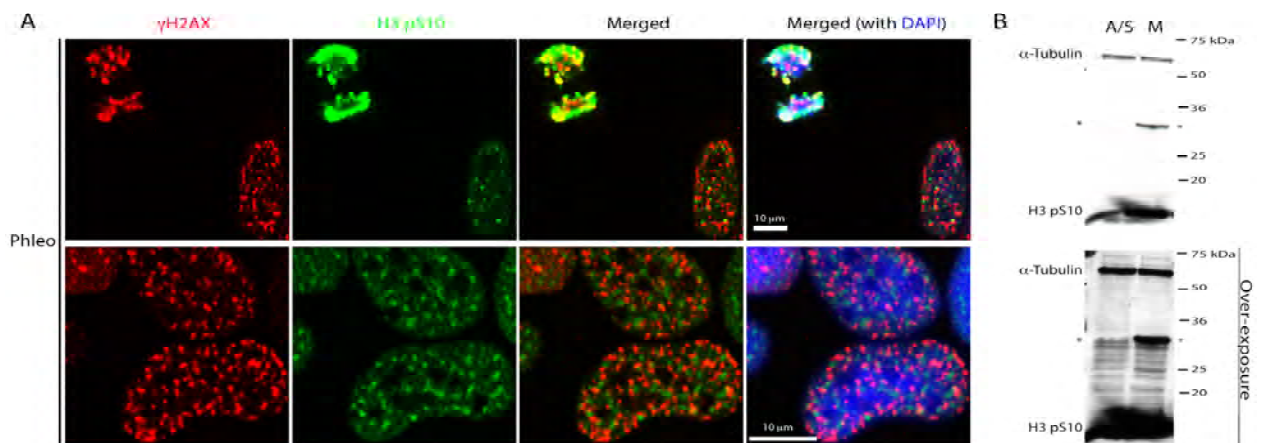


Automated quantification of  $\gamma$ H2AX average fluorescent intensity per focus, comparing interphase cells ( $n = 42$ ) versus mitotic cells ( $n = 43$ ). The error bars indicate the standard deviation within the mean of the data-set collected.

In addition to the above differences in fluorescence intensity,  $\gamma$ H2AX foci in mitosis versus interphase cells differ in relation to H3 pS10 localization. Strikingly, I observed that  $\gamma$ H2AX foci in interphase cells do not co-localize with H3 pS10 stained regions (see examples of cells in Figure 6A). In interphase, H3 pS10 marks genomic regions that are transcriptionally active (Espino et al., 2006). Therefore, the exclusion of  $\gamma$ H2AX foci from H3 pS10-stained regions represents a novel read-out to corroborate recent findings showing that actively transcribed regions are refractory to  $\gamma$ H2AX spreading (Iacovoni et al., 2010). The difference between  $\gamma$ H2AX being excluded from transcription regions marked by H3 pS10 in interphase and  $\gamma$ H2AX foci being embedded in H3 pS10 stained mitotic chromosomes during M-phase prompted me to evaluate the reasons for these cell cycle differences. It is possible that transcription, occurring within H3 pS10-stained areas in interphase, prevent H2AX phosphorylation. Accordingly, transcription inhibition during

mitosis allows  $\gamma$ H2AX foci formation. In this regard, histone modifications other than H3 pS10 may be responsible for exclusion of  $\gamma$ H2AX foci from regions of active transcription. Alternatively, H3 pS10 is further modified in mitosis and these additional modifications might render the H3 pS10 marked chromatin accessible for H2AX modifications following DNA damage. My observation that a highly modified form of H3 pS10 arises specifically in mitotic cells (Figure 6B) would favour the latter hypothesis.

**FIGURE 6. H3 pS10 localization and modifications in interphase and mitosis and its relationship to  $\gamma$ H2AX foci**

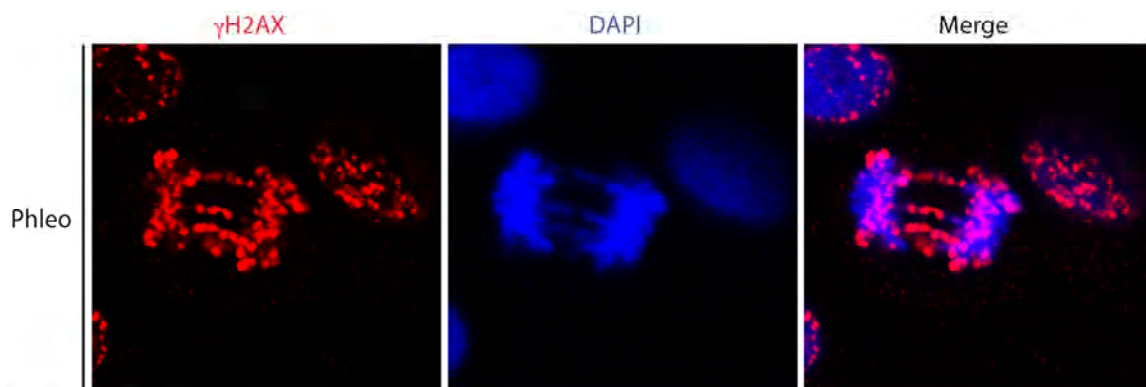


Immunofluorescence staining with phospho-antibodies against  $\gamma$ H2AX and H3 pS10. H3 pS10 displays a speckled staining in interphase cells, marking transcription sites; these are refractory to  $\gamma$ H2AX foci, formed after treatment with 30  $\mu$ g/ml of phleomycin. In mitosis, H3 is globally phosphorylated, marks mitotic chromosomes and co-localizes with  $\gamma$ H2AX (A). H3 pS10 is enriched in samples synchronized using the thymidine-nocodazole method (M) and can be detected strongly at 16 kDa. Moreover, H3 pS10 is differentially modified specifically in mitotic cells displaying a strong band at  $\sim$ 30 kDa (asterisk), possibly due to SUMOylation (one SUMO moiety is  $\sim$ 15 kDa) or to ubiquitylation by a short chain of ubiquitins (each ubiquitin is about 8 kDa).

The formation of mitotic DNA bridges between anaphase chromosomes that interconnect the two sister chromatids is a hallmark of genomic instability. The DNA bridges supposedly originate from concatenated, late-replicating DNA, carried into mitosis before duplication of the site by DNA synthesis is completed. In mitosis, the decatenation checkpoint is in place to resolve mitotic structures where entangled or catenated DNA

prevents chromosome segregation (reviewed in Damelin and Bestor, 2007). The decatenation process that resolves mitotic DNA bridges requires factors such as the WRN and BLM helicases and DNA topoisomerases – including Topo II and III – that release DNA coiling (Holm et al., 1989; Franchitto et al., 2003; Seki et al., 2006a). During my analyses, I noticed that some U2OS cancer cells displayed mitotic DNA bridges in anaphase. This phenomenon readily increased upon treatment with genotoxins. Interestingly, I found that, in cells treated with DNA damaging agents such as phleomycin, mitotic bridges are coated by  $\gamma$ H2AX foci, indicating the presence of DNA breaks on this fine DAPI-stained chromatin fibres (Figure 7). This infers that DSB found in the bulk of the mitotic chromosomes or on fine DNA bridges between the sisters chromatids are equally marked by the focal accumulation of  $\gamma$ H2AX.

**FIGURE 7. DSBs on mitotic DNA bridges are marked by  $\gamma$ H2AX foci**

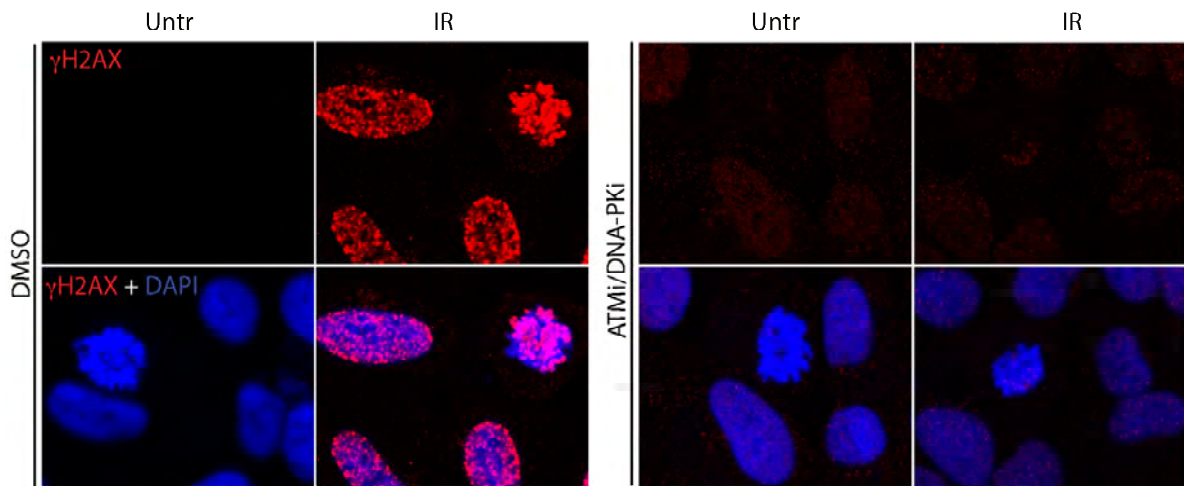


In asynchronous samples treated with phleomycin, mitotic cells found interconnected by DNA bridges between the anaphase/telophase chromosomes display  $\gamma$ H2AX foci. The concatenation must be resolved to avoid failure in chromosome segregation, eventually leading to mitotic catastrophe and cell death.

### ***3.3.III Activation of apical PIKK kinases ATM and DNA-PK leads to H2AX phosphorylation in mitosis***

To understand the dependencies of  $\gamma$ H2AX focus formation in mitotic cells, I examined the role of the apical PIKK kinases, ATM and DNA-PK, during mitosis. In interphase cells, these kinases act semi-redundantly to phosphorylate the H2AX C-terminal tail in chromatin flanking DSB sites (Burma et al., 2001; Hickson et al., 2004; Stiff et al., 2004; Wang et al., 2005). I assessed whether IRIF formation in mitotic cells required ATM and DNA-PK kinase activities, by using small-molecule inhibitors specific to each kinase (Hickson et al., 2004; Leahy et al., 2004). Partial redundancy between the two kinases in mediating H2AX phosphorylation and IRIF formation were observed (Figure 8). Consistent with previous studies in interphase cells, ATM inhibition markedly reduced IRIF intensity (data not shown), whereas combined treatment using ATM and DNA-PK inhibitors completely abrogated IRIF in M-phase cells (Figure 8). By contrast, DNA-PK inhibition alone did not markedly affect H2AX phosphorylation and IRIF formation (data not shown); however, DNA-PK inhibitor's additive effect on abolishing  $\gamma$ H2AX foci indicates that DNA-PK kinase can be activated in mitosis and acts in a compensatory manner in the absence of ATM.

**FIGURE 8. ATM and DNA-PK mediate  $\gamma$ H2AX IRIF formation in mitosis.**

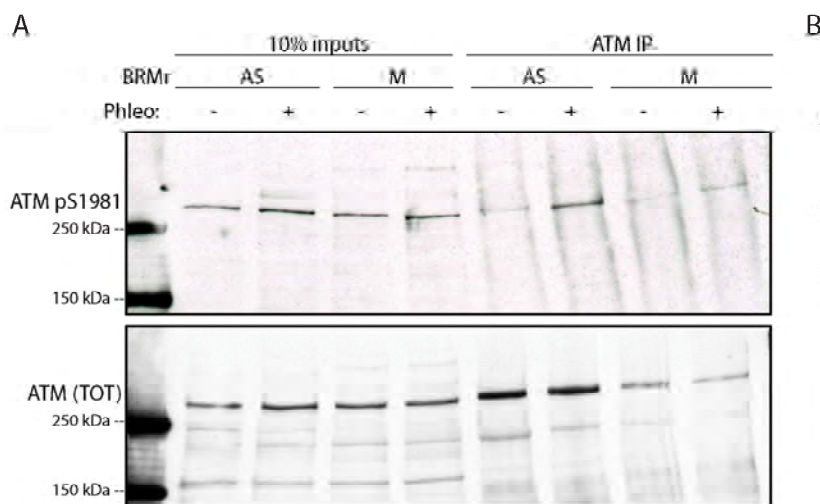


Asynchronous U2OS were co-stained for  $\gamma$ H2AX and DAPI. Upon treatment with 5 Gy of IR formation of  $\gamma$ H2AX foci occurs and this is abrogated in both mitotic and interphase cells when cells are pre-treated for 1 hour with combination of ATM and DNA-PK inhibitors before irradiation.

In order to verify ATM activation during mitosis, I monitored the presence of the auto-phosphorylated form of ATM on S1981 (Bakkenist and Kastan, 2003). Because most commercial phospho-antibodies against ATM pS1981 are not highly specific and mainly recognize various ATM target protein phosphorylations, such as those on 53BP1, I performed an ATM IP from asynchronous and thymidine-nocodazole mitotic extracts in the presence or absence of DNA damage. In line with DNA damage leading to ATM activation in interphase cells (Bakkenist and Kastan, 2003), ATM S1981 was found to be phosphorylated in extracts from IR-treated mitotic cells (Figure 9A and van Vugt et al., 2010). To further corroborate the finding that ATM is fully active in mitotic cells, I collaborated with Rimma Belotserkovskaya, a postdoctoral researcher in Steve Jackson laboratory. We assessed ATM-dependent phosphorylation of targets other than histone H2AX in a DNA damage-induced manner. Phosphorylation of KAP1 on serine 824, an ATM-dependent modification, showed a similar profile to  $\gamma$ H2AX, where a weak signal is present in the untreated mitotic samples while, following treatment with 2 Gy of IR, the

phospho-signal in the mitotic sample increased significantly, and to essentially the same extent as it did in the asynchronous cells (Figure 9B). Collectively, these data indicate that a basal level of activated ATM is present in mitotic cells (Figure 9A), possibly due to constitutive activation of ATM during mitosis (Oricchio et al., 2006) and/or to the synchronization method. However, upon induction of DNA damage, ATM becomes fully activated and it promotes robust DNA damage dependent phosphorylations of selected targets, to similar levels as those seen in interphase cells.

**FIGURE 9. ATM is activated by DNA damage and phosphorylates selected substrates in mitosis**



**Content not visible due to copyright limitations**

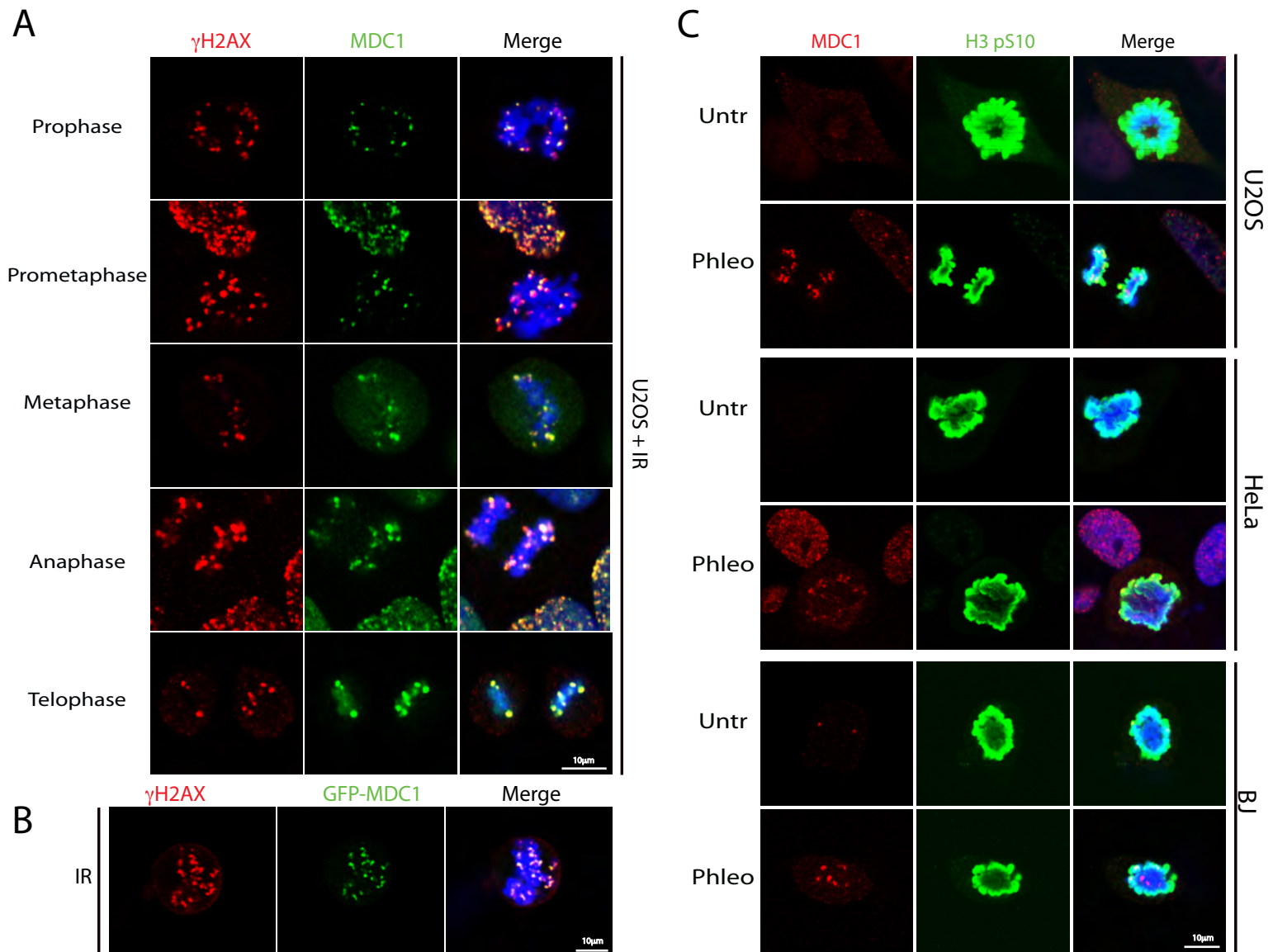
ATM is auto-phosphorylated on S1981 following IR (2 Gy) treatment of either asynchronous (AS) or mitotic (M) cells. ATM was immunoprecipitated with anti-ATM antibody (Table 1) and then detected with an antibody recognizing phosphorylated S1981 (top panel). Although a background phospho-band is observed in untreated samples, the phospho-signal increases after irradiation. The lower level of total ATM (lower panel) IPed from mitotic cells and a mild phosphorylation-induced smear suggests that the proportion of phosphorylated ATM is similar to that in interphase (A). BioRad molecular weight markers are shown (BRMr). Phosphorylation of KAP1 on ATM-target site serine 824. KAP1 is phosphorylated to the equivalent extent after irradiation in mitotic (M) and interphase cells (AS). A faint phospho-signal is detected before damage in mitosis (B; panel B from Collaborator).

### ***3.3.IV Mitotic MDC1 is recruited to IRIF and is competent to bind $\gamma$ H2AX***

MDC1 acts as a mediator protein in the DDR cascade, inciting signal transduction events following induction of a DSB. MDC1 is one of several DDR mediators, like BRCA1, 53BP1 and TopBP1, to contain BRCT domains. BRCT domains are autonomously folding modules consisting of about 100 amino acids capable of mediating protein-protein interactions (Callebaut and Mornon, 1997). MDC1 tandem twin BRCTs, located at the C-terminus of the protein, have specific affinity for the  $\gamma$ H2AX phospho-epitope (Stucki et al., 2005). Since phosphorylated S139 of H2AX creates a docking site for MDC1, I assessed whether MDC1 was recruited to DSB sites in mitosis. By using two different anti-MDC1 antibodies, as well as cells stably expressing a green-fluorescent protein (GFP)-MDC1 fusion protein, I found that MDC1 formed foci in mitotic cells that had been treated with IR or phleomycin (Figure 10A, 10B and 10C) and co-localized with  $\gamma$ H2AX (Figure 10A and 10B). MDC1 foci were also detected in mitotic cells arising from asynchronously growing HeLa and BJ cells (Figure 10C).

MDC1 foci were not as easily discerned as  $\gamma$ H2AX foci in mitotic cells (Figure 13E), as well as in interphase cells, due to a diffuse pan-nuclear staining that partially hindered foci visualization. To overcome this issue, I used a phospho-antibody raised against MDC1 phospho-SDTD motifs (pS329 and pT331; Chapman and Jackson, 2008) that was found to selectively detect MDC1 associated with DSB-flanking chromatin with reduced pan-nuclear background (Figure 10A prophase and prometaphase panels) compared to the antibody against the total protein (Figure 10A, metaphase panel). Detailed analyses with this antibody revealed that  $\gamma$ H2AX and MDC1 IRIF were present and co-localized in all mitotic stages (Figure 10A).

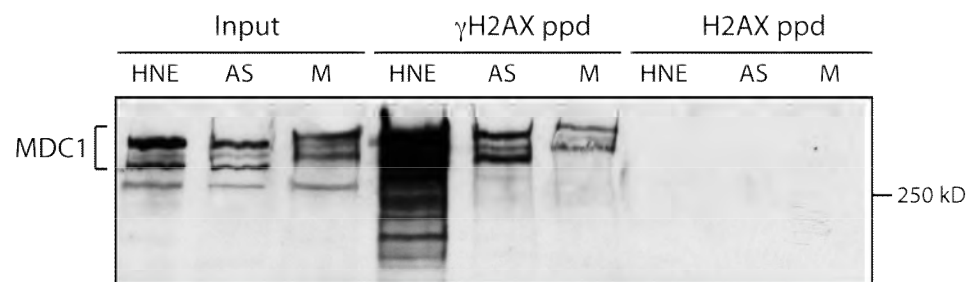
**FIGURE 10. MDC1 localizes to sites of DSB after induction of DNA damage during mitosis**



MDC1 co-localizes with  $\gamma$ H2AX foci in various mitotic stages of U2OS cells after IR (5 Gy; A). Prophase and prometaphase panels were co-stained for  $\gamma$ H2AX and MDC1 phospho - SDTD antibody, while the other panels show the diffused pan-nuclear staining of MDC1 total antibody underlying the IR foci (A). GFP-MDC1 accumulates in  $\gamma$ H2AX foci upon IR treatment (B). Formation of MDC1 IRIF in U2OS, HeLa and BJ cells upon DSB induction by 30  $\mu$ g/ml phleomycin (Phleo) but not in untreated cells. Cells were grown on coverslips, treated as indicated and processed for immunofluorescence 30 min after treatments. Mitotic chromosomes were co-stained for histone H3pS10 (C).

To confirm the capability of mitotic MDC1 to physically bind to the phosphorylated S139 epitope of  $\gamma$ H2AX, I performed *in vitro* peptide pull-down experiments with synthetic peptides corresponding to the unmodified and phosphorylated H2AX C-terminus. Consistent with the above observations, I found that the hyper-phosphorylated, slower migrating forms of MDC1 derived from mitotically-arrested cells (Xu and Stern, 2003) were capable of binding to the  $\gamma$ H2AX peptides, as was MDC1 from asynchronous cell extracts (Figure 11).

**FIGURE 11. The hyper-phosphorylated mitotic MDC1 binds to  $\gamma$ H2AX**



Mitotic MDC1 is competent to bind to the  $\gamma$ H2AX phospho-peptide, in spite of its hyper-phosphorylated mitotic status, as shown. Phosphorylated H2AX C-terminal, but not the unmodified peptides, pulls down MDC1 from all extracts. Inputs represent 10% of the total protein. The whole cell extracts were prepared from asynchronous (AS) and mitotic (M) cells, or using commercially available HeLa nuclear extract (HNE).

Next, I assessed ATM-dependent phosphorylation of mitotic MDC1 on threonine 719 within a consensus ATM target motif (TQXF) by using a phospho-specific antibody directed against this site (Kolas et al., 2007). MDC1 was constitutively phosphorylated in untreated mitotic cells and this phosphorylation increased upon irradiation (data not shown), with similar phosphorylation profiles displayed by other ATM targets, such as  $\gamma$ H2AX and KAP1 (Figure 9B). These data imply that MDC1 recruitment to the site of DSBs is fully proficient in mitosis and occurs in the same molecular fashion as in interphase cells.

### ***3.3.V The Mre11-Rad50-Nbs1 complex localizes to DSB sites in mitosis and may serve to hold DNA ends together***

The MRN complex is a heterotrimeric unit composed of Mre11, Rad50 and Nbs1. The activity of MRN is important for multiple steps in the DDR. MRN acts as a sensor and is also essential for full ATM activation (Uziel et al., 2003). MRN-dependent DNA unwinding and tethering activities are required to recruit ATM firstly to the direct proximity of the DNA ends (Williams et al., 2007), and in turn, promote ATM binding to the chromatin around the break *via* MRN ability to bind MDC1, aiding DDR propagation.

In accord with ATM activation being mediated by the MRN complex, I wanted to verify MRN recruitment to DSB sites in mitosis. In collaboration with Rimma Belotserkovskaya, we monitored the localization of Nbs1 before and after DNA damage. Antibodies against total Nbs1 show high levels of background signal, which hinders detection of nuclear foci following DNA damage in both mitotic and interphase cells. To circumvent this problem, we performed pre-extraction to remove the pan-nuclear Nbs1 and retain only the chromatin bound fraction of Nbs1 localized at DSB sites. Thymidine-nocodazole synchronized U2OS cells were collected by mitotic shake-off and, following CSK pre-extraction, a cytospin centrifuge was used to attach mitotic cells to a poly-L-lysine-coated coverslip and permit their detection by immunostaining analysis. We observed focal accumulation and co-localization of Nbs1 with  $\gamma$ H2AX on mitotic chromosomes after irradiation (Figure 12). Similarly to its role in interphase cells, the MRN complex recruitment to DSBs during mitosis might serve as a scaffolding platform for enrichment and spreading of ATM,  $\gamma$ H2AX and MDC1 into the chromatin flanking the DSB, to regulate ATM activation and carry out initial resection steps at the DSB site. Furthermore, the physical structure of the

MRN complex could serve to hold ends together *via* the DNA end tethering activity of Mre11 (Williams et al., 2008) Altogether, these data show that mitotic DSBs are marked by PIKK-dependent  $\gamma$ H2AX, MDC1 and MRN foci formation during mitosis.

**FIGURE 12. The MRN subunit Nbs1 is recruited to IRIF in mitosis**



**Content not visible due to copyright limitations**

Nbs1 co-localizes  $\gamma$ H2AX in mitotic cells treated with IR (5 Gy; image from Collaborator). After treatment, cells were harvested by mitotic shake-off, CSK pre-extracted, and attached to coverslips by cytospin for 5 minutes at 500 rpm before co-staining with  $\gamma$ H2AX and Nbs1.

### **3.3.VI *53BP1 fails to be recruited to sites of DNA damage during mitosis***

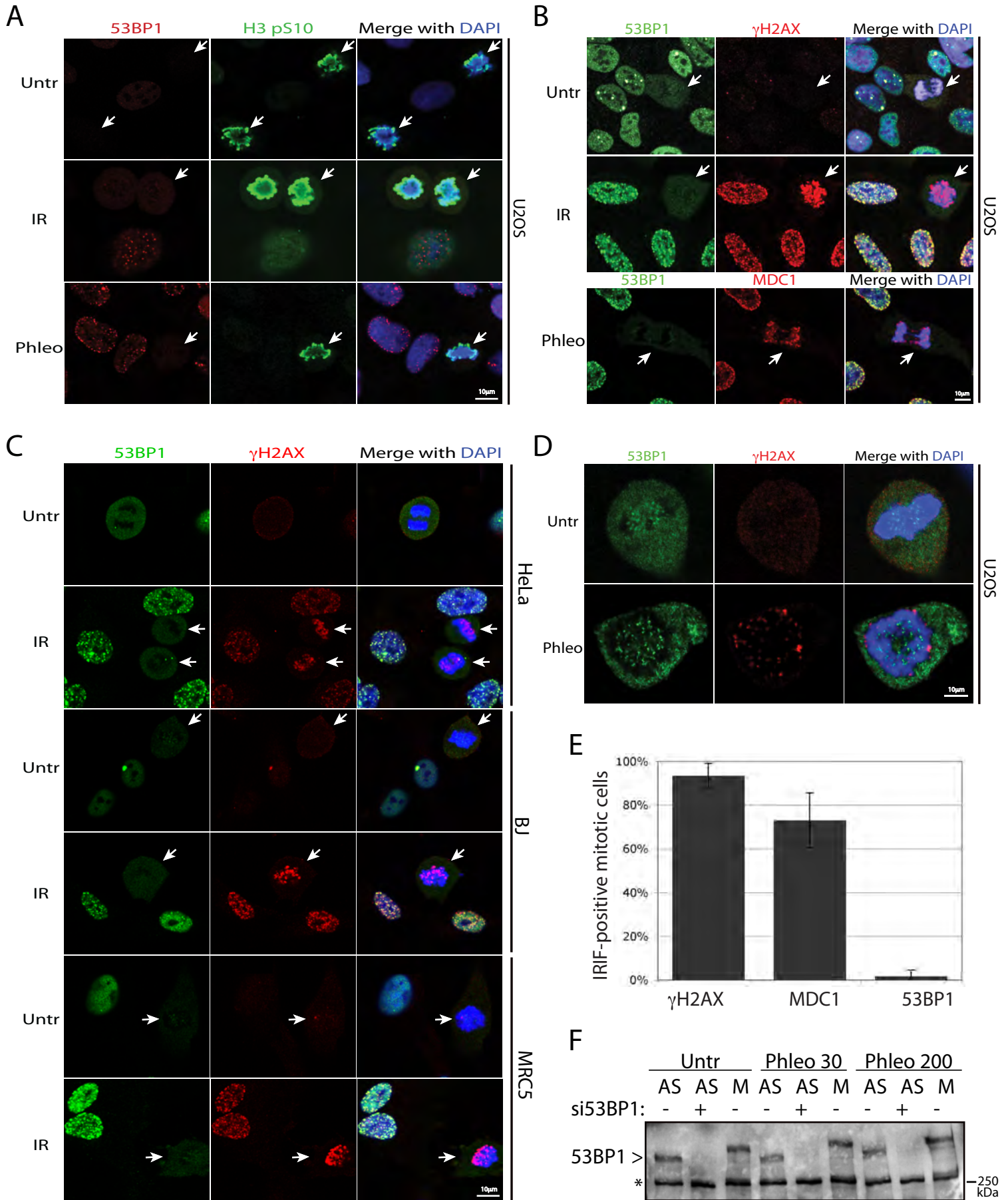
Having demonstrated that mitotic cells respond to DSB induction by ATM activation, phosphorylation of  $\gamma$ H2AX and by the recruitment of MDC1 and MRN to the DSB sites, I next examined the behaviour of another mediator protein, 53BP1. Although live imaging of interphase cells has shown that 53BP1 binds within seconds after DSB formation (Bekker-Jensen et al., 2005), its visualization within foci requires accumulation of many molecules, spreading over a large chromatin domain surrounding the lesion and follows

chromatin rearrangements (Schultz et al., 2000), placing it in the ‘second wave’ of DDR recruitment.

A striking feature of mitotic cells exposed to DNA damage is the failure to recruit 53BP1. Using an anti-53BP1 antibody, I found that endogenous 53BP1 not only failed to be recruited to IRIF and did not co-localize with  $\gamma$ H2AX and MDC1 after irradiation or treatment with phleomycin, but was also mostly excluded from chromatin during mitosis in U2OS cells (Figure 13A and 13B). Indeed, in mitotic cells, 53BP1 antibodies faintly stain a diffuse smear surrounding the chromatin, before and after damage, suggesting that mitotic 53BP1 is unable to bind to DNA. Using U2OS cells stably expressing GFP-53BP1, no focal recruitment or chromatin co-localization of GFP-53BP1 was observed after irradiation (data not shown), indicating that failed detection of 53BP1 foci was not due to impaired antibody penetrability. In line with exclusion of 53BP1 from IRIF in mitotic U2OS cells, 53BP1 also did not form readily discernible IRIF in mitotic HeLa, BJ or MRC5 cells (Figure 13C). Thus, 53BP1 exclusion from mitotic chromatin is not a cell-line specific phenomenon.

Immunoblot analyses demonstrated that 53BP1 protein levels were similar throughout the cell cycle and, in agreement with an earlier study (Jullien et al., 2002), mitotic 53BP1 displayed slower gel mobility due to hyper-phosphorylation in M-phase (Figure 13F). Thus, the overall low intensity of 53BP1 immunostaining observed in mitotic cells is not caused by reduced proteins level but can be explained by dispersal of the protein throughout the whole volume of the cell upon nuclear envelope breakdown.

**FIGURE 13. 53BP1 is excluded from DNA damage-induced foci during mitosis**



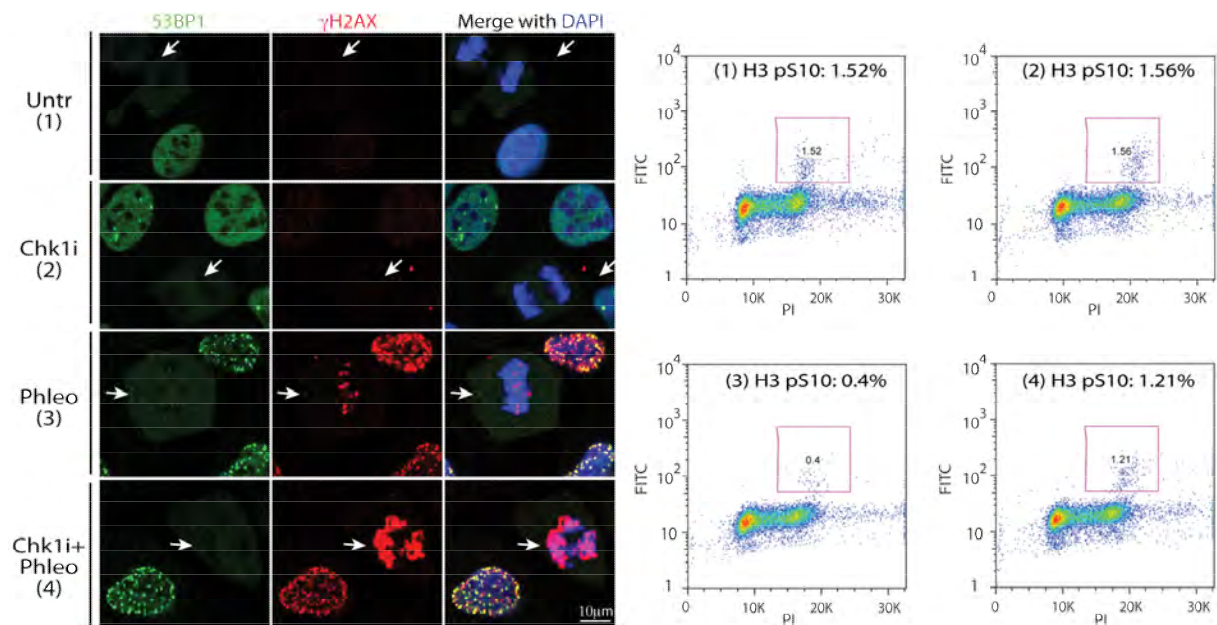
Co-staining for 53BP1 and H3pS10 before or after irradiation (5 Gy) or phleomycin treatment of asynchronously growing U2OS cells (A). Co-staining of either mock- or IR-treated cells with 53BP1 and  $\gamma$ H2AX antibodies; phleomycin-treated cells co-stained for 53BP1 and MDC1 (B). HeLa, BJ and MRC5 cells co-stained for  $\gamma$ H2AX and 53BP1 also display no 53BP1 focal accumulation (C). White arrows point to mitotic cells. Enlarged mitotic cell images show lack of co-localization between the punctate 53BP1 staining and  $\gamma$ H2AX damage foci (D). The histogram represents a quantification of  $\gamma$ H2AX, MDC1 and 53BP1 focus-positive mitotic cells after IR treatment from three independent experiments (n>200). Error bars indicate standard deviation (E). Immunoblot of 53BP1 in asynchronous (AS), si53BP1-transfected and synchronized mitotic (M) cells, untreated or treated with 30 or 200  $\mu$ g/ml of phleomycin. Asterisk indicates a cross-reacting band (F).

In addition, and consistent with the previously reported 53BP1 association with kinetochores (Jullien et al., 2002), I observed a fine, punctuated staining of 53BP1 on condensed pro-metaphase chromosomes in both untreated and irradiated cells (Figure 13D); however, those foci never co-localized with  $\gamma$ H2AX (Figure 13D). Thus, even though  $\gamma$ H2AX, MDC1 and MRN form foci in mitotic cells in a similar manner and with similar dynamics to those in interphase cells, 53BP1 is never recruited to mitotic chromatin (Figure 13E), in marked contrast to its behaviour in interphase cells.

To determine whether 53BP1 is actively excluded from IRIF upon mitotic entry, I irradiated asynchronously growing U2OS cells in the presence or absence of AZD7762, an inhibitor of the DNA damage checkpoint kinases Chk1/2 (Zabludoff et al., 2008), and then measured mitotic indices by FACS with H3pS10 antibody (Juan and Darzynkiewicz, 2004). Chk1 inhibitor was used to override the G2/M checkpoint and allow damaged interphase cells to enter mitosis. In the undamaged samples, both untreated and treated with the Chk1 inhibitor, approximately 1.5% of cells were in mitosis (Figure 14). A small increase in the mitotic index of samples treated with Chk1 inhibitor alone may be due to a minor proportion of asynchronously growing cells suffering endogenous DNA damage, yet failing to activate the G2/M checkpoint in the absence of Chk1, and entering mitosis. After a two-hour phleomycin treatment, however, the mitotic index dropped to 0.4% because the G2/M checkpoint prevents damaged cells proceeding into mitosis, while a large proportion of cells damaged in mitosis progress into G1 within the two-hour time frame. By contrast, when the G2/M checkpoint was inactivated by pre-incubating cells with the Chk1 inhibitor prior to phleomycin treatment, the mitotic index was restored to 1.2% (Figure 14), as has been observed previously in combination with other DNA damaging agents (Zabludoff et al., 2008). These data thereby imply that in the latter situation the majority of such mitotic

cells would have arisen from damaged G2 cells progressing into mitosis within the two-hour phleomycin treatment. Under these experimental settings – where damaged cells with an inhibited G2/M checkpoint entered mitosis – I still did not observe 53BP1 foci in mitotic cells (Figure 14). These data are in agreement with a recent report demonstrating that 53BP1 dissociates from endogenously arising DSBs at the G2/M boundary (Nelson et al., 2009), and suggest that 53BP1 is actively removed from mitotic chromatin.

**FIGURE 14. 53BP1 is actively excluded from IRIF upon entry into mitosis**



Active exclusion of 53BP1 in mitotic cells (white arrows). Asynchronously growing U2OS cells were left untreated (Untr; 1) or treated with 30  $\mu\text{g/ml}$  of pleomycin for 2 hours (Phleo; 3). Following a 3-hour incubation with 50 nM of Chk1 inhibitor (Chk1i; 2), cells were treated with pleomycin for 2 hours (Chk1i + Phleo; 4) and co-stained for 53BP1 and  $\gamma\text{H2AX}$ . Mitotic indices (purple boxes) were determined by FACS analysis of cells co-stained with PI (x axis) and H3pS10 antibody (FITC, y axis).

In parallel with the above studies, live-cell imaging of asynchronous U2OS cells stably expressing GFP-53BP1 was used to assess 53BP1 localization when cells irradiated during mitosis re-entered G1. Interphase cells present in the field next to M-phase cells formed 53BP1 foci within few minutes following irradiation. By contrast, 53BP1 staining

remained diffuse in mitotic cells until division was complete and nuclei re-formed as cells entered G1, at which stage 53BP1 started accumulating within IRIF. Equivalent results were also obtained for cells treated with the DSB-inducing agent neocarzinostatin (data not shown). Collectively, these findings suggested that inhibition of 53BP1 recruitment to DSBs is limited to mitosis, and that association of 53BP1 with IRIF is concomitant with nuclear envelope formation and chromatin decompaction in G1.

### ***3.3.VII Investigating the mechanisms of 53BP1 exclusion in mitosis***

To gain further insight into the mechanisms of 53BP1 exclusion from mitotic chromatin, I collaborated with Rimma Belotserkovskaya to examine whether 53BP1 requirements to bind to the damaged chromatin were satisfied in mitosis. In interphase cells, 53BP1 focal accumulation is a multifactorial process, which is influenced by a plethora of upstream events and epigenetic modifications, including phosphorylation, ubiquitylation, acetylation and methylation. Constitutive epigenetic marks such as di-methylated H3K79 and H4K20 are a prime chromatin requirement for binding and retention of 53BP1 to the sites of DNA damage by the Tudor domain (FitzGerald et al., 2009). Firstly, we monitored the presence of the methylated form of these histone marks in mitosis and their dynamics during the cell cycle. H3K79me2 and H4K20me2 are present in mitosis (Figure 15) and their levels are maintained constant throughout the cell cycle.

**FIGURE 15. Methylated marks on histones H3K79 and H4K20 are retained in mitosis**

**Content not visible due to copyright limitations**

Di-methylated histones H4K20 and H3K79 epigenetic marks serve for 53BP1 to bind to chromatin and are present on mitotic chromatin at similar levels as in interphase cells; also, their levels do not show overt changes before and after IR (5 Gy; image from Collaborator).

Next, we examined the role of mitosis-specific PTMs in preventing 53BP1 recruitment. 53BP1 has slower electrophoretic gel migration properties during M-phase (Figure 13F), likely reflecting hyper-phosphorylation in mitosis that is characteristic of many proteins (Poon, 2007). Hence, we reasoned that induction of mitotic-specific phosphorylations might hamper the ability of 53BP1 to bind to DSBs.

**Content not visible due to copyright limitations**

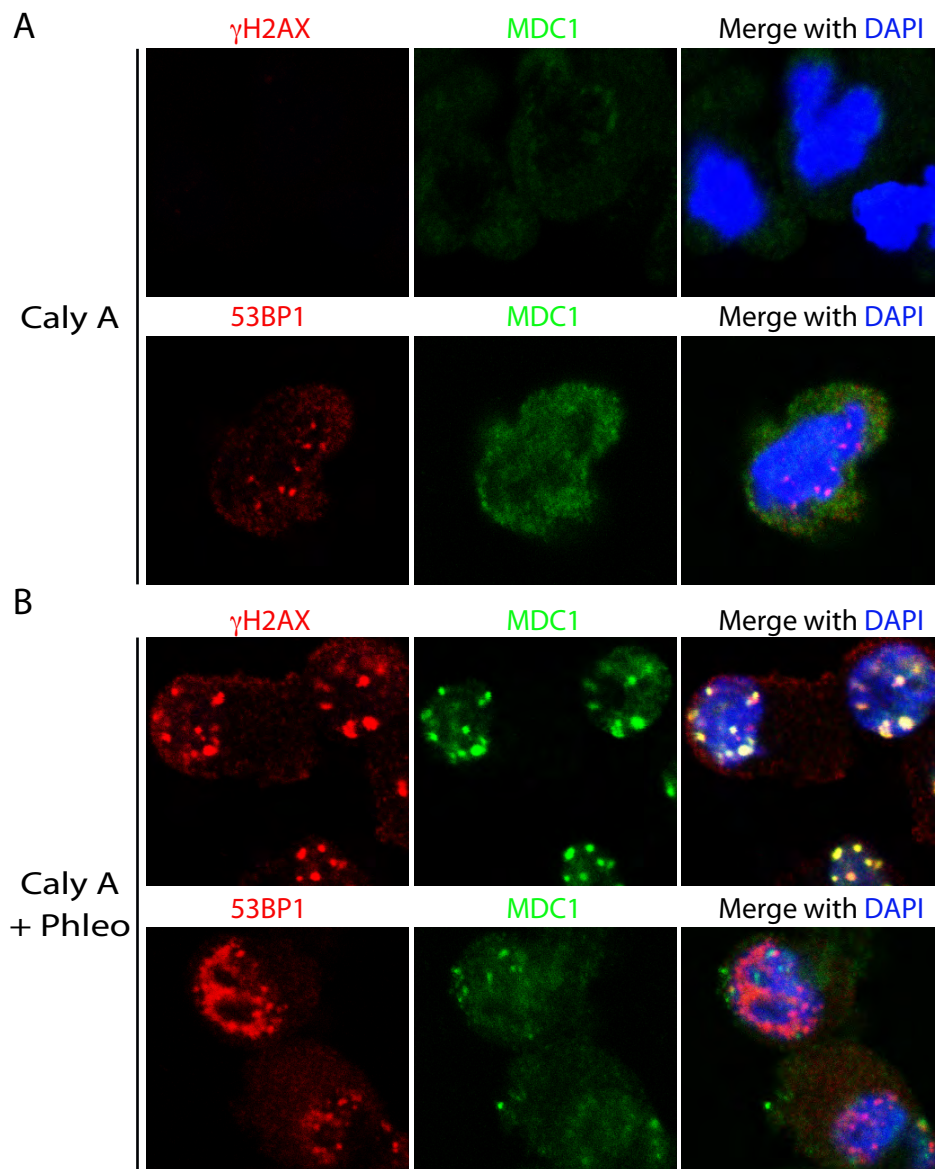
Our analyses of the epigenetic marks and 53BP1 mitosis-specific PTMs did not elucidate the underlying mechanisms of 53BP1 exclusion from mitotic chromatin. However, although methylated histone marks are present in mitosis, highly compacted chromatin, typical of mitotic chromosomes, may mask methylated histones rendering them inaccessible; indeed, 53BP1 exclusion is timed with the compaction of DNA into mitotic chromatin in early prophase. In addition, other requirements for 53BP1 IRIF retention may not be fulfilled.

### **3.3.VIII Impact of mitotic chromatin structure on the DDR**

To assess whether the recruitment of 53BP1 to DSB in mitosis was hampered by physical inaccessibility to damaged DNA due to chromatin compaction in mitosis, the chromatin conformation was manipulated with several chromatin-disrupting agents. Chromatin organization in mitotic cells can be altered by chloroquine, HDAC inhibitors and hypotonic conditions to induce relaxation of chromatin in the context of mitotic chromosomes. On the other hand, Okadaic acid, calyculin A and taxol are used to mimic mitotic state by causing premature chromatin condensation in interphase.

Calyculin A is an inhibitor of serine/threonine protein phosphatases that induces PCC in interphase cells within minutes of treatment. During PCC, the chromatin increases in compaction, mimicking mitotic DNA (Ishida et al., 1992; Alsbeih and Raaphorst, 1999; Kanda et al., 1999). I used Calyculin A to induce PCC and monitor the ability of 53BP1 to form IRIF under these conditions. Although Calyculin A has been shown to impact on  $\gamma$ H2AX phosphorylation, DNA damage-induced  $\gamma$ H2AX foci formation is not compromised following calyculin A treatment (my own observation and Svetlova et al., 2007). The use of calyculin A for less than 10 minutes was sufficient to induce rounding of cells due to chromatin compaction, visible under light microscope. Next, U2OS cells were treated with phleomycin for 45 minutes, in the presence of calyculin A. Although calyculin A treatment *per se* induced MDC1 and 53BP1 staining in the absence of DNA damage, an obvious accumulation of DDR foci was observed in most PCC cells treated with phleomycin. The DDR factors monitored were recruited to DDR foci in spite of the compacted chromatin induced by calyculin A (Figure 17), suggesting that the physical barrier enforced by the compacted mitotic chromatin cannot be the only factor responsible for the exclusion of 53BP1 from DNA damage foci in mitosis.

**FIGURE 17. 53BP1 forms IRIF following Calyculin A-induced premature chromosome condensation in interphase cells**



DNA damage foci formation following induction of PCC by treatment with 2nM of Calyculin A. Calyculin A alters the DNA morphology of asynchronous U2OS cells, causing a visible compaction of chromatin, as shown by the bright DAPI staining of the prematurely compacted DNA and the change in nuclear morphology, closely resembling those of mitotic cells (A and B). Treatment with Calyculin A was performed for 40 minutes to match the prolonged treatment in damaged samples. Immunofluorescence analyses were performed using  $\gamma$ H2AX, MDC1 and 53BP1 antibodies. 53BP1 formed sparse foci, whereas MDC1 showed a faint diffused staining in Calyculin A cells in absence of DNA damaging agents (A). However, cells that underwent 10-minutes treatment with Calyculin A, followed by 30 minutes co-treatment with 30  $\mu$ g/ml of phleomycin, showed obvious  $\gamma$ H2AX, MDC1 and 53BP1 foci formation at damage sites during PCC.

These results were confirmed using GFP-MDC1 and GFP-53BP1 stable cell lines (data not shown). In addition, upon calyculin treatment, 53BP1 exhibited slower gel mobility, likely reflecting its hyperphosphorylated status (calyculin is a potent inhibitor of protein phosphatases 1 and 2A). 53BP1 phosphorylation status following calyculin treatment mimicked that in mitotic cells. Yet, hyper-phosphorylated 53BP1 remained associated with IRIF, even after PCC induction. I therefore concluded that calyculin-induced chromatin compaction and non-specific protein hyperphosphorylation are not sufficient to render 53BP1 refractory to recruitment into IRIF.

Nevertheless, chromatin manipulation by calyculin A presented several experimental caveats. Firstly, being a phosphatase inhibitor, calyculin A altered the dynamic equilibrium of protein phosphorylation, possibly leading to DDR activation in the absence of DNA damage. It is also unclear whether calyculin A induces chromatin compaction in all stages of the cell cycle and uniformly compacts all regions of DNA within the nucleus. PCC is rapidly induced upon calyculin A treatment in S-phase and G2, but possibly not to the same extent in G1, due to low cyclin B levels (Kanda et al., 1999). In my experiments, all cells displayed a similar rounded morphology, with visibly compacted chromatin. Nonetheless, I could not assess if the DNA of cells residing into S-phase at the time of the analysis was compacted to the same extent as G1 and G2 cells. Furthermore, induction of PCC by calyculin A treatment affected the balance between the amounts of chromatin-bound and soluble 53BP1 (data not shown), suggesting it does not only impinges on chromatin structure.

In parallel with the above studies, I used the intercalating agent chloroquine to induce relaxation of mitotic chromatin by partial unwinding of DNA. However, the treatment severely altered both chromatin and cellular morphology and lead to activation of ATM and  $\gamma$ H2AX in a non-DSB related manner (data not shown). These conditions rendered unsuitable the use of chloroquine for the purposes of this analysis. These and other attempts to manipulate chromatin conformation by HDAC inhibitors- and chloroquine-mediated chromatin relaxation led to inconclusive results.

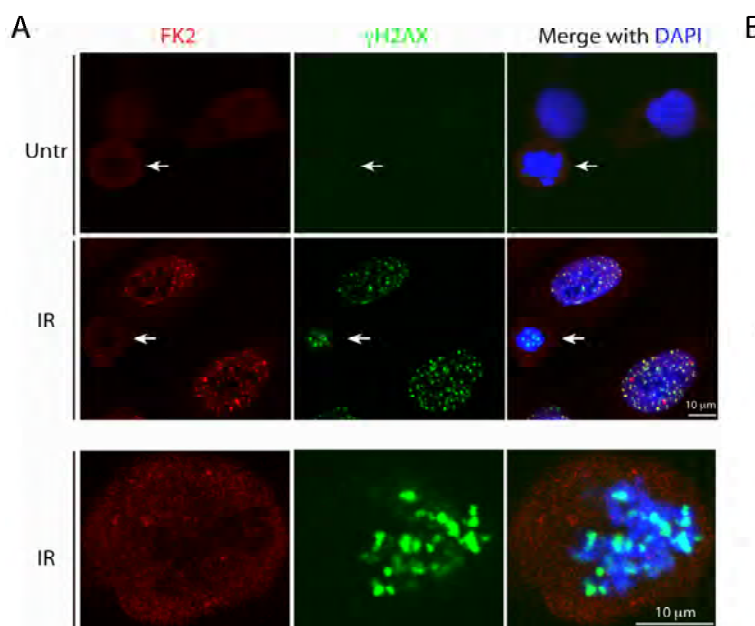
The data showing that 53BP1 is capable of binding to condensed chromatin outside of mitosis indicates that the mitotic chromatin status is unlikely to represent a physical limitation to 53BP1 recruitment *per se*, especially considering that chromatin is not maximally condensed during mitosis and retains a certain degree of plasticity.

### ***3.3.IX Association of ubiquitin conjugates with DNA damage sites is absent during mitosis***

Ubiquitylation of local nucleosomes is a main epigenetic mark of DNA DSBs. Given ubiquitylation represents one of the chief requirements for 53BP1 recruitment, I next assessed the ubiquitylation status of cells during mitosis. Previous work has shown that ubiquitylated H2A (ubH2A) is essentially absent from mitotic chromatin (Wu et al., 1981) and that active H2A de-ubiquitylation by the ubiquitin-processing protease USP16 at the G2/M transition is required for chromatin condensation (Matsui et al., 1979; Cai et al., 1999; Joo et al., 2007). The ubH2A appears to be mutually exclusive with phosphorylation of H3 S10, indicating that H2A deubiquitination is critically involved in cell cycle progression (Joo et al., 2007). In agreement with these data, a drastic reduction in the

immunoblotting signals for ubiquitylated H2A, and also for H2AX, was observed in mitotic cells, whether or not they had been irradiated (Figure 18B). Although ubiquitylation of H2AX partially increased after DNA damage, it did not reach the level of asynchronous damaged samples. Focal accumulation of ubiquitin induced by DNA damage can be cytologically visualised as nuclear aggregates in interphase cells using FK2 antibody that detects protein-ubiquitin conjugates. In mitotic cells, however, no protein-ubiquitin foci detected by the FK2 antibody were observed in spite of the presence of  $\gamma$ H2AX foci, implying that ubiquitin conjugates are not effectively formed in DSB foci during mitosis (Figure 18A). Furthermore, FK2 staining was excluded from DAPI stained chromosomes, indicating the absence of ubiquitin onto mitotic chromatin.

**FIGURE 18. Ubiquitin conjugates do not accumulate to IRIF in mitotic cells**

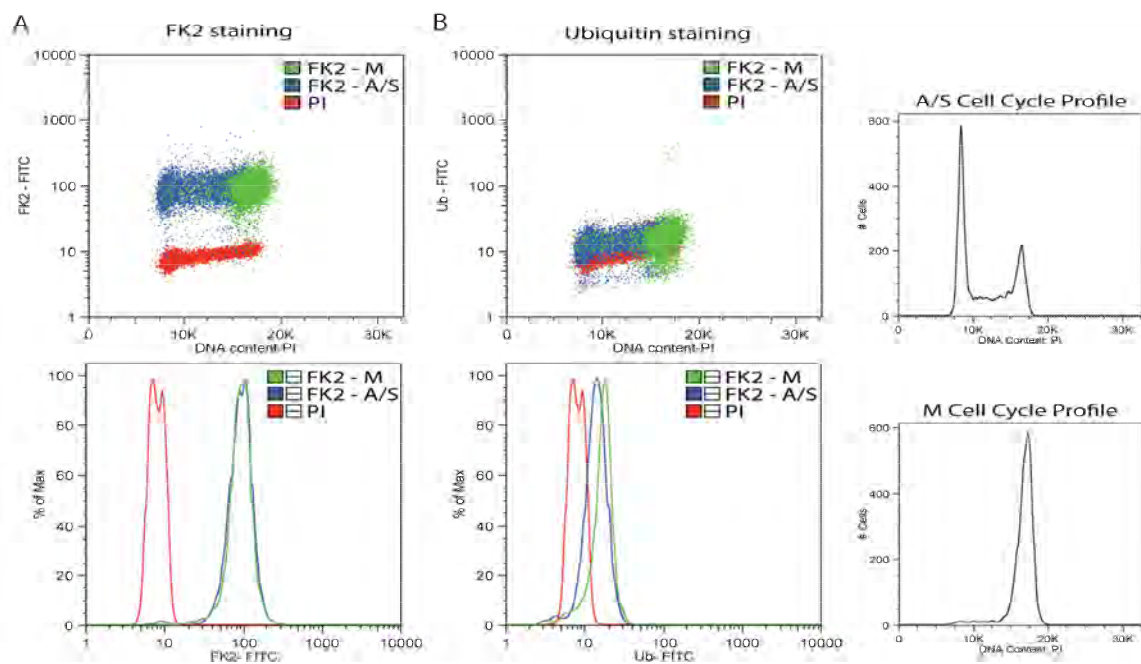


**Content not visible due to copyright limitations**

Ubiquitin conjugates are marked using FK2 antibody staining. FK antibody does not detect ubiquitin conjugates on mitotic chromosomes upon irradiation and do not co-localize with phosphorylated H2AX foci or DAPI stained regions in mitosis (A). Histones H2A and H2AX are de-ubiquitylated in mitosis. Arrows point to non-ubiquitylated forms and asterisks mark ubiquitylated forms of the proteins. Asynchronous (AS) and M-phase cells were left untreated or treated with 5 Gy of IR. The robust increase in ubiquitylated  $\gamma$ H2AX after irradiation of asynchronous cells does not take place in mitosis (B; panel B from Collaborator).

These data showing failed co-localization of FK2 staining with mitotic chromatin and exclusion of ubiquitin conjugated to H2A-type histones in mitosis, prompted me to verify changes in the level of free and conjugated ubiquitin during the cell division cycle. Although conjugated ubiquitin moieties are in a constant status of rapid dynamic equilibrium with the pool of free ubiquitin during progression through the cell cycle, to the best of my knowledge, it had not been tested whether their levels changed during the cell cycle. Using flow cytometry, I was able to show that levels of ubiquitin, of both the free ubiquitin pool and conjugated ubiquitin aggregates, are unchanged throughout the cell cycle. Moreover, levels of free and conjugated ubiquitin were equal when directly comparing mitotically-arrested cells to asynchronous cells (Figure 19).

**FIGURE 19. Free and conjugated ubiquitin levels are constant during the cell cycle**



Flow cytometry of asynchronous (A/S; in blue) and thymidine-nocodazole synchronized (M; in green) cells co-stained for PI (DNA) and FITC-FK2 antibody (for mono- and poly-ubiquitin conjugates; A) or FITC-ubiquitin antibody (monitoring free ubiquitin; B). Negative control samples are stained for PI-only and represent background signal, shown in red. For conjugated ubiquitin levels (A), the antibody gave a better staining, as higher above the background signal, compared to the free ubiquitin antibody (B), whose signal is just above background. However, in both cases, the level of fluorescence intensity of the FITC signal is the same for A/S, from G1, S, to G2/M (blue), and M-cells (green), in both graphs, indicating that ubiquitin levels are unchanged throughout the cell cycle.

Thus, these novel observations show that ubiquitylation events are not globally impaired in mitosis, yet productive association of conjugated ubiquitin to the sites of DSBs is defective. Lack of sufficient ubiquitylation localized at DSBs may be contributory factor for failed 53BP1 recruitment to damage loci in mitotic cells.

### ***3.3.X Localization analysis of the E3 ubiquitin ligases RNF8, RNF168 and BRCA1 in unperturbed and challenged mitosis***

To address the underlying reasons for failed formation of 53BP1 and ubiquitin foci upon irradiation of mitotic cells, I went on to investigate the recruitment of the E3 ubiquitin ligases that participate in the DDR. In interphase cells, the sequential recruitment of three E3 ligases RNF8, RNF168 and BRCA1 to IRIF induces local accumulation of ubiquitin conjugates at the site of breaks, mediating effective cellular responses to genotoxic stress. Histones primed by RNF8-mediated ubiquitylation serve as docking sites for the recruitment of the second E3 ligase in the cascade, RNF168, which synergize with RNF8 to augment ubiquitin conjugates at DSBs. Ubiquitin-mediated conformational changes allow for recruitment of the third E3 ligase, BRCA1, and also 53BP1, to DSBs (reviewed in Stewart, 2009). The complex regulation of the ubiquitylation pattern induced by DNA breakage is ultimately required for repair of the lesion and restoration of genome integrity.

### ***3.3.XI The E3 ubiquitin ligases RNF8 is not recruited to mitotic IRIF***

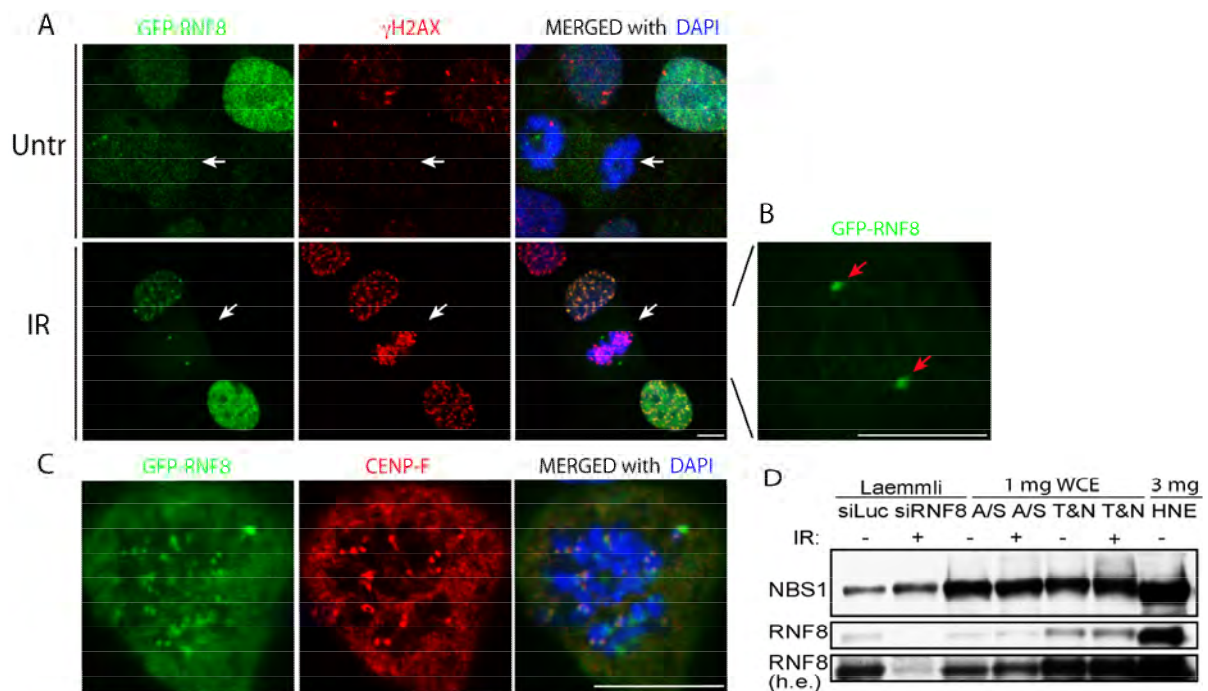
A major player that mediates a key transition in the DNA damage signalling cascade is RNF8. Remarkably, RNF8 contains two structurally relevant modules found in other DDR proteins, a phospho-threonine-binding FHA domain at the amino-terminus and a RING

finger domain at the carboxyl end. RNF8 RING finger domain is required to simultaneously bind the E2 ubiquitylation enzymes, including UBC13, and the substrates, conjugating K48 and K63 polyubiquitin chains (Ito et al., 2001; Plans et al., 2006). In interphase, RNF8 association with chromatin flanking the break site requires the ATM-dependent phosphorylation of MDC1 TQXF clusters. MDC1 phosphorylated TQXF motifs, in turn, serve as a docking site for RNF8 FHA domain. Then, chromatin-associated RNF8 induces ubiquitylation events on H2A-type histones that mediate chromatin rearrangements for the access of downstream mediators to the damaged template. Interestingly, RNF8 has also been implicated in controlling mitotic exit. Its ubiquitin ligase activity is required for mitotic arrest following treatment with nocodazole and modulates the rate of completion of mitosis by controlling timely degradation of cyclin B1 (Tuttle et al., 2007; Plans et al., 2008).

I used U2OS cells stably expressing GFP-RNF8 to investigate the nuclear localization of RNF8 in mitosis, before and after DNA damage. Strikingly, I found that RNF8 was excluded from mitotic chromatin and did not co-localize with  $\gamma$ H2AX foci upon IR or phleomycin treatment (Figure 20A and data not shown). In addition to RNF8 localization to the midbody as previously shown (Tuttle et al., 2007; Plans et al., 2008), further examinations revealed that GFP-RNF8 associated with two other mitotic structures: centrosomes (Figure 20A and 20B) and kinetochores, as evidenced by co-localization with CENP-F (Figure 20C). These data, together with the previously described function of RNF8 in mitotic-exit control (Tuttle et al., 2007; Plans et al., 2008), suggest that RNF8 plays an important role in the regulation of mitosis that might be independent of its involvement in the DDR. A previous study reported a drastic reduction in RNF8 levels in late mitotic stages (Plans et al., 2008). To verify whether the reason for failed RNF8

recruitment to DNA damage foci was due to lack of RNF8 in mitosis, I performed immunoblot analysis using two different RNF8 antibodies and GFP-RNF8 cell extracts to monitor the endogenous levels of RNF8 and to check protein turn-over. No marked changes were observed in RNF8 levels during mitosis (Figure 20D), indicating that failed recruitment to IRIF was not due to sub-optimal protein levels in mitosis. However, I cannot exclude that dispersal of proteins in mitosis due to nuclear envelope breakdown may hinder adequate local accumulation of certain factors; a critical threshold may be required for sufficient RNF8 concentration and foci detection.

**FIGURE 20. RNF8 accumulates to mitotic structures, centrosomes and kinetochores, but does not co-localize with  $\gamma$ H2AX IRIF in mitosis**



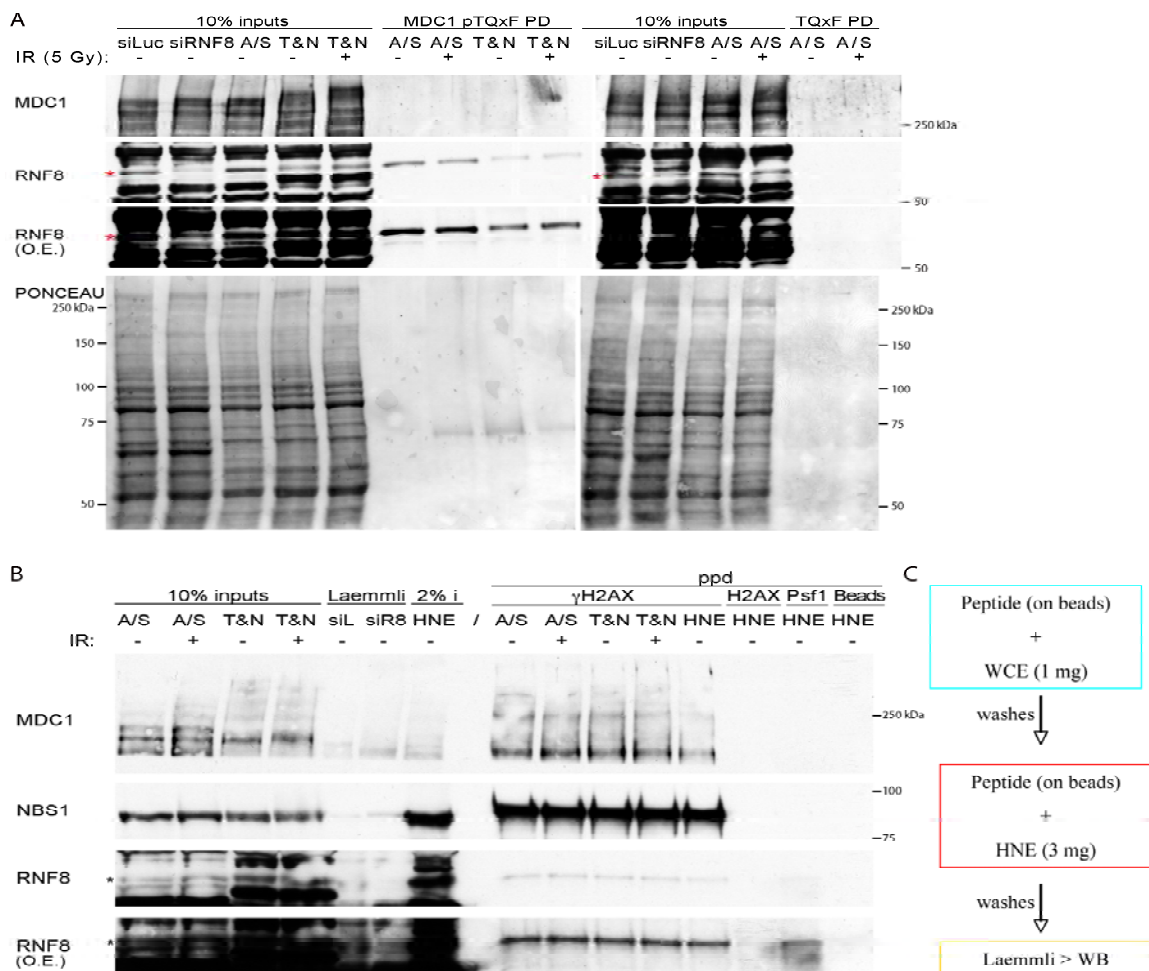
IF of GFP-RNF8 stably expressed in U2OS cells, stained for  $\gamma$ H2AX and treated with 5 Gy of IR. White arrows indicate mitotic cells (A). RNF8 association with nuclear structures in mitosis shown by localization at centrosomes (A, and zoomed in B), indicated by red arrows (B) and co-localization with CENP-F at kinetochores (C). Levels of endogenous RNF8 in extracts from asynchronous (A/S) and thymidine-nocodazole arrested mitotic (T&N) cells show that RNF8 is present in mitosis. siLuciferase (siLuc) and siRNF8 laemmli extracts are included. A small mobility shift of mitotic RNF8 is visible compared to A/S cells. High exposure (h.e.) of the RNF8 WB is shown (D). Scale bars are 10  $\mu$ m.

To gain additional insight into the underlying reasons for RNF8 failed recruitment, I performed peptide pull-downs using MDC1 synthetic peptides with the phosphorylated and unphosphorylated form of T719, one of the MDC1 TQXF clusters phosphorylated by ATM in interphase and mitotic cells after DNA damage. Mitotic RNF8 was capable of binding MDC1 phospho-peptide in a similar fashion to RNF8 from asynchronously-derived extracts and the association was unchanged before and after DNA damage (Figure 21A). These *in vitro* data indicate that the FHA domain of RNF8 has strong affinity for the MDC1 phospho-epitope and does not necessitate post-translational modifications on RNF8 to promote DNA damage dependent binding to MDC1. RNF8 is extensively phosphorylated in mitosis, as shown by a shift in gel mobility (Figure 21A and 20D). In mitosis, RNF8 post-translational modifications could possibly contribute to its exclusion from mitotic IRIF. Although pull-down experiments suggest that RNF8 mitotic hyperphosphorylation does not inhibit binding to MDC1 peptides, I cannot exclude that high concentration of phosphorylated epitopes *in vitro* might override potential regulatory mechanisms that exist *in vivo* to inhibit these interactions during mitosis.

To address the ability of mitotic RNF8 to bind to the full length MDC1 protein during mitosis, I performed peptide pull-downs using  $\gamma$ H2AX phospho-peptides.  $\gamma$ H2AX peptides avidly pull-down MDC1. Phosphorylated MDC1 from damaged extracts should bind to RNF8. However, due to the RNF8 being a very low abundance protein in the cell, no RNF8 was detected in pull-downs using  $\gamma$ H2AX peptides from U2OS whole cell extracts, as previously reported (Kolas et al., 2007). To enrich for RNF8, following  $\gamma$ H2AX peptides pull-downs of MDC1 from untreated and irradiated asynchronous and M-phase extracts, the complex was incubated with HeLa nuclear extracts to assess ability of RNF8 to bind (Figure 21C). Unexpectedly, RNF8 bound to  $\gamma$ H2AX-MDC1 complexes from all extracts

(Figure 21B). However, using a peptide for a phosphorylated SQXF motif on Psf1 similar to  $\gamma$ H2AX site as negative control, I also pulled-down a small amount of RNF8 (Figure 21B), indicating that RNF8 may have some specificity to bind  $\gamma$ H2AX and other similar phospho-epitopes directly, rendering pull-downs experiments unsuitable for further investigations.

**FIGURE 21. Mitotic RNF8 is competent to bind to MDC1 phospho-peptides**



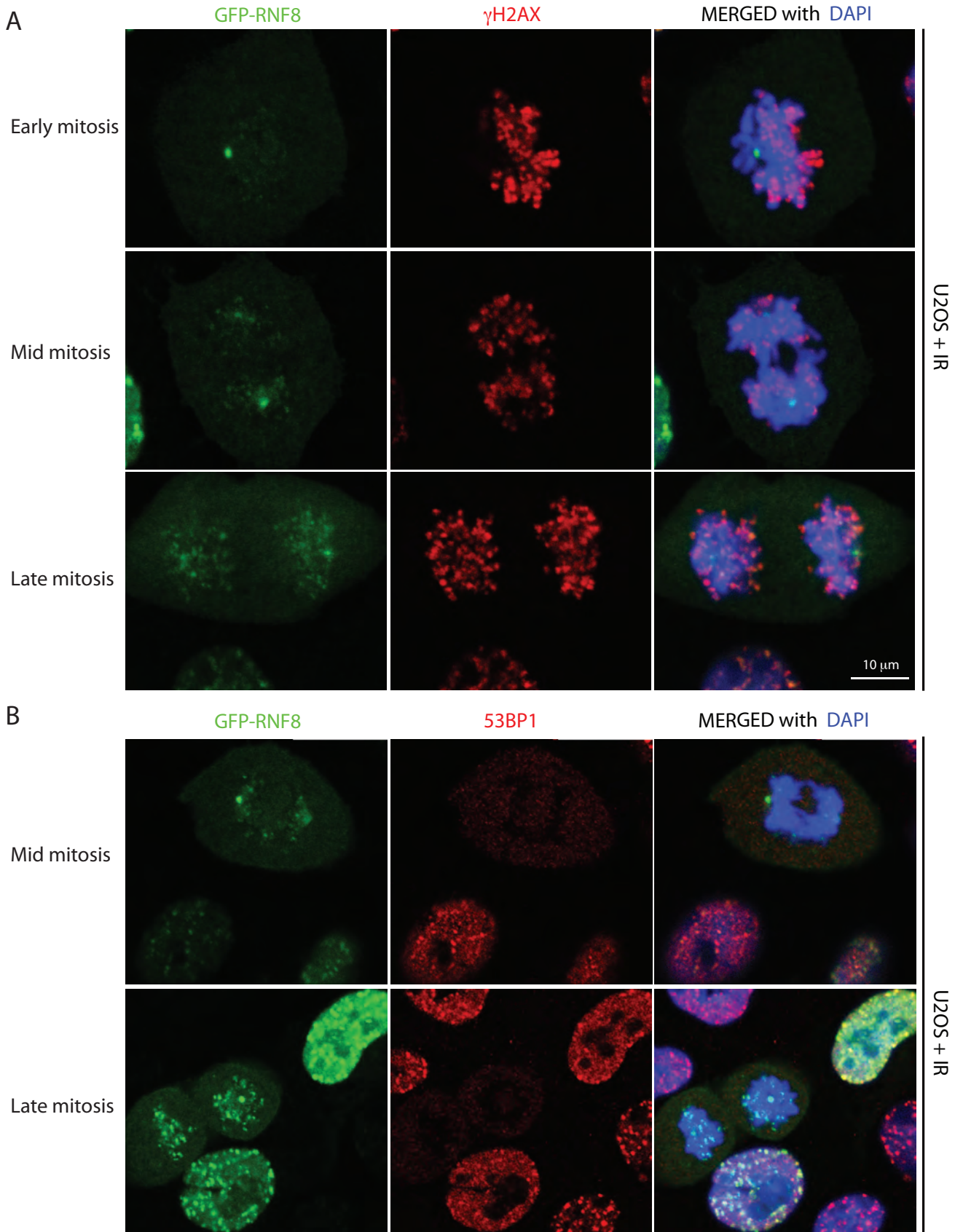
Mitotic RNF8 binds to MDC1 phospho-peptides; MDC1 phosphorylated (pTQx F) or unphosphorylated (TQx F) peptides were used to pull-down from 1 mg of untreated or irradiated (5 Gy) asynchronous (A/S) or thymidine-nocodazole -arrested mitotic (T&N) extracts. RNF8 over-exposure (O.E.) shows that RNF8 levels are not decreased in mitotic samples but appear less due to mitotic phospho-dependent gel shift (A). Pull-downs using  $\gamma$ H2AX phospho-peptides ( $\gamma$ H2AX), unphosphorylated H2AX peptide (H2AX), Psf1 phospho-SQXF peptides (Psf1) or beads-only (Beads).  $\gamma$ H2AX peptides selectively pulls-down MDC1 and Nbs1 from the indicated extracts (1 mg). After incubation in HeLa nuclear extract (3 mg/ppd; C), WB for RNF8, Nbs1 and MDC1 is shown (B). siL stands for siLuciferase; siRNF8 (siR8) lane indicates RNF8-corresponding band (marked by asterisks, red in A and black in B).

Further experimental analyses on RNF8 failed recruitment in mitosis were hindered by RNF8's mitotic role. Several synchronization and cell cycle manipulation attempts on cells with altered levels of RNF8 led to rapid induction of cell death. U2OS cells knocked-down for RNF8 by siRNA failed to synchronize in mitosis and initiated apoptosis. Similarly, in RNF8 over-expression studies, no cells were found in mitosis (data not shown). These observations, together with my novel evidence of RNF8 recruitment to diverse mitotic structures and the previously described function of RNF8 in mitotic-exit control (Tuttle et al., 2007; Plans et al., 2008), suggest that RNF8 plays important roles in the regulation of mitosis entry as well as exit.

Time-course analyses revealed that RNF8 accumulation to IRIF was resumed in late mitosis, yet 53BP1 foci were not detected in these cells (Figure 22). Accordingly, a GFP-tagged construct where the MDC1 twin BRCT domains, required for direct binding to the  $\gamma$ H2AX phospho-site, were fused to RNF8 was transformed in U2OS and forced tethering of RNF8 to  $\gamma$ H2AX after DNA damage. Despite GFP-RNF8<sub>MDC1[BRCT]</sub> hybrid protein being recruited to sites of DSBs, 53BP1 remained excluded from mitotic IRIF (data not shown). Therefore, a multi-layered control exists to prevent activation of secondary DDR responses to IRIF during mitosis. RNF8-mediated transition, comprising alteration in the chromatin status, may be unfeasible in the context of highly compacted mitotic chromosomes and may be blocked on several levels until cells have completed karyokinesis and entered G1.

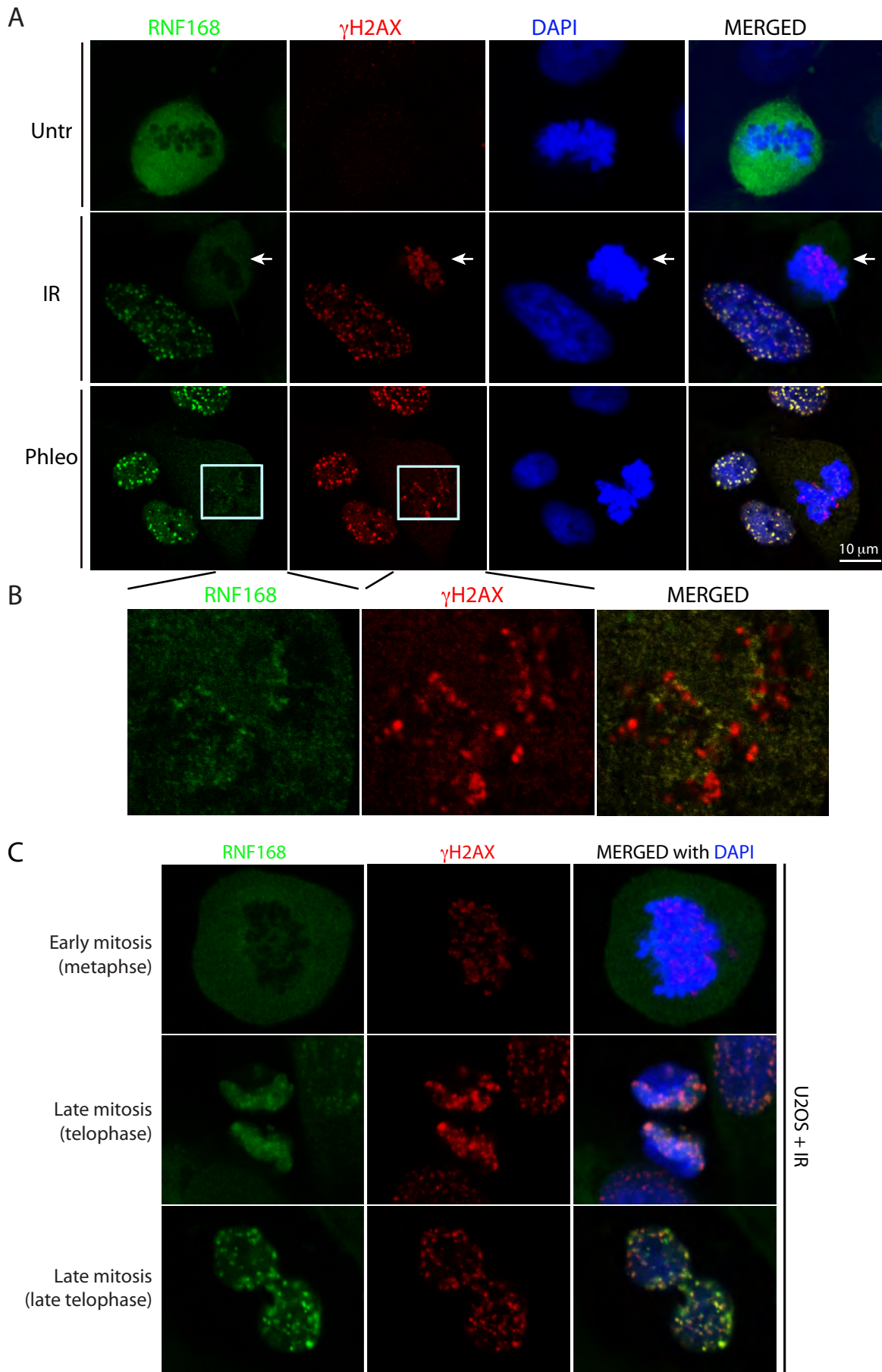
Altogether, the data and observation presented suggest that lack of RNF8 recruitment in mitosis is likely to be due to a combination of post-translational modifications (Figure 21A and 20D), as well as sequestration of RNF8 to mitotic structures (Figure 20A).

**FIGURE 22. RNF8 foci formation at late mitotic stages does not lead to 53BP1 recruitment to DSBs**



RNF8 binding to IRIF is differentially regulated in early, mid and late stages of mitosis. GFP-RNF8 asynchronously growing U2OS cells were stained for  $\gamma$ H2AX and treated with 5 Gy of IR. RNF8 is largely excluded from mitotic chromatin in early and mid mitosis. In late mitotic stages, RNF8 starts to form IRIF, co-localizing with  $\gamma$ H2AX foci (A). Productive association of RNF8 with IRIF in late mitosis does not lead to accumulation of mitotic 53BP1 to DSBs (B). RNF8 co-localizes strongly with centrosomes at all stages, as detected by 1 or 2 large, bright RNF8 dots (A and B).

**FIGURE 23. RNF168 is excluded from mitotic chromatin and IRIF until late mitosis**



Asynchronously growing U2OS stable cell lines expressing GFP-RNF168 were stained for  $\gamma$ H2AX. RNF168 is excluded from mitotic chromatin and does not co-localize with  $\gamma$ H2AX foci following irradiation (A) or phelomycin-treatment (A and B). An insert of panel A, outlined by the blue square, is enlarged in panel B to show that RNF168 forms fine dots, corresponding to the mitotic kinetochores, but does not co-localize with  $\gamma$ H2AX (B). RNF168 recruitment to IRIF is resumed in late mitosis, following the anaphase to telophase transition (C), with similar kinetics to RNF8 indicating their close succession to DSBs.

### ***3.3.XII RNF168 is not recruited to DNA damage foci in mitosis, but localizes to kinetochores***

The RING finger E3 ubiquitin ligase RNF168 associates with damaged chromatin *via* two UIMs that bind RNF8-mediated polyubiquitin chains on H2A. In turn, RNF168 binds the E2 ligase UBC13 and catalyzes the formation of K63-linked conjugates on H2A and H2AX. The epistatic recruitment of RNF168, downstream of RNF8, synergizes to locally enrich the ubiquitylation level to a threshold capable of inducing dynamic structural changes to the chromatin and propagating the DDR signal to downstream factors.

Consistent with the exclusion of RNF8 from IRIF during mitosis, I found that GFP-RNF168, stably expressed in U2OS, was not recruited to DSB and did not co-localize with mitotic chromatin (Figure 23A). Although RNF168 was mostly excluded from mitotic chromatin, further examination revealed that GFP-RNF168 associated with kinetochores in mitosis, yet the fine punctuated RNF168 staining at kinetochores did not co-localize with  $\gamma$ H2AX DNA damage foci (Figure 23B). Unlike RNF8, however, no obvious staining was observed at centrosome or at the midbody in late mitosis.

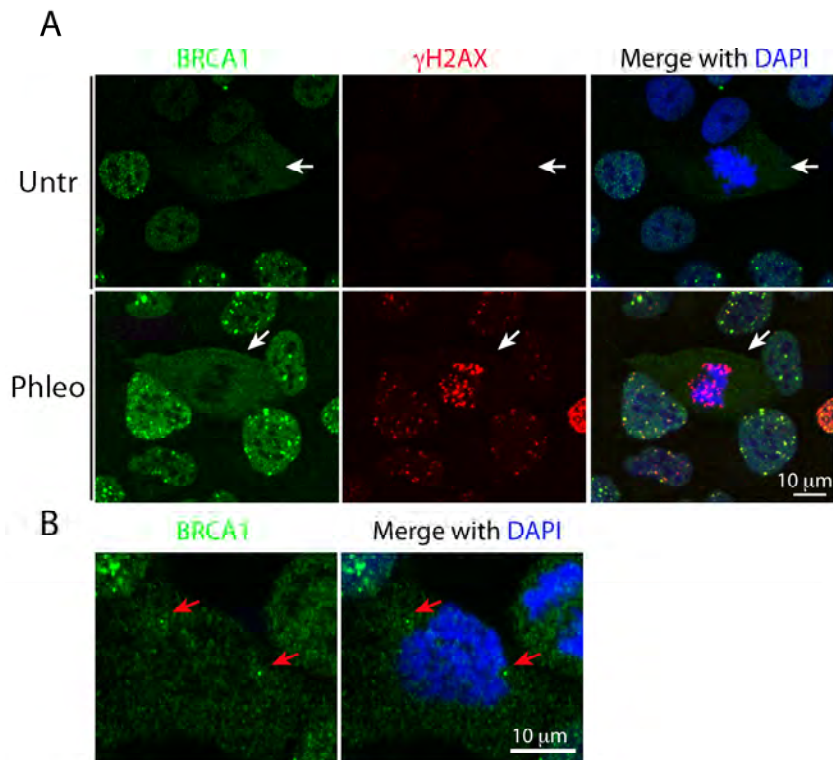
RNF8 (Figure 22A) and RNF168 (Figure 23C) share similar localization kinetics in their resumption of recruitment to IRIF in late mitosis. Indeed, these factors are recruited to DNA damage foci and co-localize with  $\gamma$ H2AX only once mitotic cells pass the metaphase-to-anaphase transition and enter telophase. Presumably, the pre-emptive recruitment of RNF8 and RNF168 to DSB sites serves to prepare the chromatin for conformational rearrangements anticipatory to 53BP1 binding once the nuclear envelope reforms and the cell enters G1. In addition, the ability of RNF8 and RNF168 to bind to DSBs within the

compacted mitotic chromatin in late mitosis infers that chromatin compaction is unlikely to play a major role in the exclusion of these factors in earlier mitotic stages.

### ***3.3.XIII The DDR mediator BRCA1 is also excluded from mitotic IRIF***

RNF8 and RNF168-dependent ubiquitin-mediated conformational changes allow for recruitment of the third E3 ligase, BRCA1. In mitosis, exclusion of RNF8 and RNF168 from IRIF causes failed association of BRCA1 to IRIF. Indeed, both live cell imaging using U2OS stably expressing GFP-BRCA1 and immunofluorescence of the endogenous protein with BRCA1 antibody revealed that BRCA1 was undetectable in mitotic  $\gamma$ H2AX foci (Figure 24A and data not shown). As previously reported, I found BRCA1 localization at centrosomes in mitosis (Figure 24B), where it actively plays a role in centrosome duplication (Hsu and White, 1998). In accord with RNF8, RNF168 and 53BP1, protein levels of BRCA1 also showed no marked changes throughout the cell cycle (data not shown).

**FIGURE 24. BRCA1 is excluded from mitotic chromatin and fails to localize to sites of DSB during mitosis**



Immunofluorescence analysis co-staining cells for BRCA1 and  $\gamma$ H2AX shows that BRCA1 does not co-localize with DAPI-stained mitotic chromosomes and is not recruited to  $\gamma$ H2AX-marked DNA damage foci. White arrows point to mitotic cells (A). BRCA1 forms two bright spots at either side of mitotic cells, indicating accumulation of BRCA1 to the centrosomes (red arrows; B).

Different phosphorylation statuses exist for BRCA1 during the cell cycle, which have been implicated in its sub-cellular compartmentalization (Okada and Ouchi, 2003). Like many other proteins, BRCA1 had altered gel migration properties during M-phase, in line with its mitotic hyper-phosphorylation (data not shown; Poon, 2007). Perhaps surprisingly, a sub-pool of mitotic BRCA1 in its hypo-phosphorylated form preferentially associates with  $\gamma$ -tubulin and localized to centrosomes (Hsu and White, 1998). It is possible to envisage a scenario whereby mitotic cells impart a dual regulation on DDR proteins. Firstly, the truncation of the DNA damage signalling cascade at the level of RNF8 prevents recruitment of downstream factors, and this is further controlled by several inhibitory

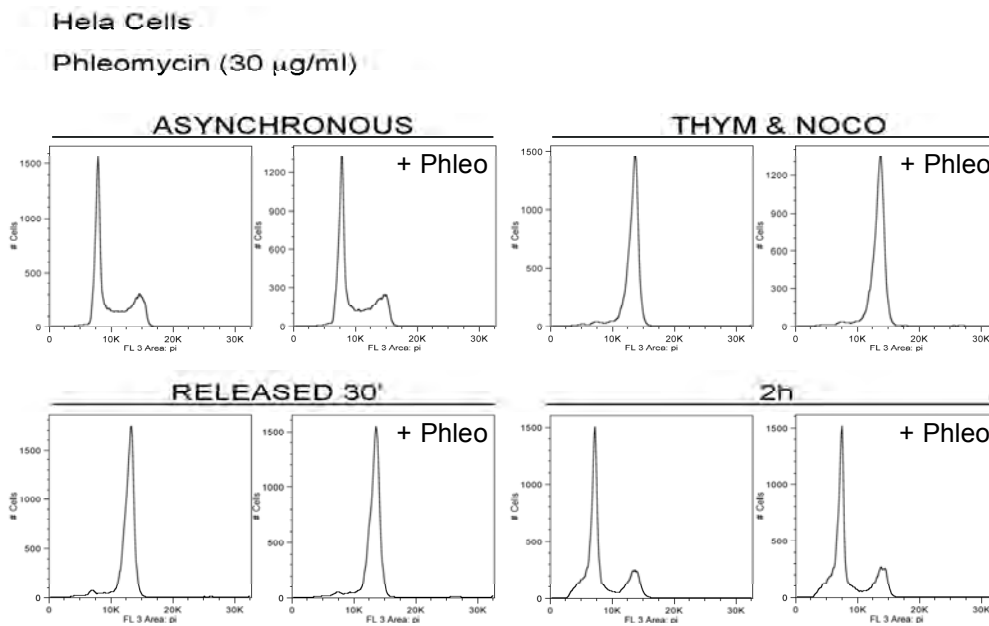
mechanisms. Also, mitotic-specific hyper-phosphorylation, by nuclear exclusion of phosphatases or activation of mitosis-specific kinases (Poon, 2007), may impair protein activities within the DDR network; only DDR factors required for physiological mitosis are sequestered into specific mitotic structures and are post-translationally regulated to be maintained active in a compartment-dependent manner.

Collectively, these data show that E3 ubiquitin ligases RNF8, RNF168 and BRCA1 are not recruited and DDR-mediated ubiquitylation does not take place at DSB sites in mitosis; this truncation of the DDR is likely to be regulated on multiple levels, both by alterations of the DSB compartment, through PTMs and sequestration of individual proteins during mitosis.

### ***3.3.XIV Absence of a DNA damage checkpoint in mitosis correlates with failed activation of checkpoint kinases***

Several lines of evidence support the idea of a lack of the DNA damage checkpoint in mitosis (Rieder and Cole, 1998; Mikhailov et al., 2002). To investigate the consequences of DSB induction on the progression through mitosis, I synchronized cells and released them into mitosis in the presence or absence of the DSB-causing agent, phleomycin. The progression of mitotic cells into G1 is not delayed by DSBs as observed in both HeLa and U2OS cells (Figure 25 and 27), supporting the idea that the presence of DSBs *per se* does not lead to cell cycle arrest in mitosis.

**FIGURE 25. Presence of DSBs does not trigger a DNA damage checkpoint delay in the progression through mitosis and re-entry into G1**



Mitotic cells were synchronized by thymidine-nocodazole arrest and harvested by shake-off, treated as indicated and 30 minutes later released into fresh medium. Samples were collected for FACS analyses after 30 minutes and 2 hours post-release. Damaged and undamaged cells display the same kinetics in progressing through and exiting mitosis, and re-entering into the following G1, indicating lack of significant DNA damage-induced delay in mitotic exit of HeLa cells.

To investigate the reasons for the absence of a mitotic DNA damage checkpoint, we examined the molecular mechanisms of checkpoint activation. Indeed, phosphorylation of downstream ATM substrates, including checkpoint effector kinases, occurred to a lesser extent in mitotic cells than in interphase cells in response to DSB induction. Mitotic samples displayed a reduced level of phosphorylation of Chk2 on T68 (Figure 26 and 28) and Chk1 on serine 345 in response to DNA damage, compared to interphase cells (Figure 26). Smc1 phosphorylation on serine 966, a classical ATM target, is also abolished in mitosis (Figure 26), in spite of the presence of damage-activated ATM autophosphorylation on S1981 and  $\gamma$ H2AX-containing IRIF. Interestingly, in line with the lack of 53BP1 recruitment, ATM-mediated 53BP1 serine 25 phosphorylation was not induced by DNA damage in mitotic cells (Figure 26). These data strongly suggest that the

absence of DNA damage-induced delay and attenuation of checkpoint signalling during mitosis may be related phenomena.

**FIGURE 26. The absence of DNA damage checkpoint in mitosis correlates with impaired activation of Chk1, Chk2 and other canonical ATM targets**



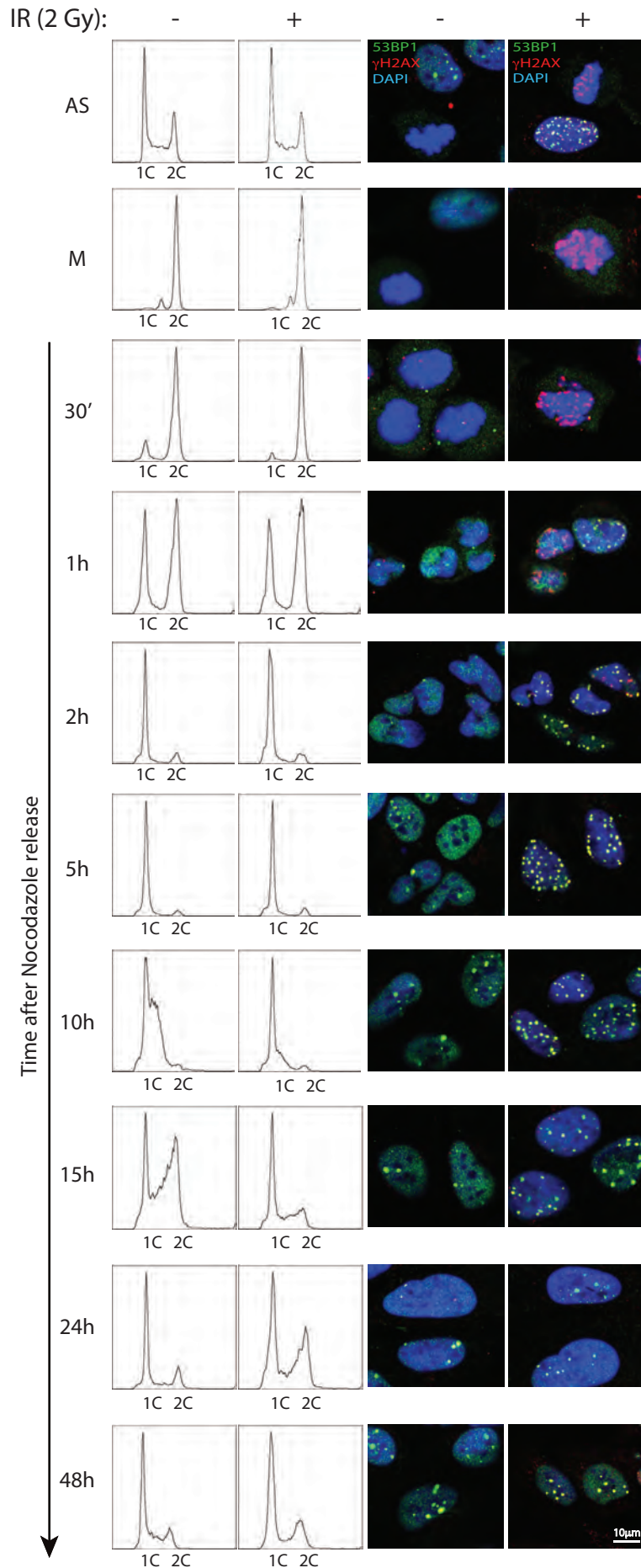
**Content not visible due to copyright limitations**

Diminished phosphorylation of ATM targets in IR-treated (2 Gy) mitotic cells (M) as compared to asynchronous cells (AS). M-phase cells were obtained from thymidine-nocodazole synchronization. Phosphorylation of ATM-target sites on 53BP1 (S25), SMC1 (S966), Chk2 (T68) and Chk1 (S345) is monitored by western blotting and was found impaired in mitotic cells.

### **3.3.XV Mitotic cells mark sites of DSBs prior to full DDR activation in G1**

Next, I wanted to monitor the behaviour of cells damaged in mitosis as they progressed into the following cycle of cell division. To see whether DSBs carried over from mitosis are able to trigger full DDR activation in G1, mitotic cells were collected from a pre-synchronized culture, treated with IR, released from nocodazole block and then analyzed at different time-points for cell cycle distribution, presence of 53BP1 in IRIF and Chk2 phosphorylation.

**FIGURE 27. Exclusion of 53BP1 from mitotic IRIF precedes its association and checkpoint activation in G1**

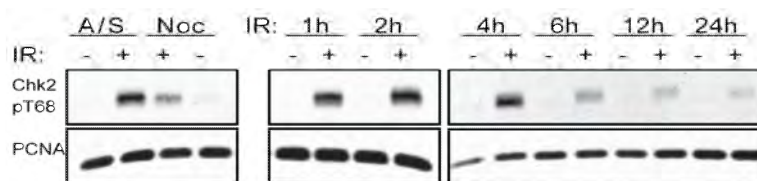


Untreated or irradiated (2 Gy IR) mitotic cells were released from nocodazole-block, collected at the indicated times and monitored for cell cycle progression by FACS and 53BP1 recruitment to IRIF by immunofluorescence of endogenous 53BP1, co-stained with  $\gamma$ H2AX and DAPI.

Cells damaged in M-phase progressed into G1 with kinetics similar to that of untreated cells for up to 5 hours after release from nocodazole (Figure 27). Irradiated cells exhibited slower entry and/or progression through S-phase, as well as a delay in G2 (Figure 27; see 10-24 hour time-points). Similar to the findings with EGFP-53BP1 in live-cell imaging experiments, endogenous 53BP1 started forming foci 1-2 hours after G1 entry (Figure 27). Furthermore, few IRIF were still detectable 24 hours after irradiation, indicative of ongoing DSB repair.

Parallel examination of IR-induced Chk2 phosphorylation on T68 revealed that this modification was reduced in M-phase in comparison with asynchronous cells (Figure 28 and 26). Nevertheless, once cells progressed into G1, T68 became highly phosphorylated (Figure 28), supporting the notion that an attenuated DDR during mitosis is then fully activated in the following interphase. Six hours after irradiation, Chk2 phospho-signal starts attenuating, becoming very low at 24 hours, indicating repair of the DNA insults and resumption of cell cycle progression.

**FIGURE 28. Proficient phosphorylation of Chk2 T68 upon re-entry into G1**



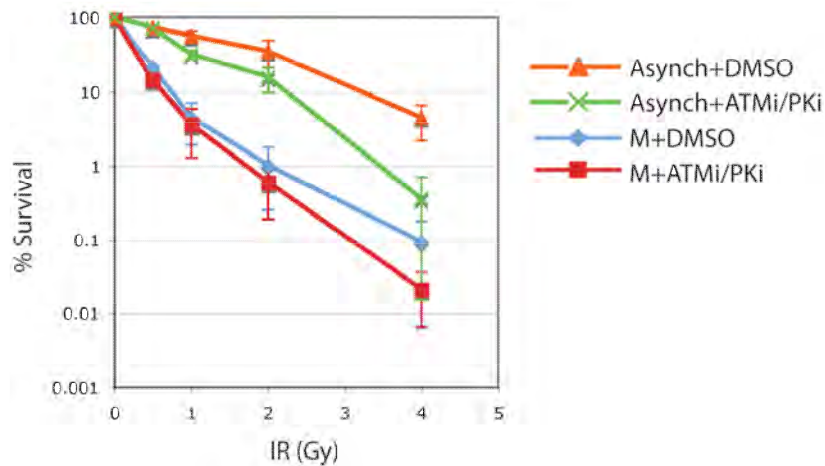
Cells were treated as in Figure 28. Immunoblot analysis of Chk2 T68 phosphorylation in cells released into G1 after IR treatment (2 Gy) in mitosis shows full Chk2 activation when mitotic cells bearing DSBs exit mitosis and enter the following G1 (1, 2 and 4 h time-points).

Collectively, these data indicate that, upon entry into G1, DSBs carried through from mitosis elicit a full DDR activation and trigger the DNA damage checkpoint, allowing time to repair the DNA lesion in the following cell cycle.

### ***3.3.XVI Biological significance of the 'primary' DDR in mitosis***

Having established that mitotic cells respond to DSB with induction of a primary DDR, comprising ATM,  $\gamma$ H2AX, MDC1 and MRN, but exclude events downstream of RNF8, and checkpoint activation, I next asked whether activation of early DDR events in mitosis is a biologically important phenomenon. To assess the potential physiological significance of DSB marking in mitosis, together with Rimma Belotserkovskaya, I performed clonogenic survival assays on asynchronous and mitotic cells that had been irradiated either in the absence or presence of ATM and DNA-PK inhibitors. In agreement with earlier studies (Stobbe et al., 2002), mitotic cells displayed much higher radio-sensitivity compared to asynchronous cells (Figure 29). Furthermore, acute PIKK inhibition, at a dose sufficient to ablate  $\gamma$ H2AX IRIF formation, further enhanced the killing of mitotic and asynchronous cells (Figure 29). As cells were extensively washed following DSB induction to remove the inhibitors, this result was unlikely to reflect residual PIKK inhibition still taking place because the effect of PIKK inhibition on  $\gamma$ H2AX was readily reversible within 1 hour (Figure 30). This indicates that, although mitotic cells are intrinsically radio-sensitive, inhibition of primary responses to DSB in mitosis induces further radio-sensitivity.

**FIGURE 29. Primary DDR in mitosis is biologically important for cell survival**



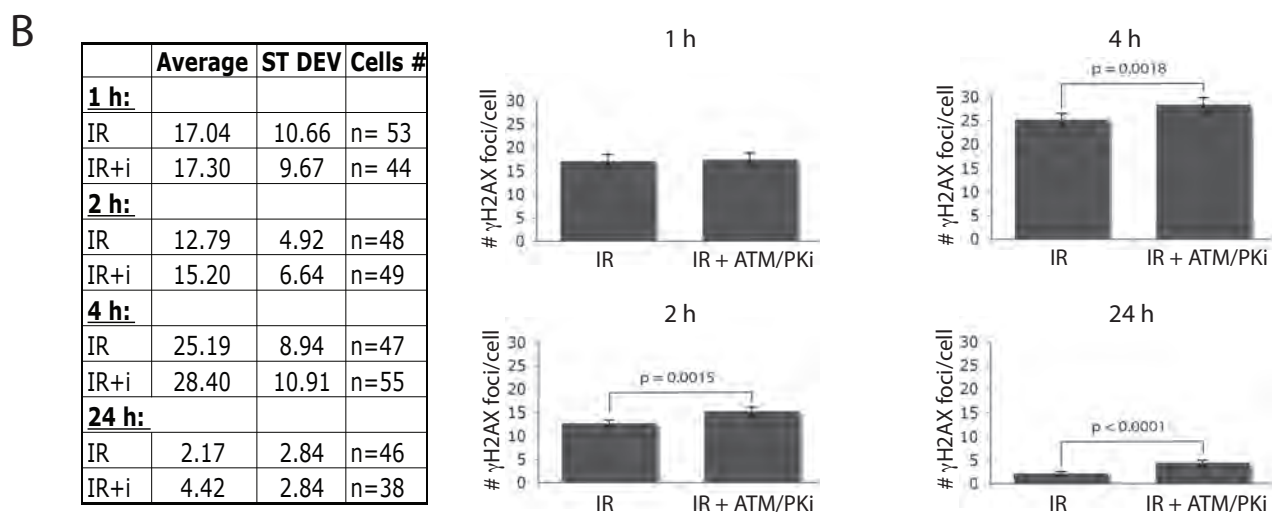
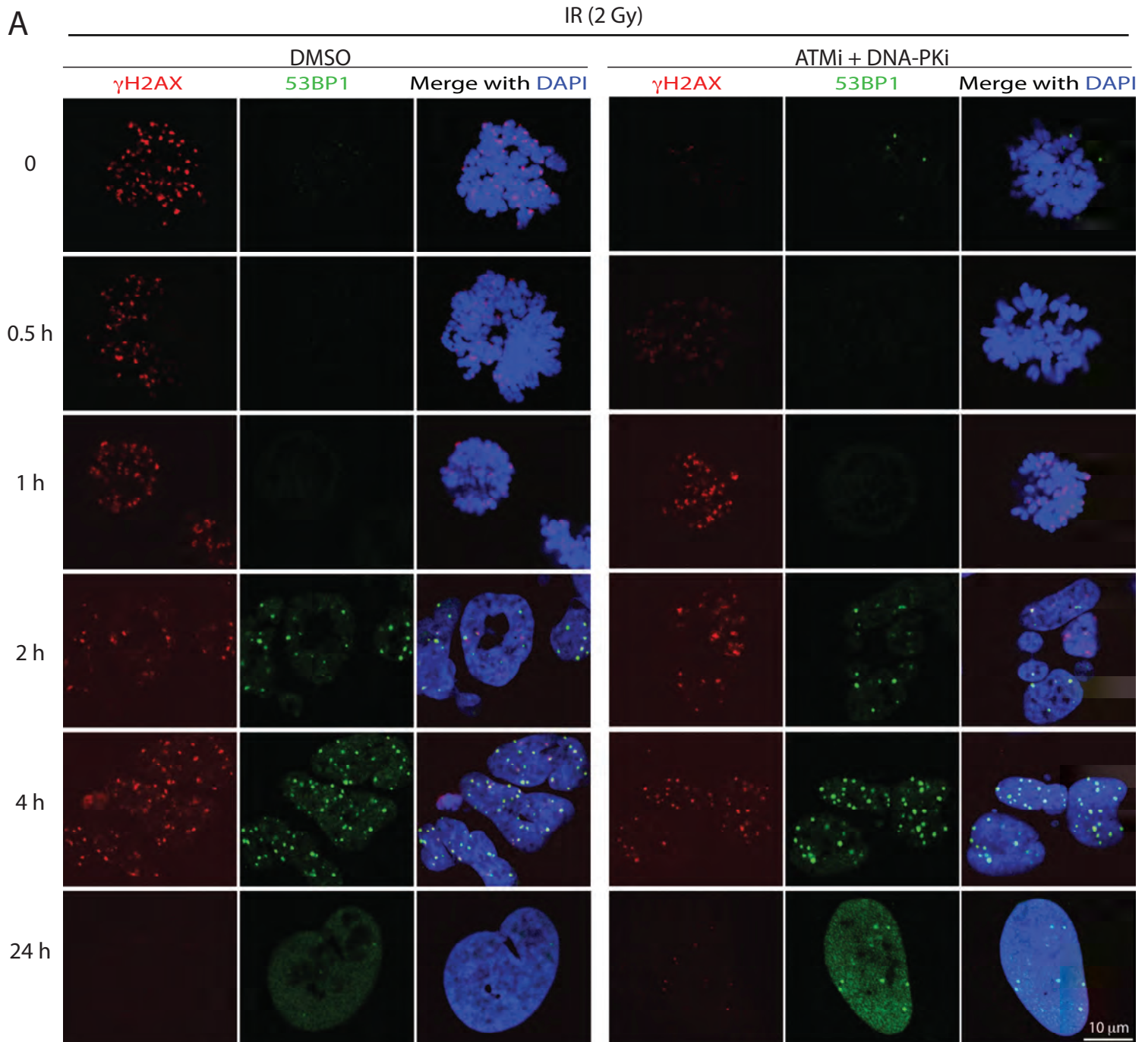
Radio-sensitivity of asynchronous and mitotic cells pre-treated with DMSO or a combination of ATM and DNA-PK inhibitors for 1 hour and then exposed to various doses of IR, as indicated. ATM and DNA-PK inhibitors are used to abolish the primary DDR in mitotic cells. 30 minutes after irradiation, the inhibitors were removed by extensive washing and cells were plated in fresh medium. Error bars represent standard deviations of the means from six independent experiments. *P* values were calculated at the standard 0.05 threshold. For both asynchronous and mitotic cells, radiation has a statistically significant increase in the killing effect of PIKK inhibitors treated cells versus DMSO-treated cells. In asynchronous cells,  $p = 0.00015$ . In the mitotic cells,  $p = 0.041$ .

To assess how PIKK inhibition during mitosis could lead to radio-sensitization, I quantified  $\gamma$ H2AX foci at various time-points after release from inhibitor treatment and nocodazole block. Notably, after 1 hour, similar numbers of foci were present in cells that had been mock- or PIKK-inhibitor-treated (Figure 30A), indicating that similar amounts of damage were generated, and that the majority of DSBs generated in mitosis were not repaired before G1 entry. Lack of ongoing DSB repair in mitosis is also supported by the difference in PIKK-inhibitor-mediated radio-sensitization between asynchronous and mitotic cells: the effect of the PIKK inhibitors on mitotic cells is ~3-fold lower than on asynchronous cells (Figure 29). I did, however, observe significant differences in IRIF numbers between mock- and inhibitor-treated cells at 2, 4 and 24 hours time-points. The inhibitor-treated cells showed 2-fold more residual foci after 24 hours (Figure 30A and 30B), suggesting that a subset of lesions, perhaps more complex DSBs, requires the ‘primary’ DDR in mitosis in order to be efficiently repaired in the next cell cycle and to promote cell survival.

Collectively, these data suggest that activation of early DDR steps in mitosis, including the *marking* of such sites by H2AX phosphorylation, MDC1 and MRN recruitment is a biologically important response and contributes to preserving genomic integrity, possibly by facilitating recognition of breaks and their repair in the following cell cycle.

Taken together, the data presented in this study support a model in which mitotic cells treated with DSB-inducing agents prioritize timely passage through mitosis over activation of a full DDR. The latter is likely to involve substantial changes in chromatin structure proximal to DSB sites that would presumably not be feasible in the context of highly condensed mitotic chromosomes and might otherwise perturb mitotic progression. Nevertheless, the mitotic cells activate a *primary* DDR, which is important for cell survival.

**FIGURE 30. Primary DDR in mitosis promotes DSB repair in the following cell cycle**



Transient inhibition of ATM and DNA-PK activity in mitosis is reversed upon removal of the inhibitors. U2OS cells were treated as in Figure 29 and exposed to 2 Gy of IR. Cells were co-stained for  $\gamma$ H2AX and 53BP1 (A). Counting of  $\gamma$ H2AX foci number per cell was performed using Volocity software and the average number of foci was reported in table and graph formats (B). Error bars represent standard errors calculated from the following formula:  $SE = SD/\sqrt{n}$ , where SD is the standard deviation of the means, and n is the number of cells counted treated as independent variables. Note that the average number of foci counted per cell at 2 hours post-release is less than that at 1 hour due to impairment focus visualization caused by the irregular morphology of cells in early G1, prior to full reattachment and flattening, that affects foci imaging and counting.

### 3.4 Discussion

#### 3.4.1 *Analysis of DNA damage responses in mitosis: exclusion of secondary DDR factors from IRIF*

The study of DNA damage signalling undertaken during my PhD has revealed a differential mode of responding to life-threatening lesions such as DSBs between interphase and mitotic cells. I have outlined the signalling cascade that unfolds in a DSB-dependent manner in mitotic cells by monitoring the behaviour of all known components of the DDR signalling cascade. Importantly, this study specifically focussed on DNA damage induced while cells were in mitosis. Considering that 2 Gy of IR causes about 50-60 DSBs, damage induced in G2 would prevent mitotic entry *via* activation of the G2/M checkpoint. Also, samples were fixed within 30 minutes after DNA damage induction to avoid loss of mitotic cells through mitotic exit, indicating that the immunofluorescence analyses show mitotic cells that have been damaged while already in mitosis.

The observation that DDR mediators 53BP1 and BRCA1 fail to be recruited to damage foci following treatments with IR and phleomycin during mitosis suggests that multiple factors impact on the recruitment of downstream players in the DDR cascade. Several aspects involved in the effective recruitment of DDR factors, like RNF8, may play a role in mitosis to prevent their binding. The pronounced compaction of chromatin during mitosis may represent a physical barrier to the recruitment of factors to damaged loci. Epigenetic modifications, specific to the mitosis phase, may alter the DDR compartment, delaying or preventing the remodelling of chromatin required for certain factors, including 53BP1, to bind to DNA. The modification of chromatin flanking the break sites by PTMs is particularly intricate during mitosis. For instance, in H3 pS10 immunoblots, I have observed a high molecular weight band appearing only in mitotically-arrested samples,

suggesting that phosphorylated H3 is further modified by ubiquitylation and possibly SUMOylation in a mitosis-specific manner. In addition, the decrease in ubiquitylated H2A-type histone is actively promoted upon entry into mitosis and does not correlate with a general loss of ubiquitylation, in line with my findings that conjugated ubiquitin levels do not change during the cell cycle.

In addition, modifications applied to the protein may directly hinder binding of factors. Numerous DDR proteins are hyper-phosphorylated during mitosis, which may affect their binding ability directly or indirectly. Another possibility of regulation may include mitosis-specific nuclear localization of DDR factors. Although difficult to analyse experimentally, it is possible that sequestration of proteins into mitotic structures jeopardizes their recruitment to damaged chromatin. 53BP1 is loaded to the kinetochore during prophase, where it co-localizes with CENP-E. In addition, I have shown for the first time that RNF168 also localizes at kinetochores and RNF8 not only co-localizes with the midbody in late mitosis, but is also recruited to centrosomes and kinetochores during unperturbed mitosis. It would be interesting to investigate the mitotic role that these proteins play at these structures. Especially, the observation that RNF8, RNF168 and 53BP1 localize to kinetochores in mitosis raises the possibility that their recruitment follows a similar epistatic relationship with analogous molecular dynamics as localization of DDR factors at DNA damage sites in interphase. Because kinetochores are subjected to tensional forces from the spindle microtubules, it is possible to envisage a scenario whereby genomic surveillance mechanisms are constitutively active to monitor these fragile sites and to promote rapid mending of spontaneously-arising DNA break. On the other hand, mitotic structures that harbour only RNF8 accumulation, like centrosomes and the midbody, may have different binding requirements, serve different functions and simultaneously work to sequester the protein from sites of DNA damage in mitosis. The results presented

emphasize that, whereas in interphase cells DDR factors play a major role in the responses to DNA double strand breaks, in unchallenged conditions these same DDR factors may have a role in monitoring and enabling physiological processes like mitosis. Both roles may be pivotal in maintaining genome stability.

Despite our best effort to solve the puzzle of the failed binding of RNF8 FHA to the MDC1 phospho-epitope, this still remains one of the major unanswered questions of this study. The data collected suggest that a combination of mitosis-specific protein modifications and sequestration, controls the recruitment of DDR factors, like RNF8, to mitotic IRIF. It would be interesting to investigate the mitotic recruitment of E2 ubiquitin-conjugating enzymes, like Ubc13, that work in partnership with E3 ligases to promote local accumulation of ubiquitin conjugates and may also be required to stabilize RNF8 binding and endorse its focal recruitment. In addition, SUMOylation has recently been shown to be another post-translational modification to control recruitment of DDR factors to IRIF and amplification of the DNA damage signalling. Despite occurring downstream of RNF8, SUMO modifications are required for the productive association of ubiquitin, RNF168, 53BP1 and BRCA1 to sites of damage (Galanty et al., 2009; Morris et al., 2009). Therefore, it would be interesting to explore how SUMOylation is regulated in the context of mitotic cells.

In addition, the understanding of molecular dynamics within the compacted chromatin status of mitosis may relate to other nuclear compartments, such as in heterochromatic regions. Penny Jeggo's laboratory has shown that repair of DSB in heterochromatin is heavily reliant on ATM-mediated regulation of KAP1 that enables transient relaxation of chromatin and promotes DSB repair (Goodarzi et al., 2009). However, mitotic cells regulate HP1 chromatin binding *via* Aurora B-dependent phosphorylation of H3 pS10;

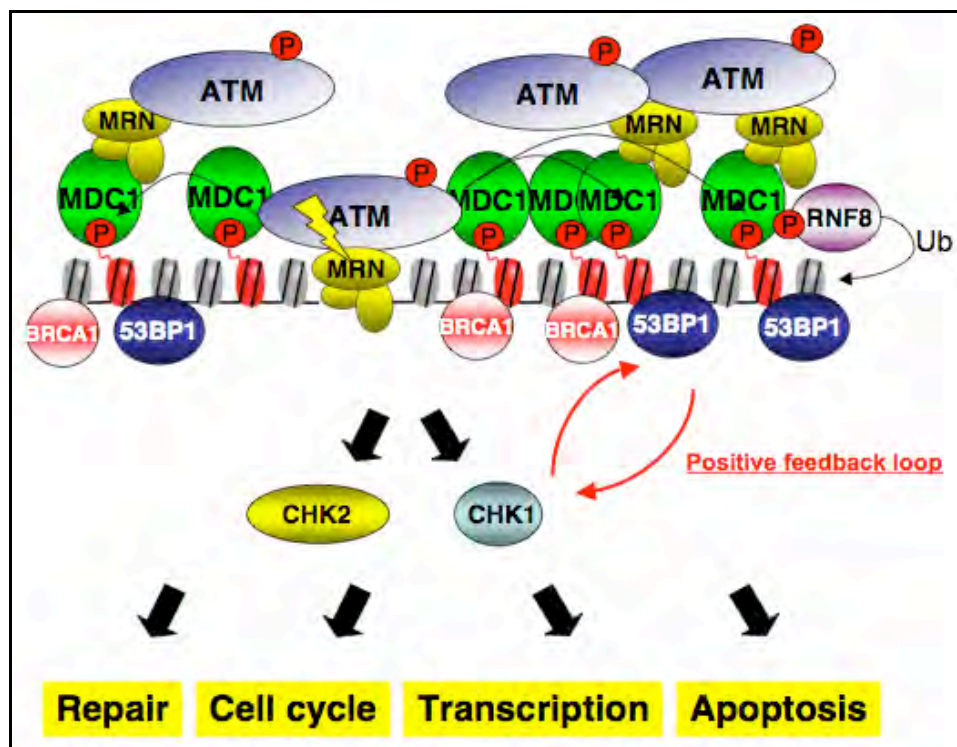
similarly to HP1, KAP1 is released from mitotic chromatin, suggesting that mitotic chromatin is considerably different from heterochromatic regions. It would also be interesting to investigate how the DDR in mitosis relates to responses to DSBs on the inactive X chromosome. Not much is known about DDR in this context, yet BRCA1 has been found to associate with the inactive X chromosome during S-phase (Chadwick and Lane, 2005), indicating that rather than compacted chromatin *per se*, it is the epigenetic marks typical of these different chromatic statuses that affect DDR factors' recruitment.

### ***3.4.II Modulation of DNA damage checkpoint during mitosis***

Treatment with DSB-causing agents in mitosis leads to activation of ATM,  $\gamma$ H2AX focal accumulation and increased phosphorylation of certain ATM targets, such as KAP1 and MDC1. However, the phosphorylation of typical ATM targets, Chk1, Chk2, Smc1, 53BP1 and possibly others, is impaired in damaged mitotic cells. Attenuation of certain ATM-mediated phosphorylations in mitosis is in agreement with a recent report by van Vugt et al., (2010) which shows that Plk1 targets 53BP1 and Chk2 for inhibitory phosphorylation, initiating a negative feedback network to inactivate the ATM-Chk2 branch of the DNA damage checkpoint in mitosis. In addition, here I show that substrates like Chk1 and Smc1 are also not phosphorylated after DNA damage in mitosis. Therefore, this suggests that some ATM substrates require a higher level of regulation to be retained in their phosphorylation status. The parallels between failed recruitment of 53BP1 to IRIF and lack of Chk2 T68 phosphorylation following DSB induction in mitosis might reflect the previously described inter-dependencies between 53BP1 and Chk2 in DDR activation (Wang et al., 2002). Truncation of mitotic DDR at the level of RNF8, and absence of DDR mediators BRCA1 and 53BP1, may compromise a positive feedback loop that acts to

enhance mitotic signalling and convey it to downstream transducer kinases like Chk1 and Chk2, for activation of the DNA damage checkpoint (Diagram 8). Therefore, the peculiarities of the DDR in mitosis, outlined by this and other studies, may be exploited as a model to understand more complex feedback mechanisms of regulation of the DNA damage signalling at different levels of the cascade.

**DIAGRAM 8. Mitotic data support the existence of a positive feedback loop between recruitment of DDR mediators and checkpoint activation**



A model describing that the unfolding of a full DDR cascade following DSB induction requires recruitment of mediators, including 53BP1 and BRCA1, to sites of DNA damage, in order to trigger proficient phosphorylation-dependent activation of Chk1 and Chk2 and stimulate a plethora of DNA damage induced responses. In mitosis, the absence of a putative positive feedback loop mediated by cross-talk between mediator and checkpoint kinases may impact on the subsequent activation of checkpoint signalling.

The study presented in this thesis experimentally demonstrates that the cell has devised several mechanisms to restrict secondary DDR activation in mitosis, by inhibiting ubiquitylation-dependent chromatin remodelling, downstream mediators recruitment and

Chk1 and Chk2-mediated activation of the DNA damage checkpoint. Thus, I suggest that activation of the secondary DDR and the DNA damage checkpoint do not occur in mitosis as deleterious to the cell in several ways. In the complex scenario of mitosis, where the nuclear envelope has broken down and the chromatin is irreversibly compacted, chromatin-remodelling events brought about by the secondary DDR cascade might result in local dismantling of mitotic chromosomes and may interfere with the process of karyokinesis. Furthermore, DSB-induced activation of the checkpoint may delay progression through mitosis, leading to mis-coordination of accurately timed mitotic events, potentially inducing mitotic catastrophe. Taking into consideration the DNA damage hyper-sensitivity of mitotic cells, both the brevity of mitosis and prioritizing the progression through mitosis in such a short time over activation of a full DDR cascade may represent evolutionarily selected traits.

### ***3.4.III Biological significance of the primary DDR in mitosis: marking and tethering***

Although secondary aspects of the DDR are not present in mitosis, mitotic cells do not ignore life-threatening lesions like DSB as was previously postulated. Mitotic cells mark the site of damage, using  $\gamma$ H2AX, MDC1 and MRN. Significantly, the data from this study shows that the primary DDR in mitosis is important for cell survival. I hypothesise that the effect of the primary DDR in mitosis is two-folds. Firstly,  $\gamma$ H2AX mediates a robust marking of the sites of DSB in mitosis. The *marking* may facilitate the identification of damaged sites in G1 and, thus, accelerate recruitment of repair factors and prompt a more rapid DDR activation. Moreover, the recruitment of MRN to mitotic DSBs could be instrumental in holding the broken DNA ends together until G1 and this might be mediated by the DNA end tethering activity of Mre11 (Williams et al., 2008). Simpler lesions might

be held together by the compacted chromatin structure, typical of mitotic chromosomes, while more complex lesions could benefit from the MRN-dependent DNA bridging activity, facilitating the repair process in the ensuing cell cycle. In line with this hypothesis, I show that a subset of DSBs remains unrepaired 24 hours after DNA damage when primary DDR activation is prevented in mitotic cells. These are likely to represent more complex lesions that would have benefited from the marking and end tethering immediately after DNA damage formation. The persistence of these DSBs can lead to increased mortality as cell progress through subsequent cell cycles. Thus, while secondary DDR responses are inhibited as presumably incompatible with the spatio-temporal set-up of mitosis, primary responses act in mitosis to favour DNA damage recognition and repair in the following cell cycle, representing a pivotal feature in maintaining genomic integrity and promoting cell survival.

#### ***3.4.IV Absence of DNA damage repair in mitosis***

The data presented in this study also infer that no repair occurs in mitotic cells. I found that one hour after the removal of the ATM/DNA-PK inhibitors, mock- and inhibitor-treated cells exhibited similar numbers of IRIF, which suggests that the majority of DSBs generated in mitosis are not fully repaired before the cell enters G1 phase. However, it was recently reported that DSBs are repaired in M-phase as well as interphase with similar kinetics (Kato et al., 2008). In the study presented by Kato et al., DSB repair was measured by pulse-field gel electrophoresis, which requires very high doses of damage (10-100 Gy). The fact that DSB repair was similar in mitotic and G1 cells could be explained by such high doses of radiation causing major perturbations in the chromatin organization of the cells as well as overall cellular metabolism. It is also possible that, upon irradiation with

these high doses, mitotic cells lose some of their unique qualities and persistent activation of the SAC may lead to atypical induction of DNA repair; indeed, a large amount of DNA damage is more likely to impact on the process of cell division itself, by impairing spindle attachment or causing loss of large portions of chromosomes, inducing prolonged activation of the SAC to act as a barrier to retain genomic protection during mitosis. Whatever the case, mitotic cells subjected to damage treatment of such magnitudes certainly do not progress into G1 and largely undergo cell death, as implied by the survival data showed in Figure 29. Therefore, it is very difficult to compare the data presented here to the previously published report by Kato et al. Notably, however, the IRIF dynamics as assessed by Kato et al., when they used 100-fold lower dose of IR, are similar to the one reported in this study: IRIF formed in mitosis persist into the following G1. Furthermore, close examination of the survival data presented in Figure 29 demonstrates that the PIKK inhibitors affect the radio-sensitivity of asynchronous cells much more strongly than that of mitotic cells. Even though further sensitisation of the mitotic cells by the PIKK inhibitors is statistically significant, when compared pair-wise, the differences at 0.5, 1 and 2 Gy are less than 2-fold and 4-fold at 4 Gy. At the same time, the difference is increasing progressively for the asynchronous cells, which have active DSB repair, and is more than 12-fold at 4 Gy. Taken together, these results suggest that the inhibition of DSB repair is not the major component contributing to cell killing upon transient inhibition of ATM and DNA-PK in mitotic cells. Instead,  $\gamma$ H2AX marking and MRN-dependent end tethering of the break until G1 may be sufficient to enable chromosome segregation and exit from mitosis, without perturbing cell division with invasive repair and chromatin remodelling apparatuses.

### ***3.4.V Different kinetics of DDR activation: breathing chromatin versus mitotic chromosomes***

Although the physical chromatin conformation of mitotic chromosomes *per se* does not obviously impact on local recruitment of factors to the DSB compartments, chromatin compaction renders cells intrinsically sensitive to DNA damage. Therefore, compacted chromatin may not cause local barriers to the damaged DNA but may globally affect the signalling cascade following DNA damage. Conversely, it is tempting to speculate that chromatin plasticity facilitates genomic surveillance. For instance, chromatin relaxation by expressing reduced levels of the linker histone H1 correlated to a hyper-responsiveness to DSB and resistance to DNA damaging agents (Murga et al., 2007). Similarly, transcriptional up-regulation of chromatin remodellers in pluripotent stem cells (Gaspar-Maia et al., 2009) increases plasticity of chromatin, which may correlate with stem cells' faster dynamics in their responses to DNA damage and repair of the DNA lesion (Maynard et al., 2008). Based on these data and those presented in this study, a model can be drawn where human cells in interphase, which have mixed chromatic environments of euchromatin and heterochromatin, display standard DDR signalling cascade and repair kinetics. Pluripotent stem cells, and other cells whose chromatin is in a more open conformation, show a more dynamic response to DSB, with increased signalling and repair capabilities. Mitotic cells, on the other hand, where chromatin is highly compacted, are characterized by an impaired DDR and strong radio-sensitivity. Although the exact causes of the phenotypic effect of different chromatin arrangements are still unclear, a correlation is starting to emerge between chromatin status and *intensity* of the DDR. Moreover, the status of chromatin directly impacts on propagation of the DNA damage signal and on the physical mending of the DNA insult. Attenuated DDR in mitosis is especially relevant in view of DSBs triggering DDR-dependent global relaxation process. A global relaxation

may facilitate responses to DNA breaks by enabling faster access of DDR factor to the DSB site to facilitate genomic surveillance; in mitosis, however, global relaxation may have disastrous consequences and human cells may have evolved to prioritize mitosis over full DDR activation and repair, and compacted chromatin may play a direct or indirect role in exerting this regulation.

The peculiarities of the DDR in mitosis, outlined by this and other studies, may be exploited as a model system to understand more complex feedback mechanisms of regulation of the DNA damage signalling at different levels of the cascade. Therefore, this study not only demonstrates how mitotic cells respond to DNA damage, but it also offers novel insight into the minute regulation of the DNA damage signalling cascade that are highly relevant in understanding DNA damage responses in all cell cycle phases.

### **3.5 Conclusions and future prospective**

The impact of DNA damage in mitosis is a phenomenon that has been largely overlooked in mammalian cells. In particular, no molecular data existed on the consequence of DSB induction in mitosis when this project started.

The aim of this study was to analyze how mitotic cells respond to an extremely cytotoxic form of DNA damage, DSBs. The notion that mitotic cells do not have a DNA damage checkpoint and do not arrest in response to irradiation had led to the assumption that no DDR was elicited by DSB during mitosis. However, I started the project with a simple observation.  $\gamma$ H2AX foci formed in mitosis, implying that mitotic cells did not simply ignore DNA lesions including DSBs and that certain responses to DNA damage were

elicited in mitosis. On the other hand, the observation that the DDR mediator 53BP1 was not recruited to DSB in mitotic cells prompted further analysis to dissect the differential regulation of DNA damage responses between mitosis and interphase.

Herein, I showed that that mitotic cells treated with DSB-inducing agents exhibit apical aspects of the DDR, but not downstream DDR components, such as RNF8, RNF168, 53BP1 and BRCA1 and lack of a DNA damage checkpoint. RNF8 represents a critical cut-off point in the DNA damage signalling cascade. Importantly, however, RNF8, RNF168 and 53BP1 become associated with IRIF after mitotic cells bearing DNA damage enter G1, when the full DDR activation occurs. Moreover, activation of primary DDR in mitosis is important for cell viability, possibly facilitating foci repair in the following cell cycle (Giunta et al., 2010).

The data presented by this study on the signalling mechanisms following induction of DNA damage in mitosis may be useful to gain a better understanding of the action of anti-mitotic agents on cancer cells. Hyper-sensitivity of mitotic cells and the understanding of the molecular mechanisms by which mitotic cells deal with DNA insults may impact on the creation of novel therapeutics against hyper-proliferating cancer cells.

Although this study provides a comprehensive analysis of the signalling responses elicited by DSB in mitosis and offers a first assessment of how mitotic cells deal with DSBs, numerous questions remain unanswered. A key challenge for the future will be to understand how exactly RNF8 is regulated in mitosis and what is the main mechanism to prevent its recruitment to IRIF. Understanding these aspects of mitotic regulation of RNF8 would help to gain more insight into the DDR cascade in interphase cells as well. In addition to RNF8, understanding how the DNA damage checkpoint is modulated in mitosis

would be of major interest. In this regard, confirming the existence of an essential cross-talk between mediators and checkpoint kinases would be extremely exciting and would provide a complex platform of regulation in a non-linear cascade. Outside of the responses to DNA damage under challenged conditions, more studies are required to understand the physiological role of DDR factors in mitotic structures. Especially, RNF8, RNF168 and 53BP1 recruitment to the kinetochores begs further investigations. Answering these and many more questions regarding mitotic DDR and the role of DDR factors in unperturbed mitosis would represent substantial progress toward gaining a better understanding of the signalling cascade initiated by DSBs and the process and regulation of mitosis; furthermore, it may allow us to gain a better understanding of the action of chemotherapeutic drugs on cancer cells and may be exploited to improve chemotherapeutics in a near future.

## 4 ANALYSIS OF THE GINS COMPLEX SUBUNIT PSF1

### 4.1 Summary

The connection between DNA damage responses and the mechanisms of arrest of DNA replication is still largely unclear. The GINS complex is an evolutionarily conserved component of the DNA replication machinery that has been suggested to coordinate DNA unwinding at the leading strand with priming of DNA synthesis at the lagging strand. In addition to its essential roles for DNA replication, I speculated that GINS may be an ideal candidate for transferring the DNA damage signal to the replication apparatus, thereby mediating DNA replication arrest and/or preventing firing of new replication origins.

Here, I show the identification of a conserved ‘SQ’ (serine-glutamine) site at the carboxyl end of two subunits of the GINS complex, Psf1 and Psf2, that conforms to the target consensus for the key DNA damage activated kinases ATM, ATR and DNA-PK. In *S. cerevisiae*, a single amino acid mutation in Psf1, switching the conserved serine to a glutamic acid (S187E), is lethal, indicating that the site is crucial for the protein function. In human cells, Psf1 C-terminus interacts *in vitro* with the UV-DDB, a heterodimeric complex involved in diverse cellular processes such as repair and ubiquitylation. Moreover, I show that the human *PSF1* gene product is involved in maintaining GINS complex stability and plays a role in DNA replication and cell cycle progression.

Altogether, the data presented in this chapter provide novel experimental support for a role of the Psf1 C-terminus consensus motif in modulating GINS complex activity in human and yeast cells.

## 4.2 Introduction

### 4.2.1 *The GINS complex is an evolutionarily conserved component of the replisome*

GINS is a heterotetrameric protein complex found in all eukaryotic cells. The four distinct subunits of the GINS complex are Sld5 (Synthetically Lethal with *Dbp11-1* five), Psf1, Psf2, and Psf3 (Partners of Sld5 1, 2 and 3; Takayama et al., 2003). Sld5 was initially identified in a synthetic lethal screen to map genetic interactions using a Dpb11 thermo-sensitive allele in *S. cerevisiae* (Kamimura et al., 1998). It is noteworthy that Dpb11 itself had been hitherto uncovered in a genetic screen where it suppressed mutations in two essential DNA polymerase  $\epsilon$  subunits and was found to be required for both DNA synthesis and intra-S-phase checkpoint activation (Araki et al., 1995). Subsequent to its identification in the 1990s, Sld5 remained unstudied until 2003, when its analysis led to the discovery of the other GINS subunits and thus of the whole GINS complex (which stands for 'go' 'ichi' 'ni' 'san': 5, 1, 2, 3 in Japanese; Kubota et al., 2003; Takayama et al., 2003).

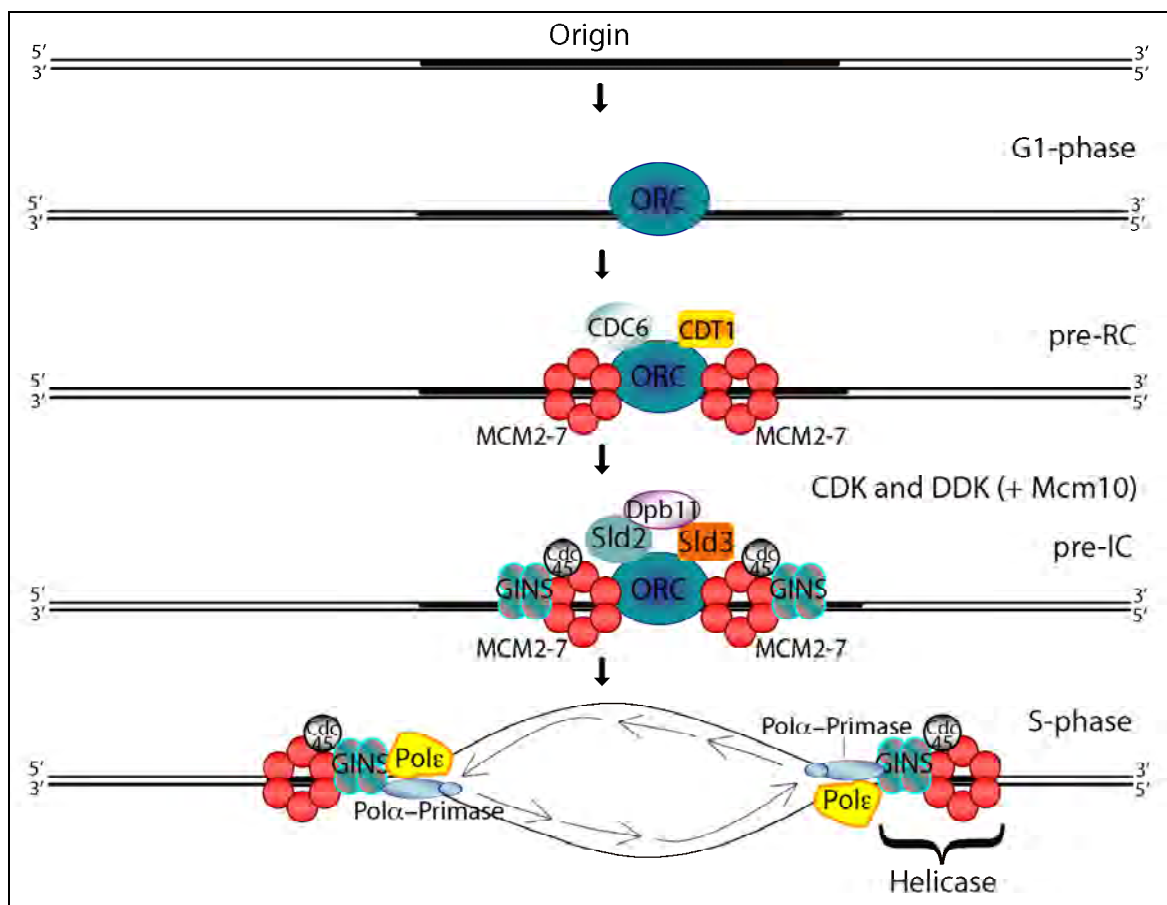
The GINS complex is structurally and functionally conserved throughout evolution. From archaea, yeast and frog, through to human, the GINS complex displays a quaternary structural arrangement and has been shown to hold an ancient fundamental role in DNA replication (Kubota et al., 2003; Takayama et al., 2003; Marinsek et al., 2006). The four paralogous GINS subunits are phylogenetically related in all eukaryotes. In archaea, the GINS core tetramer contains two homodimers of Gins23 and Gins51, which are distantly related to the eukaryotic GINS in terms of sequence homology. Duplication of the ancestral archeo-genes gave origin to the conserved heterotetramer found in all eukaryotes (Makarova et al., 2005; Marinsek et al., 2006). The complete depletion of one of the GINS

polypeptides causes lethality to eukaryotic cells, due to GINS pivotal function in DNA synthesis and cell cycle progression. In 2005, Ueno et al. showed the requirement for the GINS subunit Psf1 in early mouse embryogenesis. *PSF1* knock-out mice died *in utero* due to the absence of cell proliferation (Ueno et al., 2005), recognizing GINS essential role in genome duplication and GINS disruption being incompatible with life.

GINS function in DNA replication initiation and DNA unwinding has been characterized in *Drosophila*, *Xenopus* and, extensively, in budding and fission yeast. The GINS heterotetramer is part of the CMG complex, a candidate eukaryotic DNA replication helicase. The CMG complex comprises Cdc45, the ring-shaped MCM hexamer and the four GINS proteins (Moyer et al., 2006). In *Drosophila* and *Xenopus*, the CMG is present at sites of DNA unwinding during replication and it displays intrinsic DNA helicase activity *in vitro* (Moyer et al., 2006; Pacek et al., 2006). The MCM2-7 double hexamer represents the core of the CMG macromolecular ‘unwindosome’ machinery. Cdc45 and the GINS complex, on the other hand, have auxiliary functions as helicase cofactors, enhancing MCM2-7 unwinding activity (chapter 1.2.II). It remains unclear whether Cdc45 and GINS supporting role is fundamental for MCM-mediated DNA unwinding. In the context of DNA unwinding, GINS may function as a structural co-factor that facilitates interactions with DNA, base pair separation and translocation speed (Aparicio et al., 2006). In addition to the auxiliary role in DNA unwinding, budding yeast GINS has been shown to be an accessory factor for DNA polymerase  $\epsilon$  *in vitro* (Seki et al., 2006b), possibly coordinating DNA unwinding and polymerization during DNA synthesis. Moreover, genetic studies in *S. cerevisiae* have mapped the sequential incorporation of replication factors, including GINS, at the nascent fork (Diagram 9). In G1, the MCM-containing pre-replication complex (pre-RC) does not include the GINS complex, which becomes

associated upon the CDK/Cdc7-dependent transition from pre-RC to pre-IC (pre-initiation complex), also requiring Sld3 and Cut5. Association of GINS to the pre-IC is needed to stabilize Cdc45 in the active replisome and to promote fork progression during S-phase (Kanemaki and Labib, 2006 ; see Diagram 9 and chapters 1.2.II and 1.2.III for details).

**DIAGRAM 9. Ordered assembly of the replisome for initiation of replication in *S. cerevisiae***



A model for the sequential assembly of factors to the replication fork in budding yeast. The origins of replication sites are bound by ORC. In G1, Cdt1 and Cdc6 serve to enable the loading of the MCM2-7 ring to pre-RC. CDK-dependent phosphorylation of Sld2 and Sld3 and interaction with Dpb11 create a molecular bridge to facilitate loading of cdc45 and GINS to the pre-IC. Sld3 is then removed from the pre-IC and a plethora of other factors associate with the replication fork during the transition from G1 to S-phase to enable initiation and elongation of replication.

Investigations in fission yeast revealed that GINS are required for the chromatin association to the replication origin of the Dpb11 homologue Cut5, as well as Cdc45 and the DNA polymerase  $\epsilon$  (Yabuuchi et al., 2006); yet, DNA polymerase  $\alpha$  is successfully recruited to chromatin when GINS is inactivated (Pai et al., 2009). Nevertheless, GINS may interact with DNA polymerase  $\alpha$  during replication, directly or indirectly by binding to the Pol  $\alpha$ -interacting factors Ctf4 in budding yeast (my own result and Gambus et al., 2009) and may be required for the activity of the DNA polymerase  $\alpha$ -primase complex. The archaeal GINS associates with DNA primase and stimulates its activity *in vitro*. Thus, GINS interactions with factors at the replication fork may be necessary for coupling MCM progression with priming events (Marinsek et al., 2006). This hypothesis, yet to be verified, would reconcile the two fundamental roles of the GINS complex in replication: DNA unwinding and DNA synthesis. However, *Xenopus* egg extracts treated with the DNA polymerase inhibitor aphidicolin displayed enrichment of GINS, Cdc45 and MCM2-7 to paused replication sites, but not of the DNA polymerases, suggesting that the helicase complex is physically uncoupled from the replication apparatus (Pacek et al., 2006). Furthermore, GINS interacts with Drc1, Mrc1 (homologue of human Claspin), Tof1 and several other replication factors, suggesting that complex functional interfaces regulate GINS during DNA synthesis and other S-phase-specific activities for the GINS complex are likely to exist.

In 2006, when this PhD project started, the investigation of GINS physiological role in mammalian cells had yet to be addressed; new data from the Italian group of Dr. Pisani in 2007 confirmed the interactions between the human GINS and DNA polymerase  $\alpha$ -primase complex (De Falco et al., 2007). The human GINS complex was then shown to bind to Cdc45 and the Mcm2-7 complex, where Cdc45 bridges the replicative helicase

with the processive DNA polymerases  $\delta$  and  $\epsilon$  (Bauerschmidt et al., 2007), strengthening the idea that GINS may coordinate unwinding and DNA synthesis. Similarly to budding yeast, the assembly of human CMG helicase requires Ctf4, RecQL4 and Mcm10 proteins (Im et al., 2009). These findings outline a strong degree of conservation in the molecular mechanisms of the replication initiation and elongation in eukaryotes, of which GINS is a central nexus.

**DIAGRAM 10. The GINS complex activities at the replication fork during DNA synthesis**



**Content not visible due to copyright limitations**

The eukaryotic GINS heterotetramer is composed of Sld5 (in blue), Psf1 (in green), Psf2 (pink) and Psf3 (yellow; Psf2 and Psf3 are placed behind the Sld5-Psf1 dimer). GINS have been directly associated with DNA pol  $\epsilon$ , pol  $\alpha$ -DNA primase, as well as being part of the CMG helicase complex, with the MCM2-7 ring and Cdc45, suggesting roles in DNA unwinding and DNA synthesis.

Image modified from Chang et al., 2007

#### ***4.2.II Structural organization of the GINS complex in the context of the DNA replication fork***

Several structural conformations of the GINS complex have been suggested by electron microscopy images and gel filtration data to support the functional link with Mcm2-7, Cdc45 and DNA polymerases  $\epsilon$  and  $\alpha$ -primase. Initially, GINS was thought to be a ring-shaped molecule (Kubota et al., 2003) that acted as a molecular link between Cdc45 and the MCM ring, where both complexes formed rings that, juxtaposed, made a central channel for ss and dsDNA to pass through (Moyer et al., 2006). Furthermore, the idea of GINS shaped as a closed ring encircling the DNA prompted the theory of it functioning in a similar fashion to the trimeric polymerase-accessory-ring PCNA, as a 'sliding clamp' for DNA polymerase  $\epsilon$ , promoting initiation of DNA duplication (Aparicio et al., 2006).

In 2007, analysis of the crystallized human GINS complex described it as a globular ellipse with a small central channel (Chang et al., 2007; Choi et al., 2007; Kamada et al., 2007). The complex has a pseudo two-fold axis of symmetry, where Sld5-Psf1 dimer sits 'on top' of the Psf2-Psf3 dimer, constituting the heterotetramer. Each GINS subunit comprises two distinct protein domains; an A-domain made largely of  $\alpha$ -helices, and a smaller B-domain composed of  $\beta$ -sheet – located at the C-terminus of Sld5 and Psf1 (Diagram 11). Structurally, Sld5 and Psf2 resemble Psf1 and Psf3, respectively, indicating that they evolved from one common ancient ancestor.

Resolution of the crystal structure of the human GINS complex (Chang et al., 2007; Choi et al., 2007; Kamada et al., 2007) added yet more controversy to the molecular organization and mode of DNA interaction of the complex. Kamada et al. and Choi et al.

showed that GINS central cleft is too small for either ss or dsDNA to pass through it (Diagram 11; Choi et al., 2007; Kamada et al., 2007). However, Chang and colleagues supported the idea that a short, 16-residues peptide on the flexible Psf3 N-terminus can move to enlarge the central channel by 80% and regulate accessibility of the DNA (Chang et al., 2007).

### DIAGRAM 11. The molecular structure of the human GINS complex



**Content not visible due to copyright limitations**

The GINS complex is arranged in a pseudo-two-fold symmetry between the Sld5-Psf1 and Psf2-Psf3 dimers. The pseudo-symmetry extends at the structural level of individual subunits, showing that the morphology of Sld5 and Psf2 resemble those of Psf1 and Psf3, respectively. Each subunit is made of two types of structural domains, A and B, and a linker region connects them. The C-terminus of Psf1 is truncated in the crystal structure (dotted circle). The right panel shows GINS central cleft (zoom). Due to the cleft's dimension, GINS is unlikely to make contact to the DNA *via* this central channel.

Images modified from Kamada et al., 2007

Another study, using single-particle electron microscopy and three-dimensional reconstruction analyses, suggested that GINS complex shows a 'horseshoe' shape and is arranged as an open ring that can accommodate ss and dsDNA. The GINS complex partially encircles and directly binds to DNA, with higher affinity for ssDNA. Based on these observations, the authors speculate a possible role for the GINS complex as 'strand

displacement unit' during MCM-dependent DNA unwinding (see chapter 1.2.II and diagram 1; Boskovic et al., 2007).

#### ***4.2.III Functional relevance of Psf1 carboxyl terminal domain in mediating initiation of replication***

Despite discrepancies in the structural information provided by the crystallized human GINS complex, both Kamada et al. (2007) and Chang et al. (2007) uncovered areas undetectable by electron density maps and difficult to crystallize, representing highly flexible, unstructured regions in the GINS complex. These disordered regions are located on the C-terminal domains of Sld5 (residue 65-71), Psf3 (194-216) and the very C-terminus of Psf1 (from residue S145 to end) and are likely to be important functional and protein-binding interfaces (Chang et al., 2007). Whereas the Psf1 carboxyl tail is dispensable for the stability of the GINS complex, the Sld5 C-terminus is pivotal for the core complex assembly. Psf1 B domain is a structurally distinct region, anchored to the rest of the complex *via* a linker region (Diagram 11). Truncation of the Psf1 B-domain at the carboxyl end of the protein results in the assembly of a stable core complex, which is, however, non-functional. No initiation of replication was detected in *Xenopus* extracts where Psf1 full-length protein was replaced by its truncated counterpart (Kamada et al., 2007). Thus, Psf1 C-terminal end is the functional interface of the entire complex, mediating chromatin binding and DNA replication activities. The exposed position of the Psf1 C-terminal end is meaningful as it provides a docking site for interactions with other proteins involved in DNA replication and beyond. Therefore, the B domains on Sld5 and Psf1 are essential for the GINS complex and function both to stabilise the interfaces

between the layers of the complex and to form higher-order protein complexes with additional factors, respectively.

In conclusion, several studies in the last decade have enriched our knowledge about the GINS complex across and beyond the animal kingdom (for review, see MacNeill, 2010). Yet, significant uncertainties remain as to the exact structural conformation, mode of action and coordination dynamics between the various functional interfaces of the GINS complex.

#### ***4.2.IV Alternative roles for the GINS complex: do all roads come from Rome?***

In addition to the evolutionarily conserved functions of the GINS complex in DNA replication, several additional roles have been recently described, that may represent novel functions of the complex, or may be indirect consequences of GINS essential role in DNA replication.

The identification of the GINS subunit Psf2 as a multi-copy suppressor of the mutated fission yeast protein Bir1, the human homologue of Survivin, inferred a role for the GINS complex in chromosome segregation. Bir1 is a conserved chromosomal passenger factor, whose suppression leads to aberrant cell division and cytokinesis. Loss of Psf2 in the fission yeast *S. pombe* caused failed localization of Bir1 to elongating spindles and resulted in chromosomes mis-segregation. The same study reported a dramatic chromosome mis-segregation phenotype when *PSF2* was knocked-down by siRNA in human HeLa cancer cells, which resulted in aneuploidy and growth arrest. Psf2 may play a conserved role in promoting high-fidelity chromosome segregation and mitotic division; however, this may

be an indirect effect of GINS role during S-phase, possibly through regulation of centromere replication (Huang et al., 2005a). In support of a direct role for the GINS complex in mitosis, I have observed recruitment of the GINS subunit Psf1 to the mitotic structure of the midbody in late anaphase and telophase (Figure 41). In addition, GINS levels are maintained constant across the cell cycle, inferring for additional roles outside of S-phase. Nonetheless, a recent study investigated the putative mitotic role of GINS in human dermal fibroblasts (HDF) and found absence of gross chromosomal abnormalities and mitotic defects in Psf1/Psf2-depleted cells. The authors point to defects in the progression through S-phase and in delayed mitotic entry as the underlying cause of chromosome aberrations in GINS down-regulated cells (Barkley et al., 2009). In addition, siPFS1/2-induced S-phase delay caused replicative stress, including formation of DNA damage – as monitored by  $\gamma$ H2AX foci formation – and activation of the ATM/Chk2-dependent checkpoint – indicated by robust Chk2 T68 phosphorylation – in the absence of genotoxins. Interestingly, the ATR/Chk1 branch fails to be activated in Psf1/2-depleted HDF (Barkley et al., 2009), suggesting that the key role of GINS in maintaining replicative helicase activity is necessary for generating RPA-coated ssDNA and initiating the intra-S-phase checkpoint by Chk1.

Given accurate replication and repair of DNA is crucial for maintaining genomic stability and ensure faithful genome duplication, DDR activation has been shown to be an hallmark of pre-malignant tissues (reviewed in Halazonetis et al., 2008), indicating the presence of mutational damage which may lead to malignant transformation. Therefore, Psf1/2 down-regulation leads to a precarious scenario of genomic instability, characterized by DDR activation, possibly leading to subsequent chromosome mis-segregation. Conversely, GINS role in promoting cell proliferation represents the other face of the same coin. In

fact, up-regulation of GINS subunit drives cancer cell proliferation. Psf3 was shown to be over-expressed in colon cancer cells and its depletion results in cancer cell growth arrest, rendering Psf3 suitable as a biomarker for diagnosing progression of colon cancer, as well as a target for novel cancer therapeutics (Nagahama et al., 2010). More examples of GINS over-expression in malignancy include elevated levels of Psf2 in intrahepatic cholangiocarcinoma tissues (Obama et al., 2005), Psf1 and Sld5 in aggressive melanoma (Hayashi et al., 2006) and also Psf1 in MCF7 human breast carcinoma cells, where *PSF1* was identified as an estrogen target (Ryu et al., 2007). These findings suggest a scenario where *GINS* down-regulation leads to genomic instability and contributes to pre-malignancy. A later role of *GINS* up-regulation in malignancy serves to promote cancer cell hyper-proliferation and further mutagenic transformations. Accordingly, *GINS* mRNA levels are tightly regulated in human and mouse tissues, with the highest expression observed in the embryo, given GINS is essential for embryogenesis. Studies in *Xenopus* showed that Psf2 is specifically required for eyes and brain early development (Walter et al., 2008). GINS expression is lowered in adult tissues, made exceptions for the areas where the stem cell system is active, like bone marrow and testis. In the testis, transcriptional up-regulation of *PSF1* is essential for spermatogenesis (Han et al., 2009). Psf1 was also shown to be required for maintenance of immature haematopoietic SC and bone marrow regeneration (Ueno et al., 2009).

Therefore, maintenance of physiological levels of the GINS complex is pivotal for propagation of life, as both the under and over-expression statuses have equally deleterious consequences on human cells. Similarly to GINS, MCM had previously been shown to mark cell replicative potential (Musahl et al., 1998; Madine et al., 2000; Stoeber et al., 2001) and display dysregulated expression in a range of neoplastic conditions. MCM has

been shown to be a marker of dysplasia (Todorov et al., 1998; Freeman et al., 1999) and its over-expression correlates with increasing tumour grade and poor prognosis (Gonzalez et al., 2005). Thus, MCM is currently being exploited as a diagnostic and prognostic cancer biomarker (reviewed in Coleman and Laskey, 2009). Whether pre-RC components, like the MCM, Cdc6 or ORC complexes, have direct oncogenic potential is still under debate (Lau et al., 2007), yet other pre-RC and pre-IC proteins, including GINS, may be exploited to monitor changes in cellular replicative capabilities.

In a physiological scenario, GINS is essential to drive embryogenesis by ensuring sustained cell division, modulate tissue differentiation and promoting proliferation-dependent maintenance of the stem cells pool. Instead, in the aberrant environment of the cancer cell, GINS may contribute to hyper-proliferation, facilitating the propagation of the tumour. Therefore, the balance between endorsing physiological cell division and preventing uncontrolled cell growth by tight regulation of replication must be maintained to sustain life.

### **4.3 Results**

#### **4.4 Analysis of the GINS subunit Psf1 in human cells**

##### ***4.4.1 Psf1 and Psf2 subunits of the GINS complex contain an evolutionarily conserved DNA damage related motif at the C-terminus***

The GINS complex functions at the interface between two essential processes of replication: DNA synthesis and DNA unwinding. The functional activity of GINS in coordinating these events places it under the spot light as a key factor to ensure accuracy of the replicative process and to preserve replication fork integrity. Therefore, GINS complex may be an important target to modulate DNA replication in the presence of genotoxic alterations and function to maintain genomic stability.

To identify novel proteins containing ‘SQ’ (serine-glutamine) sites, which conform to the consensus target site for phosphorylation by the key DNA damage activated kinases ATM, ATR and DNA-PK, I performed *in silico* searches for this motif. Phosphorylation of these motifs may play a functional role in controlling cellular responses to DNA insults. With the help of Mike Gilchrist, the Gurdon institute bioinformatician, I performed a Blast search against the human genome for the closest homologue to the (S/T)QxF/Y motif located at the C-terminal end of proteins. One of the hits of the blast search was the SQEY-COOH consensus motif in human H2AX (Table 6), a main target site of PIKK kinases, validating the screen. The first hit of the bioinformatics search was the SQDF-COOH site in the GINS subunit, Psf2 (Table 6), also located at the very carboxyl end of the protein, similarly to H2AX.

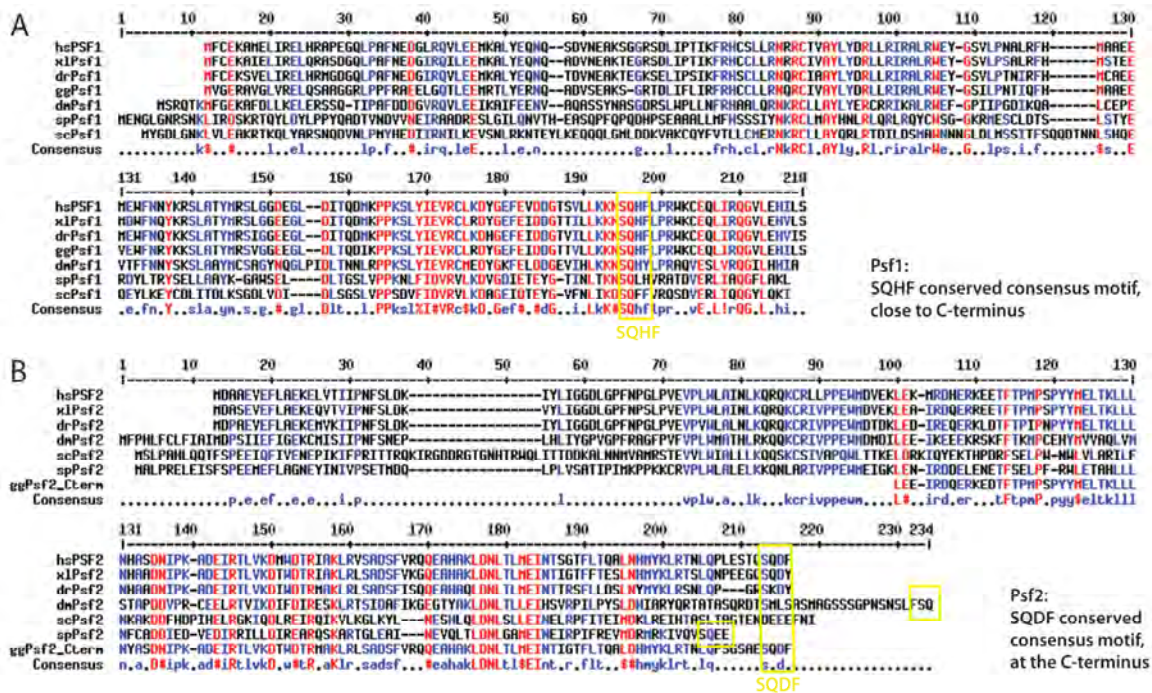
**TABLE 6. *In silico* search for C-terminal consensus (S/T)QXF peptide motifs across the human genome**

<b>Motif</b>	<b>Proteins</b>
SQDF*	DNA replication complex GINS protein Psf2
SQDF*	Protein ARV1 (hARV1)
SQEY*	Histone H2A.x (H2A/x)
SQGY*	Synaptogyrin-1
SQKF*	Centaurin-beta 2 (Cnt-b2)
SQPY*	Melanoma-associated antigen B5 (MAGE-B5 antigen)
SQRY*	Keratin 6L
TQIY*	UDP-GlcNAc:betaGal beta-1,3-N-acetylglucosaminyltransferase 3
TQQF*	CDK5 and ABL1 enzyme substrate 2 (interactor with CDK3 2)
TQTY*	Clorf113 protein (Fragment).

Blast search for human proteins containing sites homologous to the (S/T)QXF motif at the very C-terminus (\* = COOH). The 10 resulting protein hits are shown, along with the site's sequence

Strikingly, Psf1, another subunit of the GINS complex, also contains an evolutionarily conserved ATM consensus motif within its C-terminus, present in eukaryotes from yeast to human (Figure 31). ATM sits at the apex of the DDR cascade and, upon induction of DNA damage, it phosphorylates a plethora of substrates, mediating a range of cellular responses (Shiloh, 2003). The consensus motifs on Psf1 and Psf2 carboxyl termini may also be targeted for phosphorylation by ATM and may serve as a means to control replication fork elongation and/or unwinding in the presence of DNA lesions.

**FIGURE 31. Multispecies alignment of Psf1 and Psf2 proteins sequences**



Psf1 (A) and Psf2 (B) sequence alignment in different eukaryotic species: human, *Xenopus*, zebrafish, chicken, *Drosophila*, budding and fission yeasts. Human Psf1 and Psf2 share high sequence identity with their counterparts in different species with the highest conservation at the C-terminus, including the ‘SQXF’ consensus site.

#### 4.4.II A candidate approach to test the BRCT phospho-peptide binding hypothesis

The evolutionarily conserved SQXF motifs on Psf1 and Psf2 (in human, SQHF and SQDF, respectively) resemble phospho-epitopes acting as docking sites for binding to selected BRCT-containing substrates, similarly to the phosphorylated S139 of  $\gamma$ H2AX, within a consensus SQ C-terminal motif, that recruits the twin BRCTs of MDC1. The BRCT phospho-binding modules are present in several DDR proteins such as MDC1, 53BP1, BRCA1 and TopBP1, mediating signal transduction events of the DDR cascade. In addition, Psf1 and Psf2 SQ sites both share a conserved phenylalanine amino acid in the +3 position (3 residues C-terminal with respect to the phospho-serine). BRCA1 BRCTs have

been shown to bind with high affinity phospho-serine peptide targets that contain a phenylalanine residue in +3 position (Manke et al., 2003; Yu et al., 2003). The crystal structure of the interacting interface revealed that, along with the phospho-serine, the +3 phenylalanine is a key binding pocket for the BRCT hydrophobic groove (Clapperton et al., 2004; Williams et al., 2004). The conservation of the interacting residues suggests that BRCT proteins recruitment to phospho-epitopes is an evolutionary conserved mechanism in the signalling of DNA damage.

Because the human BRCT-containing DNA damage mediator TopBP1 (topoisomerase II binding protein 1) is homologue to Dpb11 in *S. cerevisiae* and Cut5 in *S. pombe*, that have been genetically and physically associated with the GINS complex, I wanted to test whether these motifs on Psf1 and Psf2 may represent binding interfaces for TopBP1 recruitment to the replication fork. Furthermore, to address if phosphorylation may regulate these putative interactions, similarly to recruitment of other BRCT-containing DDR factors by DNA damage-dependent phosphorylation, I used synthetic biotinylated peptides for the phosphorylated and unphosphorylated forms of Psf1 and Psf2 SQXF motifs (Table 7). A candidate approach was undertaken to assess if the binding of potential interactors was either positively or negatively regulated by phosphorylation. In addition, in the Psf1 peptide, the amino acid in the +3 position was modified from a phenylalanine to an alanine (F176A), still in the presence of the phosphorylated serine in Psf1, to assess the binding potential of candidate BRCT domain-containing proteins through their BRCT binding interface.

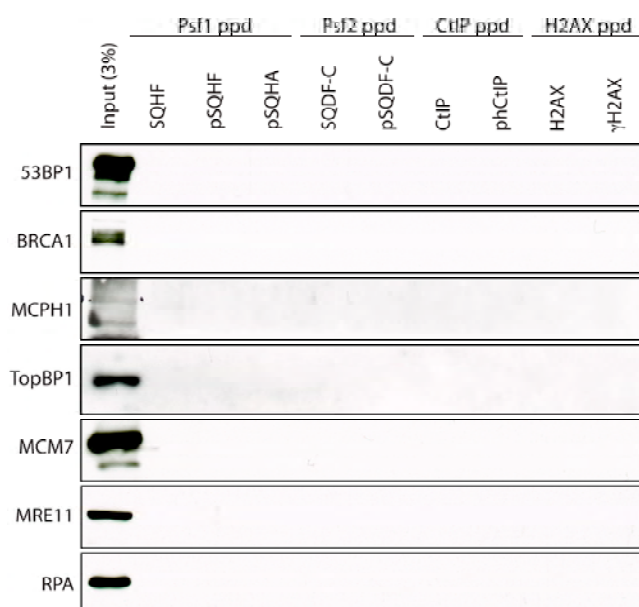
**TABLE 7. Synthetic peptides of Psf1 and Psf2 used for pull-downs experiments**

Name	Synthetic peptide
Psf1 SQHF	Biotin-SGS-GTSCVLLKKN <u>SQH</u> FLPR-NH <sub>2</sub>
Psf1 pSQHF	Biotin-SGS-GTSCVLLKKN( <b>pS</b> )QHFLPR-NH <sub>2</sub>
Psf1 pSQHA	Biotin-SGS-GTSVLLKKN( <b>pS</b> )QH <b>A</b> LPR- NH <sub>2</sub>
Psf2 SQDF	Biotin-SGS-YKLRTNLQPLESTQ <b>SQ</b> DF-COOH
Psf2 pSQDF	Biotin-SGS-YKLRTNLQPLESTQ( <b>pS</b> )Q <b>D</b> F-COOH

Human Psf1 (164-179) and hPsf2 (168-185) peptides in their unphosphorylated and phosphorylated forms (Psf1 pS173 and Psf2 pS182) are shown, where the consensus motif is underscored. An additional phospho-peptide was used for Psf1 with a mutation of the F176 to alanine, shown in bold.

Pull-downs from HNE showed that RPA, MRE11, BRCA1, 53BP1, TopBP1, MCPH1 and MCM7 failed to bind to any of the peptides tested in either their phospho- or unphosphorylated-forms (Figure 32).

**FIGURE 32. Peptide pull-down experiments and WB for selected candidates**



Psf1 and Psf2 C-termini are used to *fish* for BRCT-containing DDR proteins: 53BP1 (214 kDa), BRCA1 (220 kDa), MCPH1 (110 kDa) and TopBP1 (180 kDa). Binding of MCM7 (81 kDa), MRE11 (80) and RPA (p70, 70 kDa subunit) was also tested. MDC1 (Figure 33) but not MRE11 bound to phosphorylated H2AX peptide, as only direct interactions would be retained under the conditions used.



Psf1 bands from silver gels were sent for protein identification by tandem mass spectrometry (MS/MS). Seven silver stained bands were identified as proteins binding to Psf1 peptides (Table 8).

**TABLE 8. Psf1 peptides-binding proteins identified by mass spectrometry**

Serial #	Protein name	Gi #	Identified peptide	Coverage (%)
1	put. Beta-actin [ <i>Mus musculus</i> ]	49868	8	30
2	acetyl-CoA carboxylase 1 Isoform 2 Isoform 1 [ <i>Homo sapiens</i> ]	33112885 38679967 38679960	17	11
3	PREDICTED: similar to Prostate, ovary, testis expressed protein on chromosome 2 [ <i>Homo sapiens</i> ]	113413194	1	1
4	acetyl-CoA carboxylase 1 Isoform 2 Isoform 1 [ <i>Homo sapiens</i> ]	33112885 38679967 38679960	13	9
5	Xeroderma Pigmentosum Group E Complementing protein; DNA damage binding protein 1 (Damage-specific DNA binding protein 1, DDB p127) [ <i>Homo sapiens</i> ]	2632123	2	5
6	major vault protein [ <i>Homo sapiens</i> ]	19913410	6	12
7 (a)	lacritin precursor [ <i>Homo sapiens</i> ]	15187164	1	9
7 (b)	nasopharyngeal carcinoma-associated proline rich 4 [ <i>Homo sapiens</i> ]	22208536	1	11
7 (c)	proline rich 4 [ <i>Homo sapiens</i> ]	6005802	1	10

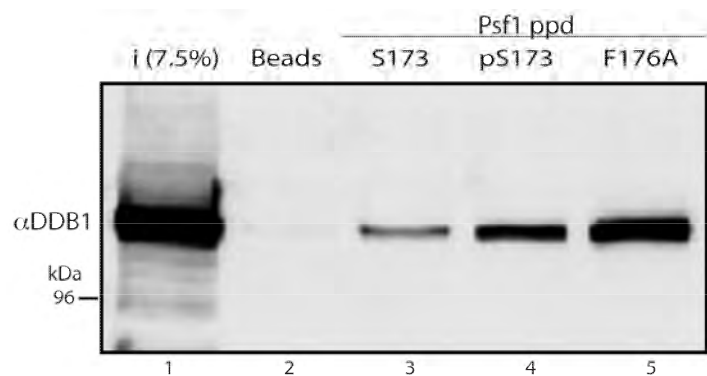
Proteins identified by MS/MS. Interestingly, band 5 was identified as DDB1, a 127 kDa protein that corresponded to a silver stained band of the expected size. Two peptides for DDB1 were identified by mass spec analysis: IGRPSETGIIGIIDPEC(+57)R and IEVQDTSGGTTALRPSASTQALSSSVSSSK which had strong homology for DDB1.

#### **4.4.IV UV-DDB protein complex binds to Psf1 C-terminus in vitro**

DDB1 was identified by MS/MS in the screen for proteins interacting with Psf1 SQXF C-terminal motif. DDB1 is a 127 kDa subunit of the DNA damage binding complex UV-DDB, involved in the repair of UV radiation photoproducts by nucleotide excision repair

(NER). To verify that DDB1 was a *bona fide* binding partner of Psf1, I analyzed their interactions by western blotting. The pull-downs recapitulated the interaction between Psf1 and DDB1, which occurred constitutively with the unphosphorylated peptide; furthermore, the interaction was strengthened by phosphorylation of Psf1 S173 and further increased when F176 was mutated to alanine (Figure 34).

**FIGURE 34. Psf1 C-terminus peptides bind to DDB1 and the interaction is stabilized by phosphorylation**

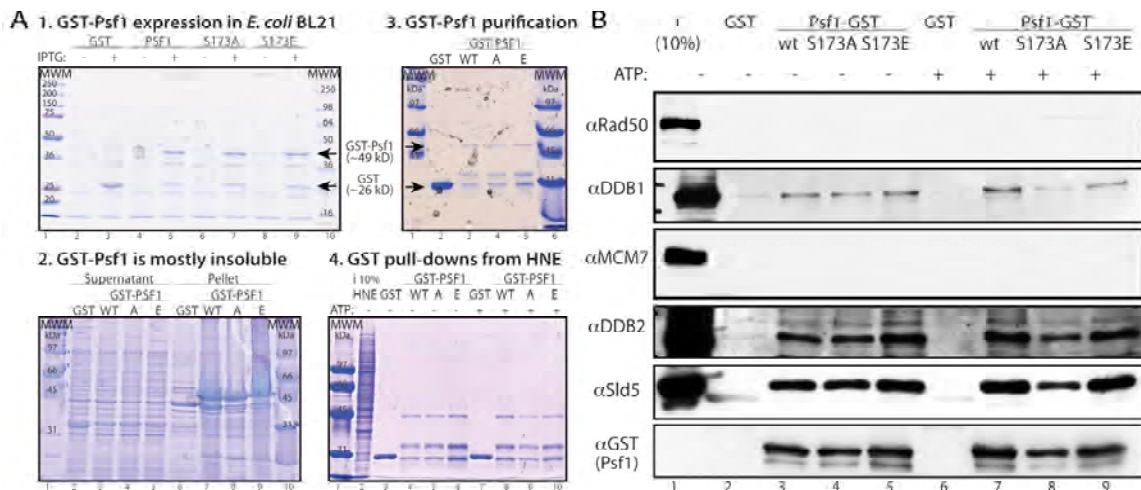


Peptide pull-downs from 1 mg of HNE were carried out as in Figures 32-33. The samples were analyzed by western blotting using a goat polyclonal antibody against hDDB1 (1128-1140 synthetic peptide DLIKVVEELTRIH, ab9194; Table 1).

To confirm interactions between full length Psf1 and DDB1, I cloned, expressed and purified recombinant GST-Psf1 protein from *E. coli*. Expression of recombinant protein in bacteria was optimized by overnight incubation with 0.1 mM IPTG at 16°C (Figure 35A, panel 1). Although most Psf1 was insoluble (Figure 35A, panel 2), a small amount of full length GST-Psf1 from the supernatant was bound to the beads (Figure 35A, panel 3) and was able to pull-down DDB1, as well as the smaller 48 kDa subunit, DDB2, from HNE (Figure 35B). In addition to pulling down the UV-DDB complex, the other GINS subunits were also retrieved when using full-length GST-Psf1 (Figure 35B). This suggests that binding of Psf1 to DDB1 did not hinder interactions with other GINS subunits and GINS complex formation. In addition, the fact that Psf1 C-terminus peptide did not pull-down

other GINS subunits, whereas full-length Psf1 did, infers that the binding interface for Psf1 to assemble into the GINS complex lies outside of the C-terminus of the protein. These observations are in agreement with data from the human GINS crystal structure, which indicates that the Psf1 C-terminus is dispensable for GINS complex formation and stability, but is an essential functional interface for binding to other factors (Kamada et al., 2007).

**FIGURE 35. Full-length GST-Psf1 expression, purification and pull-downs**



GST-Psf1 recombinant protein was expressed in a pGEX-6P-3 vector in *E. coli* using 0.1 mM IPTG overnight at 16°C (A). A band corresponding to Psf1 was observed at ~49 kDa (Psf1 = 23 kDa + GST = ~26 kDa; black arrows) only in IPTG-induced lanes (panel 1). After lysis, the soluble (supernatant) and the insoluble (bacterial pellet) fractions were analysed, showing Psf1 is mostly insoluble (panel 2). The supernatant contained a small amount of Psf1 that was conjugated to GSH-sepharose beads and run at ~49 kDa, as expected (top arrow; Panel 3). Full length GST-Psf1 bound to the beads was used for pull-down experiments from 1 mg of HNE. Psf1 was pulled-down as shown by Coomassie stained gel (Panel 4; A). Western blotting of GST, DDB1, DDB2, Sld5, Mcm7 and Rad50 is shown in B.

To address the regulation of DDB1 and DDB2 binding to Psf1, I mutated S173 to alanine (A), which cannot be phosphorylated, or to glutamic acid (E), which may represent a phospho-mimicking mutant. Importantly, both mutants behaved like wild-type Psf1 in binding other GINS subunits (Figure 35), indicating that site-specific mutagenesis of S173 in Psf1 does not disrupt GINS complex formation and stability. This was expected due to

the truncation of Psf1 C-terminus (aa 140-196) not affecting complex stability (Kamada et al., 2007). No differences were observed in the ability of DDB1 to bind Psf1 when the serine was mutated to alanine or glutamic acid, indicating that the binding interface between Psf1 and DDB1 may be outside of the SQ site and is not phosphorylation-dependent. The pull-down experiments showing decreased DDB1 binding using F176A mutant peptides (Figure 34) suggest that the binding may be modulated by the conserved phenylalanine residue (F176), which is exposed on the peripheral surface of the complex. Indeed, Kamada et al. (2007) identified this conserved hydrophobic residue as functionally important for Psf1 association with target proteins (see discussion chapter 4.6.I for details).

#### ***4.4.V Phosphorylation of human Psf1 after DNA damage***

While my investigations were ongoing, Steve Elledge and colleagues performed a large-scale proteomic screen that revealed the C-terminal SQ site of human Psf2 to be phosphorylated by ATM/ATR in response to DNA damage (Matsuoka et al., 2007). This prompted me to investigate whether the consensus SQ site on Psf1 was also phosphorylated by the PIKK kinases in response to DNA damaging agents or possibly to replicative stress.

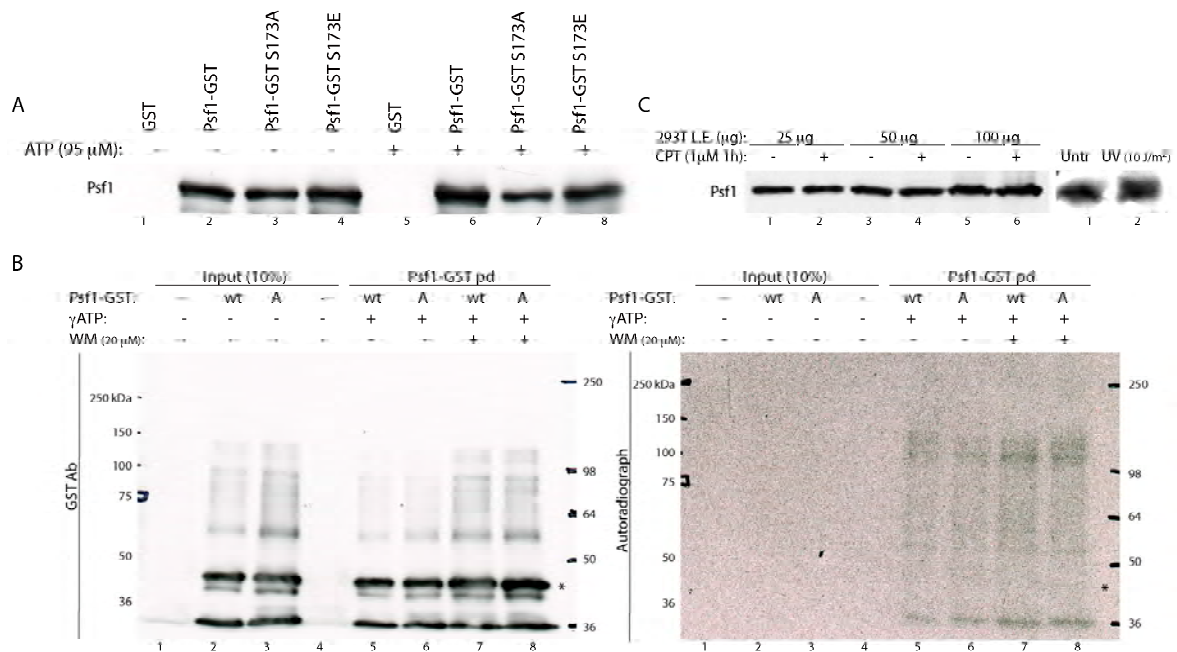
Initially, I used a similar experimental technique as described in the Matsuoka screen; Psf1 was immunoprecipitated by irradiated or untreated U2OS cell extracts and phosphorylation was assessed by using a phospho-antibody that generally recognizes substrates phosphorylated by ATM and/or ATR on S/TQ sites. However, IP experiments using Psf1 were greatly hindered by the proximity of Psf1 with the IgG light chain that runs at about

25 kDa on western blot. The use of TrueBlot™ antibodies that preferentially detect the native disulfide form of the IgG reduced but did not clear the signal from the denatured IgG light chain, making it difficult to assess the presence of phospho-bands.

To address whether Psf1 was phosphorylated *in vitro*, I performed pull-downs using GST-Psf1 recombinant protein incubated in HNE in the presence or absence of ATP. A small electrophoretic mobility shift was observed on SDS-PAGE when Psf1 was incubated with ATP and when Psf1 S173E mutant was used, even before addition of ATP (Figure 36A), suggesting that the protein may be post-translationally modified by phosphorylation. I repeated the GST pull-down experiments using radiolabelled [ $\gamma$ 32P]-ATP. Autoradiography showed very faint signals corresponding to GST-Psf1 (Figure 36B). However, the signal persisted when the alanine mutant was used for the pull-down and in the presence of 20  $\mu$ M wortmannin (Figure 36B), a dose inhibiting ATM and DNA-PK (Izzard et al., 1999), suggesting that Psf1 may be phosphorylated in a PIKK-independent manner on sites other than S173.

In addition, I used the electrophoretic mobility shift assay to monitor the presence of a phosphorylation-dependent change in Psf1 protein mobility *in vivo* following incubation with increasing doses of camptothecin (CPT). CPT is a cytotoxic alkaloid that binds to and inhibits DNA topoisomerase I causing DNA breaks. The toxicity of CPT treatment is mostly observed during S-phase, when ongoing replication converts single-strand breaks into double-strand breaks upon collision of the fork. At high dose of CPT, a smear was observed in the antibody staining against Psf1, indicative of phosphorylation. Furthermore, a similar shift was observed following UV (Figure 36C).

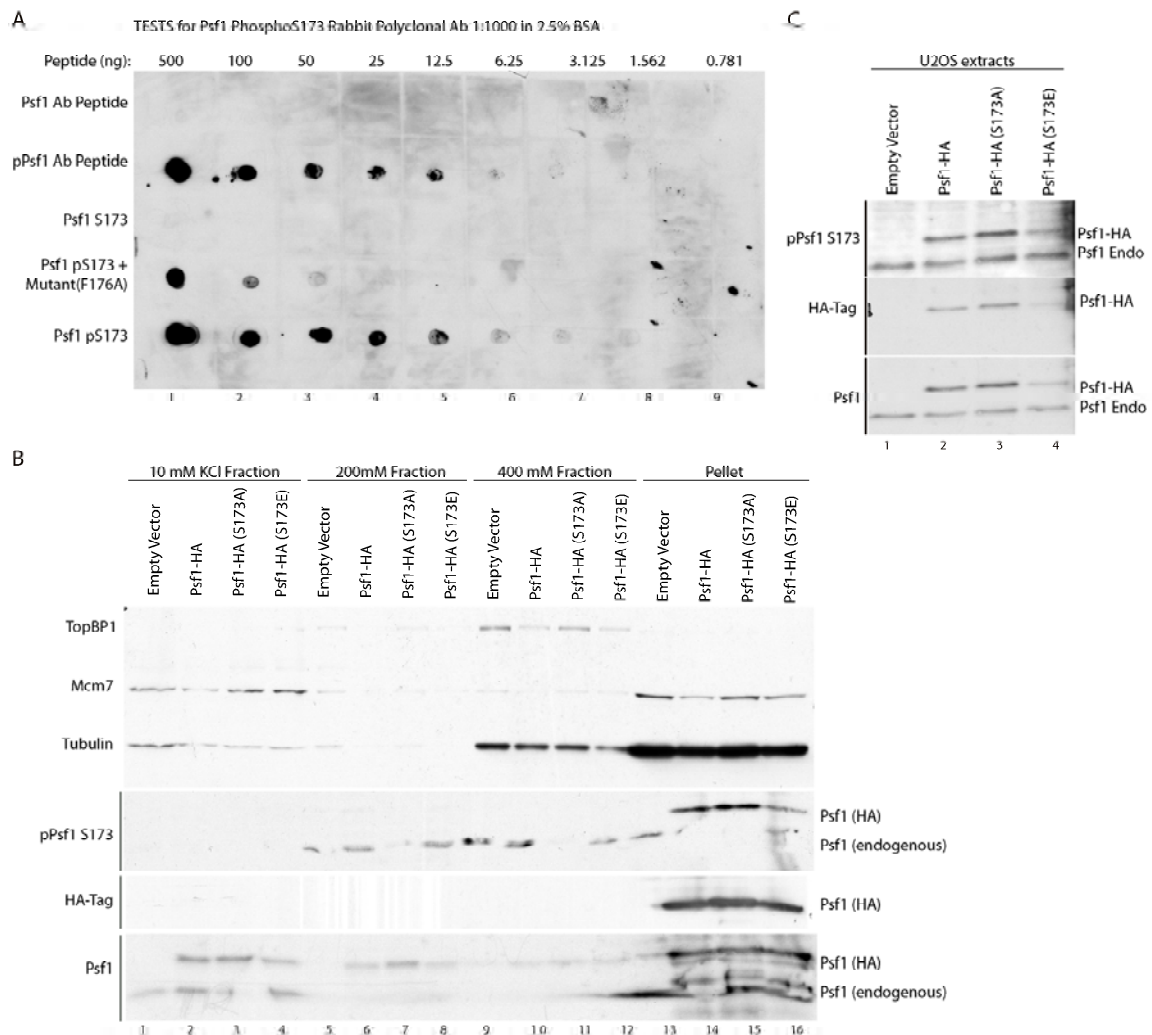
**FIGURE 36. Addressing Psf1 phosphorylation *in vitro* and *in vivo***



Empty vector (GST), Psf1-GST wild-type and mutant forms (S173A and S173E) were incubated in HNE in the presence or absence of 95  $\mu$ M ATP (A). GST pull-down experiments were repeated with Psf1 WT and S173A mutant ('A') using radiolabelled [ $\gamma$ 32P]-ATP (0.37 MBq/tube; 10  $\mu$ Ci/ $\mu$ l per reaction). Reactions were analysed by SDS-PAGE followed by western blotting (left) and autoradiography (right). A very faint signal was observed corresponding to GST-Psf1 (~51 kDa, as Psf1 ~23 kDa and the GST tag is ~28 kDa) in the autoradiograph. Signals other than Psf1 were detected by autoradiography between 100 and 150 kDa, possibly representing phosphorylated Psf1 binding partners, including the 127 kDa protein, DDB1, and at 36 kDa, possibly representing Psf1 degradation products (B). Electrophoretic mobility shift assay show a phosphorylation-dependent change in Psf1 protein mobility *in vivo* (lane 6; C) following incubation with the indicated dose of CPT for 1 hour. Treatment with 10 J/m<sup>2</sup> of UV for 1 hour shows a similar phospho-shift (C).

An antibody was raised against the phosphorylated form of Psf1 S173 to assess whether this site is phosphorylated *in vivo*. However, the pS173 antibody was found to be non-specific, detecting the Psf1 mutant with an unphosphorylatable form of the site (S173A; Figure 37). Therefore, this antibody could not be used to unequivocally address the outstanding question of whether Psf1 is phosphorylated on S173 within the conserved C-terminal consensus ATM phosphorylation motif.

**FIGURE 37. Psf1 Phospho-S173 rabbit polyclonal antibody tests**

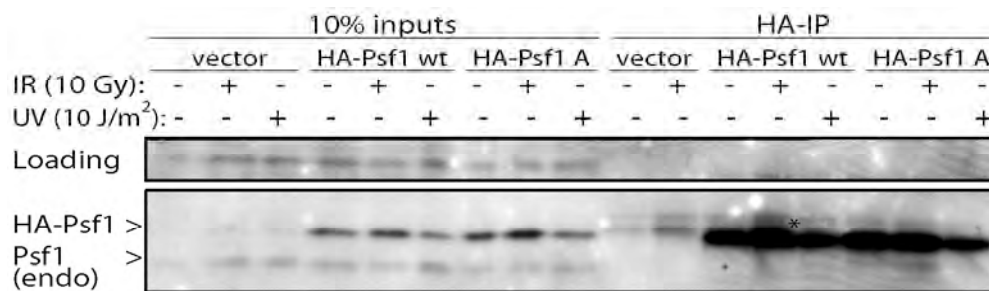


A phospho-specific antibody was raised against human Psf1 pS173. Spot test was used to test the antibody at a concentration of 1:1000 in 2.5% BSA/TBS-T solution using Psf1 and pPsf1 Ab Peptides, used to immunize the rabbit, and Psf1 synthetic peptides as from Table 7. Interestingly, mutation of F176A reduces phospho-antibody recognition (A). Cellular fractionation (B) or Laemmli extracts (C) of U2OS cells transfected with Psf1-HA, S173A and S173E mutants. Most Psf1 is found in the chromatin bound fraction (B). pPsf1 S173 antibody recognizes Psf1 alanine mutant (B and C).

Interestingly, Psf1 S173A and S173E mutants expressed and bound to chromatin similarly to the wild-type protein (Figure 37B) and expression of Psf1 mutants did not affect the stability of Psf1 (Figure 37C) and other GINS subunits (data not shown), suggesting that C-terminus motif mutants behave similarly to Psf1 in terms of DNA binding dynamics.

Psf1 levels, for both endogenous and HA-tagged transiently transfected proteins, are unchanged after irradiation and treatment with UV, indicating that DNA damage does not cause failed stabilization or proteosomal degradation of Psf1 proteins, or transcriptional inhibition of the *PSF1* gene. In addition, even after IR, a shift was observed in IR-treated samples where HA-Psf1 was immunoprecipitated, and the mobility shift was reduced using HA-Psf1 S173A mutant, suggesting that S173 may be phosphorylated following irradiation of human cells (Figure 38).

**FIGURE 38. Level of endogenous and transiently-transfected Psf1 proteins is unchanged after DNA damage**



Psf1 protein levels are unchanged after treatment with DNA damaging agents, IR (10 Gy) and UV (10 J/m<sup>2</sup>). Endogenous (endo) and transiently transfected HA-tagged Psf1 in U2OS were monitored using rabbit Psf1 polyclonal antibody. IP was performed using monoclonal antibody against HA-tag. HA-Psf1 wild-type, but not HA-Psf1 A (S173A) mutant, shows a smear after irradiation (marked by asterisk).

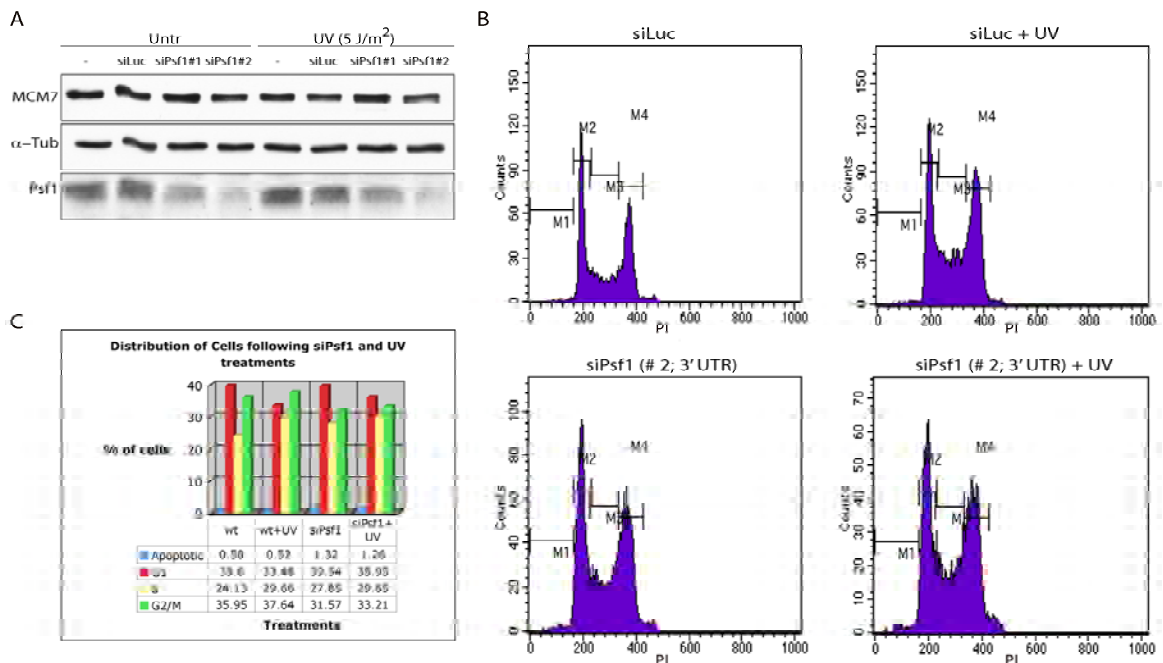
#### 4.4.VI Analysis of Psf1 subunit of the GINS complex in the cell cycle

The role of the GINS complex in human cells was largely elusive when this project started. Consequently, I set to investigate the physiological function of Psf1 and how it is modulated in response to DNA damage in human cells.

To address the affect of *PSF1* down-regulation on cell cycle progression, I used small interfering RNA (siRNA)-mediated knock-down (KD) of *PSF1* in U2OS human cancer

cells. siRNAs against *PSF1* open reading frame (ORF; siPSF1 # 1) and against the 3' untranslated region (3'-UTR; siPSF1 # 2) were tested, with the latter showing the highest level of down-regulation (Figure 39A). siPSF1#2 cells were harvested for FACS analysis 48 hours post-transfection and compared with siLuciferase cells. As expected, Psf1 depletion showed an increase in S-phase cells, indicative of slower replication. Moreover, fewer cells were found in G2/M, suggesting that Psf1 depletion activates replication arrest possibly through the induction of intra-S-phase checkpoints (Figure 39B and 39C). These data are in agreement with a recent report that shows that siPFS1/PSF2 lead to accumulation in S-phase of primary cells (Barkley et al., 2009). Data in HeLa cells, where entry into mitosis followed by mitotic catastrophe was observed following siPFS2 (Huang et al., 2005a), can be reconciled by the fact that, unlike U2OS, HeLa cells lacking functional p53 cannot support proficient intra-S-phase checkpoint arrest (Zhu et al., 2004). In line with GINS subunits being essential for cell viability, siPSF1 increased the sub-G1 population from 0.58% in siLuciferase to 1.32% (Figure 39B and 39C), probably indicating cell debris due to apoptotic death or necrosis. In addition, siPSF1 cells showed about 30% confluency on the dish, against 50-60% for siLuciferase, at 24 hours post-transfection (data not shown). The decrease in confluency in siPSF1 cells is caused by an increased cell death and, not mutually exclusive, a slower proliferation rate. It is noteworthy that no more than ~70% protein depletion was observed using siPSF1 (Figure 39A), suggesting that reduction of Psf1 below a certain threshold is incompatible with cell survival. Indeed, the level of Psf1 down-regulation may affect the choice between cell death and cell cycle delay, as a critical level of Psf1 may be sufficient to enable cell survival in spite of slower replication events.

**FIGURE 39. Psf1 down-regulation affects progression through S-phase**



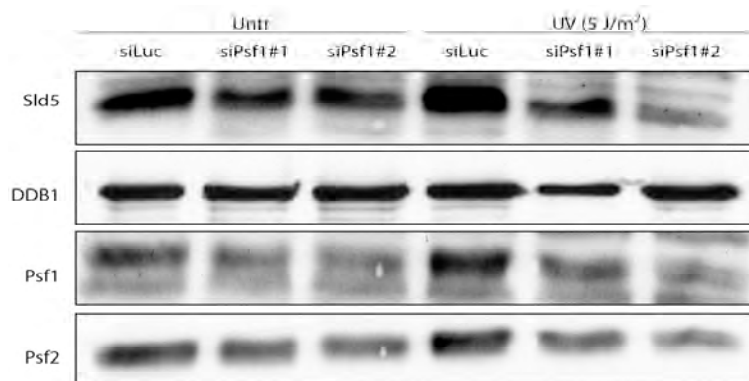
Psf1 depletion by siRNA against the ORF (siPsf1 #1) or the 3'-UTR (siPsf1 #2) in U2OS. WB shows good depletion using siPsf1 #2 and no changes in MCM7 levels (A). FACS analysis of siPsf1 (#2) and siLuciferase (siLuc) before and after UV irradiation (5 J/m<sup>2</sup>; B). A graphical representation of the number of cells in sub-G1 (cell debris), G1, S and G2/M for each treatment are shown in panel C.

To monitor how cells knocked-down for Psf1 behaved in the presence of DNA damaging agents, I compared cell cycle progression of siPFS1 or siLuciferase cells treated with 5 J/m<sup>2</sup> of UV. Treatment with UV on its own caused S-phase delay, similarly to siPFS1 alone. This suggests that 5 J/m<sup>2</sup> of UV light cause enough photoproducts to slow down replication fork progression similarly to depletion of Psf1. Yet, UV treatment caused more cells to accumulate in G2 and less to re-enter G1, suggesting that UV also causes checkpoint activation at the G1/S and G2/M boundaries (Figure 39B and 39C); thus, UV impacts on all cell cycle stages, whereas Psf1 specifically acts in S-phase. These data are in agreement with the epistatic requirements for replication initiation. Loss of MCM, an essential component of the pre-RC complex, arrests cells in G1 and prevents entry into S-phase. On the other hand, reduction of the GINS complex, loaded upon the G1/S transition onto the pre-IC complex, does support entry into S-phase but hamper replication fork

elongation and replisome activity. Interestingly, combination of siPFS1 and UV gave a decrease in G1 compared to siPFS1 alone, inferring that UV robustly activates the G2/M in a Psf1-independent manner. Moreover, S-phase index was also slightly increased (Figure 39B and 39C), indicating that the residual DNA synthesis in siPFS1 is further slowed down by the presence of UV-induced photoproducts.

I also monitored how siPsf1 might affect the level of DDR and replication proteins, in the presence or absence of UV. ATM, ATR, MCM7, DDB1, DDB2 and p53 levels were unchanged (Figure 39A, 40 and data not shown). However, the levels of other GINS subunits, including Psf2 and Sld5, were decreased accordingly to Psf1 down-regulation (Figure 40), indicating that full length Psf1 is essential for the stability of the complex. Thus, reduction in one GINS subunit triggers destabilization and proteosomal degradation of the whole complex or leads to inhibition of GINS transcription.

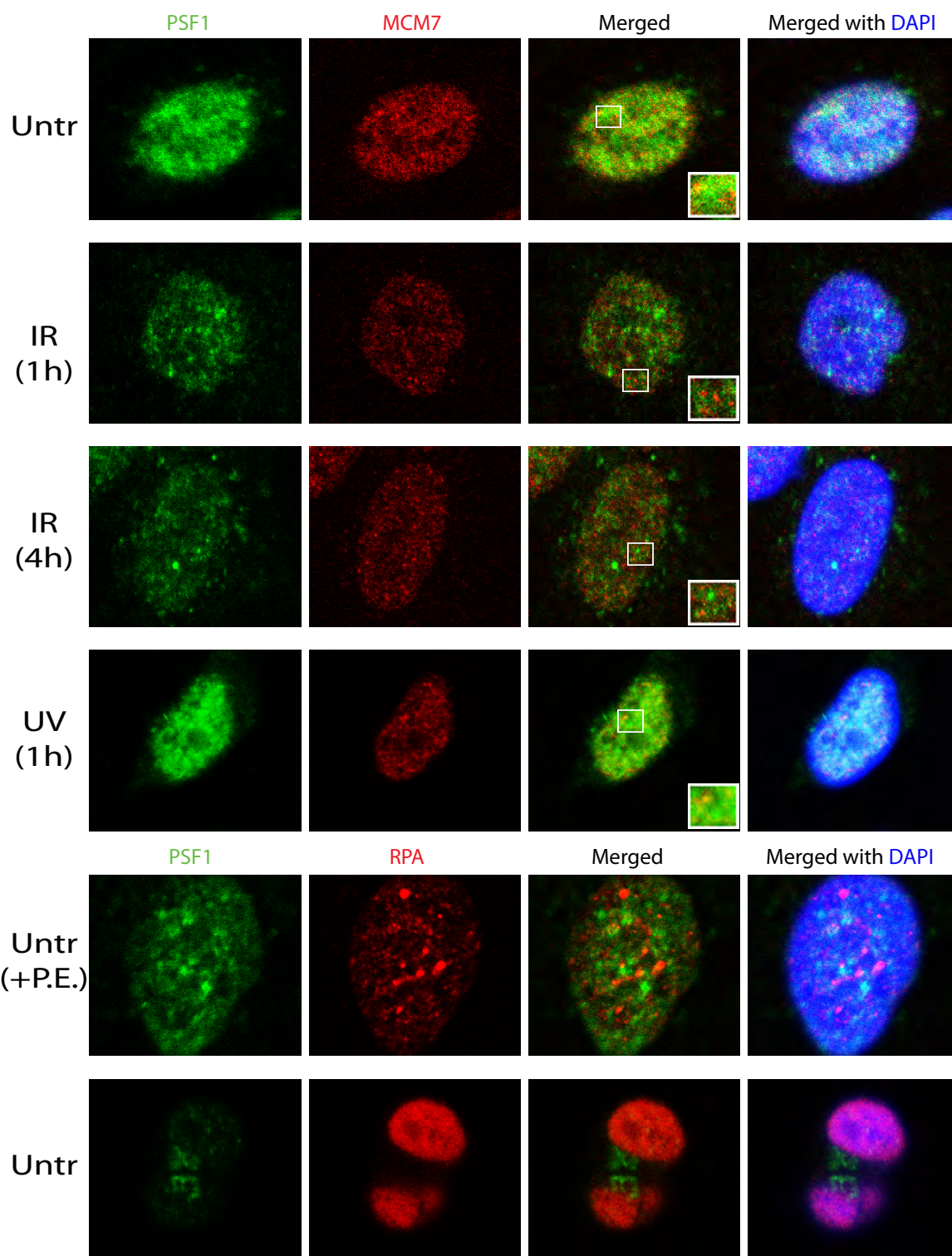
**FIGURE 40. Down-regulation of *PSF1* by siRNA causes reduction in protein level of other GINS subunits**



Protein levels of DDB1 are unchanged. Treatment with 5 J/m<sup>2</sup> of UV does not affect the endogenous proteins level of Psf1, Psf2, Sld5 and DDB1.

Next, I wanted to investigate the localization of the GINS complex in U2OS cells using antibodies raised against human Psf1 (Figure 41).

**FIGURE 41. Localization of human Psf1 is altered by DNA damage following irradiation**



Immunofluorescence analysis of Psf1 in human U2OS cancer cells. Psf1, stained in green, was co-stained with MCM7, part of the MCM ring, or RPA, staining single stranded DNA regions. Psf1 pan nuclear pattern, which co-localize with MCM and RPA, and is altered following irradiation with 5 Gy of IR, when the pan-nuclear staining diminish. Psf1 speckles are largely excluded from MCM staining. After pre-extraction, Psf1 speckles persisted, indicating staining of chromatin-bound proteins. Psf1 also localizes to the mid-body in late mitosis.

Immunofluorescence analyses revealed that Psf1 has a diffused nuclear pattern, with few brighter discretely-staining regions. Psf1 nuclear aggregates were retained following CSK pre-extraction (Figure 41), suggesting that these nuclear aggregates contain chromatin-bound Psf1. However, these Psf1 nuclear aggregates do not effectively co-localize with the MCM7 subunit of the MCM helicase, or RPA-marked ssDNA at the replication fork. Thus, Psf1 nuclear aggregates may represent regions other than the replication origins or active replisomes. Strikingly, irradiation caused an alteration in Psf1 staining, with a decrease in pan-nuclear fluorescent intensity, yet persistence of brightly-stained regions (Figure 41). This suggests that Psf1 may be degraded, although no evidence for this was found by western blotting (Figure 38), or, more likely, may be re-localized after IR. MCM and RPA staining remain unperturbed by the presence of DNA damage. This change in Psf1 nuclear pattern occurs selectively following irradiation, as treatment with UV rays did not cause obvious changes in Psf1 staining. In addition, Psf1 staining was reproducibly observed on the spindle midzone in the mitotic structure of the midbody during late mitosis, suggesting that the GINS complex may indeed play a role in cytokinesis and in promoting mitotic exit.

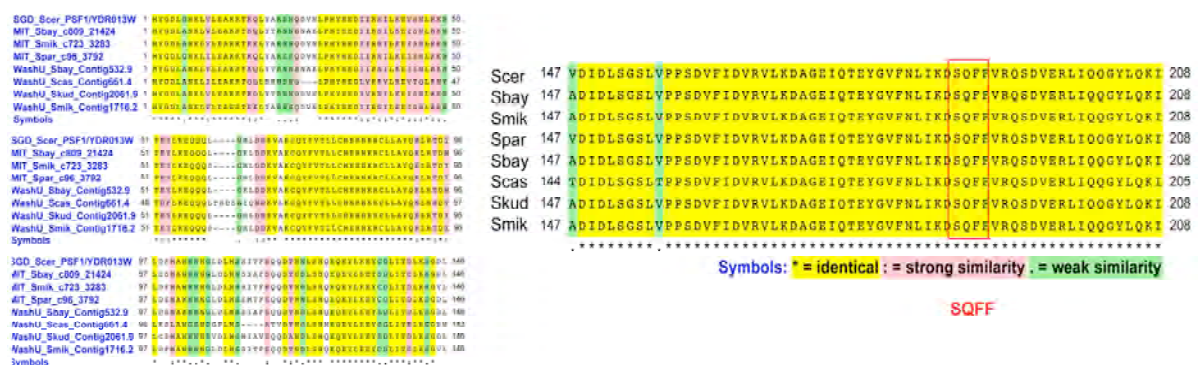
Collectively, these data show that Psf1 is required for S-phase progression and, ultimately, for cell proliferation and viability. Reduction in Psf1 causes a reduction in the level of other GINS subunits, leading to delayed replication, suggesting that the role of GINS in replication is conserved in higher eukaryotes. Finally, GINS staining was found to be altered following irradiation of human cancer cells, suggesting that perturbation of cellular metabolism following DNA damage impacts on Psf1 localization and, possibly, interactions with other replisome components.

## 4.5 A C-terminal motif of Psf1 is essential for the GINS complex activity in *Saccharomyces cerevisiae*

### 4.5.1 Analysis of the conserved SQ motif at the C-terminus of Psf1

To further investigate the role of the Psf1 C-terminus conserved SQXF motif, I adopted the budding yeast *S. cerevisiae* as model organism. The SQ site of Psf1 C-terminus is present in *S. cerevisiae* (Figure 31A) and is highly conserved in fungi (Figure 42).

**FIGURE 42. Conservation of fungal Psf1 carboxyl terminus and SQFF motif**



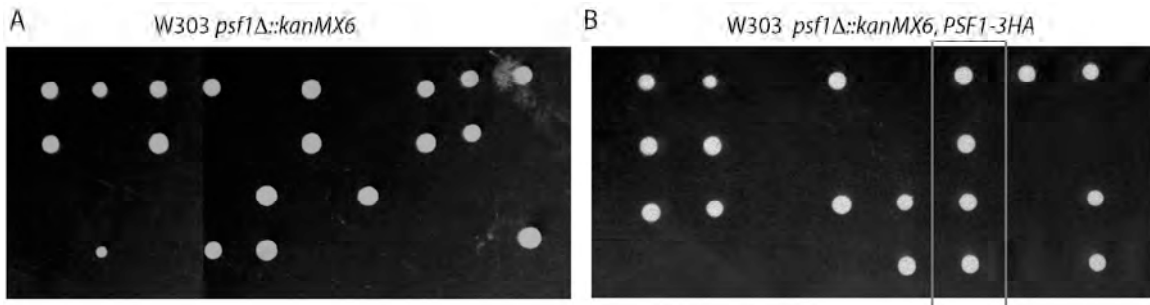
ClustalW alignments of *S. cerevisiae* Psf1 protein sequences with those of other fungi from the Saccharomyces Genome Database (SGD) website (<http://www.yeastgenome.org>). The alignment shows a striking conservation of the C-terminus (147 to end, enlarged panel on the right), corresponding to the GINS functional interface identified by Kamada et al., 2007. The SQXF motif is highly conserved and corresponds to a SQFF motif in fungi (red box), where the serine is S187.

### 4.5.II Analysis of *S. cerevisiae* psf1 null and 'SQ' motif mutant strains

I constructed a diploid W303 wild-type (W303A, *RAD5*) strain heterozygous for *PSF1* gene deletion. After sporulation and dissection, haploid spores lacking the chromosomal copy of *PSF1* gene could not germinate (Figure 43A). Thus, as previously shown and similarly to mammalian cells, deletion of *PSF1* in budding yeast is lethal. Lethality caused

by deletion of *PSF1* was reversed by expressing a plasmid copy of *PSF1* cDNA prior to sporulation, which allowed haploid spores to grow normally (Figure 43B).

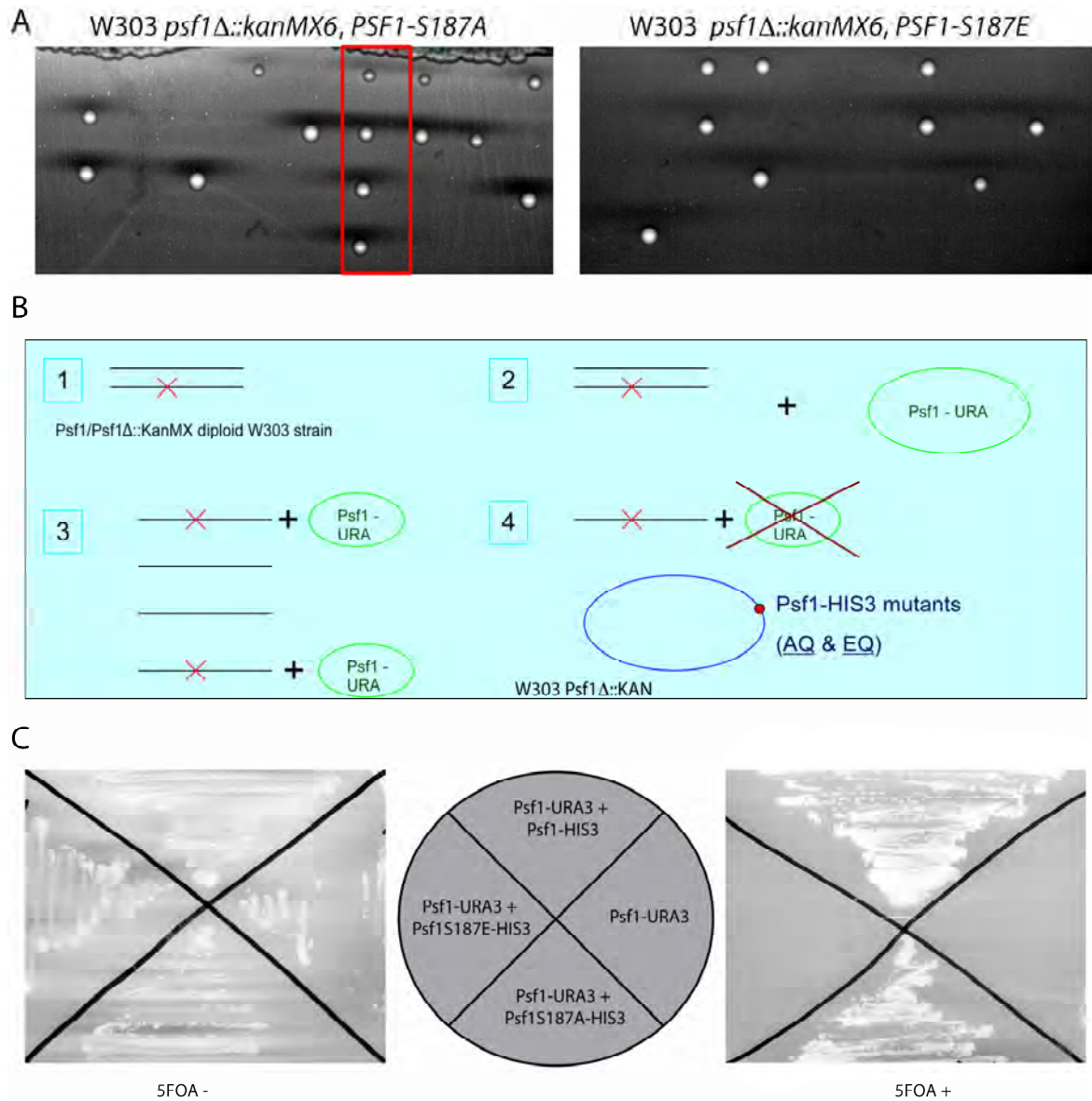
**FIGURE 43. Yeast *psf1* deletion mutant is unviable and lethality is rescued by a plasmid copy of *PSF1* cDNA**



*Psf1*Δ haploid strain is dead, as only spores containing a chromosomal copy of *PSF1* survived and grew on plate (A). Lethality is rescued by expression of *PSF1*-3HA plasmid; only yeast containing either a chromosomal copy or a plasmid copy of *PSF1* survived and grew similarly on plate (B).

To examine the function of the *Psf1* SQ motif, I employed a method called the plasmid shuffle technique (see Methods 2.11.V and Figure 44B). I performed site-directed mutagenesis to obtain a single amino acid substitution of *Psf1* serine 187 to a phospho-deficient alanine (*Psf1*<sup>S187A</sup>) or to a phospho-mimicking glutamic acid (*Psf1*<sup>S187E</sup>). Haploid *psf1*Δ strains expressing *URA3* plasmids containing wild-type *PSF1* were transformed with *HIS3* plasmids expressing *psf1*-S187A, *psf1*-S187E or *PSF1*. When plated on 5-FOA, expression of either *PSF1*-*HIS3* or *psf1*-S187A-*HIS3*, but not *PSF1*-*URA3* containing strain, conferred growth on 5-FOA-containing medium and rescued the lethality of *PSF1* chromosomal deletion (Figure 44C). *psf1*-S187E was lethal (Figure 44C), indicating that the phospho-mimicking mutant of *psf1* is unable to rescue the *PSF1* null lethality.

**FIGURE 44. Yeast *psf1Δ* strain complementation experiments with *psf1-S187A* and *psf1-S187E* and analysis by plasmid shuffle technique**

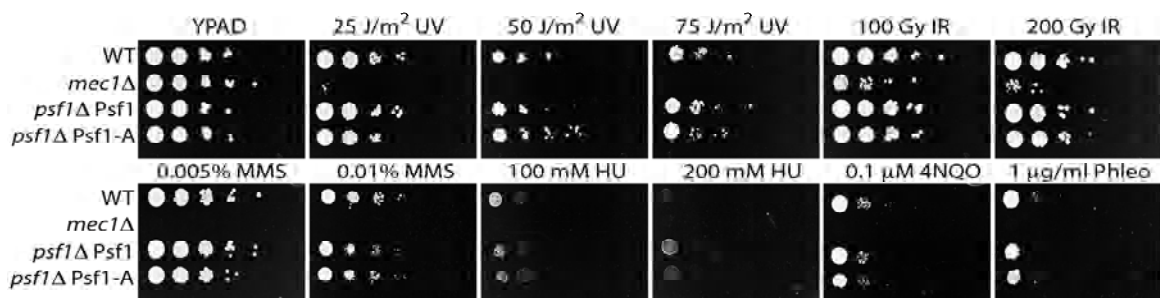


*Psf1Δ* expressing  $\text{Psf1}^{\text{S187A}}$ , but not  $\text{Psf1}^{\text{S187E}}$  protein, displayed four surviving tetrad following microdissections of diploid *psf1Δ* cells (A). The plasmid shuffle technique was used where diploid *psf1Δ* heterozygous strain (1) is transformed with a *URA3* plasmid expressing *PSF1* (2). Diploid yeasts were sporulated and haploid spores were microdissected and selected for spores that contained the *PSF1-URA3* vector and lacked the chromosomal copy of *PSF1* (3). These haploid yeasts were transformed with *HIS3* selectable marker plasmids encoding for wild-type *Psf1*,  $\text{Psf1}^{\text{S187A}}$  or  $\text{Psf1}^{\text{S187E}}$  (4), and were then plated on 5-FOA-containing medium to kill *URA3*-containing strains (C).

#### 4.5.III Analysis of the *psf1-S187A* mutant

Next, I went on to characterize functional aspects of *psf1* deletion mutant expressing  $\text{Psf1}^{\text{S187A}}$  protein under challenged conditions. *psf1-S187A* strain grew like wild-type yeast on YPAD and showed no overt sensitivity in response to a range of genotoxic agents, including IR, UV, MMS, HU, the UV-mimetic drug 4NQO and phleomycin (Figure 45), suggesting that the site is not involved in responses to DNA damage, yet it may be a pivotal site for DNA replication, given *psf1-S187E* lethality.

**FIGURE 45. Spot test for *psf1-S187A* colony formation upon treatment with DNA damaging agents**



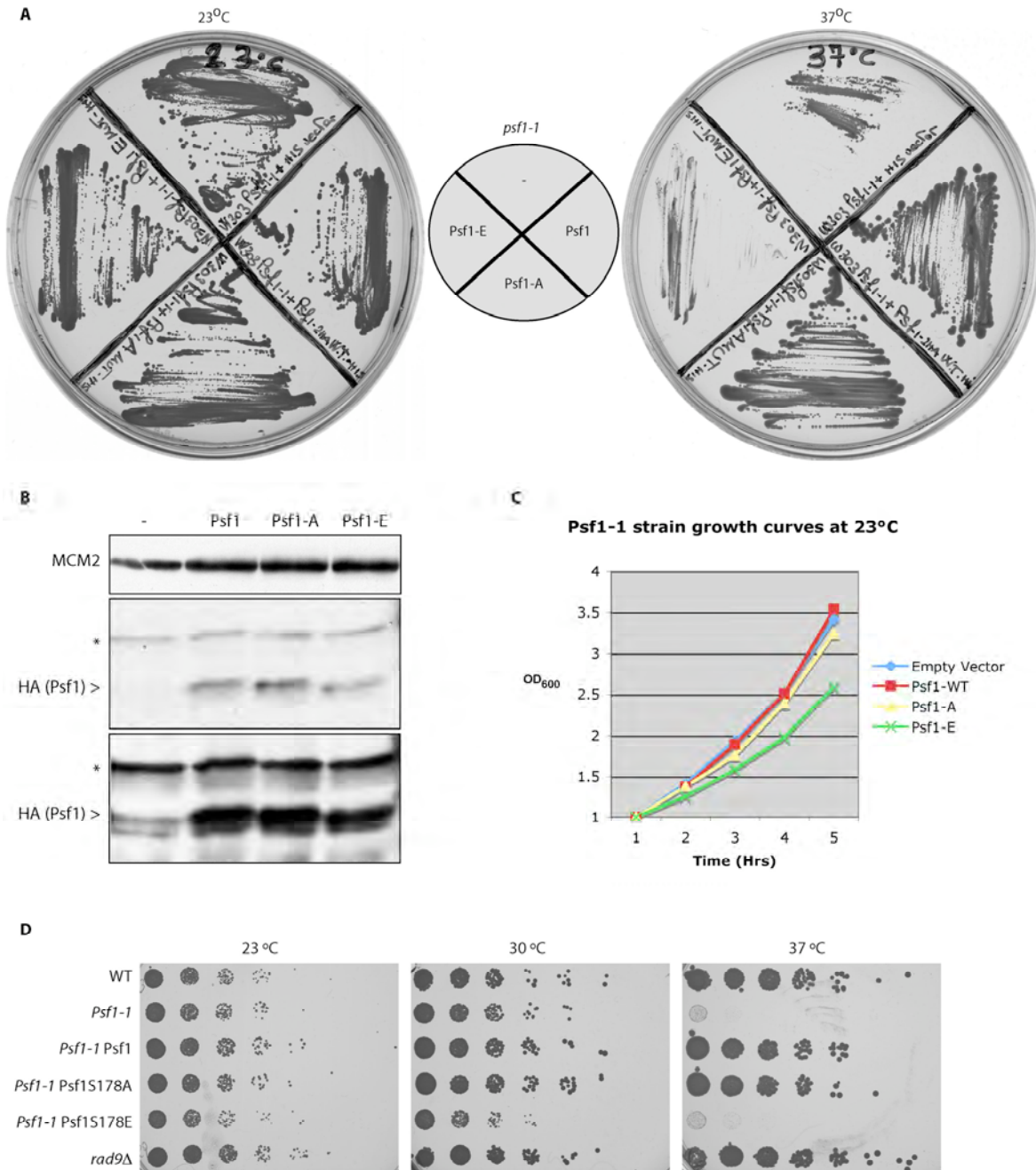
*psf1-S187A* is not sensitive to DNA damage. W303 (WT), *mec1*Δ and *psf1*Δ strain expressing WT Psf1 (*psf1*Δ Psf1) or Psf1 S187A mutant (*psf1*Δ Psf1-A) were grown overnight, diluted to an  $\text{OD}_{600\text{nm}}$  of 0.5 before dilutions (10-fold) were spotted on YPAD alone or on YPAD containing the indicated drug.

#### 4.5.IV Analysis of *psf1-S187A* and *psf1-S187E* mutants in a *psf1-1* strain

To characterize the role of the C-terminus S187 site, I used a *psf1-1* thermosensitive mutant strain, isolated by Hiro Araki and colleagues (Takayama et al., 2003). Plasmids containing *HIS3* selectable marker expressing *psf1-S187A*, *psf1-S187E*, wild-type *PSF1* or an empty vector were introduced into *psf1-1* and grown in THULL synthetic medium to

select for the *HIS3* marker. At 37°C, the restrictive temperature, both *psf1-1* expressing empty vector and *psf1-S187E* cells were dead, due to complete depletion of endogenous Psf1 at this temperature. All other strains grew similarly under these conditions (Figure 46A and 46D). This finding corroborates previous data using the plasmid shuffle method, indicating that S187E single amino acid mutation in Psf1 is lethal. Interestingly, at the permissive temperature of 23°C, only *psf1-1* expressing Psf1<sup>S187E</sup> protein showed a mild growth defect (Figure 46C and 46D). At the semi-permissive temperature of 30°C, when levels of endogenous Psf1 are partially reduced, *psf1-1* cells transformed with the empty vector showed a mild growth defect, whereas those transformed with *psf1-S187E* showed considerable growth impairment (Figure 46D), suggesting this mutant may behave as a dominant negative. Importantly, wild-type Psf1, Psf1<sup>S187A</sup> and Psf1<sup>S187E</sup> proteins were expressed to the same level in the *psf1-1* strain (Figure 46C). This indicates that the phospho-mimicking mutation does not destabilize Psf1 and that lethality caused by Psf1<sup>S187E</sup> expression is not due to protein's absence or lowered expression levels. In addition, Psf1<sup>S187E</sup> mutant protein is unlikely to cause a problem in the GINS complex's assembly and stability, as several lines of evidence have reported that truncation of the last 50 amino acids in the C-terminus of *Xenopus* and yeast Psf1 leads to formation of a stable, yet inactive, GINS complex (Chang et al., 2007; Kamada et al., 2007).

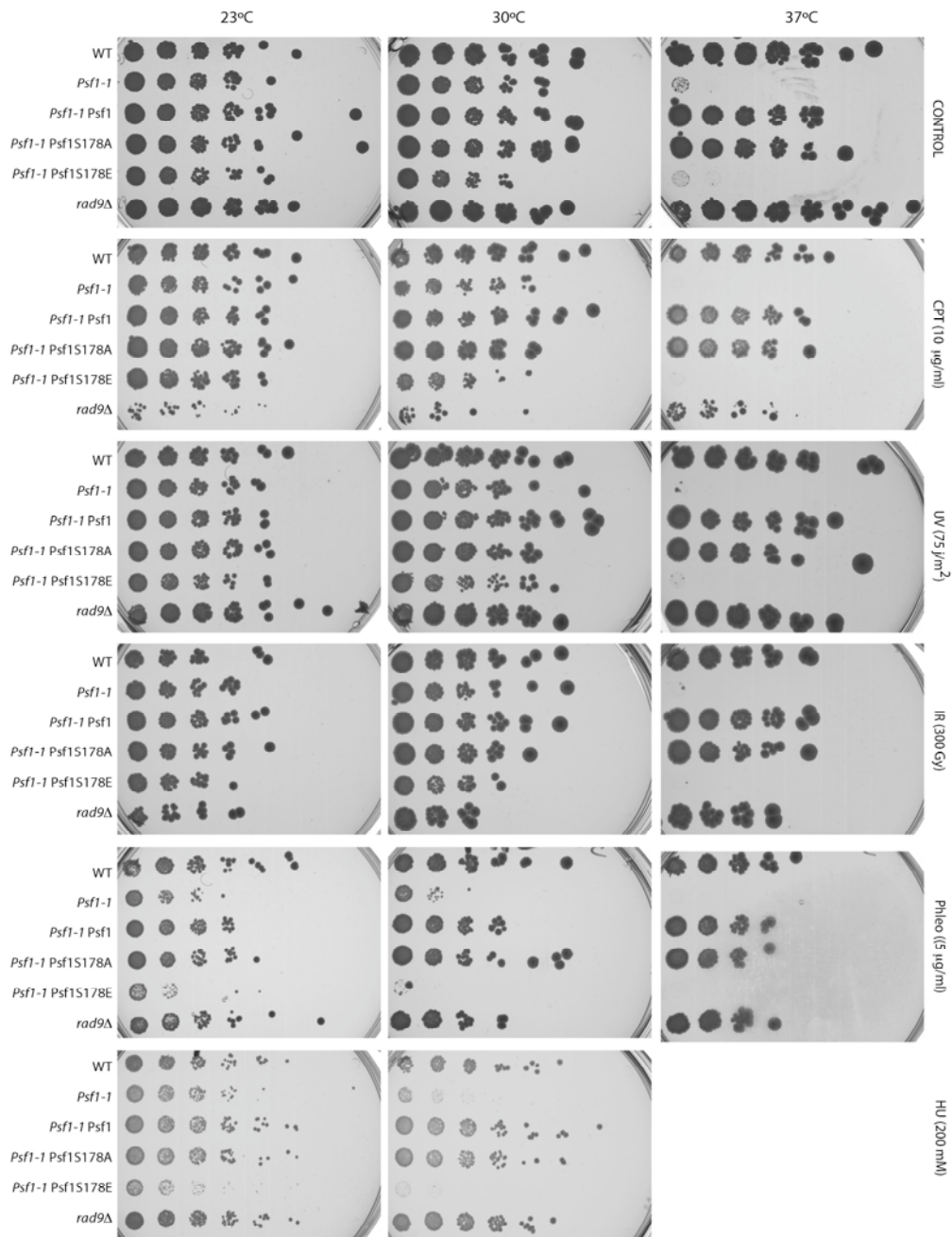
**FIGURE 46. Lethality of Psf1<sup>S187E</sup> in the *psf1-1* mutant strain**



*Psf1-1* expressing empty vector (-), *PSF1*, *psf1-S187A* or *psf1-S187E* were plated on selection medium lacking histidine (-THULL) for 3 days. At 23°C, colonies grew on plate for all strains. At restrictive temperature (37°C), *psf1-1* expressing empty vector or Psf1-E mutant (S187E) showed very little growth (A). TCA preps for western blotting of HA-tagged Psf1, Psf1<sup>S187A</sup> or Psf1<sup>S187E</sup> proteins expressed from a single-copy plasmid. MCM2 was used as loading control. Asterisks indicate cross-reacting band. The third panel from the top is a higher-exposure of the second panel (B). *Psf1-1* strains were grown to saturation into 10 ml selection medium, diluted to an OD<sub>600nm</sub> of 0.06 and grown to an OD<sub>600nm</sub> of 0.3 at 23°C. Cultures were then re-diluted to an OD<sub>600nm</sub> of 0.06 and the absorbance measured every hour for five hours (C). The indicated strains were grown overnight, diluted to an OD<sub>600nm</sub> of 0.5 before 10-fold dilutions were spotted on selection medium and grown at the indicated temperature for 3 days (D).

I then repeated the sensitivity assay using *psf1-1* mutant strains to assess Psf1<sup>S187E</sup> functional relevance in the presence of genotoxic agents. At permissive temperature, Psf1<sup>S187E</sup> showed overt sensitivity to phleomycin and HU (Figure 47), suggesting that this mutant may disrupt Psf1 regulation under challenged conditions. At 30°C, *psf1-S187E*, but not *psf1-1*, was sensitive to irradiation, to a similar extent as *rad9Δ* strain. As Rad9 controls activation of DNA damage checkpoints in *S. cerevisiae* (Weinert and Hartwell, 1988), *rad9* null mutant is hyper-sensitive to DNA-damaging agents (Weinert and Hartwell, 1990) and was used as a positive control in this experiment. In addition, both *psf1-1* and *psf1-S187E* resulted sensitive to phleomycin and HU, with Psf1<sup>S187E</sup> displaying additional sensitivity compared to the *psf1-1* strain (Figure 47). These data suggest that the growth defect phenotype caused by reduced levels of wild-type Psf1 protein at semi-permissive temperature is exacerbated upon exposure to DNA breaks and replication stress induced by phleomycin and HU, respectively. In addition, the Psf1<sup>S187E</sup> mutant protein works in an antagonistic manner to the residual expression of endogenous Psf1 and shows additional sensitivity upon exposure to phleomycin, HU and also IR. At the restrictive temperature, death of the *psf1-1* strain is fully rescued by plasmid expression of wild-type Psf1 and Psf1<sup>S187A</sup> mutant proteins (Figure 47). Strikingly, and in accord with my previous data obtained with the plasmid shuffle system, the Psf1<sup>S187A</sup> mutant protein behaves like a wild-type protein, displaying no sensitivity to DNA damaging agents (Figure 47).

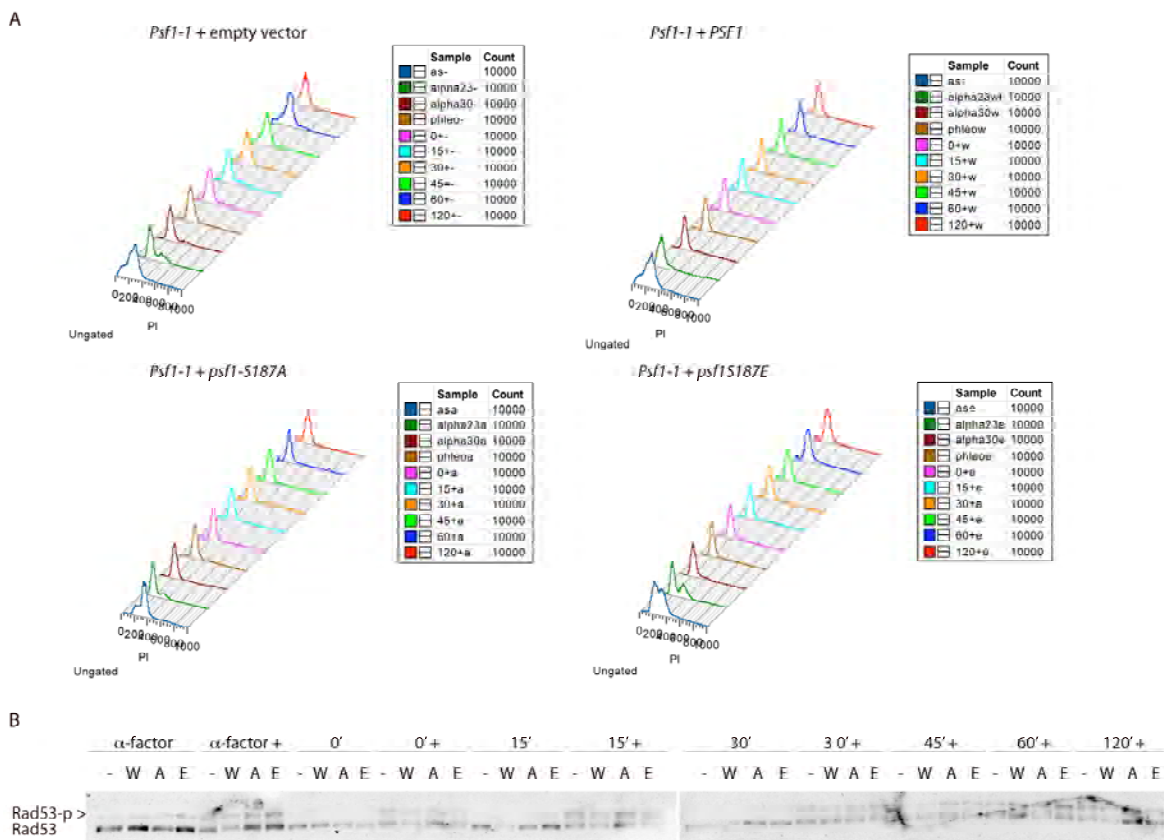
**FIGURE 47. *Psf1-S187E* displays hyper-sensitivity to specific DNA damaging agents, whereas *psf1-S187A* behaves like a wild-type strain**



*Psf1-S187E* is sensitive to irradiation, phleomycin and HU treatments. The indicated strains were grown overnight, diluted to an OD<sub>600nm</sub> of 0.5 before dilutions (10-fold) were spotted on selection medium containing the indicated drugs and grown at the indicated temperature for 3 days.

To gain additional insight into the molecular activity of Psf1 mutant proteins, I monitored their ability to progress into S-phase in the presence of the DSB-inducing agent phleomycin at 30°C. FACS of cells released from  $\alpha$ -factor G1 arrest was used to monitor entry and progression through S-phase and advancement into the cell cycle for up to 200 minutes post-release. In addition, immunoblot monitored activation of Rad53 by the appearance of a phospho-dependent upper band upon treatment with DNA damage. Rad53 was shifted in all samples pre-treated with phleomycin, indicating that lowering of Psf1 wild-type levels, or expression of mutant Psf1<sup>S187A</sup> and Psf1<sup>S187E</sup> proteins *per se* did not induce a Rad53-dependent checkpoint activation. Similar levels of Rad53 activation were observed across all damaged samples, indicating that activation of Rad53 is proficient in these yeast strains. This observation is supported by FACS data, where all strains remained arrested upon release from  $\alpha$ -factor into 5  $\mu$ g/ml phleomycin, indicating robust activation of the DNA damage checkpoint. FACS profiles of asynchronous cells at semi-permissive temperature, however, showed that expression of Psf1<sup>S187E</sup> caused cells to accumulate in S-phase in the absence of DNA damage, inferring a role for this site in replication.

**FIGURE 48. Proficient Rad53 phosphorylation and activation of the G1/S checkpoint in *psf1* mutant strains**

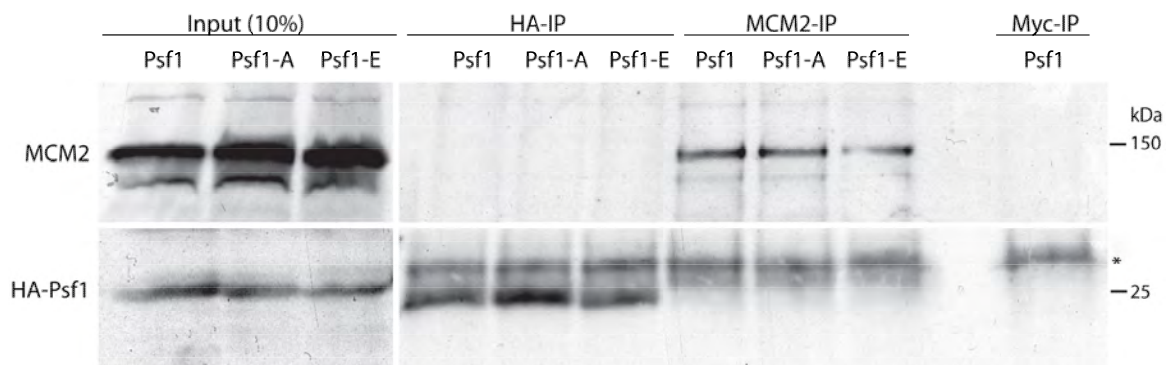


*Psf1-1* strains containing *PSF1*, *psf1-S187A*, *psf1-S187E* or empty vector were grown logarithmically into selection medium at the permissive temperature of 23°C and arrested into  $\alpha$ -factor for 2 hours. Once yeast cells were synchronized in G1, the temperature was shifted to 30°C (semi-permissive) and kept into  $\alpha$ -factor for an additional hour. Half of the cultures were then treated with phleomycin (5  $\mu$ g/ml) for 1 hour, in the presence of  $\alpha$ -factor.  $\alpha$ -factor and phleomycin were then washed out and cells were allowed to progress into S-phase at 30°C. Samples were collected for FACS and immunoblot analyses for up to 3 hours. Both failed progression into S-phase by FACS and continued Rad53 phosphorylation show that the G1/S checkpoint is induced and maintained in the timeframe analysed in all strains.

Next, I attempted to verify Psf1 and mutant proteins' ability to bind to the MCM helicase. To this end, I took advantage of protocols for yeast lysates provided by Karim Labib's laboratory, including the yeast 'spaghetti' or popcorn technique using liquid nitrogen (Gambus et al., 2006) and benzonase extracts (Gambus et al., 2009) and performed IP experiments using asynchronous as well as synchronous S-phase population. Although all Psf1 constructs expressed equally and the HA-tagged proteins were IP-ed to the same

level, no interaction with MCM2 subunit of the MCM ring was observed. The reverse IP, using antibodies against MCM2 to IP for Psf1, also showed no detectable binding (Figure 49). I cannot exclude that the N-terminal HA-tag may interfere with binding to MCM, hindering the interactions.

**FIGURE 49. HA-Psf1 does not co-IP MCM2 subunit of the MCM complex**



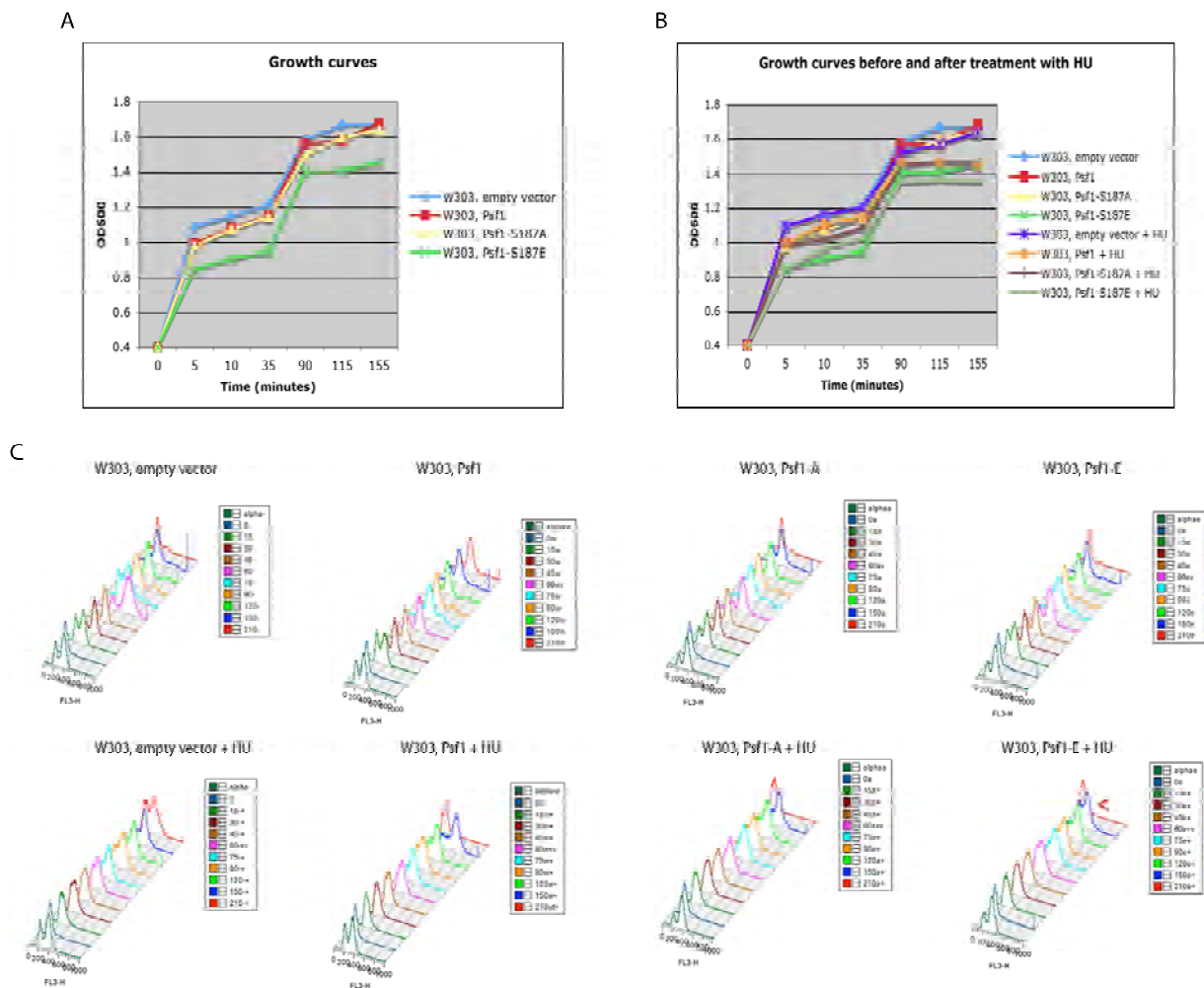
W303 strain expressing wild-type Psf1, Psf1<sup>S187A</sup> (Psf1-A) and Psf1<sup>S187E</sup> (Psf1-E) proteins were synchronized in G1, released into fresh medium for 20 minutes to synchronize them in S-phase and harvested. Cell extracts were used for co-IP experiments using HA or scMCM2 antibodies. The asterisk marks the light chains of the IgG due to antibody cross-reaction.

#### 4.5.V *Psf1-S187E is a dominant negative mutant in budding yeast*

The observations collected using *psf1-1* mutant strain suggest that *psf1-S187E* may behave as a dominant negative mutant of Psf1. To test this hypothesis, I used W303 wild-type strains expressing *PSF1*, *psf1-S187A*, *psf1-S187E* and compared their growth curves and cell cycle progression from G1 arrest. As expected, expression of Psf1<sup>S187E</sup> mutant protein showed a slower growth phenotype under unperturbed conditions and is further slowed-down by addition of HU, despite the presence of endogenous Psf1 (Figure 50A and 50B). This infers that Psf1<sup>S187E</sup> protein is a dominant negative mutant. In addition, *psf1-S187E* mutant strain displayed a mild defect in progressing into S-phase 15 minutes after  $\alpha$ -factor

release, a delay in S-phase and in progressing into G2/M in the presence of HU (Figure 50C; 150 minutes time-point), indicating that problems caused by this mutant in S-phase are exacerbated under conditions of replicative stress possibly due to the presence of unreplicated DNA.

**FIGURE 50. *Psf1-S187E* is a dominant negative mutant of yeast *PSF1***



WT W303 stains, containing *PSF1*, *psf1-S187A*, *psf1-S187E* or empty vectors were grown logarithmically into selection medium and arrested into  $\alpha$ -factor for 2 hours. Once yeast cells were synchronized in G1, they were released from the  $\alpha$ -factor block into fresh medium or medium containing HU (100 mM). Samples were collected for growth curve assays (A and B) and FACS (C) for ~3 hours. Growth curves show that expression of *psf1-S187E* in W303 cause a delay in cell growth (green line; A) and this is further reduced in the presence of HU (grey line; B), suggesting that Psf1<sup>S187E</sup> is a dominant negative mutant of Psf1.

#### 4.5.VI *A multicopy suppressor screening of psf1-S187E lethality*

To gain more insight into the functional significance of the lethality of the *psf1-S187E* mutant strain, I screened a genomic library for multicopy suppressor genes. The *LEU2*-based library was transformed in *psf1-1* mutant strain expressing Psf1<sup>S187E</sup> protein. Transformants were plated on large YPAD plates and grown at the restrictive temperature of 37°C for three days. Plating of 1/100<sup>th</sup> of yeast transformants selected for *LEU2* marker gene-containing colonies indicated that about 300,000 transformants could be obtained from the screen (Figure 51A). Considering that *S. cerevisiae* genome contains a total of about 6,000 genes, the genomic library was made up of numerous copies for each gene.

150 colonies grew at 37°C, they were picked and re-plated in medium to select for the presence of *HIS3* and *LEU2* genes and grown at 37°C overnight (Figure 51B). Genomic DNA was obtained from each colony and transformed in bacteria to isolate the plasmids containing library DNA. Sequence analysis revealed that the colonies contained *PSF1*, validating the screen. However, no additional genes were identified. Considering that *PSF3* was identified by screening for a multicopy suppressor of *psf1-1*, it is evident that over-expression of other GINS subunits is not sufficient to suppress the dominant negative phenotype of *psf1-S187E* mutant and the only suppressor of this mutant is *PSF1* gene itself. These data further emphasize the central and unique role for this Psf1 C-terminus motif in replication and cell viability.

**FIGURE 51. Screen for suppressors of *psf1-S187E* mutant lethality at 37°C**

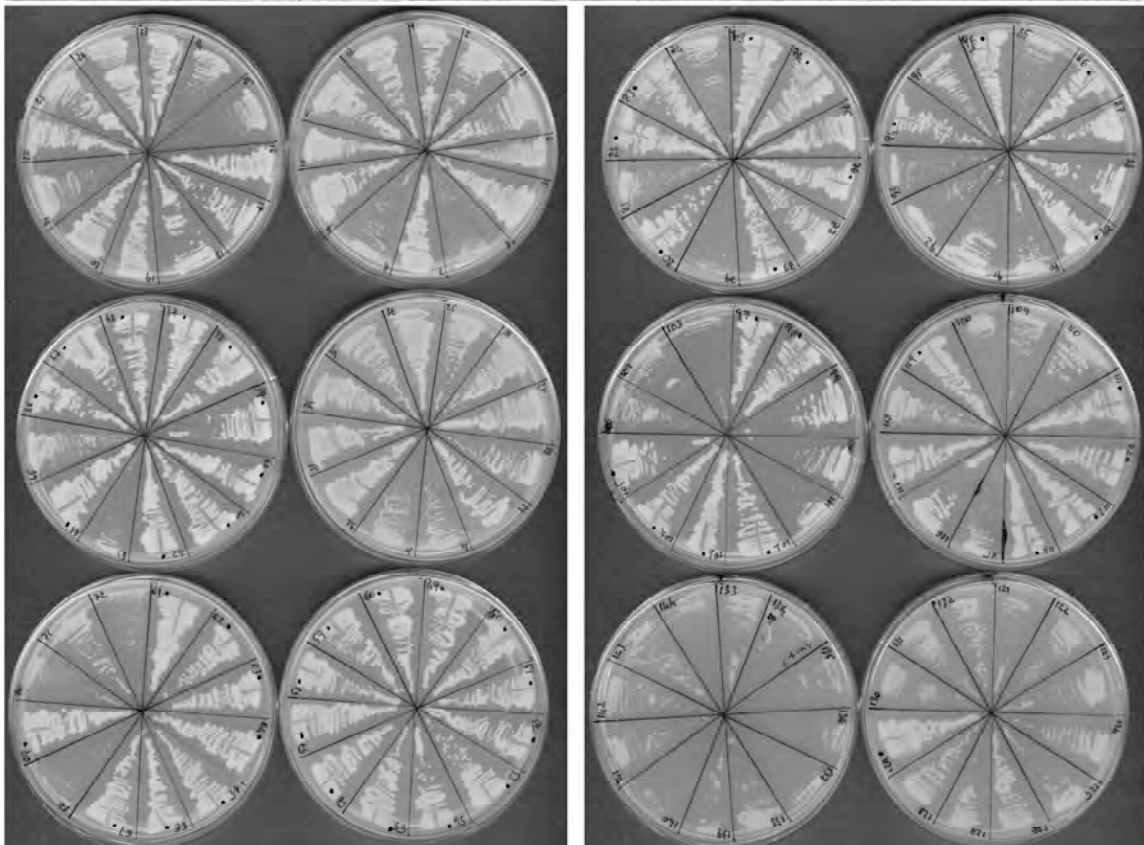
A

1/100th of suppressor library transformants selected for *LEU3*



B

*Psf1-1, PSF1-S187E* multicopy suppressor library transformants were picked and re-plated on selection at 37°C

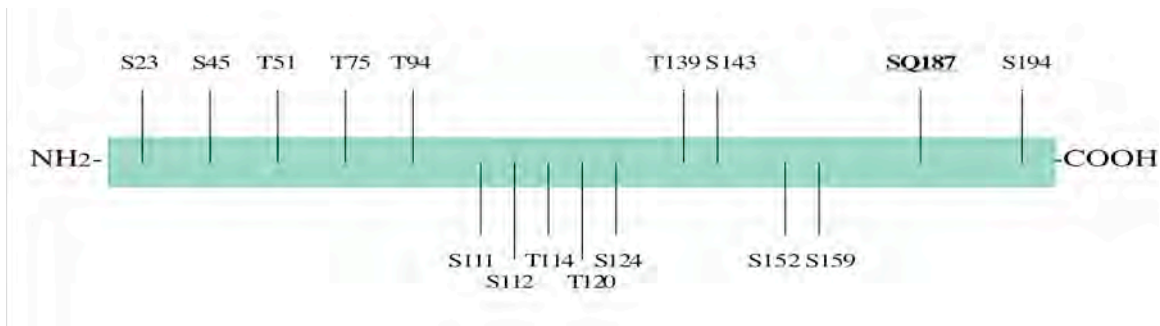


A *LEU2*-based multicopy suppressor genomic DNA library was transformed in *psf1-1* mutant strain expressing *Psf1*<sup>S187E</sup> protein. 1/100<sup>th</sup> of yeast transformants were plated on *LEU2*- selection medium at 37°C (A). 150 colonies formed at 37°C and were re-plated in *HIS3* and *LEU2* selection medium and grown at 37°C overnight (B). Sequencing of plasmid DNA from colonies revealed presence of *PSF1* gene.

#### 4.5.VII Phosphorylation of Psf1 SQXF motif in *S. cerevisiae*

To assess whether S187 site in *S. cerevisiae* Psf1 was a *bona fide* phosphorylation site *in vivo*, I performed large-scale purification of TAP-tagged Psf1 following three hours incubation with 100 mM HU, to increase the S-phase population (Gao et al., 1995). Purified Psf1 was eluted, run by SDS-PAGE and identified by coomassie staining. Psf1 was subjected to phospho-peptide mapping using liquid chromatography-tandem mass spectrometry (LC-MS/MS) at the University at Albany mass spectrometry facility. Under non-stringent conditions, Psf1 protein sequence was fully covered and 16 phosphorylation sites of the 20 potential serine/threonine phospho-sites were found to be phosphorylated (Figure 52).

**FIGURE 52. Yeast Psf1 phosphorylation sites upon incubation with HU**



Phospho-peptide mapping by LC-MS/MS identified 16 potential *in vivo* phosphorylation sites in Psf1. Amongst the 16 sites, the C-terminal conserved S187 (in bold) within the SQXF motif was phosphorylated.

The ion score is a  $-10 \cdot \log(P)$ , where  $P$  is the probability that the observed match is a random event. Individual ions scores  $\leq 3$  indicate identity or extensive homology with the suggested modification ( $p < 0.05$ ). S187 phosphorylation emerged with an ions score of 3. Other phospho-sites with a significant ion score were T139 (ion score 5) and T51 (ion score 4). However, these sites are just above or on the threshold of the 95% confidence

interval, suggesting that there may be a margin of error as to whether the detected phosphorylation occurs *in vivo*. In addition, no phosphorylation sites were identified by phospho-peptide mapping under stringent conditions.

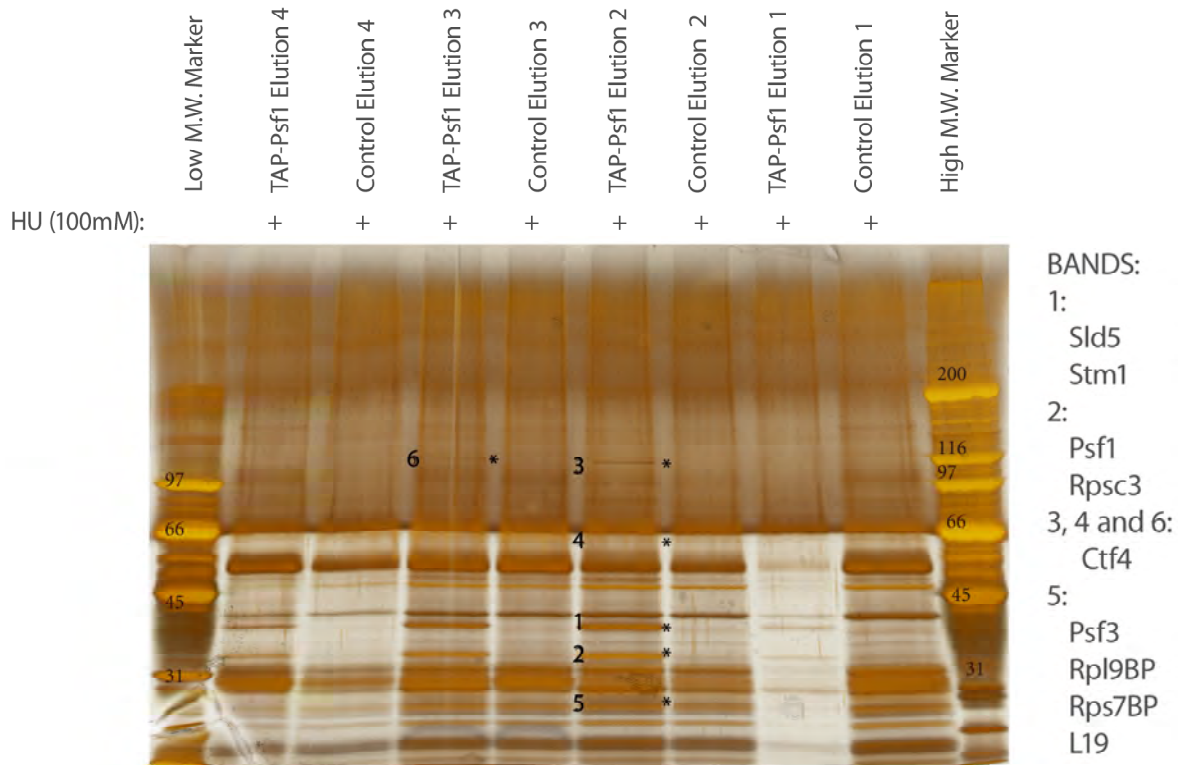
#### 4.5.VIII Identification of Psf1 interacting partners in budding yeast

At the beginning of this study, scarce data existed on Psf1 binding partners in budding yeast. To identify novel binding partners of Psf1 in S-phase, I performed affinity capture-MS interaction studies using TAP-tagged Psf1 purified from yeast extracts treated with HU, similarly to the phospho-peptide mapping analysis. Interaction partners were identified by MS/MS. Psf1, Sld5 and Psf3 were all found to associate with purified Psf1, suggesting that TAP-tagged Psf1 is proficiently incorporated in the GINS complex (Table 9 and Figure 53). As for the IP experiments (Figure 49), no MCM binding was detected under these conditions. However, novel binding partners of full-length Psf1 were identified: Rps3, Rpl9a, L19, Rps7b, Ctf4 and Stm1 (Table 9 and Figure 53).

**TABLE 9. Proteins interacting with full length Psf1**

Serial #	Protein name	Gi #	Identified peptide	Coverage (%)
1 (a)	Sld5 [ <i>Saccharomyces cerevisiae</i> ]	6320697	14	54
1 (b)	Stm1 [ <i>Saccharomyces cerevisiae</i> ]	6323179	5	23
2 (a)	Psf1 [ <i>Saccharomyces cerevisiae</i> ]	6320216	11	48
2 (b)	Rps3 [ <i>Saccharomyces cerevisiae</i> ]	6324151	9	44
3	Ctf4 [ <i>Saccharomyces cerevisiae</i> ]	6325393	5	7
4	Ctf4 [ <i>Saccharomyces cerevisiae</i> ]	6325393	9	13
5 (a)	Rpl9a / Rpl19b [ <i>Saccharomyces cerevisiae</i> ]	6321291/ 6319444	3	20
5 (b)	Ribosomal protein L19 [ <i>S. cerevisiae</i> ]	602897	2	11
5 (c)	Rps7b [ <i>Saccharomyces cerevisiae</i> ]	6324233	1	8
5 (d)	Psf3 / orf6 [ <i>Saccharomyces cerevisiae</i> ]	37362690/ 886950	1	11
6	Ctf4 [ <i>Saccharomyces cerevisiae</i> ]	6325393	1	3

**FIGURE 53. Factors interacting with full-length Psf1 upon incubation with HU in *S. cerevisiae***



TAP-Psf1 yeasts were cultured in 100 mM HU for 2 hours. Purified Psf1 was pulled-down and samples from the various elution steps were visualized on silver stained-gel. The indicated bands (asterisk) were cut and sent for MS/MS to identify Psf1 binding partners (numbered): GINS complex subunits Psf2, Sld5 and Psf3, and Psf1 itself, Stm1, Ctf4 and numerous ribosomal proteins were identified.

Collectively, the data shown in this chapter provide a preliminary assessment of Psf1 C-terminal SQXF motif in human and yeast cells. My observations suggest that the conserved serine site is important for replication in budding yeast, and may also be regulated in presence of replicative stress and DNA damage.

## 4.6 Discussion and conclusion

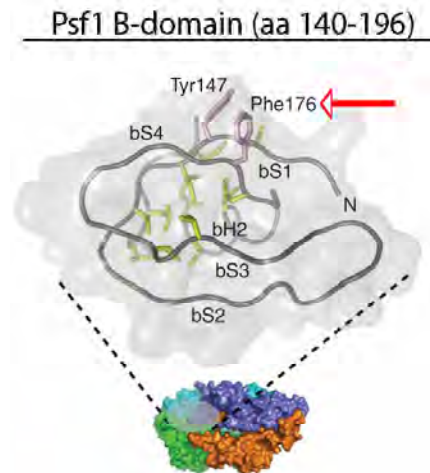
### 4.6.1 *Conserved SQXF motif on human Psf1 binds to the UV-DDB complex*

In this study, I analyzed a possible role for Psf1 in the DDR. The functional activity of GINS in coordinating DNA synthesis and unwinding makes it an appealing target to modulate replication in the presence of genotoxic alterations. Indeed, I have found that Psf1 and Psf2 GINS subunits contain an evolutionarily conserved SQXF motif at the carboxyl end, which conforms to the consensus target site for PIKK-dependent phosphorylation following DNA damage.

Interaction analyses of Psf1 C-terminus domain revealed binding to DDB1 *in vitro*. Binding to DDB1 and DDB2 (UV-DDB complex) were also confirmed using full-length recombinant Psf1. The interaction data showed no difference in the ability of DDB1 and DDB2 to bind Psf1 when the serine was mutated to an alanine or to a glutamic acid, indicating that the binding interface between Psf1 and UV-DDB may be outside of the SQ site and it may not be regulated by phosphorylation events. However, the pull-down data using synthetic peptides showed robust interactions when S173 was phosphorylated and the phenylalanine amino acid in the +3 position was mutated (F176A), suggesting that not only the SQ site, but also the surrounding amino acids, represented a binding interface and affect stability of interactions with DDB1. Indeed, Kamada et al. (2007) suggested that the binding interface of Psf1 C-terminus might reside in the conserved phenylalanine residue (F176), which is exposed on the peripheral surface of the complex (Diagram 12). Mutation of Psf1 F176 to alanine resulted in a substantially lower replication activity compared to the wild-type complex (Kamada et al., 2007). In light of my observations, where mutation of this same residue in the Psf1 phospho-S173, F176A peptide caused stronger association

of Psf1 to DDB1, this conserved hydrophobic residue on Psf1 C-terminus may be negatively regulating binding to DDB1, suggesting that DDB1 may reduce replication activity.

**DIAGRAM 12. Highly conserved, exposed phenylalanine 176 on Psf1 may regulate interaction with DDB1**



Structural model of the C-terminus (B-domain) of Psf1. The B-domain is outlined as a grey area in the GINS complex structure and is enlarged as a grey globular  $\alpha$ -carbon trace with transparent molecular surface. Yellow regions are predicted internal hydrophobic and pink regions are exposed aromatic residues, including Phe176 (red arrow).

Image modified from Kamada et al., 2007

The DNA damage binding UV-DDB complex – comprising DDB1 and DDB2 – is involved in repair of UV radiation photoproducts by nucleotide excision repair (NER) and is found mutated in the *Xeroderma pigmentosum* group E. *Xeroderma pigmentosum* is an autosomal recessive genetic disease characterized by hyper-sensitivity to UV light due to inability to perform NER. In addition to the DDB dimer, DDB1 and DDB2 are found associated with Cullin4 and ROC1 in an ubiquitin ligase complex activated in response to DNA damage (Groisman et al., 2003; Wang et al., 2006). The role of DDB1-CUL4A-ROC1 ubiquitin ligase in regulating the replication-licensing factor Cdt1 in response to DNA damage directly links DDB1 to controlling replication (Higa et al., 2003; Hu et al., 2004). DDB1 was shown to directly bind to Cdt1 enabling its proteosomal degradation

following UV damage in S-phase. Recent data shows that PCNA is an essential cofactor in this process (Hu et al., 2004). GINS was recently shown to co-localize with PCNA on extended chromatin fibres (Cohen et al., 2009) and had been previously suggested to function in a similar fashion to the trimeric polymerase-accessory-ring PCNA, as a 'sliding clamp' for DNA polymerase  $\epsilon$  (Aparicio et al., 2006), thus GINS binding to UV-DDB may follow a similar mechanism of action. It is tempting to speculate that Psf1 phosphorylation following DNA damage promotes DDB1 binding leading to replication inhibition; F176 antagonize the binding, to promote resumption of DNA synthesis. Based on my data, which do not show reduction in Psf1 levels after treatment with diverse DNA damaging agents, it is unlikely that DDB1 targets the GINS complex for proteosomal-mediated degradation. However, similarly to PCNA, GINS may serve to bridge the ubiquitin ligase to substrates such as Cdt1, yet no direct interaction between Psf1 and Cdt1 was found by co-IP in human cells (data not shown). It would also be interesting to investigate the potential interactions between Psf1 and Cullin4A and Roc1, but commercially available antibodies against these proteins have proven to be non-specific and gave very high background signal (data not shown).

DDB2 role in connection with DDB1-CUL4A is unclear. DDB2 is likely to be a substrate of the DDB1-CUL4A ligase (Nag et al., 2001), as treatment with UV induces its degradation and loss of DDB2 did not affect the catalyses of poly-ubiquitylation and proteosomal degradation of other substrates (Hu et al., 2004). On the other hand, DDB2 may associate with a subset of ubiquitin ligases, mediating substrate specificity and differential responses (Groisman et al., 2003). My data showing Psf1 binding to both DDB1 and DDB2 would be consistent with and favour the latter hypothesis.

To understand these interactions is especially interesting in light of findings showing that the C-terminal domain of Psf1 (aa 140-196) is the most exposed part of the complex and

“is crucial for chromatin binding and replication activity”. Thus, “the core GINS complex ensures a stable platform for the C-terminal domain of Psf1 to act as a key interaction interface for other proteins in the replication-initiation process” (Kamada et al., 2007). However, the exact significance of Psf1 interaction with DDB1 and DDB2 remains to be established. In all Psf1 pull-downs, I noticed that only a small percentage of DDB1 total input was pulled-down, suggesting that interactions between these factors may be very transient or present in only a small subset of cells due to cell cycle regulations. To this end, I did not observe interactions between these proteins in immunoprecipitation experiments. Perhaps, the interaction is limited to a short time window during the cell cycle *in vivo*, and *in vitro* pull-downs bypass this regulation.

No data currently exist with regard to post-translational modifications that regulate Psf1 activity and interactions. Despite extensive efforts to demonstrate phosphorylation of the SQ motif at Psf1 C-terminus, this point remains to be addressed. Psf1, however, displayed a mobility shift following treatment with DNA damaging agents *in vivo*, indicative of phosphorylation. Given the striking conservation of this motif and the location within the functional interface of the GINS complex, it would be extremely interesting to establish whether this evolutionarily conserved site is post-translationally modified.

#### **4.6.II      *Physiological roles for Psf1 in cell cycle progression in human cells***

The role of the mammalian GINS complex had yet to be addressed at the beginning of this study. Additionally to investigations of Psf1 C-terminus, I identified a role for human Psf1 in enabling cell cycle progression through S-phase, in turn affecting cell proliferation and viability. During the course of this study, two other groups also reported similar analysis of the human GINS complex, including analogous cell cycle phenotypes following down-

regulation of GINS subunits (Aparicio et al., 2009; Barkley et al., 2009). Barkley and colleagues (2009) also showed activation of the checkpoint kinase Chk2 by ATM-dependent phosphorylation on T68 and increase in  $\gamma$ H2AX signal and foci after siPsf1/2 (Barkley et al., 2009). This observation may explain the delay in S-phase progression of siPFS1 cells, possibly due to triggering of the intra-S-phase checkpoint.

After observing a cell cycle progression defect in Psf1 down-regulated cells, the next logical step was to examine whether the level of other GINS complex subunits and other replication fork-associated factors was affected by Psf1 depletion. Down-regulation of *PSF1* resulted in lowered expression of the other GINS complex subunits, likely as a result of transcriptional repression and/or proteolytic degradation of existing GINS complexes. It has been proposed that proliferation inhibition leads to a decrease in protein levels of DNA replication factors Cdc6, MCM and Cdc45 (Aparicio et al., 2009). Interestingly, I observed no obvious changes in the levels of other proteins, including human MCM ring subunit MCM7. My observations favour the hypothesis that the GINS complex stabilization is promoted by the presence of optimal levels of all subunits to prevent proteolytic degradation, rather than a global regulation of the replication-associated transcriptional program.

Immunofluorescence analysis of Psf1 revealing a change in nuclear patterning was after IR but not UV. UV radiation induces the formation of DNA photoproducts that links adjacent pyrimidines, including cyclobutane pyrimidine dimers (Lober and Kittler, 1977) and pyrimidine-pyrimidone (6-4) products (Mizukoshi et al., 2001), that block polymerase progression, causing accumulation of ssDNA and checkpoint activation. IR, on the other hand, is a potent DNA damaging agent that causes single strand breaks and base damage on multiple sites by creation of oxygen radicals (Friedberg et al., 2006), often leading to

collapsed forks. A global change in Psf1 staining might be due to the replication fork collapsing at several sites across the genome, rather than a transient stalling of the fork that meets UV photoproducts. It would be interesting to further investigate the underlying reason for this IR-dependent re-localization of Psf1 and how this may be regulated by post-translational modifications or other mechanisms.

In line with recent reports suggesting additional role for the GINS complex outside of S-phase, I have observed localization of Psf1 on the spindle midbody during mitosis. In Psf3 mutants, where the recruitment of Cut5 and Sld3 to origins is disrupted, a fraction of cells enter mitosis prior to completion of duplication of the genome (Yabuuchi et al., 2006), indicating that GINS may be involved in preventing unscheduled cytokinesis and to ensure faithful completion of replication. Furthermore, a more direct role for GINS in mediating accurate chromosome segregation has been postulated by Huang and colleagues (2005), where yeast Psf2 suppresses phenotypic defects in chromosome segregation and spindle attachment caused by *bir1/cut17* mutation and siPSF2 in human cells causes gross chromosomal aberrations (Huang et al., 2005a). Although a direct role for GINS in mitosis is yet to be confirmed, the replication licensing factor Cdc6 has been widely associated in controlling mitosis and was shown to be involved in monitoring entry into mitosis, possibly as a signal of ongoing replication, through a Chk1-dependent checkpoint mechanism (Clay-Farrace et al., 2003). Further investigation would be required to assess whether GINS plays a similar role in coordinating replication activities with cell cycle progression through S-phase and into mitosis by regulation of DNA damage checkpoints and other means.

Taken together, the data presented in this chapter show that, in human cells, *PSF1* gene product is involved in maintaining GINS complex stability and plays a role in DNA

replication and cell cycle progression. Moreover, the data showing Psf1 binding to DDB1 *via* its C-terminus motif might suggest a mechanism to regulate DNA replication in response to DNA damage. However, further studies are required to address many questions that remain unanswered, to gain additional information on the role of human GINS during cell cycle progression and possible regulations following DNA damage.

#### **4.6.III *Psf1 serine 187 is important for cell viability in *S. cerevisiae****

The function of Psf1 has been extensively studied in budding yeast (reviewed in MacNeill, 2010). Here, I show that mutational dysregulation of the conserved S187 at the carboxyl end of Psf1 to a glutamic acid (S187E) affects yeast viability. Mutation of S187 to an alanine resulted in a wild-type-like protein, which grows and tolerates genotoxic agents similarly to the wild-type strain. I uncovered that *psf1-S187E* mutant is not a functionally null allele, but an antimorphic allele encoding for a protein that behaves as a dominant negative in yeast cells. The antimorphic effect of Psf1<sup>S187E</sup> is especially obvious under challenged conditions, in the presence of the genotoxic agents HU, phleomycin and IR. Hydroxyurea (HU) depletes the dNTPs pool (Krakoff et al., 1968). Because at any given time in S-phase there are only enough dNTPs to replicate a fraction of the genome, treatment with hydroxyurea results in stalling of the polymerases, but continued advancement of the helicase leading to the accumulation of ssDNA and hence activation of the replication checkpoint. Therefore, Psf1<sup>S187E</sup> compromises the cellular metabolism during HU-mediated replication stress and fork stalling, as expected given Psf1 essential role during DNA synthesis. In addition, Psf1<sup>S187E</sup> displays additional sensitivity to IR and phleomycin, an IR-mimetic antibiotic that, similarly to IR, causes SSBs and DSBs (Povirk, 1996). These findings suggest that Psf1 is regulated following DSB and this essential

regulation is lost when the S187 site is mutated to a negatively charged glutamic acid. GINS role in the DDR has been supported by interactions with checkpoint factors like Mrc1 and Tof1, where GINS may serve to link these proteins to the MCM helicase, DNA polymerase and DNA primase (Moyer et al., 2006). In addition, human Psf2 is phosphorylated by ATM/ATR on two SQ/TQ consensus sites at the very carboxyl end of the protein (Matsuoka et al., 2007). However, at present, is not known what are the effects of these phosphorylations on GINS activity and how these relate to the DDR.

Given the S187 site was found phosphorylated in the phospho-peptide mapping analysis by mass spectrometry, it is tempting to speculate that the behaviours of the phospho-mimicking Psf1<sup>S187E</sup> and the unphosphorylatable Psf1<sup>S187A</sup> mutants reflect changes in post-translational modifications, such as phosphorylation, on this site *in vivo*. Psf1 essential role in replication may be maintained when the site is unphosphorylated and inhibition of replication may be modulated by alternative mechanisms under perturbed circumstance and at termination sites. When Psf1 becomes phosphorylated at the C-terminus S187 site (or constitutively phosphorylated, as in Psf1<sup>S187E</sup>), its activity in the context of replication is impaired, leading to cell death. How Psf1 constitutive inactivation by phosphorylation affects DNA damage sensitivity remains unclear. Although Psf1 wild-type and mutant proteins were expressed to a similar level, indicating that mutations do not affect protein stability, I was unable to verify whether the binding of MCM or other GINS subunits was affected by these mutations. It is possible that the residual level of endogenous Psf1 at semi-permissive temperature in *psf1-1* may be sufficient to retrain a functional activity of the complex; on the other hand, Psf1<sup>S187E</sup> may not get incorporated into the GINS complex, phenocopying a *psf1Δ* background strain. Although I cannot formally exclude the possibility that S187E mutation alters the stoichiometry of the GINS complex, crystallography data argue against this point (Chang et al., 2007; Kamada et al., 2007).

Collectively these data point to a role for Psf1 conserved C-terminal serine in replication and regulation after DNA damage, yet the exact functional consequences of S187 mutational changes remain to be established.

#### **4.6.IV Identification of novel Psf1 binding partners in *S. cerevisiae***

Finally, I identified novel binding partners of *S. cerevisiae* Psf1 after treatment with HU. Because of the stringent experimental conditions used in this experiment, these factors are likely to be directly associated with Psf1. Ctf4, a chromatin-associated protein required for sister chromatids cohesion in budding and fission yeast (Hanna et al., 2001; Williams and McIntosh, 2002) was found to bind to Psf1. Ctf4 was also shown to interact with DNA polymerase alpha (Pol 1), serving as an accessory factor (Formosa and Nittis, 1999) and associates with the replisome and with the CMG helicase (Gambus et al., 2006). Ctf4 has been recently shown to bind directly to GINS and this interaction persists in the presence of up to 900 mM salt (Gambus et al., 2009). These data and my own result indicate that Ctf4 binds Psf1 with high affinity, perhaps stronger than binding between GINS and the MCM ring, whose interaction may be bridged by Cdc45.

In addition, Psf1 interacts with several ribosome-associated proteins, including Rps3, Rpl9a, L19 and Rps7b. Due to their abundance, ribosomal factors were previously regarded as non-specific contaminants and discarded from genetic and physical interactome screens in *S. cerevisiae* (Krogan et al., 2006). However, the recurrence of certain ribosomes-associated factors in these screens is now shaping into a more obvious functional significance in the global landscape of these interactions (Nevan Krogan, personal communication). Indeed, a very recent genome-scale genetic map reported interaction between *PSF1* and *RPL16A* (Costanzo et al., 2010), indicating that GINS may

play a role in linking DNA replication with ribosome biogenesis. The nucleolar protein Yph1, required for 60S ribosomal subunit biogenesis, was also found to bind ORC and MCM and to be required for S-phase progression (Du and Stillman, 2002). In addition, *S. pombe* homologue of the budding yeast nucleolar complex NOC3, that is involved in origin recognition and is loaded to pre-RC complexes (Zhang et al., 2002), was recently shown to be essential for cell division and ribosome biogenesis, although it does not seem to play a role in replication (Houchens et al., 2008). Stm1, another Psf1-binding factor, is a guanine-quadruplex and purine-motif triple-helical-DNA binding protein (Nelson et al., 2000; Hayashi and Murakami, 2002). Genetically, it interacts with Cdc13 to help preserve telomere structure (Hayashi and Murakami, 2002). Interestingly, recent reports found Stm1 to be associated with ribosomes and to regulate ribosomal translation elongation by altering association to the eukaryotic elongation factor 3 under nutrient stress (Van Dyke et al., 2004; Van Dyke et al., 2006; Van Dyke et al., 2009). This establishes yet another link between the GINS complex and ribosome-associated proteins, suggesting that the interactions found in this study may have a functional significance *in vivo*.

Altogether, the data presented provide novel experimental evidences in support of a role for the Psf1 C-terminus consensus motif in modulating GINS complex activity and provide a starting point to unravel multiple roles of the GINS complex in human and yeast cells.

#### **4.6.V      *Open questions and future directions***

In this chapter, I show that, in human cells, Psf1 is involved in maintaining GINS complex stability and plays a role in DNA replication and cell cycle progression. Moreover, the data suggests a mechanism for how Psf1 binding to DDB1 *via* its C-terminus motif may regulate DNA replication in response to DNA damage. In *S. cerevisiae* mutational

dysregulation of the conserved C-terminus serine within the SQXF motif of Psf1 leads to loss of cell viability, suggesting this site is important for the GINS complex activity. Taken together, the results presented here provide a platform for future study of Psf1 carboxyl terminus and the GINS complex in the DDR pathways.

However, several questions remain to be addressed. Foremost, deciphering the exact molecular functions of the GINS complex at the replication fork would be extremely useful in furthering our understanding of the eukaryotic replication fork and the DNA helicase machinery. GINS interactions with MCM and Cdc45, as part of the CMG helicase, as well as GINS binding to the DNA polymerases, are evolutionarily conserved in eukaryotes (for a comprehensive review, see MacNeill, 2010). Recent data suggesting that GINS preferentially binds to ssDNA (Boskovic et al., 2007) support a model where GINS works as a 'ploughshare' in the proximity of DNA unwound by the MCM (Takahashi et al., 2005) and at the intersection with the replication fork, coordinating replicative polymerases with the unwinding process. In this regard, more detailed understanding of the GINS complex is hindered by our lack of knowledge of the mechanism of the MCM helicase. As discussed in chapter 1.2.II, several models have been proposed on how MCM may work as a helicase, coordinately with speculative roles for the cofactors GINS and Cdc45. However, no definite proof of MCM acting as a helicase during DNA replication has been provided as yet. A crystal structure of the CMG unwindosome complex would be helpful to clarify a model of activity for this replication machinery and perhaps suggest modes of regulating unwinding in the presence of DNA damage.

Moreover, GINS complex is not only a co-factor in DNA unwinding, but also an accessory of replicative polymerase  $\epsilon$  and the DNA polymerase  $\alpha$ -primase complex. Genetic studies showed that the processivity and stabilization of these DNA polymerases requires GINS;

however, exactly how this is mediated is currently unclear. In addition to GINS roles during S-phase, a mitotic role for GINS in maintaining chromosomes integrity during cell division has been proposed (Huang et al., 2005a). It would be key to establish whether the aberrant mitotic phenotypes observed are caused by GINS functions that are distinct and separable from the replication role of GINS during S-phase. As recently alleged, the observed mitotic defects may be a consequence of incompletely replicated chromosomes undergoing separation (Barkley et al., 2009). Further investigation is required to address this point.

GINS functions in vertebrate development and in maintenance of the stem cell pool are just beginning to emerge (see chapter 4.2.IV). *Psf1* expression is up-regulated in actively proliferating tissues and is essential for the initial stages of embryonic development in mice (Ueno et al., 2005). It is currently unclear how the role of GINS in promoting replication impacts on GINS requirement for physiological development. In addition to the role of GINS in normal embryogenesis and tissues preservation, over-expression of GINS complex subunits has been recently associated with a wide variety of cancers (Obama et al., 2005; Hayashi et al., 2006; Ryu et al., 2007; Nagahama et al., 2010). It remains to be determined if GINS aberrant expression directly contributes to malignant transformation. Ectopic expression of human MCM has already been widely implicated in induction of tumourigenesis (Pruitt et al., 2007; Shima et al., 2007b; Shima et al., 2007a). Importantly, MCM is currently being used as a cancer biomarker to stain highly proliferating cells and tissues (Coleman and Laskey, 2009). Similarly, GINS expression was recently linked to cell proliferation in human cells, where GINS marked more robustly proliferating lymphocytes, given a similar pattern to MCM3 protein (Aparicio et al., 2009).

Thus, further investigation of GINS in the context of physiological and pathological proliferation remains an exciting challenge for future research, with vast medical relevance and clinical implications.

## 5 RAD9 CONSENSUS CDK PHOSPHORYLATION SITES REGULATE CHK1 ACTIVATION IN BUDDING YEAST

### 5.1 Summary

*S. cerevisiae* Rad9 is a major checkpoint mediator protein required for Mec1/Tel1-dependent phosphorylation and activation of Rad53 and Chk1 DNA damage checkpoint kinases. Here, I present evidence for the requirement of consensus CDK phospho-sites within Rad9 for the effective phosphorylation and activation of Chk1. I found that Rad9, which is cell cycle regulated by Cdc28-dependent phosphorylation, contains consensus CDK phosphorylation sites within the CAD region at its N-terminus. Mutation of four conserved S/TP sites to alanine, but not mutation of these sites individually, confers defective Chk1 phosphorylation following treatment with various DNA damaging agents. Further investigation suggests that Rad9 regulation *via* these sites contributes to Chk1 activation in the intra-S and the M-phase checkpoints.

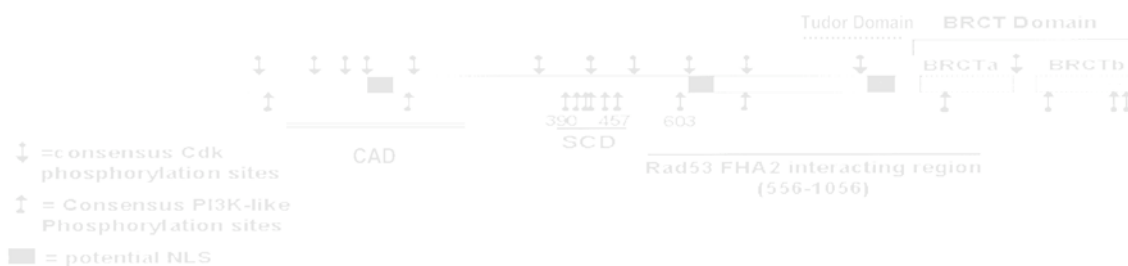
In addition, identification of conserved CDK sites in a putative CAD region in the human and chicken microcephalin proteins suggests that analogous cell cycle regulations mediate activation of Chk1 in these systems. I show that scRad9 and hMCPH1 N-termini interact with Chk1 *in vitro*. These data highlight an evolutionarily conserved pattern regulating Chk1 binding and activation, possibly through CDK-dependent phosphorylation. Further investigations are ongoing to elucidate the mechanisms of Rad9 and MCPH1 binding to Chk1 and shed light on a functional relationship between these proteins, which may be conserved throughout evolution. To this end, I have produced hybrid constructs swapping the Rad9 CAD and N-terminus for those of human and chicken MCPH1, which will be used as tools to dissect the evolutionary conservation of checkpoint activation.

## 5.2 Introduction

### 5.2.1 *Rad9 as the prototypical DNA damage checkpoint adaptor protein*

Radiation sensitive 9 (Rad9) is the prototypical DNA damage checkpoint protein in *S. cerevisiae*. The *RAD9* gene encodes a protein of 1,309 amino acids with a predicted molecular mass of 148 kDa (reviewed in Toh and Lowndes, 2003). Rad9 contains several structural regions with functional relevance for the protein's activity. At the amino-terminus is the Chk1 activation domain (CAD; Blankley and Lydall, 2004) that contains several closely-spaced consensus CDK phosphorylation sites. A cluster of 6 (S/T)Q sites consensus for Mec1/ATR and Tel1/ATM phosphorylation are found within the SCD (SQ/TQ cluster domain) between amino acids 390 and 457. The carboxyl terminus is characterized by a region of interaction with the FHA-domain of Rad53 (Emili, 1998; Sun et al., 1998; Vialard et al., 1998), tandem Tudor domains (Lancelot et al., 2007) and twin BRCT domains at very end of the protein, for binding to Tel1/Mec1-phosphorylated histone H2A (Downs et al., 2000; Hammet et al., 2007) (Diagram 13). The twin BRCTs are also required for Rad9 oligomerization in response to DNA damage (Soulier and Lowndes, 1999).

**DIAGRAM 13. Rad9 protein structural features and domains**



**Content not visible due to copyright limitations**

Rad9 is a large protein with 12 consensus CDK and 14 Mec1/Tel1 phosphorylation sites, indicating that Rad9 is regulated in response to DNA damage and during the cell cycle (Vialard et al., 1998).

Image modified from Toh and Lowndes, 2003

Despite low sequence conservation, Rad9 shares functional and structural homology with *S. pombe* Crb2, and the mammalian DDR mediator 53BP1. scRad9, spCrb2 and h53BP1 contain tandem Tudor domains for binding to methylated histones (Huyen et al., 2004; Botuyan et al., 2006; Du et al., 2006; Grenon et al., 2007) and twin BRCT motifs at the very carboxyl-end. In addition, other twin BRCT-containing DDR mediators MDC1 and BRCA1 are also putative Rad9 orthologues in higher eukaryotes. Indeed, like mammalian MDC1, Rad9 BRCTs bind to H2A phospho-epitope (Hammet et al., 2007).

Similarly to its aforementioned mammalian counterparts and *S. pombe* homologue Crb2, Rad9 is a DNA damage response factor required for checkpoint responses following DNA damage. More than 20 years ago, Weinert and Hartwell identified the *RAD9* gene as a master regulator of the G2/M cell cycle delay induced upon treatment with IR. In the same paper, the term ‘checkpoint’ was coined to describe transient arrests in cell cycle progression induced by DNA damage (Weinert and Hartwell, 1988). *RAD9* plays a role in activation of cell cycle delays induced by DNA damage at the G1/S (Siede et al., 1993; Siede et al., 1994), intra-S (Paulovich et al., 1997), as well as G2/M boundaries (Weinert and Hartwell, 1989). Given Rad9’s pivotal role in halting cell cycle progression in the presence of genotoxic lesions, the *rad9* deletion mutant shows high genomic instability and hyper-sensitivity to DNA damaging agents (Weinert and Hartwell, 1990).

### **5.2.II     *Rad9 mediates activation of the checkpoint kinases***

Rad9 functions as an adaptor-like factor to relay the DNA damage signal from the apical kinases Mec1 and Tel1 to downstream checkpoint transducer kinases Rad53 (homologue

of mammalian Chk2) and Chk1. Upon induction of DNA damage, Mec1 and Tel1 target the Rad9 SCD for phosphorylation. Phosphorylated S/TQ sites act redundantly to allow docking of Rad53 *via* its second FHA domain (FHA2). Rad9 is in a large molecular complex of about 850 kDa. Conformational changes induced by DNA damage-dependent hyper-phosphorylation cause remodelling to a smaller 560 kDa complex. This hyper-phosphorylated Rad9 is responsible for catalysing *in trans* auto-phosphorylation and activation of Rad53 (Gilbert et al., 2001). Both oligomeric assembly of Rad9 and its recruitment and retention to damaged chromatin promote a localized concentration of Rad53 to enable its auto-phosphorylation. In addition, Rad9 acts as an adaptor bridge to facilitate Mec1 phosphorylation of Rad53 (Sweeney et al., 2005). Efficient phosphorylation of Rad53 permits its release from the Rad9 complex (Gilbert et al., 2001). Once released, active Rad53 specifically targets substrates required for a variety of cellular responses, including checkpoint-induced cell cycle delay to allow for efficient repair of DNA lesions.

Although genetic and molecular data have helped to define the association between Rad9 and Rad53, the mechanistic dynamics of their interactions are still unclear. Three models have been proposed that attempt to explain Mec1-Rad9-Rad53 interaction steps (Gilbert et al., 2001; Pelliccioli and Foiani, 2005; Sweeney et al., 2005), as illustrated below in Diagram 14. In the *solid-state catalyst* model (Diagram 14, panel A) proposed by Lowndes and colleagues (2001), Rad9 molecules are hyper-phosphorylated, resulting in the recruitment and auto-phosphorylation of Rad53 kinases. Autophosphorylated Rad53 is released and activated. In a positive feedback loop, inactive Rad53 molecules get recycled into pre-active Rad9-Rad53 complexes (Gilbert et al., 2001). The *adaptor-based* model (panel B) by Durocher's group (2005), on the other hand, suggest that Rad9, hyper-

phosphorylated by Mec1 (B, step 1), recruits the inactive form of Rad53 that is subsequently phosphorylated by Mec1 (B, step 2), inducing Rad53 autophosphorylation (B, step 3), activation and release (Sweeney et al., 2005). Lastly, Pelliccioli and Foiani (2005) reconcile both previous models in the *adaptor-catalyst* model (panel C), where Mec1 phosphorylation of Rad9 continues to a threshold when hyper-phosphorylated Rad9 is able to recruit inactive Rad53 (C, step 1), which is in turn phosphorylated by Mec1 (C, step 2). Rad53 then undergoes autophosphorylation, which subsequently causes Rad9 oligomerization, amplifying the recruitment of Rad53 molecules (C, step 3). Active Rad53 molecules are then released from pre-active Mec1-Rad9-Rad53 complexes (reviewed in Pelliccioli and Foiani, 2005).

**DIAGRAM 14. Modes of Rad53 activation through the Rad9 adaptor protein**



**Content not visible due to copyright limitations**

The *solid-state catalyst* (A), *adaptor-based* (B) and *adaptor-catalyst* (C) models are shown (see text for details). Rad9 (in violet); inactive (red), pre-active (yellow) and active (green) Rad53; Mec1 (azure) are shown. Black round dots representing phosphorylated residues.

Image by Pelliccioli and Foiani, 2005

### **5.2.III    *Rad9's role in activating Chk1***

Rad9 is required for Chk1 activation in response to DNA damage (Sanchez et al., 1999; Blankley and Lydall, 2004), yet the molecular mechanisms underlying this interaction are largely elusive. Previously, it had been noticed that *rad9* yeast mutants lacking the SCD cluster were unable to activate Rad53 kinase; however, Chk1 phosphorylation and interactions with Mec1 were not disrupted by these mutations (Schwartz et al., 2002), but were abolished by *rad9* deletion. This indicates that other sites in Rad9 are involved in inducing Chk1 activation. Similarly to Rad53, Chk1 phosphorylation depends on both Mec1 and Rad9; however, Chk1 modification is independent of Rad53 and vice versa (Sanchez et al., 1999). Rad9 interacts with Chk1, as detected by two-hybrid studies (Sanchez et al., 1999), and is activated *via* a Mec1-dependent mechanism analogous to Rad53 activation (Sun et al., 1998; Vialard et al., 1998). In 2004, David Lydall's group mapped a 160 amino acid region (from 40 to 200) in Rad9 that is required for Chk1 activation, named CAD. No Mec1 consensus sites for phosphorylation are found within the CAD, but it has been shown to contain consensus CDK phospho-sites (Toh and Lowndes, 2003; Blankley and Lydall, 2004). As CDK phosphorylates Crb2, fission yeast homologue of Rad9 (Esashi and Yanagida, 1999; Caspari et al., 2002) and scRad9 is cell cycle regulated, with the phospho-shift becoming apparent not only upon irradiation, but also under unperturbed situation, following nocodazole arrest in G2/M (Vialard et al., 1998), it is possible that CDK phosphorylation of these consensus motifs promotes Chk1 recruitment and activation. Once activated, Chk1 is required for CDK inhibition and induction of cell cycle delay after DNA damage (Weinert, 1997), possibly suggesting the presence of a negative feedback loop in CDK regulation.

Chk1 regulates phosphorylation and protein levels of Pds1 to inhibit entry into anaphase and prevent mitotic exit. Because Rad53 also works in a redundant manner to control Pds1 degradation, *chk1* null mutants are only mildly sensitive to genotoxic agents. Furthermore, Chk1 plays a redundant role in maintaining replication fork stability during S-phase (Schollaert et al., 2004) and promotes HR in a *mec1-21* hypomorphic mutant, leading to a hyper-recombination phenotype and genomic instability (Fasullo and Sun, 2008). *CHK1* is also required for tolerance mechanisms in the presence of persistent single-stranded DNA breaks (Karumbati and Wilson, 2005), possibly being required for the phenomenon of adaptation in yeast. Thus, *S. cerevisiae* Chk1 differs from its mammalian homologue, whose activity not only plays a major role in activating intra-S and G2/M DNA damage checkpoints, but is also essential under normal physiological conditions to control progression through S-phase and mitosis (Chen et al., 2003; Sorensen et al., 2003). This emphasizes a diverging specialization of Chk1 protein functions in different organisms, yet a general conservation in the nature of the DNA damage checkpoint activation might have been preserved throughout evolution.

## 5.3 Results

### 5.3.1 *Rad9 contains consensus CDK phosphorylation sites within its N-terminal CAD*

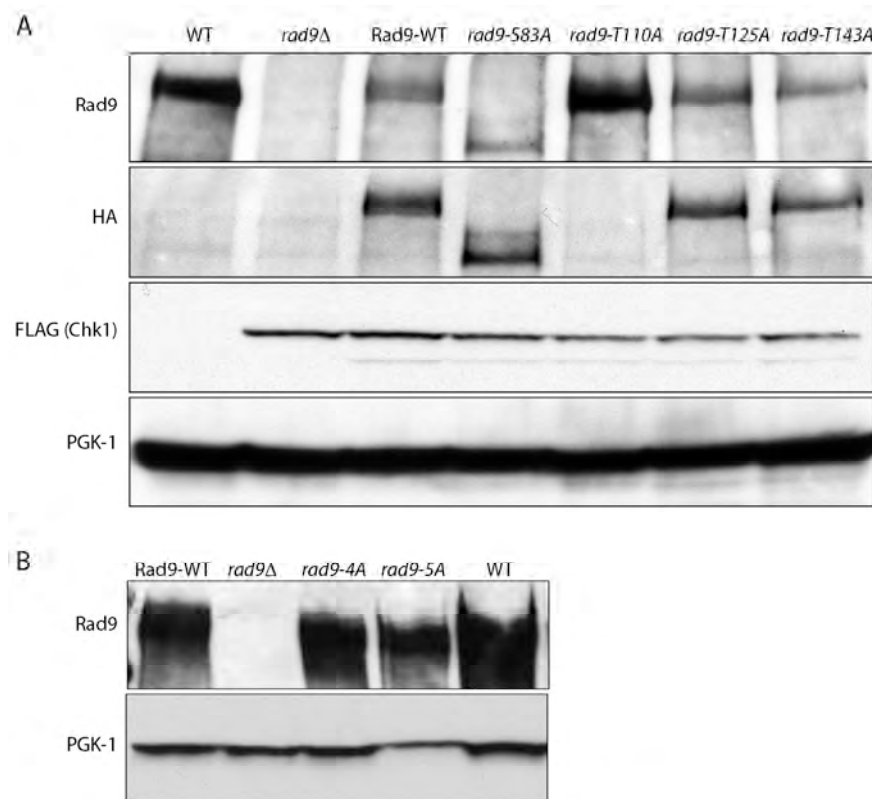
Although Mec1/Tel1-dependent phosphorylations of Rad9 have been extensively investigated, regulation of Rad9 activity by CDK during the cell cycle is still unclear. Several lines of evidence suggest that Rad9 is likely to be regulated by CDK-dependent phosphorylation (Vialard et al., 1998; Esashi and Yanagida, 1999; Caspari et al., 2002), yet direct phosphorylation of Rad9 by CDK is yet to be shown. In budding yeast, only one CDK exists, Cdc28, which can bind to nine regulatory cyclin subunits, Cln1-3 and Clb1-6. Depending on the cyclin partner, Cdc28 exercises controlled regulation to drive cells through the cell cycle (Nasmyth, 1993). As previously shown, I observed that Rad9 is constitutively phosphorylated in asynchronous, undamaged yeast cultures, as indicated by an electrophoretic mobility shift abolished by treatment with alkaline phosphatase (data not shown). In addition, using a *cdc28as*, a mutant *cdc28* sensitive to the ATP analogue 1NMPP1, I inhibited Cdc28 and saw a small reduction in Rad9 phospho-shift, suggesting that Rad9 is a target of CDK phosphorylation *in vivo* (data not shown). This is in line with data demonstrating that mutation of 18 CDK sites to alanines in Rad9 N-terminus leads to loss of cell-cycle-dependent constitutive phosphorylation (Bonilla et al., 2008).

To investigate the regulation of Rad9 during the cell cycle, I performed *in silico* searches for minimal consensus sites (S/TP) or full consensus motifs (S/TPXK/R), targeted for phosphorylation by CDK. I found 19 S/TP sites in Rad9, 12 SP sites and 7 TP sites, of which 5 and 3 match the full CDK consensus motif, respectively, the majority of which were localized at the N-terminus. The 18 N-terminal CDK phospho-sites are essential for



*S83A+T110A+T143A*), *rad9-4A* (*rad9-S83A+T110A+T125A+T143A*) and *rad9-5A* (*rad9-S56+S83A+T110A+T125A+T143A*) combination of multiple sites mutants were transformed into *rad9Δ* W303 strain and their expression was assessed (Figure 55). The N-terminal HA-tag caused a lower expression of Rad9. Removal of the tag increased expression of the Rad9 constructs from plasmid, but not to the levels of endogenous Rad9.

**FIGURE 55. Expression of *rad9* CDK mutants**

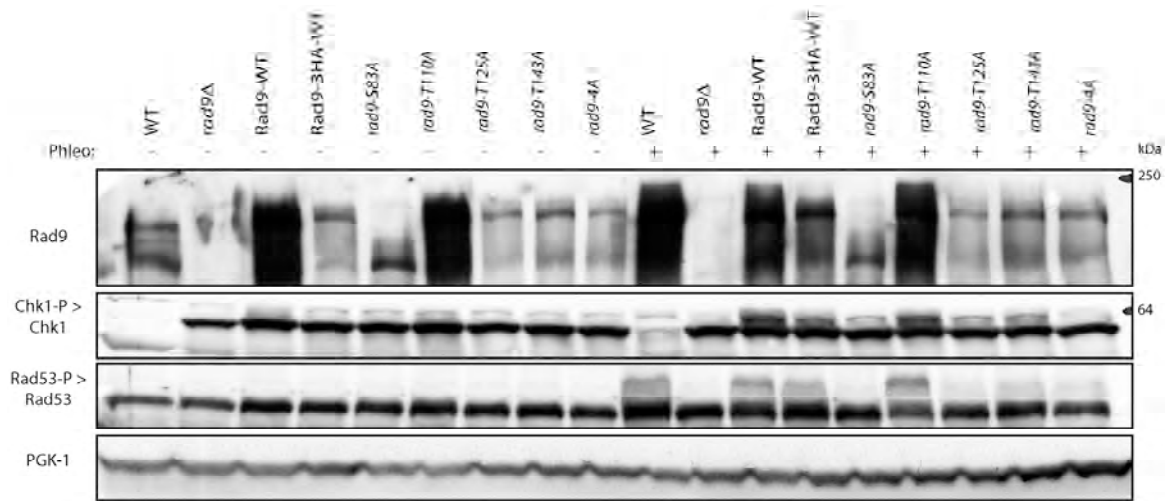


Expression of the Rad9 single CDK (A) and combination CDK mutant (B) constructs in a pRS414 plasmid was assessed by harvesting logarithmic cultures and performing TCA preparation for SDS-PAGE analysis. The constructs were transformed in *rad9Δ::HIS3, CHK1-FLAG::KanMX6* strains. WT W303 strain (WT) was used as comparison for endogenous Rad9 expression (A and B). Chk1 was tagged with FLAG inserted in the chromosomal locus. Antibodies against FLAG show that Chk1 is expressed correctly in all the *rad9Δ::HIS3, CHK1-FLAG::KanMX6* yeast strains. Note that Chk1 was not tagged in the WT W3030 strain, used as a negative control (A, lane 1). Removal of the N-terminal triple HA-tags, as in *rad9-T110A* (A), and in panel B, increased Rad9 expression. PGK-1 was used as loading control (A and B). It is noteworthy that *rad9-S83A* gives a different pattern on gel, running lower than WT Rad9. It is possible that another mutation is present, although this was not evident from sequencing. Further analyses carried out using Cdc28 inhibitors showed that *rad9-S83A* was not a hypo-phosphorylated form of Rad9.

### **5.3.III Failed Chk1 phosphorylation and activation in the *rad9-4A* mutant**

Next, I analyzed the effects of mutating these sites, collectively and individually, on Chk1 phosphorylation and activation. To assess the ability of *rad9* mutants to mediate Chk1 phosphorylation, I used an acute treatment with phleomycin to induce single and double-stranded DNA breaks in asynchronously growing cells. Single mutants did not display an obvious defect in Chk1 phosphorylation shift (Figure 56), nor did the *rad9-3A* mutant (data not shown). However, the *rad9-4A* showed an overt defect in effective Chk1 phosphorylation following phleomycin treatment. Reduction of Chk1 phosphorylation observed in the *rad9-4A* mutant was similar to the lack of Chk1 shift seen in *rad9* null cells (Figure 56). The *rad9-5A* mutant, including the S56A mutation, did not show further reduction in Chk1 phosphorylation (data not shown). Reduction of Chk1 phosphorylation observed in the *rad9-4A* mutant was also reproduced using methane methylsulfonate (MMS), another DNA damaging agent (data not shown). This result suggests that S83, T110, T125 and T143 consensus sites for CDK phosphorylation in Rad9 CAD act redundantly to promote efficient Chk1 phosphorylation and activation.

**FIGURE 56. Rad9 S83, T110, T125 and T143 are required for Chk1 phosphorylation**

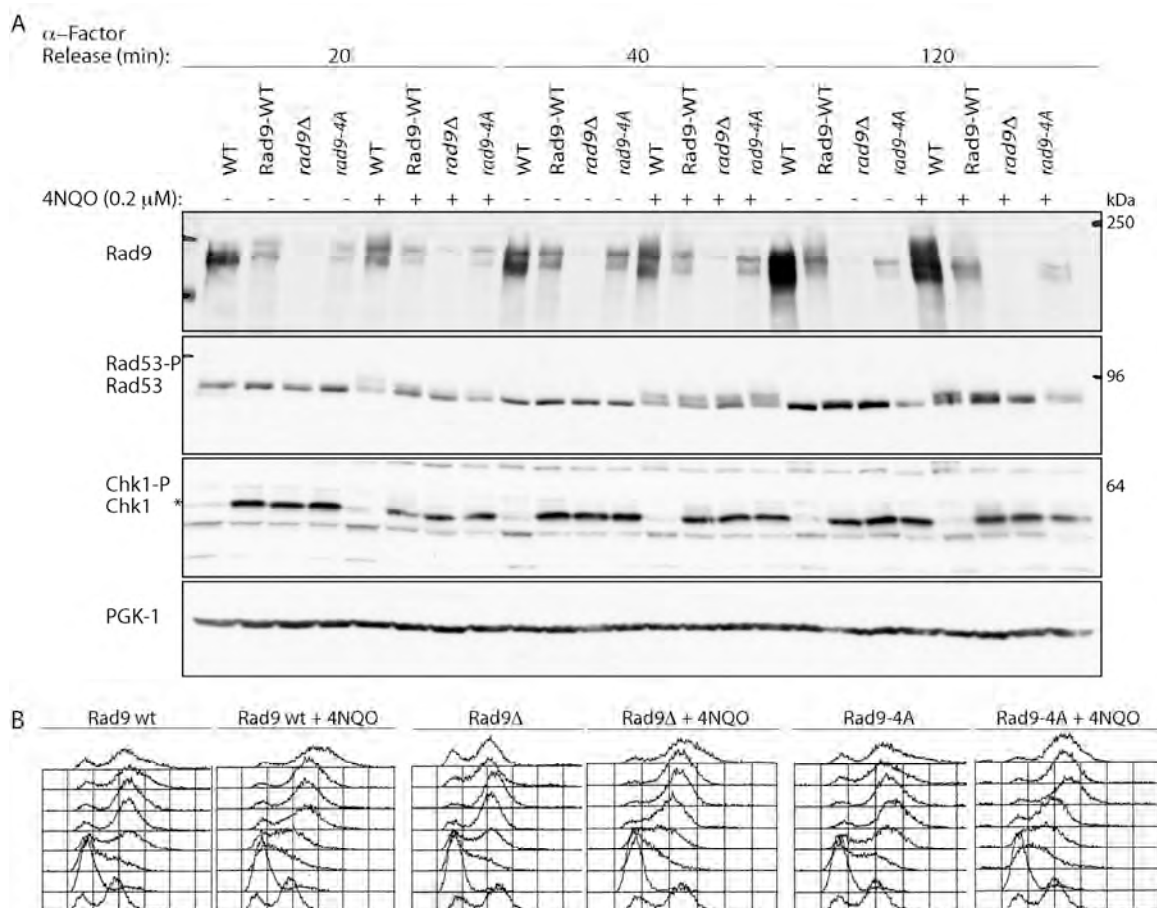


Logarithmic cultures of the indicated yeast strains were incubated in the presence and absence of 10  $\mu\text{g/ml}$  of phleomycin for 1 hour and harvested for TCA prep. 'P >' indicates phospho-bands with decrease electrophoretic mobility for Chk1 (Chk1-P) and Rad53 (Rad53-P). Similarly to *rad9Δ*, Chk1 phosphorylation is abolished in *rad9-4A* compared to *rad9* single mutants expressed to similar levels. Untagged Rad9 (Rad9-WT) expressed from plasmid has higher expression than HA-tagged Rad9 (Rad9-3HA-WT), but not as high as endogenous Rad9 (WT).

To understand the exact timing during the cell cycle when Rad9 phosphorylation by CDK impacts on Chk1 activation, I synchronized cells in G1 using  $\alpha$ -factor and released them into the cell cycle, monitoring progression into S-phase (early S, 20 minutes; late S, 40 minutes time-points), through G2/M and back into G1. I assessed Chk1 phosphorylation by WB (Figure 57A), progression through the cell cycle and activation of the DNA damage checkpoint by FACS (Figure 57B) following treatment with the radiomimetic drug, 4NQO. As expected, Chk1 did not respond to DNA damage in early S-phase (20 minutes time-point; Figure 56A). In late S-phase (40 minutes), Rad53 and Chk1 became activated by treatment with 4NQO in the presence of wild-type Rad9, whereas the *rad9-4A* strain shows a reduction in Chk1 phosphorylation (Figure 57A). Further decrease in Chk1 phosphorylation was observed at the 120 minutes time-point following  $\alpha$ -factor release,

when cells are found in G2/M (Figure 57A), indicating that CDK-phosphorylation of the four sites in Rad9 CAD is specifically important in regulating activation of Chk1 in the mitotic checkpoint, and partially in the intra-S-phase checkpoints in late S-phase. In agreement with published data, Rad53 phosphorylation was not affected by the *rad9-4A* mutant (Figure 57A), indicating that the mechanism of regulation by CDK sites in the CAD is specific to Chk1 and does not impact on Rad53 activation.

**FIGURE 57. *Rad9-4A* mutant is not proficient in mediating phosphorylation of Chk1 during late S-phase and in mitosis**



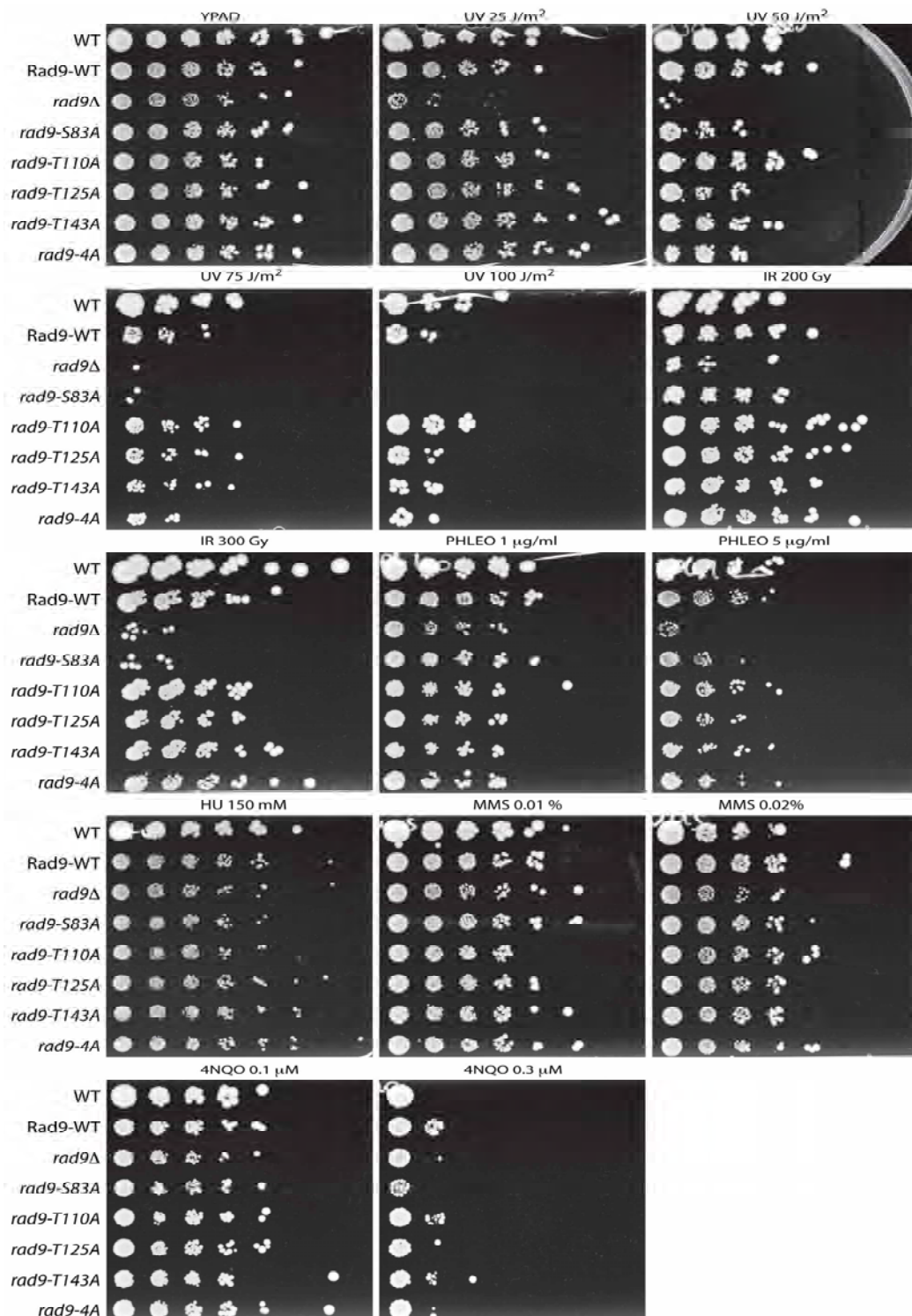
Logarithmic cultures of the yeast strains were synchronized into G1 using  $\alpha$ -factor and released into the cell cycle either into fresh medium or medium containing 0.2  $\mu$ M 4NQO. Samples were collected for western blotting analysis at 20, 40 and 120 minutes post-release (A). FACS analysis of samples of asynchronous, G1-arrested cells and cells released and collected at 20, 40, 60, 80, 100 and 120 minutes time-points (B) show that the four CDK sites in Rad9 CAD are required for Chk1 phosphorylation in late-S-phase and in G2/M and for regulation of the DNA damage checkpoint.

Failed phosphorylation of Chk1 in late-S-phase in the *rad9-4A* mutant caused a mild defect in progressing into S-phase at 20 and 40 minutes and from S-phase into G2/M at 80 minutes. However, *rad9-4A* mutant did not display an obvious over-riding of the G2/M checkpoint (Figure 57B). These data indicate that Rad9-mediated phosphorylation of Chk1 controlled through the four CDK sites is required for slowing down replication and preventing entry into G2/M with unreplicated or damage DNA, yet compensatory mechanisms may exist which allow activation of the mitotic checkpoint in the absence of active Chk1. These data are in agreement with findings that Rad53 acts in a redundant manner to Chk1 activating a parallel pathway to control the anaphase checkpoint (Sanchez et al., 1999).

Next, I assessed the phenotypical consequences of mutating the four CDK sites, individually or in combination, in response of chronic exposure to a range of genotoxic agents by sensitivity assays. In line with my previous findings, single mutants did not show sensitivity to DNA damaging agents (Figure 58). The *Rad9-4A* mutant was mildly sensitivity to UV and high doses of 4NQO (Figure 57), but not to the same extent as the *rad9Δ* strain. This was expected, since mutating the four CDK consensus sites does not impair the role of Rad9 outside of Chk1 activation, such as Rad53 activation, and *chk1Δ* is only mildly sensitive to DNA damaging agents, due to functional redundancy with Rad53 in mediating checkpoint activation.

Collectively, these data show that S83, T110, T125 and T143 consensus CDK phosphorylation sites in the Rad9 CAD act redundantly to promote Chk1 phosphorylation and activation in late-S-phase and in G2/M checkpoints; mutation of these sites leads to mild sensitization to certain genotoxins.

**FIGURE 58. Sensitivity assay of Rad9 CDK mutants**



The indicated strains were grown overnight, diluted to an  $OD_{600nm}$  of 0.5 before dilutions (5-fold) were spotted on yeast selection medium for tryptophan expression containing the indicated drug. *Rad9-4A* is mildly sensitive to high doses of UV and 4NQO. *Rad9-S83A* is sensitive to certain cytotoxic agents but, due to abnormal expression pattern in WB (Figure 55), its phenotype was disregarded. This is one representative example of the sensitivity assay; all experiments were repeated in triplicates.

Throughout this study, I noted that the *rad9Δ* strains expressing untagged Rad9 from a single-copy plasmid showed lower expression compared to endogenous Rad9 in a W303 WT strain (Figure 55A and 57A). Tagging of Rad9 using HA or FLAG tags, at the amino or carboxyl ends, caused further reduction in protein expression (Figure 55A, 56 and data not shown). Although abrogation of Chk1 phosphorylation was specifically due to combined mutagenesis of all four sites as shown in Figure 56 and 57A, and not to the reduced levels of expression, I noticed that the *rad9Δ* strains expressing Rad9 plasmids had a slightly impaired checkpoint activation (data not shown) and sensitivity to cytotoxic agents (Figure 58) compared to the WT strain. To confirm the role of Rad9 consensus CDK sites in Chk1 activation in the response to DNA damage, I established a collaboration with Prof. Noel Lowndes and Dr. Muriel Grenon (National University of Ireland Galway) to subclone the CAD mutants into a yeast integrative plasmid (Yip) to perform Yip-mediated mutagenesis by ‘pop-in pop-out’ HR-guided events for integration into the chromosomal RAD9 locus. Integration of my mutants in the endogenous gene’s locus is more rigorous and gives more reproducible results than expressing mutated genes from a plasmid. Integrated *rad9-4A* mutant, as well as individual mutants, showed endogenous levels of expression from the Rad9 genomic locus; using these strains, we were able to show that the combination of all four mutations, but not the individually mutated sites, decreased Chk1 phosphorylation, when yeast cells were arrested in nocodazole and treated with 400 Gy of IR; moreover, no additive affect was observed using the *rad9-5A* mutant strain (data not shown). This further confirms that mutational dysregulation of these four CDK sites in Rad9 CAD affects efficient Chk1 phosphorylation and activation in M-phase following a range of DNA damaging agents.

In addition, I have made serine/threonine to glutamic acid mutants of the consensus CDK sites, individually or in combination. These are currently being integrated and tested for rescuing Chk1-associated phenotype.

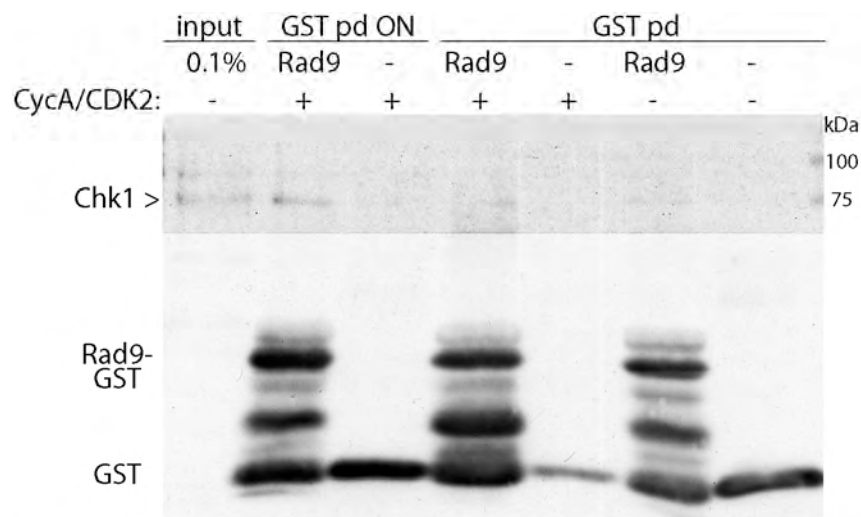
#### **5.3.IV     *Physical interactions between Rad9 and Chk1***

The Rad9-Chk1 interaction has been previously described by yeast two-hybrids (Sanchez et al., 1999; Uetz et al., 2000), yet, to date, no other biochemical evidence for a physical interaction between Chk1 and Rad9 exists. In addition, attempts by David Lydall's group to detect a direct interaction between Rad9 and Chk1 were unsuccessful, suggesting that potential binding may be very transient (Blankley and Lydall, 2004), indirect or cell cycle-regulated.

I wanted to verify the interaction between the N-terminus of Rad9 and Chk1, and test whether mutations of the four CDK sites in the CAD domain improved or hindered the binding. To address this, I sub-cloned the very N-terminal region of Rad9 containing the four CDK sites (1-166 amino acids), wild-type or mutated, into a pGEX vector and expressed the GST fusion fragments in bacteria. Once purified, I compared the capabilities of the Rad9-GST N-terminus fragments to bind and pull-down FLAG-Chk1 expressed in a *rad9Δ* strain. I found that a small amount of Chk1 bound to the N-terminus of wild-type Rad9. Pre-incubation of Rad9 with activated Cyclin A/CDK2 in an *in vitro* kinase assay slightly increased the binding (Figure 59). No obvious binding was observed in all experiments performed with the mutated N-terminus of Rad9 (data not shown). This suggests that phosphorylation may play a positive role in mediating the interaction with

Chk1, hence explain why I did not observe binding of Rad9-4A and wild-type Rad9 N-terminal fragments in the absence of phosphorylation-inducing agents.

**FIGURE 59. A small amount of Chk1 binds to Rad9 N-terminus *in vitro***



Rad9-GST N-terminus fragment on beads was added to human recombinant Cyclin A/CDK2 or to the kinase buffer only, and pre-incubated for 15 minutes. Rad9 was then used for GST pull-downs, overnight (GST pd ON) or for 2 hours (right) at 4°C. 10 mg of yeast extracts from *rad9Δ*, *CHK1-FLAG* strain was used for each pull-down. Rad9 N-terminus binds a minute fraction of Chk1 upon incubation with CDK.

### 5.3.V *Microcephalin is a novel candidate homologue of budding yeast Rad9*

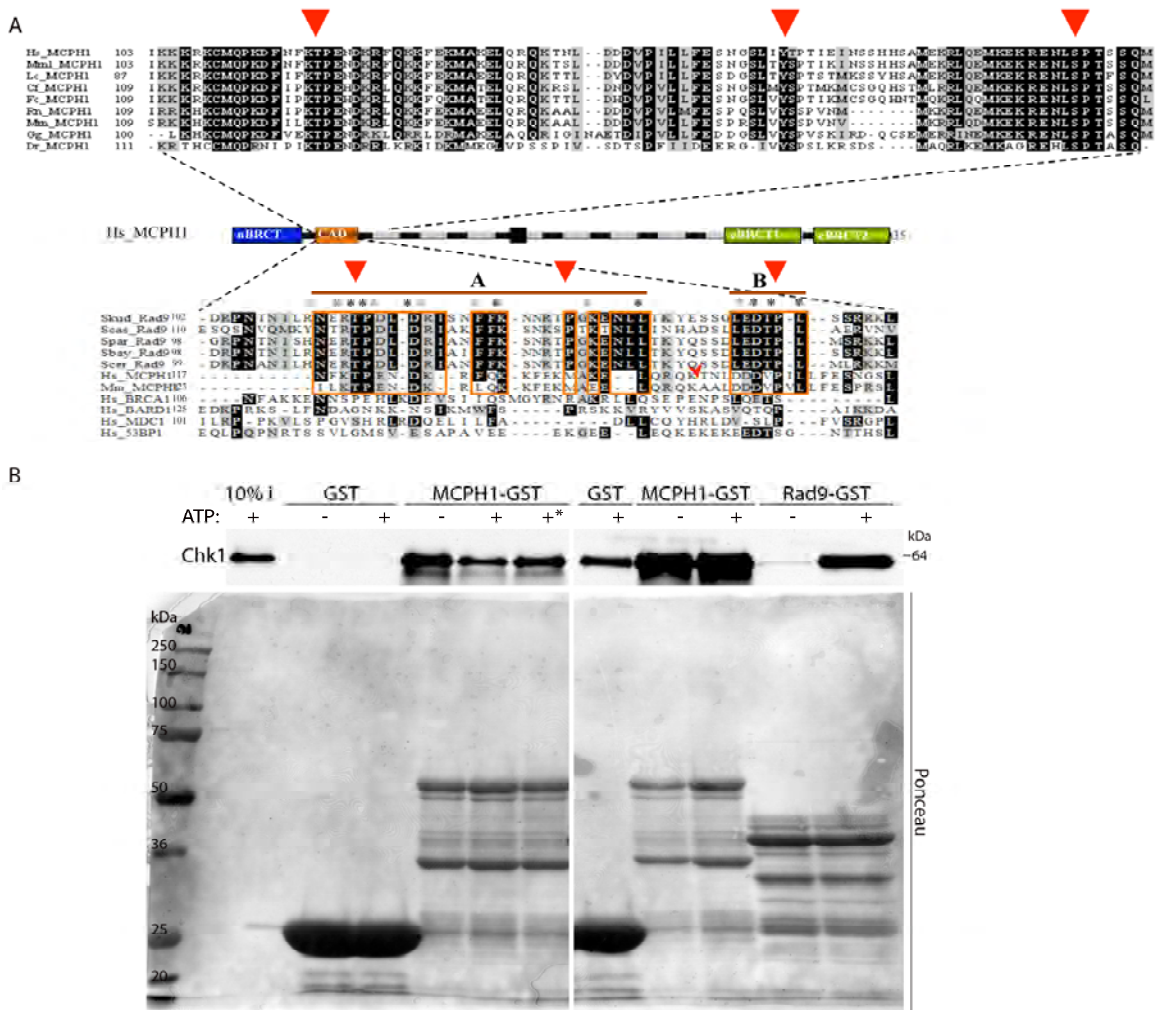
The absence of a clear homologue for *S. cerevisiae* Rad9 in mammalian cells suggests that the multitude of roles exercised by Rad9 have been separated into different, more specialized proteins during evolution. Indeed, although budding yeast Rad9, fission yeast Crb2 and metazoan 53BP1 share conserved structural homologies and display analogous modes of recruitment to sites of DNA damage, 53BP1 has limited checkpoint function, whereas Crb2 and Rad9 play a major role in checkpoint activation (Ward et al., 2006).

MCPH1 (microcephalin) is a human gene encoding a protein characterized by three BRCT domains, one at the N-terminus (BRCT1) and two twin BRCTs located at the C-terminus (BRCT2 and BRCT3; Figure 60). Mutations in this gene cause primary microcephaly, an autosomal recessive genetic disorder characterized by reduced brain size and mental retardation (Jackson et al., 2002). In addition to roles in determining human brain size during neurogenesis (reviewed in Woods et al., 2005), microcephalin localizes to  $\gamma$ H2AX DNA damage foci and functions in the execution of the intra-S and G2/M checkpoints. To this end, MCPH1 is required for stabilization of BRCA1 and Chk1, increasing their proteins levels, and for phosphorylation of Nbs1 (Xu et al., 2004; Lin et al., 2005). Thus, microcephalin is an important proximal factor in the DDR, whose inhibition leads to chromosomal abnormalities, indicating it may act as a tumour suppressor gene (Rai et al., 2006). In another study, microcephalin was found to physically interact with Chk1 and to control Cdc25A phosphatase turnover for activation of the ATR-branch of the checkpoint (Alderton et al., 2006). In addition, MCPH1 plays a physiological role in regulating mitotic entry by promoting the association of Chk1 with centrosomes, thus restraining the activation of centrosomal cyclin B–CDK1 and preventing unscheduled entry into mitosis (Tibelius et al., 2009).

Given MCPH1 is required for Chk1-dependent activation of the DNA damage checkpoint and physically binds to Chk1, I wanted to investigate whether hMCPH1 interactions with Chk1 were mediated by the protein's N-terminus and regulated by phosphorylation in a similar manner to scRad9. Interestingly, MCPH1 contains a putative CAD region located at the N-terminus of the protein – localized between amino acids ~103 and 250 – which shares conserved CDK phospho-sites with scRad9 CAD (Figure 60A; Richard Chahwan, personal communication). To verify the interaction between MCPH1 CAD domain and human Chk1, I sub-cloned hMCPH1 N-terminus (1-252 aa) into a pGEX vector and expressed the GST-fragment in *E. coli*. MCPH1 N-terminus robustly interacted with

purified Chk1 *in vitro*, both in the presence and absence of ATP (Figure 60B), suggesting that binding between MCPH1 and Chk1 occurs through the N-terminus of the protein, possibly *via* the novel CAD region, independently of phosphorylation. However, I cannot exclude that *in vivo* interactions may be regulated by phosphorylation.

**FIGURE 60. Identification of a novel CAD region in human MCPH1, which shares conserved CDK sites with scRad9 and binds to human Chk1**



Cross-species Mcph1-Rad9 alignments show presence of 3 conserved consensus CDK phospho-sites within the CAD domains. In scRad9: T110 TPDL; T125 TPGK; and T143 TPLM showed homology with hMCPH1 sites: T120 TPED; T162 TPTI; and S190 SPTS, respectively (A; image by Richard Chahwan). Human MCPH1 N-terminus avidly binds to purified Chk1 *in vitro*. GST alone, MCPH1-GST or Rad9-GST N-terminus fragments were incubated with 1  $\mu$ g of purified human Chk1 (10% input, i). 5 mM ATP was added to the reaction with GST alone, MCPH1-GST and Rad9-GST and with the input. Also, MCPH1-GST was pre-incubated with ATP (+\*), washed and then added to purified Chk1 for binding in the absence of ATP. Ponceau stained membrane prior to WB shows the expression of the recombinant constructs: GST only (~ 26 kDa), GST-MCPH1 (252 aa = ~28 kDa + GST = ~55 kDa) and GST-Rad9 (166 aa = ~18 kDa + GST = ~44 kDa) N-terminus fragments.

Next, I wanted to test the ability of *S. cerevisiae* Rad9 N-terminus fragment to bind purified human Chk1, suggesting a possible evolutionarily conserved mechanism. Binding of Rad9 to human Chk1 was increased above background upon incubation with ATP (Figure 60B). This finding is in agreement with the previous data using CyclinA-CDK2, suggesting that phosphorylation events on Rad9 N-terminus promote interactions between Rad9 and Chk1.

To investigate the functional relevance of the MCPH1 N-terminus and CAD domain interaction in the activation of Chk1, in collaboration with Muriel Grenon, I designed a strategy to make hybrids constructs where scRad9 N-terminus or CAD were swapped for human or chicken MCPH1 N-terminus and CAD, respectively (Figure 61). I performed fusion-PCR to produce the scRad9-hMCPH1<sup>N-terminus1-203</sup> and scRad9-ggMCPH1<sup>N-terminus1-199</sup> constructs and these were verified by DNA sequencing (see hybrids for N-terminal region in Figure 61). The constructs can be utilized to rescue defects caused by *rad9-4A* mutant and verify the existence of a conserved role for hMCPH1 and scRad9 in mediating Chk1 phosphorylation and activating intra-S and M-phase checkpoints. Chicken *McpH1* was cloned and analyzed by Ciaran Morrison's group (Galway), which found that cMcpH1 localized to centrosomes through the N-terminal BRCT1, and was recruited to IRIF *via* its C-terminal twin BRCTs, playing a role in the DDR (Jeffers et al., 2008), similarly to hMCPH1. Thus, testing the ability of both human and chicken MCPH1 to rescue my Rad9 CDK mutants could yield interesting results and help in defining evolutionarily convergent and divergent roles for these proteins.

**FIGURE 61. Strategy for the design of Rad9-h/ggMCPH1 hybrid constructs**



**Content not visible due to copyright limitations**

Sequence homology and experimental data were used to predict the spanning of the CAD in Rad9 and in human and chicken MCPH1. Two types of constructs were designed: Rad9 N-terminus swap, where the first 174 amino acids of scRad9 are substituted for hMCPH1 N-terminus (1-203 aa) or ggMcpH1 N-terminus (1-199 aa; panels 1.1 and 2.1). In Rad9 CAD swap, scRad9 CAD (107-174 aa) was swapped for hMCPH1 putative CAD (94-203 aa) or ggMcpH1 putative CAD (93-199 aa; panels 1.2 and 2.2 – Image by Muriel Grenon).

The constructs I have made are currently being tested in Noel Lowndes's lab for interaction with scChk1 by yeast two-hybrid and they will be used to map functional conservation of the Rad9/MCPH1-Chk1 branch of the DNA damage checkpoint in the near future.

The findings shown in this study demonstrate that *S. cerevisiae* Rad9 contains consensus sites for CDK phosphorylation within the CAD region at the N-terminus. Combined mutation of these conserved S/TP sites to alanine (S83A, T110A, T125A and T143A), confers a defect in Chk1 phosphorylation following treatment with a variety of DNA damaging agents. These sites contribute to Chk1 activation in the context of both the intra-S and M-phase checkpoints in budding yeast. Identification of conserved CDK sites in a putative CAD region in human and chicken microcephalin proteins suggests that analogous cell cycle regulation of these proteins may control phosphorylation, activation, localization and/or interaction with Chk1 in these systems. Indeed, I have shown that phosphorylation by Cyclin A/CDK2 enables the scRad9 N-terminus to bind Chk1 *in vitro*; moreover, human MCPH1 N-terminus is also capable of binding purified Chk1. Although it is unclear whether the interactions between hMCPH1 and Chk1 are positively or negatively regulated by phosphorylation, these data highlight a pattern of evolutionary conservation in the mechanisms of Chk1 regulation and binding through the N-terminus of yeast Rad9 and human MCPH1. Further investigations are ongoing to elucidate additive effects of other CDK sites in Rad9 CAD, understand the mechanisms of Rad9 and MCPH1 binding to Chk1 and shed light on a functional relationship between these proteins, which may be conserved throughout evolution.

## **5.4 Discussion and conclusion**

*S. cerevisiae* Rad9 is a major cell-cycle-regulated adaptor protein required for Mec1/Tel1-dependent phosphorylation and activation of Rad53 and Chk1-branches of the DNA damage checkpoint. The study presented in this thesis produces evidence for the requirement of specific consensus CDK phospho-sites within Rad9 CAD region for Chk1 phosphorylation and activation. The data shown in this study infers that Rad9 is regulated by CDK phosphorylation, which, in turn, affects its ability to phosphorylate Chk1 and activate Chk1-mediated cell cycle delays in response to DNA damage.

### **5.4.1 *Functional activity for Rad9 consensus CDK sites in Chk1 activation***

Identification of a functional role for 4 consensus CDK sites (S83, T110, T143 and T155) within the CAD region of Rad9 in mediating Chk1 phosphorylation suggests that CDK activity influences the activation and choice of checkpoint pathways. Indeed, mutation of these sites to alanine caused disruption in Chk1 activation, yet Rad53 phosphorylation was unperturbed. These data are in agreement with previous reports showing that Rad53 binding to Rad9 and subsequent activation is mediated by Tel1/Mec1-induced phosphorylation of Rad9 SCD, a region containing several clustered S/TQ sites (Emili, 1998; Usui et al., 2001; Schwartz et al., 2002) and is independent of Chk1 activation. The impact of putative CDK phosphorylations on Rad9 regulating activation of Chk1 is especially interesting considering that Rad9 is differentially phosphorylated in a cell cycle-dependent manner: Rad9 is hypo-phosphorylated in G1, when Chk1 is inert to DNA damage, and becomes hyper-phosphorylated in S and G2/M, when Chk1 responds to DNA damage. In support of this hypothesis, I found that Chk1 was not activated by phosphorylation upon treatment with 4NQO when cells are synchronized at early stages of

S-phase. However, Chk1 becomes selectively active in mid-to-late S-phase to monitor replication, and in mitosis for activation of the checkpoint branch that halt mitotic progression into anaphase. Furthermore, proficient activation of Chk1 in both these context require the presence of intact Rad9 CDK sites. Thus, existence of CDK sites on Rad9 to regulate Chk1 activation emphasizes a strong requirement for cell cycle control over induction of this branch of the DNA damage checkpoint in a timely manner.

Due to the low sensitivity of the *chk1* null strain to DNA damaging agents, the functional relevance of the Chk1 checkpoint in yeast is questionable. It is likely that redundancy with the Rad53-branch masks phenotypical defects of *chk1Δ* strain. Indeed, it has been shown that Rad53 and Chk1 work in parallel pathways, regulating Cdc5 and Pds1 respectively, both converging to inhibit mitotic exit and metaphase-to-anaphase transition after DNA damage (Sanchez et al., 1999). However, the mild sensitivity of the *rad4-4A* strain to high doses of UV and 4NQO suggests that Chk1 functions do not entirely overlap with Rad53. UV radiation and the UV-mimetic 4NQO induces several types of adducts and DNA “photoproducts”, that would block progression of the polymerase (Friedberg, 1996; DePamphilis et al., 2006), causing accumulation of ssDNA and checkpoint activation. In the context of late S-phase, Chk1 may play a more predominant role than Rad53 in slowing down replication in the presence of genotoxic agents. On the other hand, an independent Chk1-induced checkpoint control may exist that regulate termination of replication. Although I favour the former explanation, I currently have no evidence to exclude the latter. Thus, it would be interesting to understand the extent of the cross-talk between these two checkpoint kinases and how this changes in different cell cycle phases. In this regard, it’s tempting to speculate that CDK activity controls not only the choice between repair pathways in budding yeast (Huertas et al., 2008), but also the mode of checkpoint

activation, possibly coordinating the selection of the DNA repair mechanism with activation of the appropriate cell cycle delay machinery.

It is noteworthy that expression of *RAD9* from a single-copy plasmid resulted in lower-than-endogenous protein levels. This may be due to differences between the chromatin structures in regulating *RAD9* gene expression from the plasmid versus the endogenous genomic locus. In addition, tagging of Rad9 using HA or FLAG tags at the N-terminus resulted in a further decrease in protein levels indicating that the tags destabilized the protein. To circumvent these problems, *rad9* mutants were integrated in the chromosomal locus. Integrated *rad9-4A* confirmed defects in Chk1 phosphorylation. However, mutation of 9 consensus CDK sites located in Rad9 N-terminus completely abolished the Chk1 shift, inferring that another important or several less important sites may also be required for proficient Chk1 activation. Identification of the minimal requirements for Chk1 activation is therefore an interesting line of further enquiry. My data also show that single mutants do not display overt defects in Chk1 phosphorylation; thus, these sites act redundantly and in a concerted manner to efficiently mediate Chk1 phosphorylation by Mec1/Tel1 and checkpoint activation in late-S and G2/M.

#### **5.4.II      *Phosphorylation of Rad9 by CDK enables interaction with Chk1***

To date, evidence for a physical interaction between Rad9 and Chk1 has been very scarce. By yeast-two-hybrid, Rad9 and Chk1 interact (Sanchez et al., 1999); however, other attempts to demonstrate direct physical interactions failed (Blankley and Lydall, 2004). Attempts to IP Chk1, or a kinase-dead versions of the protein, using wild-type or Rad9<sup>4A</sup> mutant, as well as reverse IPs, were unsuccessful, indicating that interactions may be very

transient. Here, I show that, using the Rad9 N-terminus fragment, a small amount of Chk1 was pulled-down. Interestingly, binding was observed upon pre-incubation with CyclinA/CDK2 complex. These data show that a fraction of Chk1 does interact with Rad9 and the binding occurs between Chk1 and the N-terminal region of Rad9, possibly following phosphorylation by CDK. Thus, phosphorylation of Rad9, but not Chk1, by CDK is required for the two proteins to interact, corroborating the idea that CDK regulation of Rad9 N-terminus controls binding and activation of Chk1 in a cell cycle-dependent manner. It would be interesting to analyze how cell cycle regulations affect this interaction and the spatio-temporal settings for Rad9-Chk1 binding *in vivo*.

#### **5.4.III *MCPH1, a new homologue of *S. cerevisiae* Rad9 in higher eukaryotes***

Although the domain organization of mammalian Chk1 and its yeast orthologues is evolutionarily conserved (Stracker et al., 2009), the functional aspects of Chk1 have diverged during evolution. In budding yeast, the functional overlap with Rad53 renders this factor dispensable for cell viability and unnecessary for DNA damage checkpoints activation. By contrast, mammalian Chk1 not only plays a major role in intra-S and G2/M-checkpoints, but is also essential for cell viability, due to an as yet undefined role during unperturbed mitosis (Wilsker et al., 2008). Despite differences in Chk1 roles between mammals and lower eukaryotes, the molecular mechanisms of Chk1 activation may be preserved during evolution. Here, I show that the BRCT-containing mammalian DDR mediator protein MCPH1 contains a CAD-like region at the N-terminus, similar to scRad9 CAD, including three conserved consensus CDK phosphorylation sites. In addition, hMCPH1 has been previously shown to regulate the Chk1-branch of the DNA damage checkpoint pathway. Indeed, I show that hMCPH1 N-terminus binds to purified Chk1 *in*

*vitro*, suggesting that interactions between MCPH1 and Chk1 in human may be analogous to those in budding yeast. Because MCPH1 BRCT1 at the very N-terminus was shown to be required for Chk1 localization to the centrosome, I used the full N-terminal region for my experiments, as both the CAD and the first BRCT domain may be required for binding to Chk1. These preliminary observations suggest that MCPH1 is a novel homologue of scRad9 in higher eukaryotes.

#### **5.4.IV    *Open questions and future directions***

Further investigations are needed to establish the minimal consensus for Rad9 and MCPH1 binding and activation of Chk1, to address how this may be regulated by CDK-dependent phosphorylation and how this regulation impacts on Chk1 pivotal roles in mammalian cells. Addressing these questions is particularly relevant in light of the essential role of Chk1 in mammals, considering MCPH1 may be an important mediator of Chk1 activation. Although these hypotheses have yet to be tested, I have produced powerful tools to verify how the functional relationship between Rad9/MCPH1 and Chk1 has evolved during evolution. I have made hybrid constructs swapping Rad9 MCPH1 CAD or N-terminus with the respective human or chicken homologue regions. These constructs will be utilized for rescue experiments of *rad9-4A* mutant and to verify the existence of an evolutionarily conserved or divergent role for human and chicken MCPH1 and scRad9 in mediating Chk1 phosphorylation and subsequent activation of the checkpoint. Also, these studies may help in uncoupling Chk1 essential cell cycle role and Chk1 role in the DDR.

The study presented in this thesis provides a starting platform for subsequent investigations into a novel homologue of Rad9 in higher eukaryotes, MCPH1. Especially interesting is the identification of conserved sites consensus for CDK phosphorylation on human MCPH1

within a novel CAD-like region. Both budding yeast Rad9 and human MCPH1 bind to Chk1, strengthening the speculation that an evolutionarily conserved mechanism exists in mediating Chk1-dependent checkpoint activation. Several questions remain to be addressed as to how CDK regulates both scRad9 and MCPH1 impacting on checkpoint activation and, possibly, on other, essential roles of mammalian Chk1. Also, further studies might provide novel molecular evidence as to the clinical relevance of MCPH1 in brain development in human. Chk1 role in monitoring physiological cell proliferation and mitotic division may be a missing link in explaining the microcephaly phenotype and reduced body size consequent to MCPH1 mutations. Hence, more studies will be required to untangle the diverse contributions of adaptor-like proteins throughout evolution in regulating the checkpoint effector kinase Chk1, and in preserving genomic integrity and physiological homeostasis.

## DISCUSSION AND CONCLUSIONS

---

## 6 GENERAL DISCUSSION

Selective evolutionary pressure has been shaping molecular phenomena for millions of years. Biological systems have acquired a multilayered complexity to ensure an elevated level of proficiency in their cellular responses. Fundamental cellular events that guarantee the propagation of life include the faithful duplication of the genetic information, a proficient cell division program and surveillance mechanisms to maintain genomic integrity. These events must synergistically coordinate their efforts to allow cell growth while retaining high-fidelity segregation of the genetic material to the progeny. Aberrations in different aspects of these pivotal processes have widespread impacts on the genesis of a variety of human pathologies, including neoplasia.

The work presented in this thesis aims to explore interactions between cell cycle mechanisms and preservation of genome integrity. The molecular interface shared by these processes is characterized by direct cross-talk, as well as by positive and negative feedback loops that indirectly influence cellular responses in these contexts. While responses to DNA damage act to delay cell cycle progression by enforcing activation of so-called checkpoints, the DDR itself is subject to cell cycle regulation (Branzei and Foiani, 2008; Pardo et al., 2009). For instance, some DDR factors are only readily available at certain cell cycle stages, while the function of others is modulated by phosphorylation events mediated by cell cycle kinases (e.g. CDKs). In addition, the sub-cellular localization of certain DDR factors changes during the cell cycle and/or upon induction of DNA damage, affecting their activity. This communication between the cell cycle machinery and the DDR apparatus is fine-tuned depending on myriad variables, including the nature of the DNA lesion, the chromatin status of the genomic locus, availability of sister chromatids, and the phase of the cell cycle. These affect the choice of the repair pathways, the

activation of different checkpoint cascades and the selection of factors required to orchestrate these responses.

During my PhD, I have shown that DNA damage responses are heavily influenced by cell cycle regulations and that the DNA damage cascade unfolds in a different manner depending on the cell cycle phase when the cells suffers genotoxic insults. Specifically, I have found that the DDR in mitosis differs remarkably from that in interphase stages. This work has revealed that human cells have evolved a mechanism that prioritizes timely passage through mitosis over a complete activation of all the steps in the DNA damage signalling cascade. Once committed to mitosis, cells containing DNA DSBs do not perturb progression through mitosis, to achieve the timely accomplishment of chromosome segregation and cytokinesis, as they fail to activate a DNA damage checkpoint and corresponding effector kinases Chk1 and Chk2 while in mitosis.

Although the observation that mitotic cells do not delay cell cycle progression in the presence of DSBs is not novel, my studies have gone one step further to challenge the pre-existing view that the absence of a mitotic checkpoint correlates with the absence of a DDR in mitosis. Indeed, it is difficult to conceive a scenario where cells would totally ignore potentially deadly lesions such as DSBs in any cell cycle stage. My data show that mitotic cells do respond to the presence of DSBs but only activate a *primary* DDR, comprising of activation of the apical PIKK kinases ATM and DNA-PK, phosphorylation of  $\gamma$ H2AX and recruitment of MDC1 and MRN to sites of DNA damage. This, however, is where the mitotic DDR stops, lacking recruitment of the E3 ubiquitin ligases RNF8, RNF168 and BRCA1, and the DDR mediator 53BP1. The restriction in the recruitment of these *secondary* factors during mitosis is likely to be multifactorial, reflecting a combination of mitosis-specific post-translational modifications, compacted mitotic

chromatin status and sequestration of certain DDR proteins within mitotic structures. These differences emphasize the uniqueness of the mitotic phase in human cells and highlight the need to adapt responses to DNA lesions to the physiological requirements of this important cell cycle phase. In this regard, activation of the *secondary* DDR is understandably unsuited to the characteristics of mitosis because the brevity of this phase and the timely execution of karyokinesis and cytokinesis could be perturbed by full DDR and checkpoint activation. In addition, remodelling of chromatin induced by RNF8-mediated ubiquitylation events would likely be deleterious in the context of highly compacted mitotic chromosomes. Thus, it is tempting to speculate that mitotic cells prevent *secondary* DDR to ensure timely cell division and avoid disruption in the higher-order chromatin of mitotic chromosomes. Nonetheless, activation of the primary DDR in mitotic cells appears to be biologically important, as our data indicate that it promotes cell viability and confers radio-resistance. Collectively, these findings indicate that human cells have evolved a mechanism to *mark* DSB during mitosis, while guaranteeing completion of cell division. Once the daughter cells re-enter the following interphase, a full DDR activation ensues and DSBs are dealt with in the more favourable chromatin environment of the G1 cell.

In budding yeast, responses to DNA damage in mitosis differ in some regards to those in mammalian cells. In *S. cerevisiae*, not only do Mec1/Tel1, Rad9 and Rad53/Chk1 contribute to activate the mitotic checkpoint that blocks the metaphase-to-anaphase transition in the presence of DNA damage, but also the SAC protein Mad2 acts to enforce this regulation after DNA damage (Clerici et al., 2004). Thus, in *S. cerevisiae*, DDR factors and mitotic factors act in concert to activate a DNA damage-induced delay in mitosis. By contrast, in human cells, the SAC does not seem to be activated by DNA damage *per se*, unless spindle attachment to the kinetochore is affected. However, my novel observations showing the localization of DDR factors within specific mitotic structures corroborate

existing findings indicating that DDR factors may play roles in unperturbed mitosis. This suggests that in human cells, even if DDR responses are minimal in mitosis and do not seem to affect mitotic processes, DDR factors may possess both DDR and mitotic roles. In mitosis, RNF8, RNF168 and 53BP1 recruitment to kinetochores, as well as RNF8 and BRCA1 recruitment to centrosomes, is especially significant, inferring that these factors may work to control mitotic progression in similar molecular ways as they do in the DDR cascade. To this end, RNF8 was shown to be recruited to the midbody and to be required for mitotic exit (Tuttle et al., 2007; Plans et al., 2008). My observations that RNF8 depletion by siRNA causes failure to synchronize cells in mitosis suggest that RNF8 plays additional roles, including those controlling entry/progression through mitosis. It would be interesting to see how these roles correlate to RNF8's association with the various mitotic structures.

Human Chk1 is an important example of how a DNA damage-responsive factor also plays an essential role in unperturbed progression through mitosis. In *S. cerevisiae*, Chk1 does not display the essential functions present in mammalian cells, including driving cells through the cell cycle and monitoring unperturbed progression through S, G2 and M-phases, yet has retained responsiveness to DNA damaging agents in late-S-phase and in G2/M checkpoints, including regulation of the metaphase-to-anaphase transition. In this study, I show that effective Chk1 phosphorylation and activation of the Chk1-branch of the late-S-phase and G2/M delays depends on consensus CDK phosphorylation sites on the mediator protein Rad9. Thus, regulation of Chk1 activation in specific phases of the cell cycle underlines the impact of the cell cycle on DNA damage mechanisms in budding yeast, like in mammalian cells. In this case, Rad9 may be directly regulated by CDK-dependent phosphorylation events that impact on the capabilities of Rad9 to bind Chk1 and promote Mec1/Tel1 phosphorylation and activation of this checkpoint kinase.

In budding yeast, Rad9 has retained multiple roles in the DDR and checkpoint activation pathways. During evolution, Rad9 appears to have diverged into several mediator proteins in higher eukaryotes, possibly to improve fine-tuning and include additional regulations in increasingly complex biological systems. Here, I show that MCPH1 might be a novel homologue of Rad9, as it not only contains twin BRCT domains at the C-terminus, like BRCA1, 53BP1 and MDC1, but it also contains a CAD-like region with conserved consensus CDK phospho-sites, similar to those in the Rad9 CAD. Moreover, similarly to Rad9, MCPH1 binds Chk1 through its N-terminal region. This suggests that certain cell cycle regulations of mediators' functions are retained during evolution, yet the spatio-temporal settings of these processes have changed. Whereas in yeast DNA damage checkpoints can be activated in the middle of mitosis, human cells have suppressed these responses. Thus, the differences highlighted in this study between human and yeast cells help reveal how DNA damage responses and cell cycle regulations influence one another, and how these effects could be influenced by the organism's biological complexity.

The interlink between cell cycle and DNA damage can also be analyzed from a dynamic point of view, monitoring cycling cells dealing with DNA damage from one phase to the other. Pivotal cellular process like duplication of the genetic information contained in the nucleus ought to be carried out synchronously with surveillance mechanisms embedded in the replication process itself. In addition, aberrations in the replication process or the presence of DNA damage during replication not only slow down and affect S-phase progression, but also impact on subsequent activation of G2/M checkpoint, which monitors unreplicated as well as damaged DNA, and on mitotic division, that activates the decatenation checkpoint to enable separation of genomic regions left unreplicated in mitosis. Thus, the process of replication and its termination continues through and affects

G2 and sometimes M-phase, as well as progression through S-phase. Replication requires the marvellously coordinated efforts of thousands of replication forks to duplicate the entire human genome. This complex task of proficiently and precisely replicating DNA is made more difficult by replication fork stalling and possibly collapsing upon encountering damaged DNA. Responses to DNA damage in the context of S-phase must be prompt and timely to facilitate the job of the replication machinery. Thus, some components of the active replisome that travel with the fork selectively work as surveillance factors to quickly respond to challenged situations. Roles for structural components of the replication fork, such as PCNA, but also TopBP1, Claspin, Timeless and others in stabilizing the fork under unperturbed conditions and following DNA damage are just starting to emerge. For example, it has been shown that upon induction of DNA damage in S-phase, ATR, recruited to the fork by RPA-coated ssDNA, phosphorylates and activates Chk1 through interactions with mediator proteins including TopBP1 and Claspin.

GIN5 is a novel replication complex that has been shown to work at the interface between replicative polymerases and the unwinding helicase complex. In this thesis, I present the identification of evolutionarily conserved ATM/ATR consensus sites at the C-termini of two GIN5 subunits, Psf1 and Psf2. In budding yeast Psf1, mutation of the serine within the phospho-motif to a glutamic acid, possibly mimicking constitutive phosphorylation of the site, leads to loss of viability. This suggests that this site may not only be important for DNA damage-dependent phosphorylation, but also to enable replication. Further analysis of this mutant shows that it behaves like a dominant negative protein. Increased sensitivity to DNA damaging agents in the *psf1-S187E* strain suggests a potential dual role for this site in promoting and enabling replication, while responding to DNA damage during DNA synthesis. To this end, in human cells, Psf1 is phosphorylated after DNA damage and the Psf1 conserved C-terminal motif binds the UV-responsive molecular machine DDB1-

DDB2, which links DNA repair with ubiquitylation events (Sugasawa, 2009) and regulates Cdt1 degradation after UV in S-phase (Hu et al., 2004). Binding of DDB1 to GINS suggest a mechanism analogous to PCNA, where GINS serves to bridge DDB1 to replication licensing factor Cdt1 and possibly others, mediating lysine 48-linked poly-ubiquitin chains to mark targets for proteosomal degradation. GINS is important for progression through S-phase in human and yeast cells; the data presented in this thesis also suggest that it may play additional roles in regulating replication in response to DNA damage. This hypothesis awaits further investigation.

Collectively, the work described in this thesis maps cross-talks between DDR and cell cycle mechanisms. The evidence presented serves to highlight evolutionarily diverging or converging DDR pathways that interact with the cell cycle machinery to promote cell cycle progression while ensuring genomic fidelity in both human and yeast cells. These data show that, while differences exist in how simple and more complex eukaryotes deal with DNA damage during diverse cell cycle phases, the molecular mechanisms underlying activation and unfolding of the DDR and checkpoint induction are often conserved throughout evolution. The observations shown in this thesis serve as a starting point for further investigations to minutely dissect molecular interactions and the functional relevance of the DDR mechanisms during individual steps of the cell cycle.

Advances in this novel field at the boundary between cell cycle and DNA damage research might be translated into medical applications to pioneer new translational therapies based on emerging molecular data. For instance, the understanding of how cells respond to DNA damage in the radio-sensitive phase of mitosis is especially important to understand the differential impact of chemotherapeutic treatments on human cells at different stages of the cell cycle and between proliferating versus quiescent cells. Especially, the design of novel

anti-mitotic therapeutics requires an increasingly deep knowledge of the web of molecular mechanisms during physiological and challenged mitosis, with an aim of reducing side-effects and selectively targeting cancer cells. In addition, understanding the essential role of Chk1 in higher eukaryotes and how this connects to other factors like microcephalin may not only serve to define how Chk1 inhibition negatively affects certain types of tumours, but may also shed light on Chk1's role in physiological cell proliferation.

The emerging links between replication factors and malignant transformations have been clinically implemented in various aspects of cancer pathology. Replication licensing proteins, such the MCM complex, are currently being used as biomarkers for hyper-proliferation and have several translational applications, including diagnosis, prognosis and treatment assessment for a variety of cancers. The GINS complex could perhaps also be exploited as a cancer biomarker and could also provide an attractive target for novel anti-tumour drugs to inhibit proliferation of cancer cells.

The scientific knowledge gathered by research on cell and molecular biology is being gradually but surely translated into medical applications. It has been an enormously exciting and rewarding experience for me to have provided a small contribution to understanding biological phenomena and producing knowledge that can be used to better understand, detect and treat human diseases, particularly cancer.



## REFERENCES

---

- Abraham, R.T. and Tibbetts, R.S. (2005) Cell biology. Guiding ATM to broken DNA. *Science* 308:510-1.
- Adams, M.M. and Carpenter, P.B. (2006) Tying the loose ends together in DNA double strand break repair with 53BP1. *Cell Div* 1:19.
- Alderton, G.K., Galbiati, L., Griffith, E., Surinya, K.H., Neitzel, H., Jackson, A.P., Jeggo, P.A. and O'Driscoll, M. (2006) Regulation of mitotic entry by microcephalin and its overlap with ATR signalling. *Nat Cell Biol* 8:725-33.
- Alsbeih, G. and Raaphorst, G.P. (1999) Differential induction of premature chromosome condensation by calyculin A in human fibroblast and tumor cell lines. *Anticancer Res* 19:903-8.
- Anderson, L., Henderson, C. and Adachi, Y. (2001) Phosphorylation and rapid relocalization of 53BP1 to nuclear foci upon DNA damage. *Mol Cell Biol* 21:1719-29.
- Aparicio, O.M., Weinstein, D.M. and Bell, S.P. (1997) Components and dynamics of DNA replication complexes in *S. cerevisiae*: redistribution of MCM proteins and Cdc45p during S phase. *Cell* 91:59-69.
- Aparicio, T., Ibarra, A. and Mendez, J. (2006) Cdc45-MCM-GINS, a new power player for DNA replication. *Cell Div* 1:18.
- Aparicio, T., Guillou, E., Coloma, J., Montoya, G. and Mendez, J. (2009) The human GINS complex associates with Cdc45 and MCM and is essential for DNA replication. *Nucleic Acids Res* 37:2087-95.
- Araki, H., Leem, S.H., Phongdara, A. and Sugino, A. (1995) Dpb11, which interacts with DNA polymerase II(epsilon) in *Saccharomyces cerevisiae*, has a dual role in S-phase progression and at a cell cycle checkpoint. *Proc Natl Acad Sci U S A* 92:11791-5.
- Bahassi el, M., Myer, D.L., McKenney, R.J., Hennigan, R.F. and Stambrook, P.J. (2006) Priming phosphorylation of Chk2 by polo-like kinase 3 (Plk3) mediates its full activation by ATM and a downstream checkpoint in response to DNA damage. *Mutat Res* 596:166-76.
- Bakkenist, C.J. and Kastan, M.B. (2003) DNA damage activates ATM through intermolecular autophosphorylation and dimer dissociation. *Nature* 421:499-506.
- Barkley, L.R., Song, I.Y., Zou, Y. and Vaziri, C. (2009) Reduced expression of GINS complex members induces hallmarks of pre-malignancy in primary untransformed human cells. *Cell Cycle* 8:1577-88.
- Bartek, J. and Lukas, J. (2003) Chk1 and Chk2 kinases in checkpoint control and cancer. *Cancer Cell* 3:421-9.
- Bartek, J., Lukas, C. and Lukas, J. (2004) Checking on DNA damage in S phase. *Nat Rev Mol Cell Biol* 5:792-804.
- Bassing, C.H. and Alt, F.W. (2004) The cellular response to general and programmed DNA double strand breaks. *DNA Repair (Amst)* 3:781-96.
- Baudin, A., Ozier-Kalogeropoulos, O., Denouel, A., Lacroute, F. and Cullin, C. (1993) A simple and efficient method for direct gene deletion in *Saccharomyces cerevisiae*. *Nucleic Acids Res* 21:3329-30.
- Bauerschmidt, C., Pollok, S., Kremmer, E., Nasheuer, H.P. and Grosse, F. (2007) Interactions of human Cdc45 with the Mcm2-7 complex, the GINS complex, and DNA polymerases delta and epsilon during S phase. *Genes Cells* 12:745-58.

- Bekker-Jensen, S., Lukas, C., Melander, F., Bartek, J. and Lukas, J. (2005) Dynamic assembly and sustained retention of 53BP1 at the sites of DNA damage are controlled by Mdc1/NFBD1. *J Cell Biol* 170:201-11.
- Bell, S.P. and Stillman, B. (1992) ATP-dependent recognition of eukaryotic origins of DNA replication by a multiprotein complex. *Nature* 357:128-34.
- Bender, A. and Pringle, J.R. (1991) Use of a screen for synthetic lethal and multicopy suppressor mutants to identify two new genes involved in morphogenesis in *Saccharomyces cerevisiae*. *Mol Cell Biol* 11:1295-305.
- Bermejo, R., Capra, T., Gonzalez-Huici, V., Fachinetti, D., Cocito, A., Natoli, G., Katou, Y., Mori, H., Kurokawa, K., Shirahige, K. and Foiani, M. (2009) Genome-organizing factors Top2 and Hmo1 prevent chromosome fragility at sites of S phase transcription. *Cell* 138:870-84.
- Bernhard, E.J., Maity, A., Muschel, R.J. and McKenna, W.G. (1995) Effects of ionizing radiation on cell cycle progression. A review. *Radiat Environ Biophys* 34:79-83.
- Bishop, A.C., Ubersax, J.A., Petsch, D.T., Matheos, D.P., Gray, N.S., Blethrow, J., Shimizu, E., Tsien, J.Z., Schultz, P.G., Rose, M.D., Wood, J.L., Morgan, D.O. and Shokat, K.M. (2000) A chemical switch for inhibitor-sensitive alleles of any protein kinase. *Nature* 407:395-401.
- Blankley, R.T. and Lydall, D. (2004) A domain of Rad9 specifically required for activation of Chk1 in budding yeast. *J Cell Sci* 117:601-8.
- Blow, J.J. and Laskey, R.A. (1988) A role for the nuclear envelope in controlling DNA replication within the cell cycle. *Nature* 332:546-8.
- Bochman, M.L. and Schwacha, A. (2007) Differences in the single-stranded DNA binding activities of MCM2-7 and MCM467: MCM2 and MCM5 define a slow ATP-dependent step. *J Biol Chem* 282:33795-804.
- Bochman, M.L. and Schwacha, A. (2008) The Mcm2-7 complex has in vitro helicase activity. *Mol Cell* 31:287-93.
- Bochman, M.L., Bell, S.P. and Schwacha, A. (2008) Subunit organization of Mcm2-7 and the unequal role of active sites in ATP hydrolysis and viability. *Mol Cell Biol* 28:5865-73.
- Bonilla, C.Y., Melo, J.A. and Toczyski, D.P. (2008) Colocalization of sensors is sufficient to activate the DNA damage checkpoint in the absence of damage. *Mol Cell* 30:267-76.
- Boskovic, J., Coloma, J., Aparicio, T., Zhou, M., Robinson, C.V., Mendez, J. and Montoya, G. (2007) Molecular architecture of the human GINS complex. *EMBO Rep* 8:678-84.
- Botuyan, M.V., Lee, J., Ward, I.M., Kim, J.E., Thompson, J.R., Chen, J. and Mer, G. (2006) Structural basis for the methylation state-specific recognition of histone H4-K20 by 53BP1 and Crb2 in DNA repair. *Cell* 127:1361-73.
- Bousset, K. and Diffley, J.F. (1998) The Cdc7 protein kinase is required for origin firing during S phase. *Genes Dev* 12:480-90.
- Bowman, G.D., Goedken, E.R., Kazmirski, S.L., O'Donnell, M. and Kuriyan, J. (2005) DNA polymerase clamp loaders and DNA recognition. *FEBS Lett* 579:863-7.
- Branzei, D. and Foiani, M. (2008) Regulation of DNA repair throughout the cell cycle. *Nat Rev Mol Cell Biol* 9:297-308.
- Branzei, D. and Foiani, M. (2010) Maintaining genome stability at the replication fork. *Nat Rev Mol Cell Biol* 11:208-19.
- Brewerton, S.C., Dore, A.S., Drake, A.C., Leuther, K.K. and Blundell, T.L. (2004) Structural analysis of DNA-PKcs: modelling of the repeat units and insights into the detailed molecular architecture. *J Struct Biol* 145:295-306.

- Brown, G.W. and Kelly, T.J. (1998) Purification of Hsk1, a minichromosome maintenance protein kinase from fission yeast. *J Biol Chem* 273:22083-90.
- Burma, S., Chen, B.P., Murphy, M., Kurimasa, A. and Chen, D.J. (2001) ATM phosphorylates histone H2AX in response to DNA double-strand breaks. *J Biol Chem* 276:42462-7.
- Cai, S.Y., Babbitt, R.W. and Marchesi, V.T. (1999) A mutant deubiquitinating enzyme (Ubp-M) associates with mitotic chromosomes and blocks cell division. *Proc Natl Acad Sci U S A* 96:2828-33.
- Callebaut, I. and Mornon, J.P. (1997) From BRCA1 to RAP1: a widespread BRCT module closely associated with DNA repair. *FEBS Lett* 400:25-30.
- Carlson, J.G. (1969a) A detailed analysis of x-ray-induced prophase delay and reversion of grasshopper neuroblasts in culture. *Radiat Res* 37:1-14.
- Carlson, J.G. (1969b) X-ray-induced prophase delay and reversion of selected cells in certain avian and mammalian tissues in culture. *Radiat Res* 37:15-30.
- Carpenter, P.B., Mueller, P.R. and Dunphy, W.G. (1996) Role for a *Xenopus* Orc2-related protein in controlling DNA replication. *Nature* 379:357-60.
- Caspari, T., Murray, J.M. and Carr, A.M. (2002) Cdc2-cyclin B kinase activity links Crb2 and Rqh1-topoisomerase III. *Genes Dev* 16:1195-208.
- Casper, A.M., Nghiem, P., Arlt, M.F. and Glover, T.W. (2002) ATR regulates fragile site stability. *Cell* 111:779-89.
- Celeste, A., Fernandez-Capetillo, O., Kruhlak, M.J., Pilch, D.R., Staudt, D.W., Lee, A., Bonner, R.F., Bonner, W.M. and Nussenzweig, A. (2003) Histone H2AX phosphorylation is dispensable for the initial recognition of DNA breaks. *Nat Cell Biol* 5:675-9.
- Celeste, A., Petersen, S., Romanienko, P.J., Fernandez-Capetillo, O., Chen, H.T., Sedelnikova, O.A., Reina-San-Martin, B., Coppola, V., Meffre, E., Difilippantonio, M.J., Redon, C., Pilch, D.R., Oлару, A., Eckhaus, M., Camerini-Otero, R.D., Tessarollo, L., Livak, F., Manova, K., Bonner, W.M., Nussenzweig, M.C. and Nussenzweig, A. (2002) Genomic instability in mice lacking histone H2AX. *Science* 296:922-7.
- Chadwick, B.P. and Lane, T.F. (2005) BRCA1 associates with the inactive X chromosome in late S-phase, coupled with transient H2AX phosphorylation. *Chromosoma* 114:432-9.
- Chang, Y.P., Wang, G., Bermudez, V., Hurwitz, J. and Chen, X.S. (2007) Crystal structure of the GINS complex and functional insights into its role in DNA replication. *Proc Natl Acad Sci U S A* 104:12685-90.
- Chapman, J.R. and Jackson, S.P. (2008) Phospho-dependent interactions between NBS1 and MDC1 mediate chromatin retention of the MRN complex at sites of DNA damage. *EMBO Rep* 9:795-801.
- Chattopadhyay, S. and Bielinsky, A.K. (2007) Human Mcm10 regulates the catalytic subunit of DNA polymerase-alpha and prevents DNA damage during replication. *Mol Biol Cell* 18:4085-95.
- Chen, M.S., Ryan, C.E. and Piwnicka-Worms, H. (2003) Chk1 kinase negatively regulates mitotic function of Cdc25A phosphatase through 14-3-3 binding. *Mol Cell Biol* 23:7488-97.
- Chin, C.F. and Yeong, F.M. (2009) Safeguarding Entry into Mitosis: the Antephase Checkpoint. *Mol Cell Biol*.
- Choi, J.M., Lim, H.S., Kim, J.J., Song, O.K. and Cho, Y. (2007) Crystal structure of the human GINS complex. *Genes Dev* 21:1316-21.

- Chong, J.P., Hayashi, M.K., Simon, M.N., Xu, R.M. and Stillman, B. (2000) A double-hexameric archaeal minichromosome maintenance protein is an ATP-dependent DNA helicase. *Proc Natl Acad Sci U S A* 97:1530-5.
- Clapperton, J.A., Manke, I.A., Lowery, D.M., Ho, T., Haire, L.F., Yaffe, M.B. and Smerdon, S.J. (2004) Structure and mechanism of BRCA1 BRCT domain recognition of phosphorylated BACH1 with implications for cancer. *Nat Struct Mol Biol* 11:512-8.
- Clay-Farrace, L., Pelizon, C., Santamaria, D., Pines, J. and Laskey, R.A. (2003) Human replication protein Cdc6 prevents mitosis through a checkpoint mechanism that implicates Chk1. *Embo J* 22:704-12.
- Clerici, M., Baldo, V., Mantiero, D., Lottersberger, F., Lucchini, G. and Longhese, M.P. (2004) A Tel1/MRX-dependent checkpoint inhibits the metaphase-to-anaphase transition after UV irradiation in the absence of Mec1. *Mol Cell Biol* 24:10126-44.
- Cohen, S.M., Chastain, P.D., 2nd, Cordeiro-Stone, M. and Kaufman, D.G. (2009) DNA replication and the GINS complex: localization on extended chromatin fibers. *Epigenetics Chromatin* 2:6.
- Coleman, N. and Laskey, R.A. (2009) Minichromosome maintenance proteins in cancer screening. *Eur J Cancer* 45 Suppl 1:416-7.
- Coleman, T.R. and Dunphy, W.G. (1994) Cdc2 regulatory factors. *Curr Opin Cell Biol* 6:877-82.
- Coleman, T.R., Carpenter, P.B. and Dunphy, W.G. (1996) The *Xenopus* Cdc6 protein is essential for the initiation of a single round of DNA replication in cell-free extracts. *Cell* 87:53-63.
- Collins, K., Jaks, T. and Pavletich, N.P. (1997) The cell cycle and cancer. *Proc Natl Acad Sci U S A* 94:2776-8.
- Cook, P.R. (1999) The organization of replication and transcription. *Science* 284:1790-5.
- Costanzo, M., Baryshnikova, A., Bellay, J., Kim, Y., Spear, E.D., Sevier, C.S., Ding, H., Koh, J.L., Toufighi, K., Mostafavi, S., Prinz, J., St Onge, R.P., VanderSluis, B., Makhnevych, T., Vizeacoumar, F.J., Alizadeh, S., Bahr, S., Brost, R.L., Chen, Y., Cokol, M., Deshpande, R., Li, Z., Lin, Z.Y., Liang, W., Marback, M., Paw, J., San Luis, B.J., Shuteriqi, E., Tong, A.H., van Dyk, N., Wallace, I.M., Whitney, J.A., Weirauch, M.T., Zhong, G., Zhu, H., Houry, W.A., Brudno, M., Ragibzadeh, S., Papp, B., Pal, C., Roth, F.P., Giaever, G., Nislow, C., Troyanskaya, O.G., Bussey, H., Bader, G.D., Gingras, A.C., Morris, Q.D., Kim, P.M., Kaiser, C.A., Myers, C.L., Andrews, B.J. and Boone, C. (2010) The genetic landscape of a cell. *Science* 327:425-31.
- Costanzo, V., Robertson, K., Ying, C.Y., Kim, E., Avvedimento, E., Gottesman, M., Grieco, D. and Gautier, J. (2000) Reconstitution of an ATM-dependent checkpoint that inhibits chromosomal DNA replication following DNA damage. *Mol Cell* 6:649-59.
- Coster, G., Hayouka, Z., Argaman, L., Strauss, C., Friedler, A., Brandeis, M. and Goldberg, M. (2007) The DNA damage response mediator MDC1 directly interacts with the anaphase-promoting complex/cyclosome. *J Biol Chem* 282:32053-64.
- Dalton, W.B. and Yang, V.W. (2009) Role of prolonged mitotic checkpoint activation in the formation and treatment of cancer. *Future Oncol* 5:1363-70.
- Damelin, M. and Bestor, T.H. (2007) The decatenation checkpoint. *Br J Cancer* 96:201-5.
- De Falco, M., Ferrari, E., De Felice, M., Rossi, M., Hubscher, U. and Pisani, F.M. (2007) The human GINS complex binds to and specifically stimulates human DNA polymerase alpha-primase. *EMBO Rep* 8:99-103.

- Deckbar, D., Birraux, J., Krempler, A., Tchouandong, L., Beucher, A., Walker, S., Stiff, T., Jeggo, P. and Lobrich, M. (2007) Chromosome breakage after G2 checkpoint release. *J Cell Biol* 176:749-55.
- DePamphilis, M.L., Blow, J.J., Ghosh, S., Saha, T., Noguchi, K. and Vassilev, A. (2006) Regulating the licensing of DNA replication origins in metazoa. *Curr Opin Cell Biol* 18:231-9.
- Diffley, J.F. and Labib, K. (2002) The chromosome replication cycle. *J Cell Sci* 115:869-72.
- Difilippantonio, S., Gapud, E., Wong, N., Huang, C.Y., Mahowald, G., Chen, H.T., Kruhlak, M.J., Callen, E., Livak, F., Nussenzweig, M.C., Sleckman, B.P. and Nussenzweig, A. (2008) 53BP1 facilitates long-range DNA end-joining during V(D)J recombination. *Nature* 456:529-33.
- Dimitrova, D.S., Todorov, I.T., Melendy, T. and Gilbert, D.M. (1999) Mcm2, but not RPA, is a component of the mammalian early G1-phase prereplication complex. *J Cell Biol* 146:709-22.
- DiTullio, R.A., Jr., Mochan, T.A., Venere, M., Bartkova, J., Sehested, M., Bartek, J. and Halazonetis, T.D. (2002) 53BP1 functions in an ATM-dependent checkpoint pathway that is constitutively activated in human cancer. *Nat Cell Biol* 4:998-1002.
- Doil, C., Mailand, N., Bekker-Jensen, S., Menard, P., Larsen, D.H., Pepperkok, R., Ellenberg, J., Panier, S., Durocher, D., Bartek, J., Lukas, J. and Lukas, C. (2009) RNF168 binds and amplifies ubiquitin conjugates on damaged chromosomes to allow accumulation of repair proteins. *Cell* 136:435-46.
- Doksani, Y., Bermejo, R., Fiorani, S., Haber, J.E. and Foiani, M. (2009) Replicon dynamics, dormant origin firing, and terminal fork integrity after double-strand break formation. *Cell* 137:247-58.
- Donaldson, A.D. and Blow, J.J. (2001) DNA replication: stable driving prevents fatal smashes. *Curr Biol* 11:R979-82.
- Donaldson, A.D., Fangman, W.L. and Brewer, B.J. (1998) Cdc7 is required throughout the yeast S phase to activate replication origins. *Genes Dev* 12:491-501.
- Downs, J.A. and Jackson, S.P. (2004) A means to a DNA end: the many roles of Ku. *Nat Rev Mol Cell Biol* 5:367-78.
- Downs, J.A., Lowndes, N.F. and Jackson, S.P. (2000) A role for *Saccharomyces cerevisiae* histone H2A in DNA repair. *Nature* 408:1001-4.
- Downs, J.A., Kosmidou, E., Morgan, A. and Jackson, S.P. (2003) Suppression of homologous recombination by the *Saccharomyces cerevisiae* linker histone. *Mol Cell* 11:1685-92.
- Drury, L.S., Perkins, G. and Diffley, J.F. (1997) The Cdc4/34/53 pathway targets Cdc6p for proteolysis in budding yeast. *Embo J* 16:5966-76.
- Drury, L.S., Perkins, G. and Diffley, J.F. (2000) The cyclin-dependent kinase Cdc28p regulates distinct modes of Cdc6p proteolysis during the budding yeast cell cycle. *Curr Biol* 10:231-40.
- Du, L.L., Nakamura, T.M. and Russell, P. (2006) Histone modification-dependent and -independent pathways for recruitment of checkpoint protein Crb2 to double-strand breaks. *Genes Dev* 20:1583-96.
- Du, Y.C. and Stillman, B. (2002) Yph1p, an ORC-interacting protein: potential links between cell proliferation control, DNA replication, and ribosome biogenesis. *Cell* 109:835-48.
- Durocher, D. and Jackson, S.P. (2001) DNA-PK, ATM and ATR as sensors of DNA damage: variations on a theme? *Curr Opin Cell Biol* 13:225-31.

- Durocher, D., Henckel, J., Fersht, A.R. and Jackson, S.P. (1999) The FHA domain is a modular phosphopeptide recognition motif. *Mol Cell* 4:387-94.
- El-Mahdy, M.A., Zhu, Q., Wang, Q.E., Wani, G., Praetorius-Ibba, M. and Wani, A.A. (2006) Cullin 4A-mediated proteolysis of DDB2 protein at DNA damage sites regulates in vivo lesion recognition by XPC. *J Biol Chem* 281:13404-11.
- Emili, A. (1998) MEC1-dependent phosphorylation of Rad9p in response to DNA damage. *Mol Cell* 2:183-9.
- Erenpreisa, J. and Cragg, M.S. (2001) Mitotic death: a mechanism of survival? A review. *Cancer Cell Int* 1:1.
- Esashi, F. and Yanagida, M. (1999) Cdc2 phosphorylation of Crb2 is required for reestablishing cell cycle progression after the damage checkpoint. *Mol Cell* 4:167-74.
- Espino, P.S., Li, L., He, S., Yu, J. and Davie, J.R. (2006) Chromatin modification of the trefoil factor 1 gene in human breast cancer cells by the Ras/mitogen-activated protein kinase pathway. *Cancer Res* 66:4610-6.
- Falck, J., Coates, J. and Jackson, S.P. (2005) Conserved modes of recruitment of ATM, ATR and DNA-PKcs to sites of DNA damage. *Nature* 434:605-11.
- Fasullo, M. and Sun, M. (2008) The *Saccharomyces cerevisiae* checkpoint genes RAD9, CHK1 and PDS1 are required for elevated homologous recombination in a mec1 (ATR) hypomorphic mutant. *Cell Cycle* 7:2418-26.
- Fernandez-Capetillo, O., Chen, H.T., Celeste, A., Ward, I., Romanienko, P.J., Morales, J.C., Naka, K., Xia, Z., Camerini-Otero, R.D., Motoyama, N., Carpenter, P.B., Bonner, W.M., Chen, J. and Nussenzweig, A. (2002) DNA damage-induced G2-M checkpoint activation by histone H2AX and 53BP1. *Nat Cell Biol* 4:993-7.
- FitzGerald, J.E., Grenon, M. and Lowndes, N.F. (2009) 53BP1: function and mechanisms of focal recruitment. *Biochem Soc Trans* 37:897-904.
- Foiani, M., Marini, F., Gamba, D., Lucchini, G. and Plevani, P. (1994) The B subunit of the DNA polymerase alpha-primase complex in *Saccharomyces cerevisiae* executes an essential function at the initial stage of DNA replication. *Mol Cell Biol* 14:923-33.
- Forand, A., Dutrillaux, B. and Bernardino-Sgherri, J. (2004) Gamma-H2AX expression pattern in non-irradiated neonatal mouse germ cells and after low-dose gamma-radiation: relationships between chromatid breaks and DNA double-strand breaks. *Biol Reprod* 71:643-9.
- Formosa, T. and Nittis, T. (1999) Dna2 mutants reveal interactions with Dna polymerase alpha and Ctf4, a Pol alpha accessory factor, and show that full Dna2 helicase activity is not essential for growth. *Genetics* 151:1459-70.
- Forsburg, S.L. and Nurse, P. (1991) Cell cycle regulation in the yeasts *Saccharomyces cerevisiae* and *Schizosaccharomyces pombe*. *Annu Rev Cell Biol* 7:227-56.
- Franchitto, A., Oshima, J. and Pichierri, P. (2003) The G2-phase decatenation checkpoint is defective in Werner syndrome cells. *Cancer Res* 63:3289-95.
- Freeman, A., Morris, L.S., Mills, A.D., Stoeber, K., Laskey, R.A., Williams, G.H. and Coleman, N. (1999) Minichromosome maintenance proteins as biological markers of dysplasia and malignancy. *Clin Cancer Res* 5:2121-32.
- Friedberg, E.C. (1996) Relationships between DNA repair and transcription. *Annu Rev Biochem* 65:15-42.
- Funk, J.O. (1999) Cancer cell cycle control. *Anticancer Res* 19:4772-80.
- Galanty, Y., Belotserkovskaya, R., Coates, J., Polo, S., Miller, K.M. and Jackson, S.P. (2009) Mammalian SUMO E3-ligases PIAS1 and PIAS4 promote responses to DNA double-strand breaks. *Nature* 462:935-9.

- Gambus, A., Jones, R.C., Sanchez-Diaz, A., Kanemaki, M., van Deursen, F., Edmondson, R.D. and Labib, K. (2006) GINS maintains association of Cdc45 with MCM in replisome progression complexes at eukaryotic DNA replication forks. *Nat Cell Biol* 8:358-66.
- Gambus, A., van Deursen, F., Polychronopoulos, D., Foltman, M., Jones, R.C., Edmondson, R.D., Calzada, A. and Labib, K. (2009) A key role for Ctf4 in coupling the MCM2-7 helicase to DNA polymerase alpha within the eukaryotic replisome. *Embo J* 28:2992-3004.
- Gao, W.Y., Johns, D.G., Choekuchai, S. and Mitsuya, H. (1995) Disparate actions of hydroxyurea in potentiation of purine and pyrimidine 2',3'-dideoxynucleoside activities against replication of human immunodeficiency virus. *Proc Natl Acad Sci U S A* 92:8333-7.
- Garg, P. and Burgers, P.M. (2005a) DNA polymerases that propagate the eukaryotic DNA replication fork. *Crit Rev Biochem Mol Biol* 40:115-28.
- Garg, P. and Burgers, P.M. (2005b) How the cell deals with DNA nicks. *Cell Cycle* 4:221-4.
- Gaspar-Maia, A., Alajem, A., Polesso, F., Sridharan, R., Mason, M.J., Heidersbach, A., Ramalho-Santos, J., McManus, M.T., Plath, K., Meshorer, E. and Ramalho-Santos, M. (2009) Chd1 regulates open chromatin and pluripotency of embryonic stem cells. *Nature* 460:863-8.
- Gelbart, M.E., Rechsteiner, T., Richmond, T.J. and Tsukiyama, T. (2001) Interactions of Isw2 chromatin remodeling complex with nucleosomal arrays: analyses using recombinant yeast histones and immobilized templates. *Mol Cell Biol* 21:2098-106.
- Ghaemmaghami, S., Huh, W.K., Bower, K., Howson, R.W., Belle, A., Dephoure, N., O'Shea, E.K. and Weissman, J.S. (2003) Global analysis of protein expression in yeast. *Nature* 425:737-41.
- Gilbert, C.S., Green, C.M. and Lowndes, N.F. (2001) Budding yeast Rad9 is an ATP-dependent Rad53 activating machine. *Mol Cell* 8:129-36.
- Giunta, S., Belotserkovskaya, R. and Jackson, S.P. (2010) DNA damage signaling in response to double-strand breaks during mitosis. *J Cell Biol* 190:197-207.
- Goldberg, M., Stucki, M., Falck, J., D'Amours, D., Rahman, D., Pappin, D., Bartek, J. and Jackson, S.P. (2003) MDC1 is required for the intra-S-phase DNA damage checkpoint. *Nature* 421:952-6.
- Gonzalez, M.A., Tachibana, K.E., Laskey, R.A. and Coleman, N. (2005) Control of DNA replication and its potential clinical exploitation. *Nat Rev Cancer* 5:135-41.
- Goodarzi, A.A., Noon, A.T. and Jeggo, P.A. (2009) The impact of heterochromatin on DSB repair. *Biochem Soc Trans* 37:569-76.
- Goodarzi, A.A., Noon, A.T., Deckbar, D., Ziv, Y., Shiloh, Y., Lobrich, M. and Jeggo, P.A. (2008) ATM signaling facilitates repair of DNA double-strand breaks associated with heterochromatin. *Mol Cell* 31:167-77.
- Grenon, M., Costelloe, T., Jimeno, S., O'Shaughnessy, A., Fitzgerald, J., Zgheib, O., Degerth, L. and Lowndes, N.F. (2007) Docking onto chromatin via the *Saccharomyces cerevisiae* Rad9 Tudor domain. *Yeast* 24:105-19.
- Groisman, R., Polanowska, J., Kuraoka, I., Sawada, J., Saijo, M., Drapkin, R., Kisselev, A.F., Tanaka, K. and Nakatani, Y. (2003) The ubiquitin ligase activity in the DDB2 and CSA complexes is differentially regulated by the COP9 signalosome in response to DNA damage. *Cell* 113:357-67.
- Guerrero, A.A., Gamero, M.C., Trachana, V., Futterer, A., Pacios-Bras, C., Diaz-Concha, N.P., Cigudosa, J.C., Martinez, A.C. and van Wely, K.H. (2009) Centromere-

- localized breaks indicate the generation of DNA damage by the mitotic spindle. *Proc Natl Acad Sci U S A* 107:4159-64.
- Halazonetis, T.D., Gorgoulis, V.G. and Bartek, J. (2008) An oncogene-induced DNA damage model for cancer development. *Science* 319:1352-5.
- Hammet, A., Magill, C., Heierhorst, J. and Jackson, S.P. (2007) Rad9 BRCT domain interaction with phosphorylated H2AX regulates the G1 checkpoint in budding yeast. *EMBO Rep* 8:851-7.
- Han, Y., Ueno, M., Nagahama, Y. and Takakura, N. (2009) Identification and characterization of stem cell-specific transcription of PSF1 in spermatogenesis. *Biochem Biophys Res Commun* 380:609-13.
- Hanna, J.S., Kroll, E.S., Lundblad, V. and Spencer, F.A. (2001) *Saccharomyces cerevisiae* CTF18 and CTF4 are required for sister chromatid cohesion. *Mol Cell Biol* 21:3144-58.
- Hartwell, L.H. and Weinert, T.A. (1989) Checkpoints: controls that ensure the order of cell cycle events. *Science* 246:629-34.
- Hayashi, N. and Murakami, S. (2002) STM1, a gene which encodes a guanine quadruplex binding protein, interacts with CDC13 in *Saccharomyces cerevisiae*. *Mol Genet Genomics* 267:806-13.
- Hayashi, R., Arauchi, T., Tategu, M., Goto, Y. and Yoshida, K. (2006) A combined computational and experimental study on the structure-regulation relationships of putative mammalian DNA replication initiator GINS. *Genomics Proteomics Bioinformatics* 4:156-64.
- Hickson, I., Zhao, Y., Richardson, C.J., Green, S.J., Martin, N.M., Orr, A.I., Reaper, P.M., Jackson, S.P., Curtin, N.J. and Smith, G.C. (2004) Identification and characterization of a novel and specific inhibitor of the ataxia-telangiectasia mutated kinase ATM. *Cancer Res* 64:9152-9.
- Higa, L.A., Mihaylov, I.S., Banks, D.P., Zheng, J. and Zhang, H. (2003) Radiation-mediated proteolysis of CDT1 by CUL4-ROC1 and CSN complexes constitutes a new checkpoint. *Nat Cell Biol* 5:1008-15.
- Holm, C., Stearns, T. and Botstein, D. (1989) DNA topoisomerase II must act at mitosis to prevent nondisjunction and chromosome breakage. *Mol Cell Biol* 9:159-68.
- Houchens, C.R., Perreault, A., Bachand, F. and Kelly, T.J. (2008) *Schizosaccharomyces pombe* Noc3 is essential for ribosome biogenesis and cell division but not DNA replication. *Eukaryot Cell* 7:1433-40.
- Hsu, L.C. and White, R.L. (1998) BRCA1 is associated with the centrosome during mitosis. *Proc Natl Acad Sci U S A* 95:12983-8.
- Hu, J., McCall, C.M., Ohta, T. and Xiong, Y. (2004) Targeted ubiquitination of CDT1 by the DDB1-CUL4A-ROC1 ligase in response to DNA damage. *Nat Cell Biol* 6:1003-9.
- Huang, H.K., Bailis, J.M., Levenson, J.D., Gomez, E.B., Forsburg, S.L. and Hunter, T. (2005a) Suppressors of Bir1p (Survivin) identify roles for the chromosomal passenger protein Pic1p (INCENP) and the replication initiation factor Psf2p in chromosome segregation. *Mol Cell Biol* 25:9000-15.
- Huang, X., Halicka, H.D., Traganos, F., Tanaka, T., Kurose, A. and Darzynkiewicz, Z. (2005b) Cytometric assessment of DNA damage in relation to cell cycle phase and apoptosis. *Cell Prolif* 38:223-43.
- Hubscher, U., Maga, G. and Spadari, S. (2002) Eukaryotic DNA polymerases. *Annu Rev Biochem* 71:133-63.

- Huen, M.S., Grant, R., Manke, I., Minn, K., Yu, X., Yaffe, M.B. and Chen, J. (2007) RNF8 transduces the DNA-damage signal via histone ubiquitylation and checkpoint protein assembly. *Cell* 131:901-14.
- Huertas, P., Cortes-Ledesma, F., Sartori, A.A., Aguilera, A. and Jackson, S.P. (2008) CDK targets Sae2 to control DNA-end resection and homologous recombination. *Nature* 455:689-92.
- Huyen, Y., Zgheib, O., Ditullio, R.A., Jr., Gorgoulis, V.G., Zacharatos, P., Petty, T.J., Sheston, E.A., Mellert, H.S., Stavridi, E.S. and Halazonetis, T.D. (2004) Methylated lysine 79 of histone H3 targets 53BP1 to DNA double-strand breaks. *Nature* 432:406-11.
- Iacovoni, J.S., Caron, P., Lassadi, I., Nicolas, E., Massip, L., Trouche, D. and Legube, G. (2010) High-resolution profiling of gammaH2AX around DNA double strand breaks in the mammalian genome. *Embo J* 29:1446-57.
- Ichijima, Y., Sakasai, R., Okita, N., Asahina, K., Mizutani, S. and Teraoka, H. (2005) Phosphorylation of histone H2AX at M phase in human cells without DNA damage response. *Biochem Biophys Res Commun* 336:807-12.
- Im, J.S., Ki, S.H., Farina, A., Jung, D.S., Hurwitz, J. and Lee, J.K. (2009) Assembly of the Cdc45-Mcm2-7-GINS complex in human cells requires the Ctf4/And-1, RecQL4, and Mcm10 proteins. *Proc Natl Acad Sci U S A* 106:15628-32.
- Ishida, Y., Furukawa, Y., Decaprio, J.A., Saito, M. and Griffin, J.D. (1992) Treatment of myeloid leukemic cells with the phosphatase inhibitor okadaic acid induces cell cycle arrest at either G1/S or G2/M depending on dose. *J Cell Physiol* 150:484-92.
- Ishimi, Y. (1997) A DNA helicase activity is associated with an MCM4, -6, and -7 protein complex. *J Biol Chem* 272:24508-13.
- Ito, H., Fukuda, Y., Murata, K. and Kimura, A. (1983) Transformation of intact yeast cells treated with alkali cations. *J Bacteriol* 153:163-8.
- Ito, K., Adachi, S., Iwakami, R., Yasuda, H., Muto, Y., Seki, N. and Okano, Y. (2001) N-Terminally extended human ubiquitin-conjugating enzymes (E2s) mediate the ubiquitination of RING-finger proteins, ARA54 and RNF8. *Eur J Biochem* 268:2725-32.
- Izzard, R.A., Jackson, S.P. and Smith, G.C. (1999) Competitive and noncompetitive inhibition of the DNA-dependent protein kinase. *Cancer Res* 59:2581-6.
- Jackson, A.P., Eastwood, H., Bell, S.M., Adu, J., Toomes, C., Carr, I.M., Roberts, E., Hampshire, D.J., Crow, Y.J., Mighell, A.J., Karbani, G., Jafri, H., Rashid, Y., Mueller, R.F., Markham, A.F. and Woods, C.G. (2002) Identification of microcephalin, a protein implicated in determining the size of the human brain. *Am J Hum Genet* 71:136-42.
- Jackson, S.P. and Bartek, J. (2009) The DNA-damage response in human biology and disease. *Nature* 461:1071-8.
- Jazayeri, A., Balestrini, A., Garner, E., Haber, J.E. and Costanzo, V. (2008) Mre11-Rad50-Nbs1-dependent processing of DNA breaks generates oligonucleotides that stimulate ATM activity. *Embo J* 27:1953-62.
- Jeffers, L.J., Coull, B.J., Stack, S.J. and Morrison, C.G. (2008) Distinct BRCT domains in Mcph1/Brit1 mediate ionizing radiation-induced focus formation and centrosomal localization. *Oncogene* 27:139-44.
- Jenuwein, T. and Allis, C.D. (2001) Translating the histone code. *Science* 293:1074-80.
- Jiang, W. and Hunter, T. (1997) Identification and characterization of a human protein kinase related to budding yeast Cdc7p. *Proc Natl Acad Sci U S A* 94:14320-5.
- Jonsson, Z.O. and Hubscher, U. (1997) Proliferating cell nuclear antigen: more than a clamp for DNA polymerases. *Bioessays* 19:967-75.

- Joo, H.Y., Zhai, L., Yang, C., Nie, S., Erdjument-Bromage, H., Tempst, P., Chang, C. and Wang, H. (2007) Regulation of cell cycle progression and gene expression by H2A deubiquitination. *Nature* 449:1068-72.
- Juan, G. and Darzynkiewicz, Z. (2004) Detection of mitotic cells. *Curr Protoc Cytom* Chapter 7:Unit 7 24.
- Jullien, D., Vagnarelli, P., Earnshaw, W.C. and Adachi, Y. (2002) Kinetochore localisation of the DNA damage response component 53BP1 during mitosis. *J Cell Sci* 115:71-9.
- Kai, M. and Wang, T.S. (2003) Checkpoint activation regulates mutagenic translesion synthesis. *Genes Dev* 17:64-76.
- Kamada, K., Kubota, Y., Arata, T., Shindo, Y. and Hanaoka, F. (2007) Structure of the human GINS complex and its assembly and functional interface in replication initiation. *Nat Struct Mol Biol* 14:388-96.
- Kamimura, Y., Masumoto, H., Sugino, A. and Araki, H. (1998) Sld2, which interacts with Dpb11 in *Saccharomyces cerevisiae*, is required for chromosomal DNA replication. *Mol Cell Biol* 18:6102-9.
- Kamimura, Y., Tak, Y.S., Sugino, A. and Araki, H. (2001) Sld3, which interacts with Cdc45 (Sld4), functions for chromosomal DNA replication in *Saccharomyces cerevisiae*. *Embo J* 20:2097-107.
- Kanda, R., Eguchi-Kasai, K. and Hayata, I. (1999) Phosphatase inhibitors and premature chromosome condensation in human peripheral lymphocytes at different cell-cycle phases. *Somat Cell Mol Genet* 25:1-8.
- Kanemaki, M. and Labib, K. (2006) Distinct roles for Sld3 and GINS during establishment and progression of eukaryotic DNA replication forks. *Embo J* 25:1753-63.
- Karumbati, A.S. and Wilson, T.E. (2005) Abrogation of the Chk1-Pds1 checkpoint leads to tolerance of persistent single-strand breaks in *Saccharomyces cerevisiae*. *Genetics* 169:1833-44.
- Kato, T.A., Okayasu, R. and Bedford, J.S. (2008) Comparison of the induction and disappearance of DNA double strand breaks and gamma-H2AX foci after irradiation of chromosomes in G1-phase or in condensed metaphase cells. *Mutat Res* 639:108-12.
- Kato, T.A., Okayasu, R. and Bedford, J.S. (2009) Signatures of DNA double strand breaks produced in irradiated G1 and G2 cells persist into mitosis. *J Cell Physiol* 219:760-5.
- Kearsey, S.E. and Labib, K. (1998) MCM proteins: evolution, properties, and role in DNA replication. *Biochim Biophys Acta* 1398:113-36.
- Kelman, Z., Lee, J.K. and Hurwitz, J. (1999) The single minichromosome maintenance protein of *Methanobacterium thermoautotrophicum* DeltaH contains DNA helicase activity. *Proc Natl Acad Sci U S A* 96:14783-8.
- Khanna, K.K. and Jackson, S.P. (2001) DNA double-strand breaks: signaling, repair and the cancer connection. *Nat Genet* 27:247-54.
- Khanna, K.K., Lavin, M.F., Jackson, S.P. and Mulhern, T.D. (2001) ATM, a central controller of cellular responses to DNA damage. *Cell Death Differ* 8:1052-65.
- Khorasanizadeh, S. (2004) The nucleosome: from genomic organization to genomic regulation. *Cell* 116:259-72.
- Kim, E.M. and Burke, D.J. (2008) DNA damage activates the SAC in an ATM/ATR-dependent manner, independently of the kinetochore. *PLoS Genet* 4:e1000015.
- Kogoma, T. (1997) Stable DNA replication: interplay between DNA replication, homologous recombination, and transcription. *Microbiol Mol Biol Rev* 61:212-38.

- Kolas, N.K., Chapman, J.R., Nakada, S., Ylanko, J., Chahwan, R., Sweeney, F.D., Panier, S., Mendez, M., Wildenhain, J., Thomson, T.M., Pelletier, L., Jackson, S.P. and Durocher, D. (2007) Orchestration of the DNA-damage response by the RNF8 ubiquitin ligase. *Science* 318:1637-40.
- Kornberg, R.D. (1974) Chromatin structure: a repeating unit of histones and DNA. *Science* 184:868-71.
- Kouzarides, T. (2007) Chromatin modifications and their function. *Cell* 128:693-705.
- Krakoff, I.H., Brown, N.C. and Reichard, P. (1968) Inhibition of ribonucleoside diphosphate reductase by hydroxyurea. *Cancer Res* 28:1559-65.
- Kramer, A., Mailand, N., Lukas, C., Syljuasen, R.G., Wilkinson, C.J., Nigg, E.A., Bartek, J. and Lukas, J. (2004) Centrosome-associated Chk1 prevents premature activation of cyclin-B-Cdk1 kinase. *Nat Cell Biol* 6:884-91.
- Kramer, E.R., Scheuringer, N., Podtelejnikov, A.V., Mann, M. and Peters, J.M. (2000) Mitotic regulation of the APC activator proteins CDC20 and CDH1. *Mol Biol Cell* 11:1555-69.
- Krogan, N.J., Cagney, G., Yu, H., Zhong, G., Guo, X., Ignatchenko, A., Li, J., Pu, S., Datta, N., Tikuisis, A.P., Punna, T., Peregrin-Alvarez, J.M., Shales, M., Zhang, X., Davey, M., Robinson, M.D., Paccanaro, A., Bray, J.E., Sheung, A., Beattie, B., Richards, D.P., Canadien, V., Lalev, A., Mena, F., Wong, P., Starostine, A., Canete, M.M., Vlasblom, J., Wu, S., Orsi, C., Collins, S.R., Chandran, S., Haw, R., Rilstone, J.J., Gandi, K., Thompson, N.J., Musso, G., St Onge, P., Ghanny, S., Lam, M.H., Butland, G., Altaf-Ul, A.M., Kanaya, S., Shilatifard, A., O'Shea, E., Weissman, J.S., Ingles, C.J., Hughes, T.R., Parkinson, J., Gerstein, M., Wodak, S.J., Emili, A. and Greenblatt, J.F. (2006) Global landscape of protein complexes in the yeast *Saccharomyces cerevisiae*. *Nature* 440:637-43.
- Krude, T., Musahl, C., Laskey, R.A. and Knippers, R. (1996) Human replication proteins hCdc21, hCdc46 and P1Mcm3 bind chromatin uniformly before S-phase and are displaced locally during DNA replication. *J Cell Sci* 109 ( Pt 2):309-18.
- Krude, T., Jackman, M., Pines, J. and Laskey, R.A. (1997) Cyclin/Cdk-dependent initiation of DNA replication in a human cell-free system. *Cell* 88:109-19.
- Kubota, Y., Takase, Y., Komori, Y., Hashimoto, Y., Arata, T., Kamimura, Y., Araki, H. and Takisawa, H. (2003) A novel ring-like complex of *Xenopus* proteins essential for the initiation of DNA replication. *Genes Dev* 17:1141-52.
- Labib, K. and Hodgson, B. (2007) Replication fork barriers: pausing for a break or stalling for time? *EMBO Rep* 8:346-53.
- Labib, K., Diffley, J.F. and Kearsley, S.E. (1999) G1-phase and B-type cyclins exclude the DNA-replication factor Mcm4 from the nucleus. *Nat Cell Biol* 1:415-22.
- Lancelot, N., Charier, G., Couprie, J., Duband-Goulet, I., Alpha-Bazin, B., Quemeneur, E., Ma, E., Marsolier-Kergoat, M.C., Ropars, V., Charbonnier, J.B., Miron, S., Craescu, C.T., Callebaut, I., Gilquin, B. and Zinn-Justin, S. (2007) The checkpoint *Saccharomyces cerevisiae* Rad9 protein contains a tandem tudor domain that recognizes DNA. *Nucleic Acids Res* 35:5898-912.
- Laskey, R.A. and Madine, M.A. (2003) A rotary pumping model for helicase function of MCM proteins at a distance from replication forks. *EMBO Rep* 4:26-30.
- Lau, E., Tsuji, T., Guo, L., Lu, S.H. and Jiang, W. (2007) The role of pre-replicative complex (pre-RC) components in oncogenesis. *Faseb J* 21:3786-94.
- Leahy, J.J., Golding, B.T., Griffin, R.J., Hardcastle, I.R., Richardson, C., Rigoreau, L. and Smith, G.C. (2004) Identification of a highly potent and selective DNA-dependent protein kinase (DNA-PK) inhibitor (NU7441) by screening of chromenone libraries. *Bioorg Med Chem Lett* 14:6083-7.

- Lee, J.H. and Paull, T.T. (2005) ATM activation by DNA double-strand breaks through the Mre11-Rad50-Nbs1 complex. *Science* 308:551-4.
- Lee, J.K. and Hurwitz, J. (2000) Isolation and characterization of various complexes of the minichromosome maintenance proteins of *Schizosaccharomyces pombe*. *J Biol Chem* 275:18871-8.
- Lei, M., Kawasaki, Y., Young, M.R., Kihara, M., Sugino, A. and Tye, B.K. (1997) Mcm2 is a target of regulation by Cdc7-Dbf4 during the initiation of DNA synthesis. *Genes Dev* 11:3365-74.
- Lew, D.J. and Kornbluth, S. (1996) Regulatory roles of cyclin dependent kinase phosphorylation in cell cycle control. *Curr Opin Cell Biol* 8:795-804.
- Liberi, G., Maffioletti, G., Lucca, C., Chiolo, I., Baryshnikova, A., Cotta-Ramusino, C., Lopes, M., Pellicoli, A., Haber, J.E. and Foiani, M. (2005) Rad51-dependent DNA structures accumulate at damaged replication forks in *sgs1* mutants defective in the yeast ortholog of BLM RecQ helicase. *Genes Dev* 19:339-50.
- Lin, S.Y., Rai, R., Li, K., Xu, Z.X. and Elledge, S.J. (2005) BRIT1/MCPH1 is a DNA damage responsive protein that regulates the Brca1-Chk1 pathway, implicating checkpoint dysfunction in microcephaly. *Proc Natl Acad Sci U S A* 102:15105-9.
- Liu, F., Stanton, J.J., Wu, Z. and Piwnicka-Worms, H. (1997) The human Myt1 kinase preferentially phosphorylates Cdc2 on threonine 14 and localizes to the endoplasmic reticulum and Golgi complex. *Mol Cell Biol* 17:571-83.
- Lober, G. and Kittler, L. (1977) Selected topics in photochemistry of nucleic acids. Recent results and perspectives. *Photochem Photobiol* 25:215-33.
- Lopes, M., Foiani, M. and Sogo, J.M. (2006) Multiple mechanisms control chromosome integrity after replication fork uncoupling and restart at irreparable UV lesions. *Mol Cell* 21:15-27.
- MacNeill, S.A. (2010) Structure and function of the GINS complex, a key component of the eukaryotic replisome. *Biochem J* 425:489-500.
- Madine, M.A., Khoo, C.Y., Mills, A.D., Musahl, C. and Laskey, R.A. (1995) The nuclear envelope prevents reinitiation of replication by regulating the binding of MCM3 to chromatin in *Xenopus* egg extracts. *Curr Biol* 5:1270-9.
- Madine, M.A., Swietlik, M., Pelizon, C., Romanowski, P., Mills, A.D. and Laskey, R.A. (2000) The roles of the MCM, ORC, and Cdc6 proteins in determining the replication competence of chromatin in quiescent cells. *J Struct Biol* 129:198-210.
- Mailand, N., Bekker-Jensen, S., Fastrup, H., Melander, F., Bartek, J., Lukas, C. and Lukas, J. (2007) RNF8 ubiquitylates histones at DNA double-strand breaks and promotes assembly of repair proteins. *Cell* 131:887-900.
- Maiorano, D., Moreau, J. and Mechali, M. (2000) XCDT1 is required for the assembly of pre-replicative complexes in *Xenopus laevis*. *Nature* 404:622-5.
- Makarova, K.S., Wolf, Y.I., Mekhedov, S.L., Mirkin, B.G. and Koonin, E.V. (2005) Ancestral paralogs and pseudoparalogs and their role in the emergence of the eukaryotic cell. *Nucleic Acids Res* 33:4626-38.
- Manis, J.P., Morales, J.C., Xia, Z., Kutok, J.L., Alt, F.W. and Carpenter, P.B. (2004) 53BP1 links DNA damage-response pathways to immunoglobulin heavy chain class-switch recombination. *Nat Immunol* 5:481-7.
- Manke, I.A., Lowery, D.M., Nguyen, A. and Yaffe, M.B. (2003) BRCT repeats as phosphopeptide-binding modules involved in protein targeting. *Science* 302:636-9.
- Marinsek, N., Barry, E.R., Makarova, K.S., Dionne, I., Koonin, E.V. and Bell, S.D. (2006) GINS, a central nexus in the archaeal DNA replication fork. *EMBO Rep* 7:539-45.

- Masumoto, H., Muramatsu, S., Kamimura, Y. and Araki, H. (2002) S-Cdk-dependent phosphorylation of Sld2 essential for chromosomal DNA replication in budding yeast. *Nature* 415:651-5.
- Matsui, S.I., Seon, B.K. and Sandberg, A.A. (1979) Disappearance of a structural chromatin protein A24 in mitosis: implications for molecular basis of chromatin condensation. *Proc Natl Acad Sci U S A* 76:6386-90.
- Matsuoka, S., Ballif, B.A., Smogorzewska, A., McDonald, E.R., 3rd, Hurov, K.E., Luo, J., Bakalarski, C.E., Zhao, Z., Solimini, N., Lerenthal, Y., Shiloh, Y., Gygi, S.P. and Elledge, S.J. (2007) ATM and ATR substrate analysis reveals extensive protein networks responsive to DNA damage. *Science* 316:1160-6.
- Matsusaka, T. and Pines, J. (2004) Chfr acts with the p38 stress kinases to block entry to mitosis in mammalian cells. *J Cell Biol* 166:507-16.
- Maynard, S., Swistowska, A.M., Lee, J.W., Liu, Y., Liu, S.T., Da Cruz, A.B., Rao, M., de Souza-Pinto, N.C., Zeng, X. and Bohr, V.A. (2008) Human embryonic stem cells have enhanced repair of multiple forms of DNA damage. *Stem Cells* 26:2266-74.
- Mazia, D. (1961) How cells divide. *Sci Am* 205:100-20.
- Mazia, D. (1987) The chromosome cycle and the centrosome cycle in the mitotic cycle. *Int Rev Cytol* 100:49-92.
- McManus, K.J. and Hendzel, M.J. (2005) ATM-dependent DNA damage-independent mitotic phosphorylation of H2AX in normally growing mammalian cells. *Mol Biol Cell* 16:5013-25.
- Mikhailov, A., Cole, R.W. and Rieder, C.L. (2002) DNA damage during mitosis in human cells delays the metaphase/anaphase transition via the spindle-assembly checkpoint. *Curr Biol* 12:1797-806.
- Mirzoeva, O.K. and Petrini, J.H. (2001) DNA damage-dependent nuclear dynamics of the Mre11 complex. *Mol Cell Biol* 21:281-8.
- Mizukoshi, T., Kodama, T.S., Fujiwara, Y., Furuno, T., Nakanishi, M. and Iwai, S. (2001) Structural study of DNA duplexes containing the (6-4) photoproduct by fluorescence resonance energy transfer. *Nucleic Acids Res* 29:4948-54.
- Moore, C.W. (1988) Internucleosomal cleavage and chromosomal degradation by bleomycin and phleomycin in yeast. *Cancer Res* 48:6837-43.
- Morris, J.R., Boutell, C., Keppler, M., Densham, R., Weekes, D., Alamshah, A., Butler, L., Galanty, Y., Pagon, L., Kiuchi, T., Ng, T. and Solomon, E. (2009) The SUMO modification pathway is involved in the BRCA1 response to genotoxic stress. *Nature* 462:886-90.
- Moyer, S.E., Lewis, P.W. and Botchan, M.R. (2006) Isolation of the Cdc45/Mcm2-7/GINS (CMG) complex, a candidate for the eukaryotic DNA replication fork helicase. *Proc Natl Acad Sci U S A* 103:10236-41.
- Murga, M., Jaco, I., Fan, Y., Soria, R., Martinez-Pastor, B., Cuadrado, M., Yang, S.M., Blasco, M.A., Skoultchi, A.I. and Fernandez-Capetillo, O. (2007) Global chromatin compaction limits the strength of the DNA damage response. *J Cell Biol* 178:1101-8.
- Musahl, C., Holthoff, H.P., Lesch, R. and Knippers, R. (1998) Stability of the replicative Mcm3 protein in proliferating and differentiating human cells. *Exp Cell Res* 241:260-4.
- Nadal, M. (2007) Reverse gyrase: an insight into the role of DNA-topoisomerases. *Biochimie* 89:447-55.
- Nag, A., Bondar, T., Shiv, S. and Raychaudhuri, P. (2001) The xeroderma pigmentosum group E gene product DDB2 is a specific target of cullin 4A in mammalian cells. *Mol Cell Biol* 21:6738-47.

- Nagahama, Y., Ueno, M., Haraguchi, N., Mori, M. and Takakura, N. (2010) PSF3 marks malignant colon cancer and has a role in cancer cell proliferation. *Biochem Biophys Res Commun* 392:150-4.
- Nakamura, A., Sedelnikova, O.A., Redon, C., Pilch, D.R., Sinogeeva, N.I., Shroff, R., Lichten, M. and Bonner, W.M. (2006) Techniques for gamma-H2AX detection. *Methods Enzymol* 409:236-50.
- Nasheuer, H.P., Smith, R., Bauerschmidt, C., Grosse, F. and Weisshart, K. (2002) Initiation of eukaryotic DNA replication: regulation and mechanisms. *Prog Nucleic Acid Res Mol Biol* 72:41-94.
- Nasmyth, K. (1993) Control of the yeast cell cycle by the Cdc28 protein kinase. *Curr Opin Cell Biol* 5:166-79.
- Natale, D.A., Li, C.J., Sun, W.H. and DePamphilis, M.L. (2000) Selective instability of Orc1 protein accounts for the absence of functional origin recognition complexes during the M-G(1) transition in mammals. *Embo J* 19:2728-38.
- Nelson, G., Buhmann, M. and von Zglinicki, T. (2009) DNA damage foci in mitosis are devoid of 53BP1. *Cell Cycle* 8:3379-83.
- Nelson, L.D., Musso, M. and Van Dyke, M.W. (2000) The yeast STM1 gene encodes a purine motif triple helical DNA-binding protein. *J Biol Chem* 275:5573-81.
- Nguyen, V.Q., Co, C. and Li, J.J. (2001) Cyclin-dependent kinases prevent DNA re-replication through multiple mechanisms. *Nature* 411:1068-73.
- Nguyen, V.Q., Co, C., Irie, K. and Li, J.J. (2000) Clb/Cdc28 kinases promote nuclear export of the replication initiator proteins Mcm2-7. *Curr Biol* 10:195-205.
- Niedzwiedz, W., Mosedale, G., Johnson, M., Ong, C.Y., Pace, P. and Patel, K.J. (2004) The Fanconi anaemia gene FANCC promotes homologous recombination and error-prone DNA repair. *Mol Cell* 15:607-20.
- Nishitani, H. and Nurse, P. (1995) p53cdc18 plays a major role controlling the initiation of DNA replication in fission yeast. *Cell* 83:397-405.
- Nishitani, H., Lygerou, Z., Nishimoto, T. and Nurse, P. (2000) The Cdt1 protein is required to license DNA for replication in fission yeast. *Nature* 404:625-8.
- Norbury, C. and Nurse, P. (1992) Animal cell cycles and their control. *Annu Rev Biochem* 61:441-70.
- Nurse, P. (1990) Universal control mechanism regulating onset of M-phase. *Nature* 344:503-8.
- Obama, K., Ura, K., Li, M., Katagiri, T., Tsunoda, T., Nomura, A., Satoh, S., Nakamura, Y. and Furukawa, Y. (2005) Genome-wide analysis of gene expression in human intrahepatic cholangiocarcinoma. *Hepatology* 41:1339-48.
- Okada, S. and Ouchi, T. (2003) Cell cycle differences in DNA damage-induced BRCA1 phosphorylation affect its subcellular localization. *J Biol Chem* 278:2015-20.
- Olavarrieta, L., Hernandez, P., Krimer, D.B. and Schvartzman, J.B. (2002) DNA knotting caused by head-on collision of transcription and replication. *J Mol Biol* 322:1-6.
- Oricchio, E., Saladino, C., Iacovelli, S., Soddu, S. and Cundari, E. (2006) ATM is activated by default in mitosis, localizes at centrosomes and monitors mitotic spindle integrity. *Cell Cycle* 5:88-92.
- Pacek, M., Tutter, A.V., Kubota, Y., Takisawa, H. and Walter, J.C. (2006) Localization of MCM2-7, Cdc45, and GINS to the site of DNA unwinding during eukaryotic DNA replication. *Mol Cell* 21:581-7.
- Pai, C.C., Garcia, I., Wang, S.W., Cotterill, S., Macneill, S.A. and Kearsey, S.E. (2009) GINS inactivation phenotypes reveal two pathways for chromatin association of replicative alpha and epsilon DNA polymerases in fission yeast. *Mol Biol Cell* 20:1213-22.

- Pardo, B., Gomez-Gonzalez, B. and Aguilera, A. (2009) DNA repair in mammalian cells: DNA double-strand break repair: how to fix a broken relationship. *Cell Mol Life Sci* 66:1039-56.
- Parker, L.L. and Piwnica-Worms, H. (1992) Inactivation of the p34cdc2-cyclin B complex by the human WEE1 tyrosine kinase. *Science* 257:1955-7.
- Patel, S.S. and Picha, K.M. (2000) Structure and function of hexameric helicases. *Annu Rev Biochem* 69:651-97.
- Paull, T.T. and Gellert, M. (1998) The 3' to 5' exonuclease activity of Mre 11 facilitates repair of DNA double-strand breaks. *Mol Cell* 1:969-79.
- Paull, T.T., Rogakou, E.P., Yamazaki, V., Kirchgessner, C.U., Gellert, M. and Bonner, W.M. (2000) A critical role for histone H2AX in recruitment of repair factors to nuclear foci after DNA damage. *Curr Biol* 10:886-95.
- Paulovich, A.G. and Hartwell, L.H. (1995) A checkpoint regulates the rate of progression through S phase in *S. cerevisiae* in response to DNA damage. *Cell* 82:841-7.
- Paulovich, A.G., Margulies, R.U., Garvik, B.M. and Hartwell, L.H. (1997) RAD9, RAD17, and RAD24 are required for S phase regulation in *Saccharomyces cerevisiae* in response to DNA damage. *Genetics* 145:45-62.
- Peddibhotla, S., Lam, M.H., Gonzalez-Rimbau, M. and Rosen, J.M. (2009) The DNA-damage effector checkpoint kinase 1 is essential for chromosome segregation and cytokinesis. *Proc Natl Acad Sci U S A* 106:5159-64.
- Pellicioli, A. and Foiani, M. (2005) Signal transduction: how rad53 kinase is activated. *Curr Biol* 15:R769-71.
- Perry, J. and Kleckner, N. (2003) The ATRs, ATMs, and TORs are giant HEAT repeat proteins. *Cell* 112:151-5.
- Perry, J.A. and Kornbluth, S. (2007) Cdc25 and Wee1: analogous opposites? *Cell Div* 2:12.
- Peters, J.M. (2006) The anaphase promoting complex/cyclosome: a machine designed to destroy. *Nat Rev Mol Cell Biol* 7:644-56.
- Pines, J. and Rieder, C.L. (2001) Re-staging mitosis: a contemporary view of mitotic progression. *Nat Cell Biol* 3:E3-6.
- Plans, V., Guerra-Rebollo, M. and Thomson, T.M. (2008) Regulation of mitotic exit by the RNF8 ubiquitin ligase. *Oncogene* 27:1355-65.
- Plans, V., Scheper, J., Soler, M., Loukili, N., Okano, Y. and Thomson, T.M. (2006) The RING finger protein RNF8 recruits UBC13 for lysine 63-based self polyubiquitylation. *J Cell Biochem* 97:572-82.
- Pomerantz, R.T. and O'Donnell, M. (2008) The replisome uses mRNA as a primer after colliding with RNA polymerase. *Nature* 456:762-6.
- Poon, R.Y. (2007) Mitotic phosphorylation: breaking the balance of power by a tactical retreat. *Biochem J* 403:e5-7.
- Povirk, L.F. (1996) DNA damage and mutagenesis by radiomimetic DNA-cleaving agents: bleomycin, neocarzinostatin and other enediynes. *Mutat Res* 355:71-89.
- Pruitt, S.C., Bailey, K.J. and Freeland, A. (2007) Reduced Mcm2 expression results in severe stem/progenitor cell deficiency and cancer. *Stem Cells* 25:3121-32.
- Pursell, Z.F., Isoz, I., Lundstrom, E.B., Johansson, E. and Kunkel, T.A. (2007) Yeast DNA polymerase epsilon participates in leading-strand DNA replication. *Science* 317:127-30.
- Rai, R., Dai, H., Multani, A.S., Li, K., Chin, K., Gray, J., Lahad, J.P., Liang, J., Mills, G.B., Meric-Bernstam, F. and Lin, S.Y. (2006) BRIT1 regulates early DNA damage response, chromosomal integrity, and cancer. *Cancer Cell* 10:145-57.

- Rappold, I., Iwabuchi, K., Date, T. and Chen, J. (2001) Tumor suppressor p53 binding protein 1 (53BP1) is involved in DNA damage-signaling pathways. *J Cell Biol* 153:613-20.
- Reini, K., Uitto, L., Perera, D., Moens, P.B., Freire, R. and Syvaaja, J.E. (2004) TopBP1 localises to centrosomes in mitosis and to chromosome cores in meiosis. *Chromosoma* 112:323-30.
- Ricke, R.M. and Bielinsky, A.K. (2004) Mcm10 regulates the stability and chromatin association of DNA polymerase-alpha. *Mol Cell* 16:173-85.
- Rieder, C.L. and Salmon, E.D. (1998) The vertebrate cell kinetochore and its roles during mitosis. *Trends Cell Biol* 8:310-8.
- Rieder, C.L. and Cole, R.W. (1998) Entry into mitosis in vertebrate somatic cells is guarded by a chromosome damage checkpoint that reverses the cell cycle when triggered during early but not late prophase. *J Cell Biol* 142:1013-22.
- Ritzi, M., Baack, M., Musahl, C., Romanowski, P., Laskey, R.A. and Knippers, R. (1998) Human minichromosome maintenance proteins and human origin recognition complex 2 protein on chromatin. *J Biol Chem* 273:24543-9.
- Rogakou, E.P., Pilch, D.R., Orr, A.H., Ivanova, V.S. and Bonner, W.M. (1998) DNA double-stranded breaks induce histone H2AX phosphorylation on serine 139. *J Biol Chem* 273:5858-68.
- Romanowski, P., Madine, M.A., Rowles, A., Blow, J.J. and Laskey, R.A. (1996) The *Xenopus* origin recognition complex is essential for DNA replication and MCM binding to chromatin. *Curr Biol* 6:1416-25.
- Rouse, J. and Jackson, S.P. (2002) Interfaces between the detection, signaling, and repair of DNA damage. *Science* 297:547-51.
- Rowles, A., Chong, J.P., Brown, L., Howell, M., Evan, G.I. and Blow, J.J. (1996) Interaction between the origin recognition complex and the replication licensing system in *Xenopus*. *Cell* 87:287-96.
- Ryu, B., Kim, D.S., Deluca, A.M. and Alani, R.M. (2007) Comprehensive expression profiling of tumor cell lines identifies molecular signatures of melanoma progression. *PLoS One* 2:e594.
- Sabbioneda, S., Minesinger, B.K., Giannattasio, M., Plevani, P., Muzi-Falconi, M. and Jinks-Robertson, S. (2005) The 9-1-1 checkpoint clamp physically interacts with polzeta and is partially required for spontaneous polzeta-dependent mutagenesis in *Saccharomyces cerevisiae*. *J Biol Chem* 280:38657-65.
- Sambrook, J., Fritsch, E.F. and Maniatis, T. (1989) A laboratory manual, 2nd edition. *Cold Spring Harb Laboratory Press* 1.
- Sanchez, Y., Bachant, J., Wang, H., Hu, F., Liu, D., Tetzlaff, M. and Elledge, S.J. (1999) Control of the DNA damage checkpoint by chk1 and rad53 protein kinases through distinct mechanisms. *Science* 286:1166-71.
- Santocanale, C. and Diffley, J.F. (1998) A Mec1- and Rad53-dependent checkpoint controls late-firing origins of DNA replication. *Nature* 395:615-8.
- Sartori, A.A., Lukas, C., Coates, J., Mistrik, M., Fu, S., Bartek, J., Baer, R., Lukas, J. and Jackson, S.P. (2007) Human CtIP promotes DNA end resection. *Nature* 450:509-14.
- Savitsky, K., Bar-Shira, A., Gilad, S., Rotman, G., Ziv, Y., Vanagaite, L., Tagle, D.A., Smith, S., Uziel, T., Sfez, S., Ashkenazi, M., Pecker, I., Frydman, M., Harnik, R., Patanjali, S.R., Simmons, A., Clines, G.A., Sartiel, A., Gatti, R.A., Chessa, L., Sanal, O., Lavin, M.F., Jaspers, N.G., Taylor, A.M., Arlett, C.F., Miki, T., Weissman, S.M., Lovett, M., Collins, F.S. and Shiloh, Y. (1995) A single ataxia telangiectasia gene with a product similar to PI-3 kinase. *Science* 268:1749-53.

- Schollaert, K.L., Poisson, J.M., Searle, J.S., Schwanekamp, J.A., Tomlinson, C.R. and Sanchez, Y. (2004) A role for *Saccharomyces cerevisiae* Chk1p in the response to replication blocks. *Mol Biol Cell* 15:4051-63.
- Schultz, L.B., Chehab, N.H., Malikzay, A. and Halazonetis, T.D. (2000) p53 binding protein 1 (53BP1) is an early participant in the cellular response to DNA double-strand breaks. *J Cell Biol* 151:1381-90.
- Schwartz, M.F., Duong, J.K., Sun, Z., Morrow, J.S., Pradhan, D. and Stern, D.F. (2002) Rad9 phosphorylation sites couple Rad53 to the *Saccharomyces cerevisiae* DNA damage checkpoint. *Mol Cell* 9:1055-65.
- Seki, M., Nakagawa, T., Seki, T., Kato, G., Tada, S., Takahashi, Y., Yoshimura, A., Kobayashi, T., Aoki, A., Otsuki, M., Habermann, F.A., Tanabe, H., Ishii, Y. and Enomoto, T. (2006a) Bloom helicase and DNA topoisomerase IIIalpha are involved in the dissolution of sister chromatids. *Mol Cell Biol* 26:6299-307.
- Seki, T., Akita, M., Kamimura, Y., Muramatsu, S., Araki, H. and Sugino, A. (2006b) GINS is a DNA polymerase epsilon accessory factor during chromosomal DNA replication in budding yeast. *J Biol Chem* 281:21422-32.
- Shechter, D., Costanzo, V. and Gautier, J. (2004) ATR and ATM regulate the timing of DNA replication origin firing. *Nat Cell Biol* 6:648-55.
- Shechter, D.F., Ying, C.Y. and Gautier, J. (2000) The intrinsic DNA helicase activity of *Methanobacterium thermoautotrophicum* delta H minichromosome maintenance protein. *J Biol Chem* 275:15049-59.
- Shiloh, Y. (2003) ATM and related protein kinases: safeguarding genome integrity. *Nat Rev Cancer* 3:155-68.
- Shima, N., Buske, T.R. and Schimenti, J.C. (2007a) Genetic screen for chromosome instability in mice: Mcm4 and breast cancer. *Cell Cycle* 6:1135-40.
- Shima, N., Alcaraz, A., Liachko, I., Buske, T.R., Andrews, C.A., Munroe, R.J., Hartford, S.A., Tye, B.K. and Schimenti, J.C. (2007b) A viable allele of Mcm4 causes chromosome instability and mammary adenocarcinomas in mice. *Nat Genet* 39:93-8.
- Shiromizu, T., Goto, H., Tomono, Y., Bartek, J., Totsukawa, G., Inoko, A., Nakanishi, M., Matsumura, F. and Inagaki, M. (2006) Regulation of mitotic function of Chk1 through phosphorylation at novel sites by cyclin-dependent kinase 1 (Cdk1). *Genes Cells* 11:477-85.
- Shishkin, A.A., Voineagu, I., Matera, R., Cherng, N., Chernet, B.T., Krasilnikova, M.M., Narayanan, V., Lobachev, K.S. and Mirkin, S.M. (2009) Large-scale expansions of Friedreich's ataxia GAA repeats in yeast. *Mol Cell* 35:82-92.
- Siede, W., Friedberg, A.S. and Friedberg, E.C. (1993) RAD9-dependent G1 arrest defines a second checkpoint for damaged DNA in the cell cycle of *Saccharomyces cerevisiae*. *Proc Natl Acad Sci U S A* 90:7985-9.
- Siede, W., Friedberg, A.S., Dianova, I. and Friedberg, E.C. (1994) Characterization of G1 checkpoint control in the yeast *Saccharomyces cerevisiae* following exposure to DNA-damaging agents. *Genetics* 138:271-81.
- Sorensen, C.S., Syljuasen, R.G., Falck, J., Schroeder, T., Ronnstrand, L., Khanna, K.K., Zhou, B.B., Bartek, J. and Lukas, J. (2003) Chk1 regulates the S phase checkpoint by coupling the physiological turnover and ionizing radiation-induced accelerated proteolysis of Cdc25A. *Cancer Cell* 3:247-58.
- Soulier, J. and Lowndes, N.F. (1999) The BRCT domain of the *S. cerevisiae* checkpoint protein Rad9 mediates a Rad9-Rad9 interaction after DNA damage. *Curr Biol* 9:551-4.

- Soutoglou, E. and Misteli, T. (2008) Activation of the cellular DNA damage response in the absence of DNA lesions. *Science* 320:1507-10.
- Stewart, G.S. (2009) Solving the RIDDLE of 53BP1 recruitment to sites of damage. *Cell Cycle* 8:1532-8.
- Stewart, G.S., Wang, B., Bignell, C.R., Taylor, A.M. and Elledge, S.J. (2003) MDC1 is a mediator of the mammalian DNA damage checkpoint. *Nature* 421:961-6.
- Stewart, G.S., Panier, S., Townsend, K., Al-Hakim, A.K., Kolas, N.K., Miller, E.S., Nakada, S., Ylanko, J., Olivarius, S., Mendez, M., Oldreive, C., Wildenhain, J., Tagliaferro, A., Pelletier, L., Taubenheim, N., Durandy, A., Byrd, P.J., Stankovic, T., Taylor, A.M. and Durocher, D. (2009) The RIDDLE syndrome protein mediates a ubiquitin-dependent signaling cascade at sites of DNA damage. *Cell* 136:420-34.
- Stiff, T., O'Driscoll, M., Rief, N., Iwabuchi, K., Lobrich, M. and Jeggo, P.A. (2004) ATM and DNA-PK function redundantly to phosphorylate H2AX after exposure to ionizing radiation. *Cancer Res* 64:2390-6.
- Stobbe, C.C., Park, S.J. and Chapman, J.D. (2002) The radiation hypersensitivity of cells at mitosis. *Int J Radiat Biol* 78:1149-57.
- Stoeber, K., Tlsty, T.D., Happerfield, L., Thomas, G.A., Romanov, S., Bobrow, L., Williams, E.D. and Williams, G.H. (2001) DNA replication licensing and human cell proliferation. *J Cell Sci* 114:2027-41.
- Stracker, T.H., Usui, T. and Petrini, J.H. (2009) Taking the time to make important decisions: the checkpoint effector kinases Chk1 and Chk2 and the DNA damage response. *DNA Repair (Amst)* 8:1047-54.
- Strahl, B.D. and Allis, C.D. (2000) The language of covalent histone modifications. *Nature* 403:41-5.
- Stucki, M. and Jackson, S.P. (2004) MDC1/NFBD1: a key regulator of the DNA damage response in higher eukaryotes. *DNA Repair (Amst)* 3:953-7.
- Stucki, M., Clapperton, J.A., Mohammad, D., Yaffe, M.B., Smerdon, S.J. and Jackson, S.P. (2005) MDC1 directly binds phosphorylated histone H2AX to regulate cellular responses to DNA double-strand breaks. *Cell* 123:1213-26.
- Sudakin, V. and Yen, T.J. (2007) Targeting mitosis for anti-cancer therapy. *BioDrugs* 21:225-33.
- Sugasawa, K. (2009) UV-DDB: a molecular machine linking DNA repair with ubiquitination. *DNA Repair (Amst)* 8:969-72.
- Sun, Y., Xu, Y., Roy, K. and Price, B.D. (2007) DNA damage-induced acetylation of lysine 3016 of ATM activates ATM kinase activity. *Mol Cell Biol* 27:8502-9.
- Sun, Z., Hsiao, J., Fay, D.S. and Stern, D.F. (1998) Rad53 FHA domain associated with phosphorylated Rad9 in the DNA damage checkpoint. *Science* 281:272-4.
- Svetlova, M., Solovjeva, L., Nishi, K., Nazarov, I., Siino, J. and Tomilin, N. (2007) Elimination of radiation-induced gamma-H2AX foci in mammalian nucleus can occur by histone exchange. *Biochem Biophys Res Commun* 358:650-4.
- Swann, M.M. (1957) The control of cell division; a review. I. General mechanisms. *Cancer Res* 17:727-57.
- Sweeney, F.D., Yang, F., Chi, A., Shabanowitz, J., Hunt, D.F. and Durocher, D. (2005) *Saccharomyces cerevisiae* Rad9 acts as a Mec1 adaptor to allow Rad53 activation. *Curr Biol* 15:1364-75.
- Tada, S., Li, A., Maiorano, D., Mechali, M. and Blow, J.J. (2001) Repression of origin assembly in metaphase depends on inhibition of RLF-B/Cdt1 by geminin. *Nat Cell Biol* 3:107-13.

- Tak, Y.S., Tanaka, Y., Endo, S., Kamimura, Y. and Araki, H. (2006) A CDK-catalysed regulatory phosphorylation for formation of the DNA replication complex Sld2-Dpb11. *Embo J* 25:1987-96.
- Takahashi, T.S., Wigley, D.B. and Walter, J.C. (2005) Pumps, paradoxes and ploughshares: mechanism of the MCM2-7 DNA helicase. *Trends Biochem Sci* 30:437-44.
- Takayama, Y., Kamimura, Y., Okawa, M., Muramatsu, S., Sugino, A. and Araki, H. (2003) GINS, a novel multiprotein complex required for chromosomal DNA replication in budding yeast. *Genes Dev* 17:1153-65.
- Takeda, D.Y. and Dutta, A. (2005) DNA replication and progression through S phase. *Oncogene* 24:2827-43.
- Tanaka, S., Umemori, T., Hirai, K., Muramatsu, S., Kamimura, Y. and Araki, H. (2007) CDK-dependent phosphorylation of Sld2 and Sld3 initiates DNA replication in budding yeast. *Nature* 445:328-32.
- Tanaka, T., Knapp, D. and Nasmyth, K. (1997) Loading of an Mcm protein onto DNA replication origins is regulated by Cdc6p and CDKs. *Cell* 90:649-60.
- Tatsumi, Y., Tsurimoto, T., Shirahige, K., Yoshikawa, H. and Obuse, C. (2000) Association of human origin recognition complex 1 with chromatin DNA and nuclease-resistant nuclear structures. *J Biol Chem* 275:5904-10.
- Tibelius, A., Marhold, J., Zentgraf, H., Heilig, C.E., Neitzel, H., Ducommun, B., Rauch, A., Ho, A.D., Bartek, J. and Kramer, A. (2009) Microcephalin and pericentrin regulate mitotic entry via centrosome-associated Chk1. *J Cell Biol* 185:1149-57.
- Tishler, R.B., Lamppu, D.M., Park, S. and Price, B.D. (1995) Microtubule-active drugs taxol, vinblastine, and nocodazole increase the levels of transcriptionally active p53. *Cancer Res* 55:6021-5.
- Todorov, I.T., Werness, B.A., Wang, H.Q., Buddharaju, L.N., Todorova, P.D., Slocum, H.K., Brooks, J.S. and Huberman, J.A. (1998) HsMCM2/BM28: a novel proliferation marker for human tumors and normal tissues. *Lab Invest* 78:73-8.
- Toh, G.W. and Lowndes, N.F. (2003) Role of the *Saccharomyces cerevisiae* Rad9 protein in sensing and responding to DNA damage. *Biochem Soc Trans* 31:242-6.
- Townsend, K., Mason, H., Blackford, A.N., Miller, E.S., Chapman, J.R., Sedgwick, G.G., Barone, G., Turnell, A.S. and Stewart, G.S. (2009) Mediator of DNA damage checkpoint 1 (MDC1) regulates mitotic progression. *J Biol Chem* 284:33939-48.
- Tritarelli, A., Oricchio, E., Ciciarello, M., Mangiacasale, R., Palena, A., Lavia, P., Soddu, S. and Cundari, E. (2004) p53 localization at centrosomes during mitosis and postmitotic checkpoint are ATM-dependent and require serine 15 phosphorylation. *Mol Biol Cell* 15:3751-7.
- Tsvetkov, L., Xu, X., Li, J. and Stern, D.F. (2003) Polo-like kinase 1 and Chk2 interact and co-localize to centrosomes and the midbody. *J Biol Chem* 278:8468-75.
- Tuduri, S., Crabbe, L., Conti, C., Tourriere, H., Holtgreve-Grez, H., Jauch, A., Pantesco, V., De Vos, J., Thomas, A., Theillet, C., Pommier, Y., Tazi, J., Coquelle, A. and Pasero, P. (2009) Topoisomerase I suppresses genomic instability by preventing interference between replication and transcription. *Nat Cell Biol* 11:1315-24.
- Tuel-Ahlgren, L., Jun, X., Waddick, K.G., Jin, J., Bolen, J. and Uckun, F.M. (1996) Role of tyrosine phosphorylation in radiation-induced cell cycle-arrest of leukemic B-cell precursors at the G2-M transition checkpoint. *Leuk Lymphoma* 20:417-26.
- Tuttle, R.L., Bothos, J., Summers, M.K., Luca, F.C. and Halazonetis, T.D. (2007) Defective in mitotic arrest 1/ring finger 8 is a checkpoint protein that antagonizes the human mitotic exit network. *Mol Cancer Res* 5:1304-11.

- Ueno, M., Itoh, M., Sugihara, K., Asano, M. and Takakura, N. (2009) Both alleles of PSF1 are required for maintenance of pool size of immature hematopoietic cells and acute bone marrow regeneration. *Blood* 113:555-62.
- Ueno, M., Itoh, M., Kong, L., Sugihara, K., Asano, M. and Takakura, N. (2005) PSF1 is essential for early embryogenesis in mice. *Mol Cell Biol* 25:10528-32.
- Uetz, P., Giot, L., Cagney, G., Mansfield, T.A., Judson, R.S., Knight, J.R., Lockshon, D., Narayan, V., Srinivasan, M., Pochart, P., Qureshi-Emili, A., Li, Y., Godwin, B., Conover, D., Kalbfleisch, T., Vijayadamodar, G., Yang, M., Johnston, M., Fields, S. and Rothberg, J.M. (2000) A comprehensive analysis of protein-protein interactions in *Saccharomyces cerevisiae*. *Nature* 403:623-7.
- Usui, T., Ogawa, H. and Petrini, J.H. (2001) A DNA damage response pathway controlled by Tel1 and the Mre11 complex. *Mol Cell* 7:1255-66.
- Uziel, T., Lerenthal, Y., Moyal, L., Andegeko, Y., Mittelman, L. and Shiloh, Y. (2003) Requirement of the MRN complex for ATM activation by DNA damage. *Embo J* 22:5612-21.
- Van Dyke, M.W., Nelson, L.D., Weilbaecher, R.G. and Mehta, D.V. (2004) Stm1p, a G4 quadruplex and purine motif triplex nucleic acid-binding protein, interacts with ribosomes and subtelomeric Y' DNA in *Saccharomyces cerevisiae*. *J Biol Chem* 279:24323-33.
- Van Dyke, N., Baby, J. and Van Dyke, M.W. (2006) Stm1p, a ribosome-associated protein, is important for protein synthesis in *Saccharomyces cerevisiae* under nutritional stress conditions. *J Mol Biol* 358:1023-31.
- Van Dyke, N., Pickering, B.F. and Van Dyke, M.W. (2009) Stm1p alters the ribosome association of eukaryotic elongation factor 3 and affects translation elongation. *Nucleic Acids Res* 37:6116-25.
- van Veelen, L.R., Cervelli, T., van de Rakt, M.W., Theil, A.F., Essers, J. and Kanaar, R. (2005) Analysis of ionizing radiation-induced foci of DNA damage repair proteins. *Mutat Res* 574:22-33.
- van Vugt, M.A., Gardino, A.K., Linding, R., Ostheimer, G.J., Reinhardt, H.C., Ong, S.E., Tan, C.S., Miao, H., Keezer, S.M., Li, J., Pawson, T., Lewis, T.A., Carr, S.A., Smerdon, S.J., Brummelkamp, T.R. and Yaffe, M.B. (2010) A mitotic phosphorylation feedback network connects Cdk1, Plk1, 53BP1, and Chk2 to inactivate the G(2)/M DNA damage checkpoint. *PLoS Biol* 8:e1000287.
- Vas, A., Mok, W. and Leatherwood, J. (2001) Control of DNA rereplication via Cdc2 phosphorylation sites in the origin recognition complex. *Mol Cell Biol* 21:5767-77.
- Vialard, J.E., Gilbert, C.S., Green, C.M. and Lowndes, N.F. (1998) The budding yeast Rad9 checkpoint protein is subjected to Mec1/Tel1-dependent hyperphosphorylation and interacts with Rad53 after DNA damage. *Embo J* 17:5679-88.
- Voineagu, I., Surka, C.F., Shishkin, A.A., Krasilnikova, M.M. and Mirkin, S.M. (2009) Replisome stalling and stabilization at CGG repeats, which are responsible for chromosomal fragility. *Nat Struct Mol Biol* 16:226-8.
- Walter, B.E., Perry, K.J., Fukui, L., Malloch, E.L., Wever, J. and Henry, J.J. (2008) Psf2 plays important roles in normal eye development in *Xenopus laevis*. *Mol Vis* 14:906-21.
- Wang, B. and Elledge, S.J. (2007) Ubc13/Rnf8 ubiquitin ligases control foci formation of the Rap80/Abraxas/Brc1/Brcc36 complex in response to DNA damage. *Proc Natl Acad Sci U S A* 104:20759-63.
- Wang, B., Matsuoka, S., Carpenter, P.B. and Elledge, S.J. (2002) 53BP1, a mediator of the DNA damage checkpoint. *Science* 298:1435-8.

- Wang, H., Wang, M., Wang, H., Bocker, W. and Iliakis, G. (2005) Complex H2AX phosphorylation patterns by multiple kinases including ATM and DNA-PK in human cells exposed to ionizing radiation and treated with kinase inhibitors. *J Cell Physiol* 202:492-502.
- Wang, H., Zhai, L., Xu, J., Joo, H.Y., Jackson, S., Erdjument-Bromage, H., Tempst, P., Xiong, Y. and Zhang, Y. (2006) Histone H3 and H4 ubiquitylation by the CUL4-DDB-ROC1 ubiquitin ligase facilitates cellular response to DNA damage. *Mol Cell* 22:383-94.
- Wang, J.C. (2002) Cellular roles of DNA topoisomerases: a molecular perspective. *Nat Rev Mol Cell Biol* 3:430-40.
- Ward, I., Kim, J.E., Minn, K., Chini, C.C., Mer, G. and Chen, J. (2006) The tandem BRCT domain of 53BP1 is not required for its repair function. *J Biol Chem* 281:38472-7.
- Ward, I.M., Minn, K., van Deursen, J. and Chen, J. (2003) p53 Binding protein 53BP1 is required for DNA damage responses and tumor suppression in mice. *Mol Cell Biol* 23:2556-63.
- Ward, I.M., Reina-San-Martin, B., Oлару, A., Minn, K., Tamada, K., Lau, J.S., Cascalho, M., Chen, L., Nussenzweig, A., Livak, F., Nussenzweig, M.C. and Chen, J. (2004) 53BP1 is required for class switch recombination. *J Cell Biol* 165:459-64.
- Weinert, T. (1997) A DNA damage checkpoint meets the cell cycle engine. *Science* 277:1450-1.
- Weinert, T. and Hartwell, L. (1989) Control of G2 delay by the rad9 gene of *Saccharomyces cerevisiae*. *J Cell Sci Suppl* 12:145-8.
- Weinert, T.A. and Hartwell, L.H. (1988) The RAD9 gene controls the cell cycle response to DNA damage in *Saccharomyces cerevisiae*. *Science* 241:317-22.
- Weinert, T.A. and Hartwell, L.H. (1990) Characterization of RAD9 of *Saccharomyces cerevisiae* and evidence that its function acts posttranslationally in cell cycle arrest after DNA damage. *Mol Cell Biol* 10:6554-64.
- Weinreich, M. and Stillman, B. (1999) Cdc7p-Dbf4p kinase binds to chromatin during S phase and is regulated by both the APC and the RAD53 checkpoint pathway. *Embo J* 18:5334-46.
- Williams, D.R. and McIntosh, J.R. (2002) mcl1+, the *Schizosaccharomyces pombe* homologue of CTF4, is important for chromosome replication, cohesion, and segregation. *Eukaryot Cell* 1:758-73.
- Williams, R.S., Williams, J.S. and Tainer, J.A. (2007) Mre11-Rad50-Nbs1 is a keystone complex connecting DNA repair machinery, double-strand break signaling, and the chromatin template. *Biochem Cell Biol* 85:509-20.
- Williams, R.S., Lee, M.S., Hau, D.D. and Glover, J.N. (2004) Structural basis of phosphopeptide recognition by the BRCT domain of BRCA1. *Nat Struct Mol Biol* 11:519-25.
- Williams, R.S., Moncalian, G., Williams, J.S., Yamada, Y., Limbo, O., Shin, D.S., Grocock, L.M., Cahill, D., Hitomi, C., Guenther, G., Moiani, D., Carney, J.P., Russell, P. and Tainer, J.A. (2008) Mre11 dimers coordinate DNA end bridging and nuclease processing in double-strand-break repair. *Cell* 135:97-109.
- Wilsker, D., Petermann, E., Helleday, T. and Bunz, F. (2008) Essential function of Chk1 can be uncoupled from DNA damage checkpoint and replication control. *Proc Natl Acad Sci U S A* 105:20752-7.
- Wohlschlegel, J.A., Dwyer, B.T., Dhar, S.K., Cvetic, C., Walter, J.C. and Dutta, A. (2000) Inhibition of eukaryotic DNA replication by geminin binding to Cdt1. *Science* 290:2309-12.

- Woods, C.G., Bond, J. and Enard, W. (2005) Autosomal recessive primary microcephaly (MCPH): a review of clinical, molecular, and evolutionary findings. *Am J Hum Genet* 76:717-28.
- Wu, R.S., Kohn, K.W. and Bonner, W.M. (1981) Metabolism of ubiquitinated histones. *J Biol Chem* 256:5916-20.
- Xia, Z., Morales, J.C., Dunphy, W.G. and Carpenter, P.B. (2001) Negative cell cycle regulation and DNA damage-inducible phosphorylation of the BRCT protein 53BP1. *J Biol Chem* 276:2708-18.
- Xu, X. and Stern, D.F. (2003) NFBFD1/KIAA0170 is a chromatin-associated protein involved in DNA damage signaling pathways. *J Biol Chem* 278:8795-803.
- Xu, X., Lee, J. and Stern, D.F. (2004) Microcephalin is a DNA damage response protein involved in regulation of CHK1 and BRCA1. *J Biol Chem* 279:34091-4.
- Yabuuchi, H., Yamada, Y., Uchida, T., Sunathvanichkul, T., Nakagawa, T. and Masukata, H. (2006) Ordered assembly of Sld3, GINS and Cdc45 is distinctly regulated by DDK and CDK for activation of replication origins. *Embo J* 25:4663-74.
- You, Z., Komamura, Y. and Ishimi, Y. (1999) Biochemical analysis of the intrinsic Mcm4-Mcm6-mcm7 DNA helicase activity. *Mol Cell Biol* 19:8003-15.
- Yu, X., Chini, C.C., He, M., Mer, G. and Chen, J. (2003) The BRCT domain is a phospho-protein binding domain. *Science* 302:639-42.
- Zabludoff, S.D., Deng, C., Grondine, M.R., Sheehy, A.M., Ashwell, S., Caleb, B.L., Green, S., Haye, H.R., Horn, C.L., Janetka, J.W., Liu, D., Mouchet, E., Ready, S., Rosenthal, J.L., Queva, C., Schwartz, G.K., Taylor, K.J., Tse, A.N., Walker, G.E. and White, A.M. (2008) AZD7762, a novel checkpoint kinase inhibitor, drives checkpoint abrogation and potentiates DNA-targeted therapies. *Mol Cancer Ther* 7:2955-66.
- Zachos, G., Black, E.J., Walker, M., Scott, M.T., Vagnarelli, P., Earnshaw, W.C. and Gillespie, D.A. (2007) Chk1 is required for spindle checkpoint function. *Dev Cell* 12:247-60.
- Zegerman, P. and Diffley, J.F. (2007) Phosphorylation of Sld2 and Sld3 by cyclin-dependent kinases promotes DNA replication in budding yeast. *Nature* 445:281-5.
- Zhang, S., Hemmerich, P. and Grosse, F. (2007) Centrosomal localization of DNA damage checkpoint proteins. *J Cell Biochem* 101:451-65.
- Zhang, Y., Yu, Z., Fu, X. and Liang, C. (2002) Noc3p, a bHLH protein, plays an integral role in the initiation of DNA replication in budding yeast. *Cell* 109:849-60.
- Zhou, B.B. and Elledge, S.J. (2000) The DNA damage response: putting checkpoints in perspective. *Nature* 408:433-9.
- Zhu, W., Ukomadu, C., Jha, S., Senga, T., Dhar, S.K., Wohlschlegel, J.A., Nutt, L.K., Kornbluth, S. and Dutta, A. (2007) Mcm10 and And-1/CTF4 recruit DNA polymerase alpha to chromatin for initiation of DNA replication. *Genes Dev* 21:2288-99.
- Zhu, Y., Alvarez, C., Doll, R., Kurata, H., Schebye, X.M., Parry, D. and Lees, E. (2004) Intra-S-phase checkpoint activation by direct CDK2 inhibition. *Mol Cell Biol* 24:6268-77.
- Ziv, Y., Bielopolski, D., Galanty, Y., Lukas, C., Taya, Y., Schultz, D.C., Lukas, J., Bekker-Jensen, S., Bartek, J. and Shiloh, Y. (2006) Chromatin relaxation in response to DNA double-strand breaks is modulated by a novel ATM- and KAP-1 dependent pathway. *Nat Cell Biol* 8:870-6.
- Zou, L. and Elledge, S.J. (2003) Sensing DNA damage through ATRIP recognition of RPA-ssDNA complexes. *Science* 300:1542-8.



## APPENDIX

---

## PUBLICATIONS

---

S. Giunta, R. Belotserkovskaya and S. P. Jackson

**DNA damage signalling in response to double-strand breaks during mitosis**

*Journal of Cell Biology.* **190**, 197-207 (2010)